

**Manual For Model 730**

**Magnetic  
Levitation System**  
(Instructor's Edition)

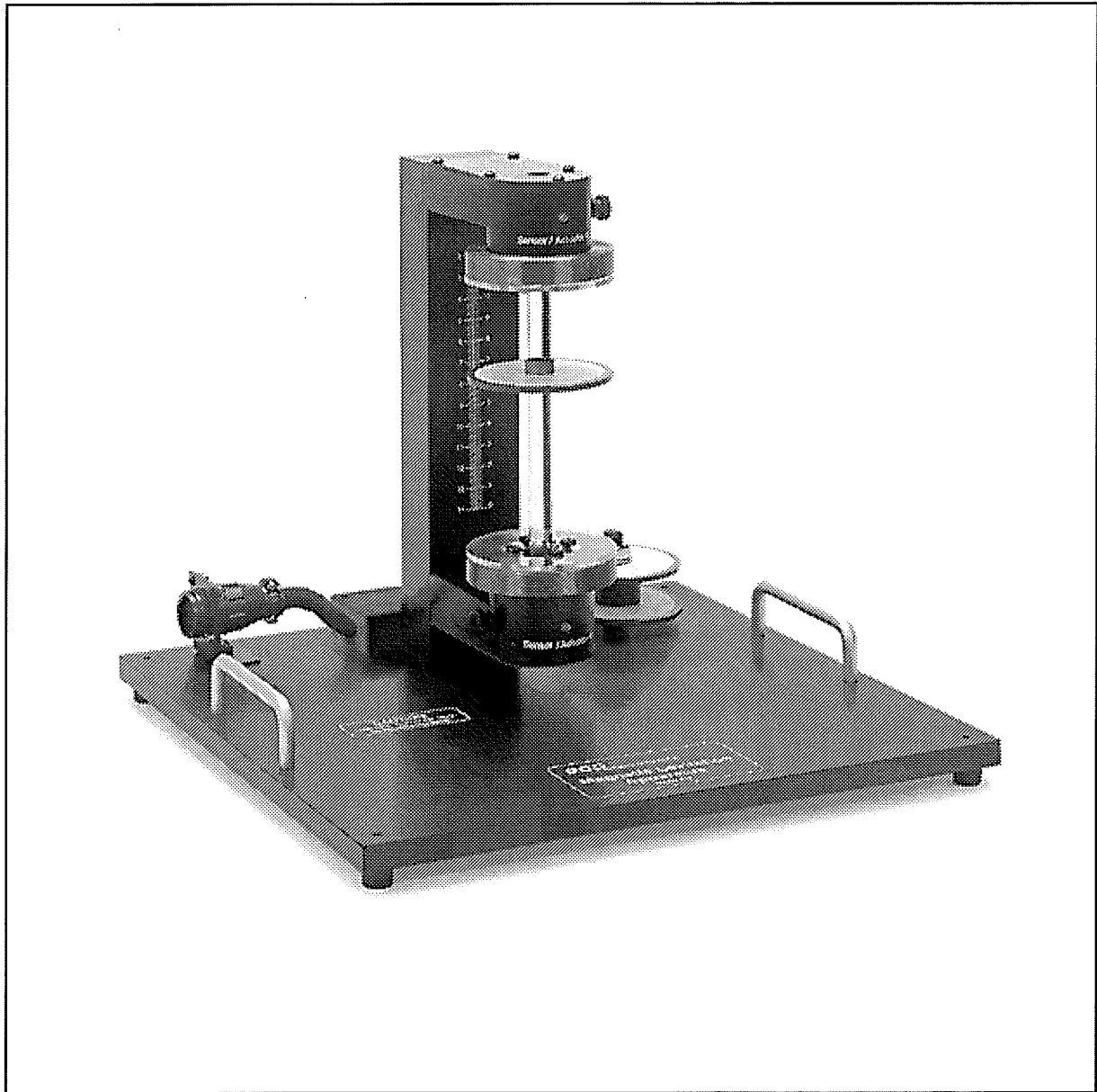
**Important Notice**

Section 2.3 of this manual contains important safety information that must be read by all users prior to operating the ECP system.

**Created & Edited By:  
Thomas R. Parks**

This manual is for use in conjunction with ECP experimental systems only and may be reproduced only for that purpose. All other use, dissemination, or reproduction in whole or in part without the written permission of ECP is strictly prohibited.

© COPYRIGHT 1991-1999 by ECP, Educational Control Products. All rights reserved.



**The Model 730 Magnetic Levitation Apparatus**

# CONTENTS

<b>1</b>	<b>Introduction</b> . . . . .	<b>1</b>
	1.1 System Overview . . . . .	1
	1.2 Manual Overview . . . . .	2
<b>2</b>	<b>System Description &amp; Operating Instructions</b> . . . . .	<b>3</b>
	2.1 ECP Executive Software . . . . .	3
	2.2 Electromechanical Plant . . . . .	32
	2.3 Safety . . . . .	37
<b>3</b>	<b>Start-up &amp; Self-Guided Demonstration</b> . . . . .	<b>41</b>
	3.1 Hardware Set-up Verification . . . . .	41
	3.2 Demonstration Of ECP Executive Program . . . . .	43
<b>4</b>	<b>Real-time Control Implementation</b> . . . . .	<b>49</b>
	4.1 Servo Loop Closure . . . . .	50
	4.2 Command Generation . . . . .	51
	4.3 Servo Motor & Amplifier . . . . .	54
	4.4 Multi-tasking Environment . . . . .	55
	4.5 Sensors . . . . .	56
	4.6 Auxiliary Analog Output . . . . .	59
<b>5</b>	<b>Plant Dynamic Models</b> . . . . .	<b>60</b>
	5.1 Full Order Nonlinear Model . . . . .	60
	5.2 Simplified Equations of Motion . . . . .	61
	5.2 Linearized Equations of Motion . . . . .	63
	5.2 Sensor/System Model Using Rawe Sensor Counts . . . . .	65
<b>6</b>	<b>Experiments</b> . . . . .	<b>67</b>
	6.1 System Identification . . . . .	68
	6.2 Nonlinear Plant Control: Linearization About Operating Point . . . . .	79
	6.3 Control of Nonlinear Compensated SISO Systems . . . . .	84
	6.4 Fundamental Properties of Second Order Systems . . . . .	88
	6.5 Disturbance Rejection of Various 1 DOF Plant Controllers . . . . .	93
	6.6 Collocated Control of SIMO Plant . . . . .	95
	6.7 Noncollocated SIMO Control . . . . .	100
	6.8 MIMO Control . . . . .	104

<b>A</b>	<b>Magnetic Levitation Principals</b>	<b>103</b>
A.1	Introduction	103
A.2	Magnetic Fields & Forces	103
A.3	Maglev Applications	117
A.4	Reference	119

**(Instructor's Manual Only)**

<b>6i</b>	<b>Instructor's Supplement To Experiments</b>	<b>122</b>
6.1i	System Identification	123
6.2i	Nonlinear Plant Control: Linearization About Operating Point	135
6.3i	Control of Nonlinear Compensated SISO Systems	141
6.4i	Fundamental Properties of Second Order Systems	146
6.5i	Disturbance Rejection of Various 1 DOF Plant Controllers	157
6.6i	Collocated Control of SIMO Plant	163
6.7i	Noncollocated SIMO Control	168
6.8i	MIMO Control	178
6.9i	Suggested Further Experiments	180
<b>Ai</b>	<b>Useful Scripts and Real-time Algorithms</b>	<b>190</b>
A.1i	Matlab® Scripts	190
A.2i	Real-time Algorithms	191

# 1 Introduction

Welcome to the ECP line of educational control systems. These systems are designed to provide insight to control system principles through hands-on demonstration and experimentation. Seen in Figure 1.1-1, each consists of an electromechanical plant and a full complement of control hardware and software. The user interface to the system is via a user-friendly, PC based environment which supports a broad range of controller specification, trajectory generation, data acquisition, and plotting features. The systems are designed to accompany introductory through advanced level courses in control systems.

The Model 730 Magnetic Levitation (MagLev) apparatus may be quickly transformed into a variety of single input single output (SISO) and multi-input multi-output (MIMO) configurations. By using repulsive force from the lower coil to levitate a single magnet, an open loop stable SISO system is created. Attractive levitation via the upper coil effects an open loop unstable system. Two magnets may be raised by a single coil to produce a SIMO plant. If two coils are used a MIMO one is produced. These may be locally stable or unstable depending on the selection of the magnet polarities and the nominal magnet positions. The plant has inherently strong nonlinearities due to the natural properties of magnetic fields. These may be compensated for in feedforward using derived or provided algorithms so that the control problem may be approached as that of a linear or nonlinear system depending on the desired course of study. Thus this system provides a dynamically rich testbed for implementation of introductory through advanced control methods.

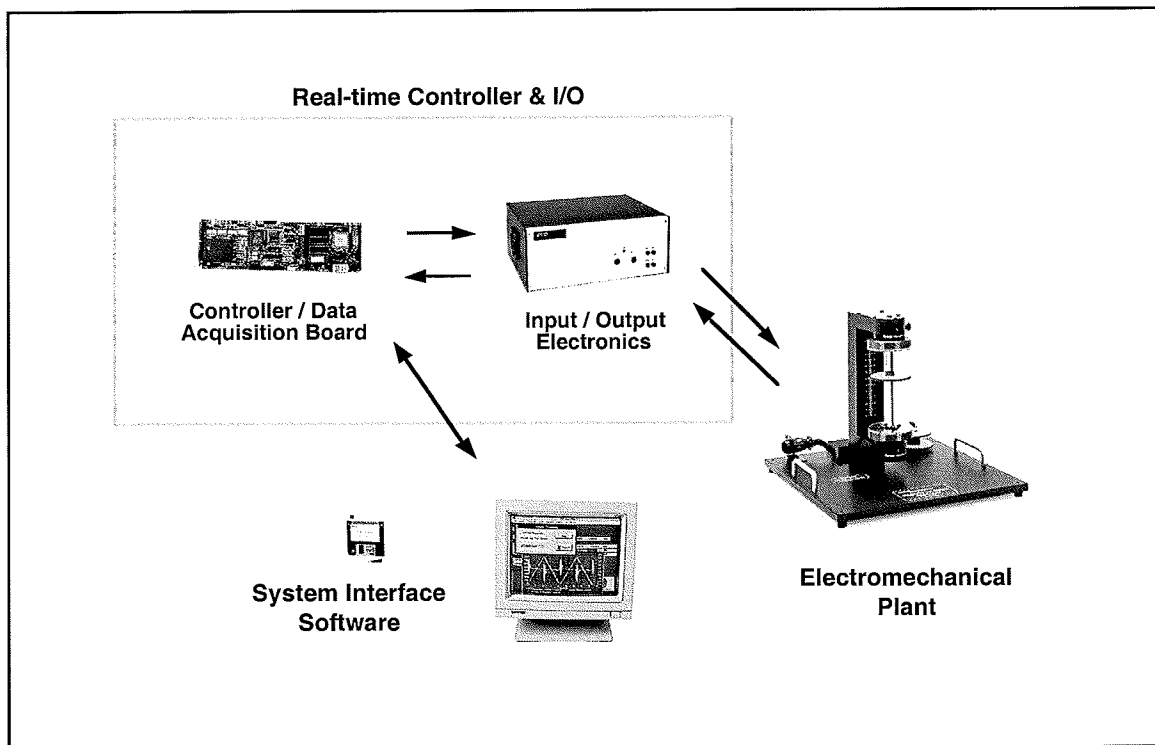


Figure 1.1-1. The Model 730 Experimental Control System

## 1.1 System Overview

The experimental system is comprised of the three subsystems shown in Figure 1.1-1. The first of these is the electromechanical plant, which consists of the MagLev apparatus including its actuators and sensors. The design features two high field density rare earth magnets and high flux drive coils to provide more than 4 cm. of controlled levitation range. Laser sensors provide non-contacting position feedback and incorporate proprietary conditioning electronics for signal noise reduction and ambient light rejection. An optional turntable incorporates a high-speed conductive spin platter that interacts with the permanent magnet in such a way as to induce a traveling current and cause the magnet to levitate. Magnet position control is accomplished through spin speed changes in the platter.

The next subsystem is the real-time controller unit which contains the digital signal processor (DSP) based real-time controller, servo/actuator interfaces, servo amplifiers, and auxiliary power supplies. The DSP – based on the M56000 processor family - is capable of executing control laws at high sampling rates allowing the implementation to be modeled as being in continuous or discrete time. The controller also interprets trajectory commands and supports such functions as data acquisition, trajectory generation, and system health and safety checks. A logic gate array performs encoder pulse decoding (optional turntable sensing). Four 16 bit analog-to-digital (ADC) converters are used to digitize the laser sensor signals. Two optional auxiliary digital-to-analog converters (DAC's) provide for real-time analog signal measurement. This controller is representative of modern industrial control implementation.

The third subsystem is the Executive program which runs on a PC under the DOS or Windows™ operating system. This graphical user interface (GUI) based program is the user's interface to the system and supports controller specification, trajectory definition, data acquisition, plotting, system execution commands, and more. Controllers are specified via an intuitive “C-like” language that supports easy generation of basic or highly complex algorithms. A built-in auto-compiler provides for efficient downloading and implementation of the real-time code by the DSP while remaining within the Executive. The interface supports a wide assortment of features that provide a friendly yet powerful experimental environment.

## 1.2 Manual Overview

The next chapter, Chapter 2, describes the system and gives instructions for its operation. Section 2.3 contains important information regarding safety and is mandatory reading for all users prior to operating this equipment. Chapter 3 is a self-guided demonstration in which the user is quickly walked through the salient system operations before reading all of the details in Chapter 2. A description of the system's real-time control implementation as well as a discussion of generic implementation issues is given in Chapter 4. Chapter 5 presents dynamic equations useful for control modeling. Chapter 6 gives detailed experiments including system identification and a study of important implementation issues and practical control approaches.

## 2 System Description & Operating Instructions

This chapter contains descriptions and operating instructions for the executive software and the mechanism. The safety instructions given in Section 2.3 must be read and understood by any user prior to operating this equipment.

### 2.1 ECP Executive Software

The ECP Executive program is the user's interface to the system. It is a menu driven / window environment that the user will find is intuitively familiar and quickly learned - see Figure 2.1-1. This software runs on an IBM PC or compatible computer and communicates with ECP's digital signal processor (DSP) based real-time controller. Its primary functions are supporting the downloading of various control algorithm parameters (gains), specifying command trajectories, selecting data to be acquired, and specifying how data should be plotted. In addition, various utility functions ranging from saving the current configuration of the Executive to specifying analog outputs on the optional auxiliary DAC's are included as menu items.

#### 2.1.1 The ECPMV Executive For Windows 95™, 98, & NT

##### 2.1.1.1 PC System Requirements

The 32-bit ECPMV Executive code runs best with a Pentium based PC having at least 16 megabytes of memory. The hard drive memory usage is less than 12 Megabytes.

##### 2.1.1.2 Installation Procedure

Enter Windows operating system, insert diskette 1 of 4 in the floppy drive of your computer and "Run" SETUP.EXE. Follow the installation dialog boxes. We strongly recommend that you do not modify the default setup of the directory structure used by the installation program.

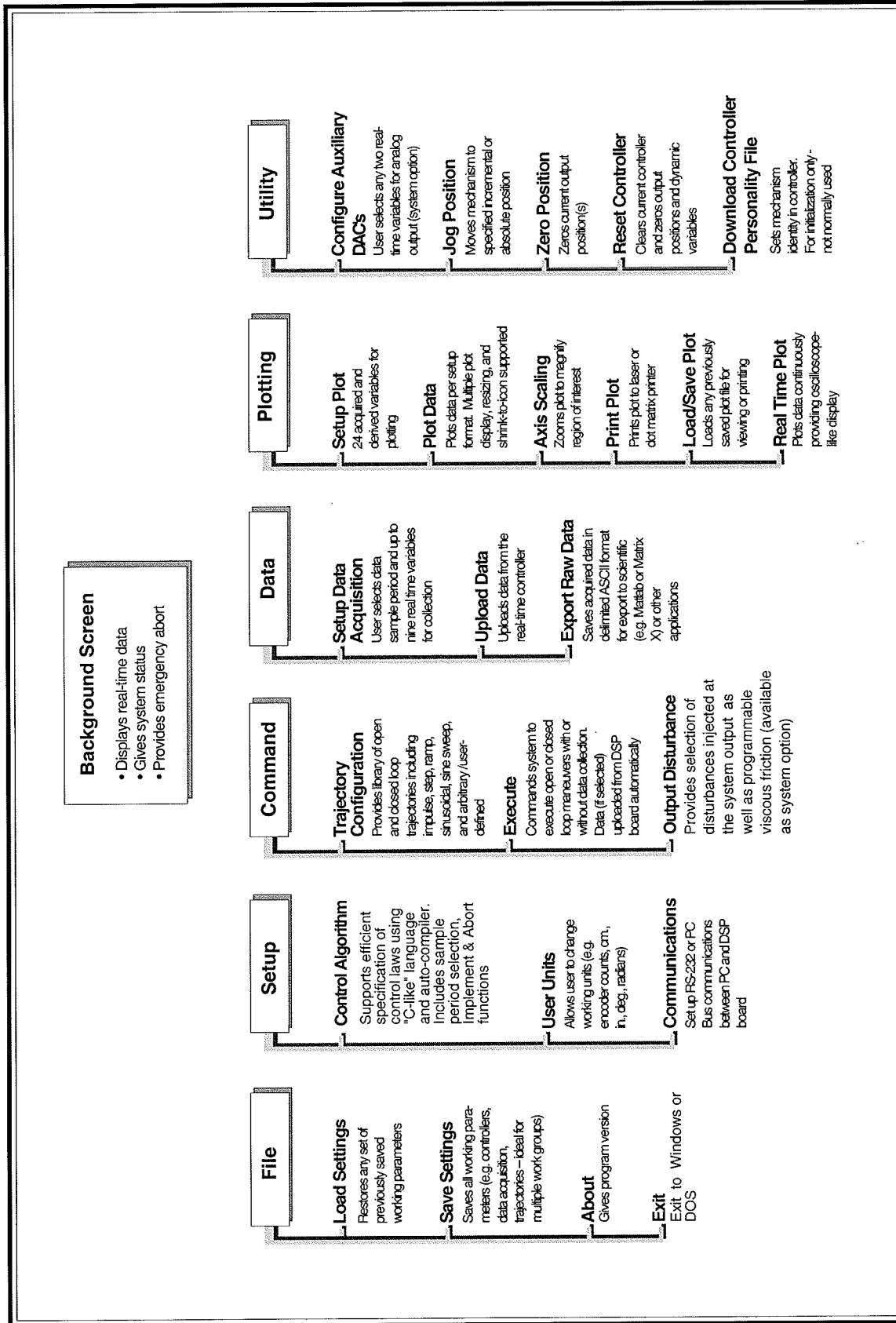


Figure 2.1-1. Structure and Key Features of Executive Program



### 2.1.3 Background Screen

The *Background Screen*, shown in Figure 2.1-1, remains in the background during system operation including times when other menus and dialog boxes are active. It contains the main menu and a display of real-time data, system status, and an *Abort Control* button to immediately discontinue control effort in the case of an emergency.

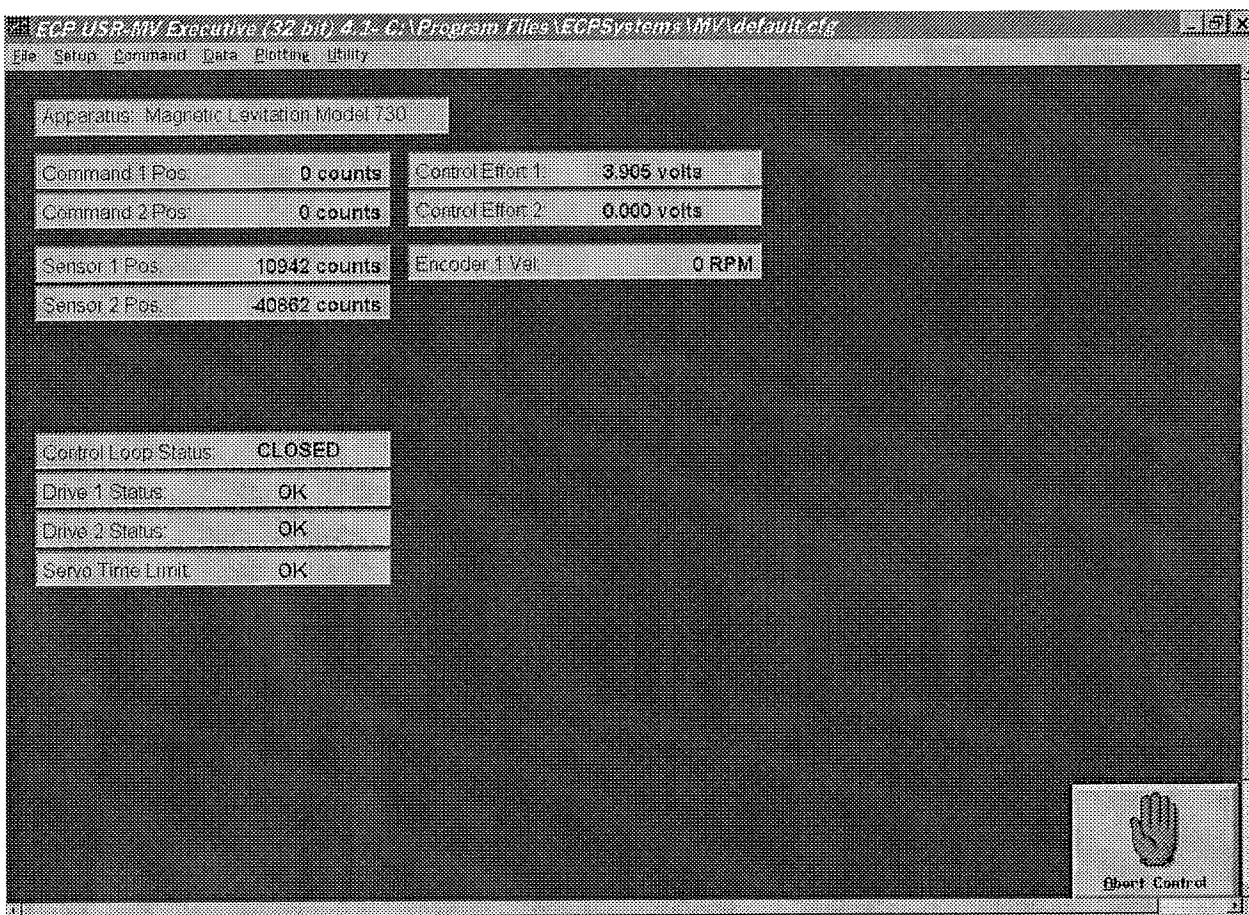


Figure 2.1-1. The Background Screen

#### 2.1.3.1 Real-Time Data Display

In the *Data Display* fields, the instantaneous commanded position, the encoder positions, the velocity of the rotor are shown. The units of the displayed data may be changed as described in

#### 2.1.3.2 System Status Display

The Control Loop Status indicates *Closed* when a \*.ALG file (an algorithm file) is compiled and downloaded to the DSP board. When this display indicates *Open* it means that the control loop is not active.

The Drive Status fields indicate *OK* unless the current limits of the respective drive coil amplifier is exceeded or a drive coil has reached a temperature limit. If either of these conditions occur, the affected field will indicate *Limit Exceeded*. To clear the current limit condition either the DSP board must be Reset via the Utility menu<sup>1</sup> or a control algorithm must be re-implemented which does not cause continuous current to exceed the set limit. If the *Limit Exceeded* indicator is due to either of the coils reaching an over-temperature condition, it will remain active for a period of time until the coil(s) cool down.

The Servo Time Limit field will indicate *OK* unless the currently implemented \*.ALG file is too long and/or complex for the chosen sampling period. In such case the *Limit Exceeded* condition will occur and the loop will be automatically opened. The user may then either increase the sampling period or edit the algorithm code to reduce the execution time. In general the combination of high sampling frequency, complex control laws and sine sweep trajectories (these require more intensive real-time processing than the other trajectories) may cause the *Limit Exceeded* condition displayed on the Servo Time Limit indicator

#### 2.1.3.3 Abort Control Button

Also included on the Background Screen is the Abort Control button. Clicking the mouse on this button simply opens the control loop. This is a very useful feature in various situations including one in which the user detects a marginally stable or a noisy closed loop system and he/she wishes to discontinue control action immediately. Note also that control action may always be discontinued immediately by pressing the red "OFF" button on the control box. The latter method should be used in case of an emergency.

#### 2.1.3.4 Main Menu Options

The *Main menu* is displayed at the top of the screen and has the following choices:

- File
- Setup
- Command
- Data
- Plotting
- Utility

#### 2.1.4 File Menu

The File menu contains the following pull-down options:

- Load Settings
- Save Settings
- About
- Exit

---

<sup>1</sup> Following a Reset Controller command, you must respecify the sensor setup options before implementing a control algorithm. See Section 2.1.5.2.

2.1.4.1 The Load Settings dialog box allows the user to load a previously saved configuration file into the Executive. Such file contains all user-specifiable data except for the control algorithm itself. A configuration file is any file with a ".cfg" extension which has been previously saved by the user using Save Settings. Any "\*.cfg" file can be loaded at any time. The latest loaded "\*.cfg" file will overwrite the previous configuration settings in the ECP Executive *but* will not effect the existing controller residing in the DSP real-time control card will not take place until the new controller is "implemented" – see Section 2.1.5.1. The configuration files include information on the last used control algorithm file, trajectories, data gathering, and plotting items previously saved. To load a "\*.cfg" file simply select the Load Settings command and when the dialog box opens, select the appropriate file from the directory.<sup>1</sup> Note that every time the Executive program is entered, a particular configuration file called "default.cfg" (which the user may customize - see below) is loaded. This file must exist in the same directory as the Executive Program in order for it to be automatically loaded.

2.1.4.2 The Save Settings option allows the user to save the current user-specifiable parameters for future retrieval via the Load Settings option. To save a "\*.cfg" file, select the Save Settings option and save under an appropriately named file (e.g. "pid1disk.cfg"). By saving the configuration under a file named "default.cfg" the user creates a default configuration file, which will be automatically loaded on reentry into the Executive program. You may tailor "default.cfg" to best fit your usage.

2.1.4.3 Selecting About brings up a dialog box with the current version number of the Executive program.

2.1.4.4 The Exit option immediately terminates the Executive program.

## 2.1.5 Setup Menu

The Setup menu contains the following pull-down options:

- Control Algorithm
- Sensor Calibration
- User Units
- Communications

---

<sup>1</sup>Its fastest to simply double-click on the desired file icon.

2.1.5.1 Setup Control Algorithm allows the user to write control algorithms, compile them, and implement them via the DSP based controller. Figure 2.1-2 shows the control algorithm dialog box. The *Sampling Period* field allows the user to change the servo period " $T_s$ " in multiples of 0.000884 seconds (e.g. 0.000884, 0.001768 etc.). The *minimum* sampling period is 0.000884 seconds (1.1 KHz). Note that if the user servo algorithm is long and/or complex the code execution may run longer than the sampling period. In such a case a *Servo Time Limit Exceeded* condition will occur which will cause the control loop to be automatically opened by the Real-time Controller. The user may then either *increase* the sampling time or edit the user servo algorithm to *reduce* execution time. In general, the combination of high sampling frequency, complex control laws and sinusoidal or sine sweep trajectories (which also require significant real-time processing) may cause the *Servo Time Limit Exceeded* condition.

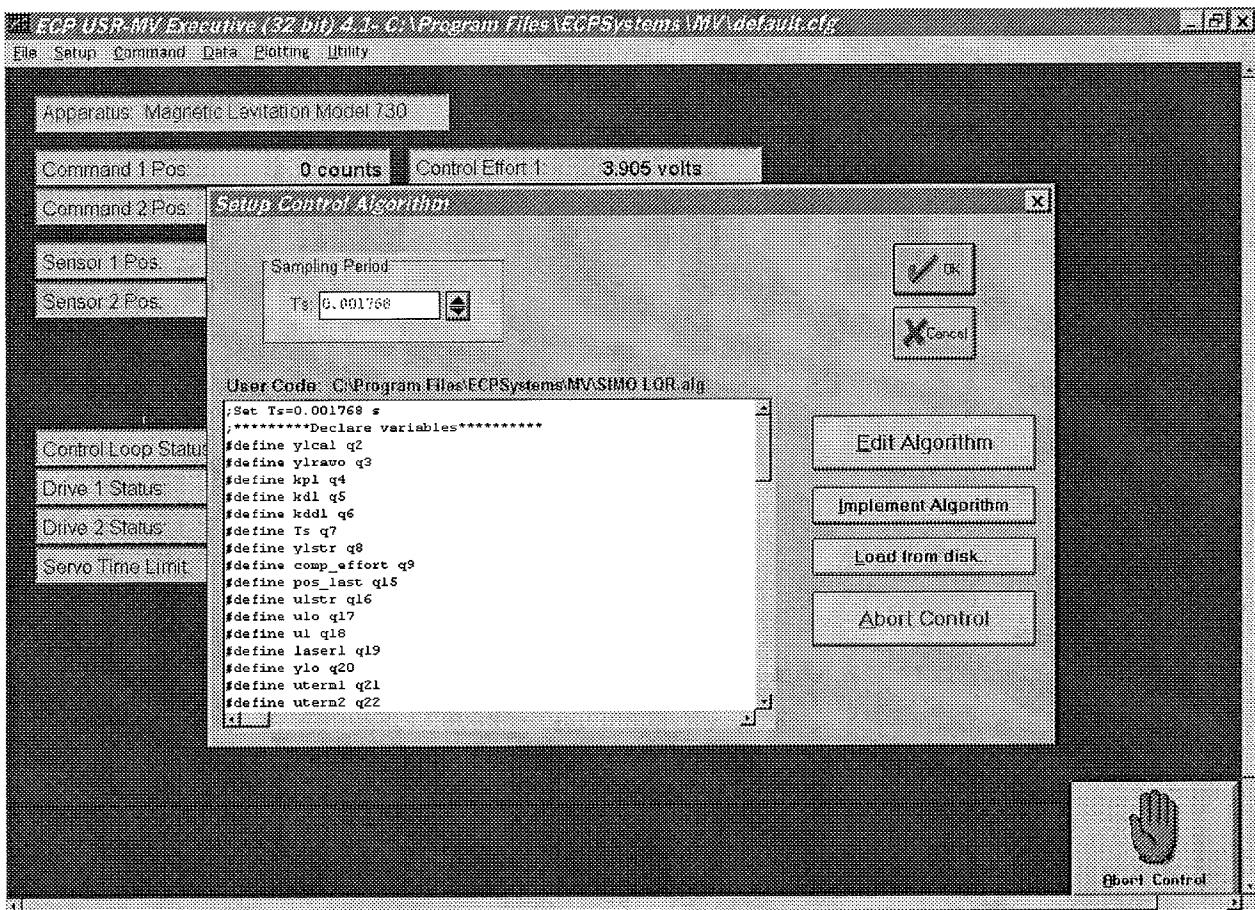


Figure 2.1-2. Setup Control Algorithm Dialog Box

The User Code view box displays the latest user servo algorithm edited or loaded from the disk. You cannot edit the algorithm via the view box. You may however browse it via the arrow keys.

Edit Algorithm opens up the ECPUSR Editor where servo algorithms may be created by the user. The Editor's features are described below.

Implement Algorithm downloads the user's code from the Editor buffer to the Real-time Controller. Load from Disk allows the user to bring into the Editor previously saved user written algorithms saved as \*.ALG files. The existing algorithm in the Editor will be automatically overwritten.

Once Edit Algorithm is invoked, the Editor Screen is displayed (see Figure 2.1-3). The user may then enter the servo algorithm text according to the structural format described in the next section. Under the File menu within the Editor Screen, the following options are available:

- New
- Load
- Save
- Save as ...
- Save changes and quit
- Cancel

```

C:\Program Files\Educational Control Products\EDSR32 - Mult Variab...
File Edit
;*****define user variables *****

#define kw2 q2      ;
#define kq4 q3      ;|
#define kw4 q4      ;
#define ka2 q5      ;
#define past_pos2 q6 ;
#define past_pos4 q7
#define past_cmd q16
#define uval q22    ; unscaled control_effort
#define gain q15   ; scaling gain
#define dac2 m127
#define speed_cmd q17
#define Ts q19
#define enc2_dif q8
#define enc2_rate q9
#define enc4_dif q18
#define enc4_rate q20

#define kp q30      ; proportional gain
#define kd q31      ; derivative gain gimbal 4 (output)
#define past_pos3 q32 ; need three memory terms
#define uvall q34   ; unscaled control_effort
#define gain1 q35   ; scaling gain
#define dac1 m100
#define enc3_dif q36
#define past_cmd1 q37
;*****Initialize variables*****
Ts=.00884
past_pos1=0      ; initialize memory term
past_cmd=0
past_pos4=0

```

**Figure 2.1-3. Control Algorithm Editor Window**

The New option enables the user to edit a completely new control algorithm text.

Load allows the user to bring into the Editor previously saved user written algorithms save as \*.ALG files. The existing algorithm in the Editor will be automatically deleted.

Save as... provides the user with the ability to save the Editor's content with a new or different name on the disk.

Save changes and quit saves the changes made in the latest editing session and returns to the Control Algorithm dialog box.

Cancel all returns to the Control Algorithm dialog box without updating the previous version of the user code with the changes made in the latest editing session.

**NOTE:** The Editor is not case sensitive. E.g. "kp" or "Kp" or "KP" will be treated as the same variable.

### 2.1.5.1.2 Structure of User Written Control Algorithm

Any user written control algorithm code is made up of three distinct sections:

- the definition segment
- the variable initialization segment
- the servo loop or real-time execution segment

When the ECPUSR program downloads the algorithm to the Real-time Controller, it uses the definition segment to assign internal q-variables (**q1..q100**) to the user variables defined in the definition segment. The variable initialization segment is to be used to assign values to the servo gains and/or coefficients that either remain constant or must be assigned some initial value prior to running the servo loop code. The servo loop code segment starts with a "**begin**" statement and ends with an "**end**" statement. All the legitimate assignment and condition statements between these two statements will be executed every Sample Period provided that the execution time of the code does not exceed the Sample Period. (If this occurs the "Servo Time **Limit Exceeded**" condition will be shown on the background screen and the loop will be opened up. The user may then reduce the complexity of the algorithm between the "**begin**" and the "**end**" statements. Alternatively, if appropriate, the Sample Period may be increased.)

#### 2.1.5.1.2.1 Definition Segment

There are 100 *general variables* **q1** to **q100** that may be used by the user for gains, controller coefficients, and controller variables. These variables are used internally by the Real-time Controller. They are stored and manipulated as 48-bit floating point numbers. For users' convenience, the **#define** statement may be used to assign to the q-variables text labels appropriate for particular servo algorithms. For example:

```
#define gain_1 q2 ;assigns to the variable q2 the name gain_1
or
#define past_pos1 q6 ;assigns to the variable q6 the name past_pos1
```

Note that all the text beyond the comment delimiter ";" are ignored by the Real-time Controller and are provided for annotation by the user. Also the special variables  $q10$ ,  $q11$ ,  $q12$  and  $q13$  may be acquired via the Data menu along with other standard collectable data. This feature allows the users to inspect critical internal variables of their specific control algorithms in addition to the command and sensor feedback positions and control effort(s).

In addition to the 100 general variables, there are eight *global variables* as follows:

```

cmd1_pos
cmd2_pos
sensor1_pos
sensor2_pos
control_effort1
control_effort2

```

The first six of these global variables are predefined to contain the instantaneous commanded positions and actual encoder positions 1 to 4 respectively. The value assigned to the `control_effort` global variable by the user algorithm will be used as the control effort (i.e. output to the DAC → servo amplifier → motor) for that particular servo cycle - see example below.

Important Note: The above global variable names must not be used as general variable names any definition statement.

#### 2.1.5.1.2.2 Initialization Code Segment

In this segment the user may predefine the algorithm constants (gains and controller coefficients) and initial values of the algorithm's variables. For example:

```

gain_1=0.78 ;assigns to gain_1 the value of 0.78
gain_1=0.78*3/gain_3 ;requires gain_3 to be previously defined
past_pos1=0.0 ; initialize the past position cell

```

Note that the above three examples assume that the `#define` statement was used in the Definition Code segment to relate one general variable  $q_i$  ( $i=1\dots 100$ ) to the text variables such as `gain_1`. Also, all initialization and constant variable assignments should be done outside the servo loop code segment to maximize the servo loop execution speed.

#### 2.1.5.1.2.3 Servo Loop Segment

This segment starts with a "`begin`" statement and terminates with an "`end`" statement. All the legitimate assignment and condition statements between these two statements will be executed every *Sample Period* provided that the execution of the code does not exceed the *Sample Period*.

#### An Example

Consider the following control algorithm program:

```

;***** Definition code segment*****
#define kpf q1 ;define kpf as general variable q1
#define k1 q2 ;define k1 as general variable q2 and so on
#define k2 q3
#define k3 q4
#define k4 q5
#define past_pos1 q6
#define past_pos2 q7
#define dead_band q8

;***** Initialization code segment *****
past_pos1=0 ;initialize algorithm variables
past_pos2=0
kpf=0.93 ;initialize constant gains etc.
k1=0.78
k2=3.14
k3=0.156
k4=7.58
dead_band=100 ;the size of dead band is set at 100 counts

;***** Servo Loop Code Segment *****
begin
    if ((abs(enc1_pos) !> dead_band)
        k1=k1+0.5
    else
        k1=0.78
    endif
    control_effort1=kpf*cmd1_pos-k1*enc1_pos-k3*enc2_pos-
k3*(enc1_pos- past_pos1)-k4*(enc2_pos-past_pos2)
    past_pos1=enc1_pos
    past_pos2=enc2_pos
end

```

This is a simple state feedback algorithm with a conditional gain change based on the size of encoder 1 position. First the required general variables are defined. Next, their values are initialized. And finally between the "begin" and the "end" statement the servo loop code is written which is intended to run every *Sample Period*. In addition, the "if" and the "else" statements are used to change the value of the k1 gain according to the *absolute* ("abs") value of encoder 1 instantaneous position.

### 2.1.5.1.3 Language Syntax For Real-time Algorithms

#### 2.1.5.1.3.1 Constants

Constants are numerical values not subject to change. They are treated internally as 48-bit floating point numbers (32-bit mantissa, 12-bit exponent) by the Real-time Controller. They must be entered in decimal format as the following examples suggest:



```

1234
3
03      ;(leading zero OK)
-27.656
0.001
.001    ;(leading zero not required)

```

#### 2.1.5.1.3.2 Variables

There are 100 general variables **q1** to **q100** that may be used by the user for gains, controller coefficients, control variables and program flow flags. Examples:

```

q1=10.05 ;(assign to the variable q1 the values of 10.05)
q2=q1*0.05;(assign to the variable q2 the value of q1*0.05)

```

Note that when the define statement is used in the Definition Code segment to give names to the appropriate q variable then the above two examples may be written as:

```

#define gain_1 q1
#define gain_2 q2
.
.
.
gain_1=10.05
gain_2=gain_1*0.05

```

#### 2.1.5.1.3.3 Arithmetic Operators

The four standard arithmetic operators are: **+**, **-**, **\***, **/**. The standard algebraic precedence rules apply: multiply and divide are executed before add and subtract, operations of equal precedence are executed from left to right, and operations inside parentheses are executed first.

There is an additional **"%"** modulo operator, which produces the resulting remainder when the value in front of the operator is divided by the value after the operator. This operator is particularly useful for dealing with roll over condition of command or actual positions.

#### 2.1.5.3.4 Functions

Functions perform mathematical operations on constants or expressions to yield new values. The general format is:

```
{function name} ({expression})
```

The available functions are **SIN**, **COS**, **TAN**, **ASIN**, **ACOS**, **ATAN**, **SQRT**, **LN**, **EXP**, **ABS**, and **INT**.

Note: All trigonometric functions are evaluated in units of radians (not degrees).

<b>SIN</b>	This is the standard trigonometric sine function
Syntax	<b>sin</b> ( {expression} )
Domain	All real numbers
Domain Units	radians
Range	-1.0 to 1.0
Range units	none
Possible Errors	N/A
<b>COS</b>	This is the standard trigonometric cosine function
Syntax	<b>cos</b> ( {expression} )
Domain	All real numbers
Domain Units	radians
Range	-1.0 to 1.0
Range units	none
Possible Errors	N/A
<b>TAN</b>	This is the standard trigonometric tangent function
Syntax	<b>tan</b> ( {expression} )
Domain	All real numbers except +/- pi/2, 3pi/2, ...
Domain Units	radians
Range	-1.0 to 1.0
Range units	none
Possible Errors	divide by zero on illegal domain. (may return max. value.
<b>ASIN</b>	This is the inverse sine (arc sine) function with range +/- pi/2
Syntax	<b>asin</b> ( {expression} )
Domain	-1.0 to 1.0
Domain Units	none
Range	-pi/2 to pi/2
Range units	radians
Possible Errors	illegal domain
<b>ACOS</b>	This is the inverse cosine (arc cosine) function with its range reduced to 0 to pi.
Syntax	<b>acos</b> ( {expression} )
Domain	-1.0 to 1.0
Domain Units	none
Range	0 to pi
Range units	radians
Possible Errors	illegal domain
<b>atan</b>	This is the inverse tangent function (arc tangent).
Syntax	<b>atan</b> ( {expression} )
Domain	all reals
Domain Units	none
Range	-pi/2 to pi/2
Range units	radians
Possible Errors	N/A

<b>LN</b>	This is the natural logarithm function (log base e)
Syntax	<code>ln ( {expression} )</code>
Domain	All positive numbers
Domain Units	none
Range	all real
Range units	none
Possible Errors	illegal domain
<b>EXP</b>	This is the exponentiation function ( $e^x$ ). Note: to implement the $y^x$ function, use $e^{x \ln(y)}$ instead. A sample expression would be <code>exp (q1 * ln (q2) )</code> to implement $q2^{q1}$ .
Syntax	<code>exp ( {expression} )</code>
Domain	All real numbers
Domain Units	none
Range	all positive reals
Range units	none
Possible Errors	N/A
<b>SQRT</b>	This is the square root function
Syntax	<code>sqrt ( {expression} )</code>
Domain	All non-negative real numbers
Domain Units	free
Range	All non-negative real numbers
Range units	free
Possible Errors	illegal domain
<b>ABS</b>	This is the absolute value function
Syntax	<code>abs ( {expression} )</code>
Domain	All real numbers
Domain Units	free
Range	all non-negative reals
Range units	free
Possible Errors	N/A
<b>INT</b>	This is a truncation function which returns the greatest integer less than or equal to the argument, e.g. ( <code>int (2.5) =2</code> , <code>int (-2.5)=-3</code> )
Syntax	<code>int ( {expression} )</code>
Domain	All real numbers
Domain Units	free
Range	integers
Range units	free
Possible Errors	none

#### 2.1.5.1.3.5 Expressions

An expression is a mathematical construct consisting of constants, variables and functions. connected by operators. Expressions can be used to assign a value to a variable or as a part of condition (see below). A constant may be used as an expression, so if the syntax calls for

{expression}, a constant may be used as well as a more complicated expression. Examples of expressions:

```
#define variable_1 q1
#define variable_2 q2
512
variable_1
variable_1 -variable_2
1000*cos(variable_1*variable2)
abs(cmd1_pos)
```

Note that the "define" statements should be used to define the user variables in terms of q variables. In additions, these variables should have been initialized.

#### 2.1.5.1.3.6 Variable Value Assignment Statement

This type of statement calculates and assigns a value to a variable. Example:

```
control_effort1= kp*(cmd1_pos-sensor1_pos)
```

#### 2.1.5.1.3.7 Comparators

A comparator evaluates the relationship between two values (constants or expressions). It is used to determine the truth of a condition in Servo Loop Code segment via the **--IF** statement (see below). The valid comparators are:

```
=      (equal to)
!=     (not equal to)
>      (greater than)
!>    (not greater than; less than or equal to)
<      (less than)
!<    (not less than, greater than or equal to)
```

Note: the comparators  $\leq$  and  $\geq$  are not valid. The comparators  $!>$  and  $!<$  , respectively, should be used in their place.

#### 2.1.5.1.3.8 Conditional Statement

In the Servo Loop Code segment between the **begin** and **end** statements, the **if** statement may be for conditional execution of parts of the control algorithm. The format is as follows:

```
if ( {condition})
    valid expression
    :
    :
endif
```

In addition, the **else** statement may be used as follows:

```
if ( {condition})
    valid expression
    . . .
else
    valid expression
    . . .
endif
```

If the {condition} is true, with no statement following on the line of the **if** statement, the Real-time Controller will execute all subsequent statements on the following lines down to the next **endif** or **else** statements.

A {condition} is made up of two expressions compared via the comparators described above. For Example:

```
if (control_effort1>16000)
    control_effort1=16000
endif
```

or,

```
If (sensor2_pos>1.1*deadband)
    kp=1.0
else
    kp=1.2
endif
```

The {condition} statement may be in a **compound** form using the **and** and the **or** operators as follows:

```
If (sensor2_pos>1.1*deadband and sensor1_pos<sensor2_pos)
    kp=1.0
else
    kp=1.2
endif
```

Note that the condition in the **if** statement line must be surrounded by parenthesis. Also avoid nesting more than three layers of **if** statements.

2.1.5.2 The Setup Sensor Calibration dialog box, shown in Figure 2.1-4, allows the user to select to use the raw sensor counts or to use calibrated sensor data. The calibration function is shown and parameter values are entered to perform the linearization/calibration of each sensor<sup>1</sup>. When *Use Raw Sensor Counts* is selected, the Sensor 1 Pos and Sensor 2 Pos fields in the background screen displays raw sensor counts and the global variables **sensor1\_pos** and **sensor2\_pos** are the instantaneous raw sensor counts. Similarly when *Calibrate Sensor* is selected these signals are the calibrated/linearized values. The *Apply Thermal Compensation* option provides for thermal correction of the laser output. This is done through temperature feedback to the ADC and background compensation in the DSP board. Normally this option should be selected.

---

<sup>1</sup> Default sensor calibration coefficients are supplied with each unit. These should be updated with unit -specific values according to the procedure of Section 6.1

Note: If *Reset Controller* is selected (Utility menu - see Section 2.1.9) the sensor mode is automatically set to *Raw Sensor Counts*. In order to use calibrated sensor values, the user must enter Setup Sensor Calibration and select *Calibrate Sensor* and then OK.

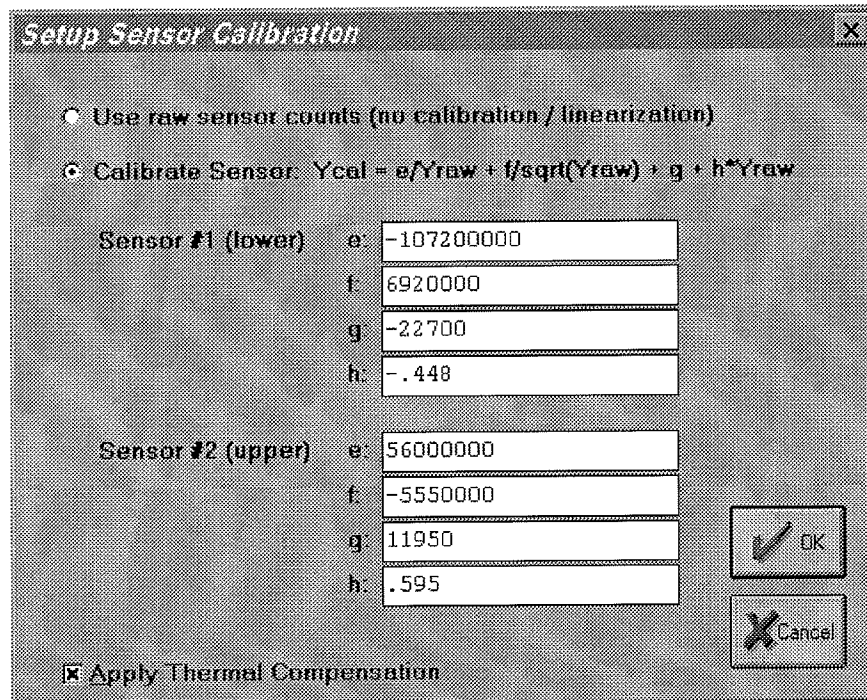


Figure 2.1-4. The Setup Sensor Calibration Dialog Box

2.1.5.3 The User Units dialog box provides various choices of angular or linear units for several ECP systems. For Model 730, the units are fixed. They are “counts” for the two laser position sensors and optical encoder of the optional turntable and for the commanded positions, units of rpm for the displayed value of the optional turntable disk speed, and units of volts for the displayed control effort values. For Model 730, there are 32,768 counts per 10 V. of the sensor output if *Use Raw Sensor Counts* is selected in Setup Sensor Calibration – see Section 2.1.5.2. If *Calibrate Sensor* is selected, the scaling is nominally 10,000 counts per cm.

2.1.5.4 The Communications dialog box is usually used only at the time of installation of the real-time controller. The choices are serial communication (RS232 mode) or PC-bus mode – see Figure 2.1-4. If your system was ordered for PC-bus mode of communication, you do not usually need to enter this dialog box unless the default address at 528 on the ISA bus is conflicting with your PC hardware. In such a case consult the factory for changing the appropriate jumpers on the controller. If your system was ordered for serial communication (v. direct installation of the DSP board on the PC bus) the default baud rate is set at 34800 bits/sec. To change the baud rate consult factory for changing the appropriate jumpers on the controller. You may use the Test Communication button to check data exchange between the PC and the real-time controller. This should be done after the correct choice of Communication Port has been made. The Timeout should be set as follows:

ECP Executive For Windows with Pentium Computer: Timeout  $\geq$  50,000  
ECP Executive For Windows with 486 Computer: Timeout  $\geq$  20,000

### 2.1.6 Command Menu

The Command menu contains the following pull-down options

Trajectory . . .  
Disturbance . . .  
Execute . . .

2.1.6.1 The Trajectory Configuration dialog boxes (see Figure 2.1.-5) provide a selection of trajectories or reference inputs with which the apparatus can be maneuvered. These become the “commanded position” signals while they are being executed. There are two such boxes, one for each of the two available system inputs.

Impulse  
Step  
Ramp  
Parabolic  
Cubic  
Sinusoidal  
Sine Sweep  
User Defined

A mathematical description of these is given later in Section 4.1.

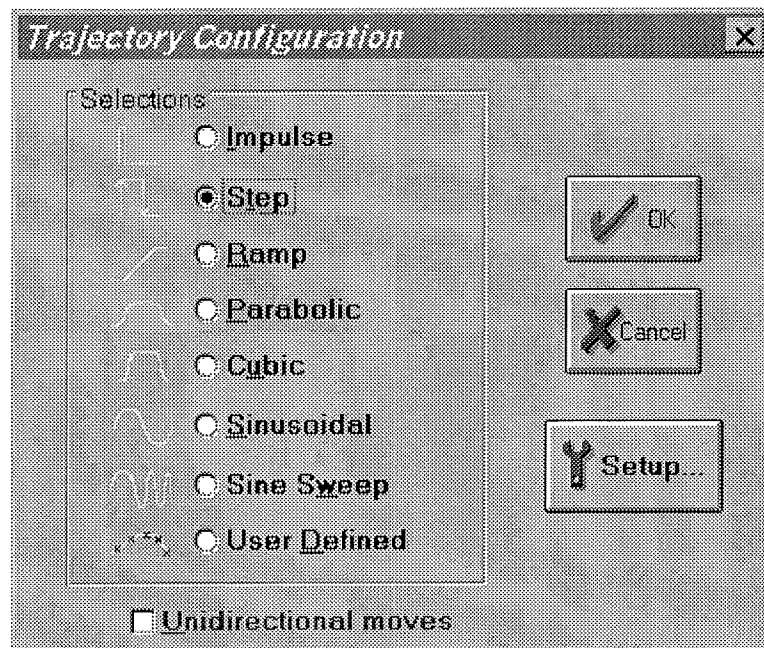


Figure 2.1-5. The Trajectory Configuration Dialog Box

All *geometric* input shapes – Impulse through Cubic – may be specified as Unidirectional or Bi-directional. Examples of these shape types are shown in Figure 2.1-6. The bi-directional option should normally be selected whenever the system is configured to have a *rigid body mode* (one that rotates freely) and the system is operating open loop. This is to avoid excessive speed or displacement of the system.

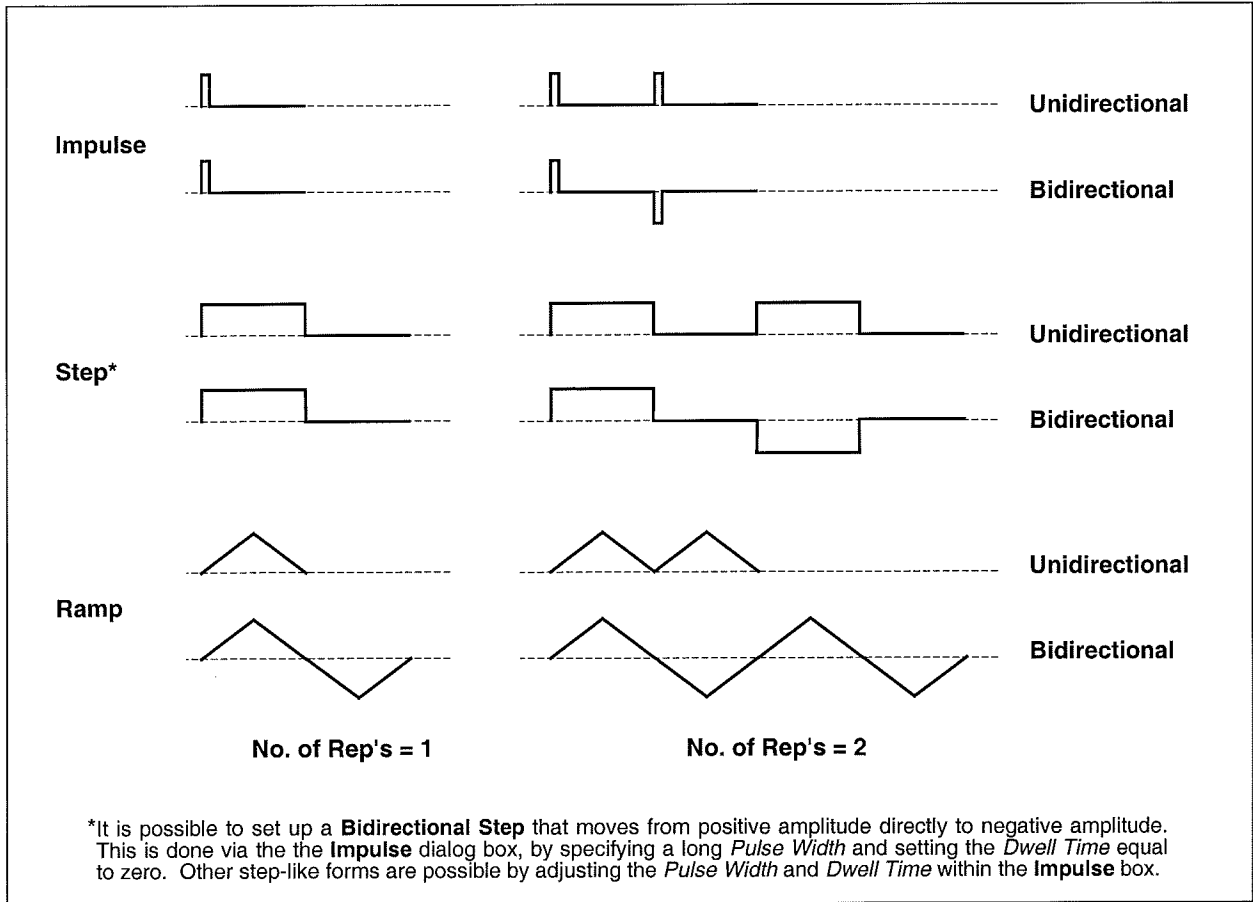


Figure 2.1-6. Example Geometric Trajectories



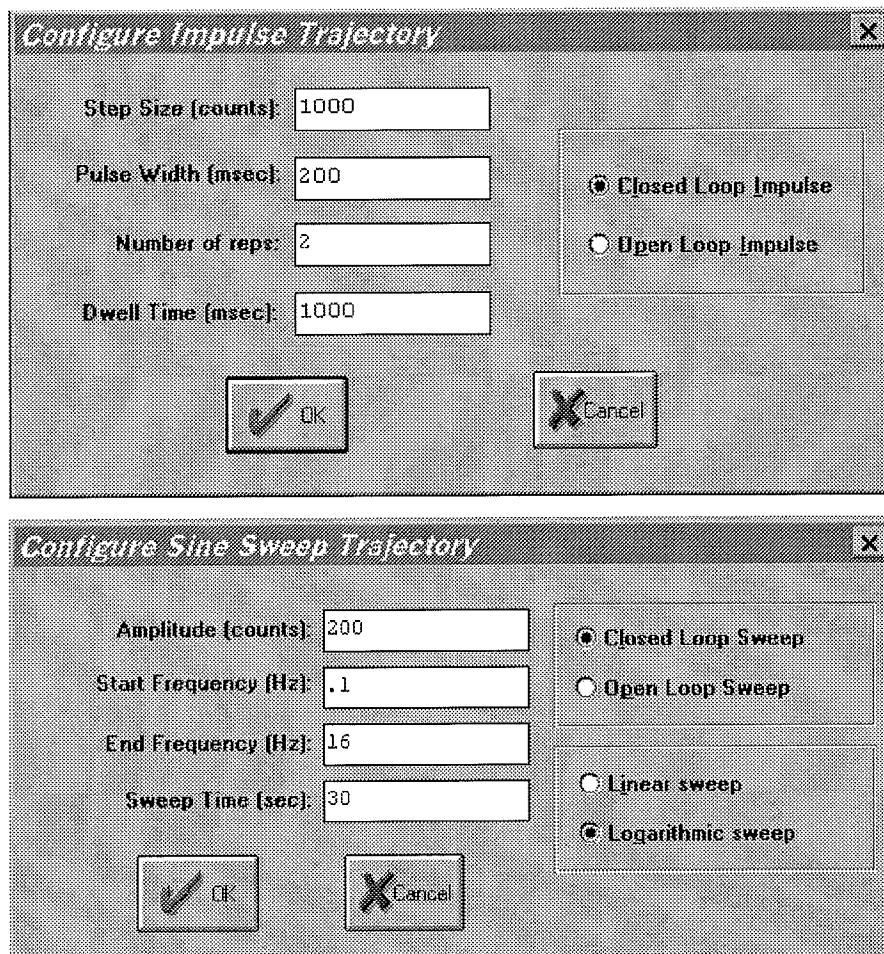


Figure 2.1-7. Example "Setup Trajectory" Dialog Boxes

The Impulse dialog box provides for specification of amplitude, impulse duration, dwell duration, and number of repetitions.<sup>1</sup> The Step box supports specification of step amplitude, duration, and number of repetitions with the dwell duration being equal to the step duration. The Ramp shape is specified by the peak amplitude, ramp slope (units of amplitude per second), dwell time at amplitude peaks, and number of repetitions. The Parabolic shape is specified by the peak amplitude, ramp slope (units of  $\text{ampl./s}$ ), acceleration time, dwell time at amplitude peaks, and number of repetitions. In this case, the acceleration (units of  $\text{ampl./s}^2$ ) results from meeting the specified amplitude, slope, and acceleration period. The Cubic shape is specified by the peak amplitude, ramp slope (units of  $\text{ampl./s}$ ), acceleration time, dwell time at amplitude peaks, and number of repetitions. In this case, the "jerk" (units of  $\text{ampl./s}^3$ ) results from meeting the specified amplitude, slope, and acceleration period where the acceleration increases linearly in time until the specified velocity is reached.

<sup>1</sup>If the specified "impulse" duration becomes long enough, the resulting torque becomes more step-like than impulsive. Thus the Setup Impulse dialog box may also be used for Step input shapes where the dwell (zero excitation) period may be specified independently of the step duration.

Note that the only difference between a parabolic input and a cubic one is that during the acceleration/deceleration times, a constant acceleration is commanded in a parabolic input and a constant jerk is commanded in the cubic input. Of course, in a *ramp* input, the commanded acceleration/deceleration is infinite at the ends of a commanded displacement stroke and zero at all other times during the motion. For safety, there is an apparatus-specific limit beyond which the Executive program will not accept the amplitude inputs for each geometric shape.

The Sinusoidal dialog box provides for specification of input amplitude, frequency and number of repetitions.

The Sine Sweep dialog box accepts inputs of amplitude, start and end frequencies (units of Hz), and sweep duration. Both linear and logarithmic frequency sweeps are available. The linear sweep frequency increase is linear in time. For example a sweep from 0 Hz to 10 Hz in 10 seconds results in a one Hertz per second frequency increase. The logarithmic sweep increases frequency logarithmically so that the time taken in sweeping from 1 to 2 Hz for example, is the same as that for 10 to 20 Hz when a single test run includes these frequencies. There is an apparatus-specific amplitude limit beyond which the Executive will not accept the inputs.

Important Note #1: The logic as to whether to include the Sine Sweep plotting options is driven by the currently selected shape under Trajectory 1. Sine Sweep must be selected in the Trajectory 1 Configuration dialog box in order for these options to be available in Setup Plot. E.g. if a sine sweep is desired for Trajectory 2 only, the user should also select Sine Sweep for Trajectory 1, and then select *Execute Trajectory 2 Only* under Execute – see Section 2.1.6.3. Conversely, if Trajectory 2 is not to be a sine sweep, then Sine Sweep should not be selected under Trajectory 1.

Important Note #2: A large open loop<sup>1</sup> amplitude combined with a low frequency may result in an over-power condition in the corresponding drive power circuits. This will be detected by the real-time controller and cause the system to shut down (see Section 2.3). In addition, high frequency, large amplitude tests may result in a shut down or *Limit Exceeded* condition. Any of these conditions will cause the test to be aborted and one or more of the System Status displays in the Background Screen to indicate Limit Exceeded. To run the test again you should reduce the input shape amplitude and then Reset Controller (Utility menu). Then select *Calibrate Sensor* (via Setup Sensor Calibration – if this is the intended sensor mode) and re-Implement a stabilizing controller (via Setup Control Algorithm). In general, all trajectories that generate either too large a deflection, or otherwise cause excessive actuator power will cause this condition – see Safety, Section 2.3. For a further margin of safety, there is an apparatus-specific amplitude limit beyond which the Executive program will not accept the inputs.

The User Defined shape dialog box provides an interface for the specification of any input shape created by the user. In order to make use of this feature the user must first create an ASCII text file with an extension ".trj" (e.g. "random.trj"). This file may be accessed from any directory or disk drive using the usual file path designators in the filename field or via the Browse button. If the file exists in the same directory as the Executive program, then only the file name should be entered. The content of this file should be as follows:

---

<sup>1</sup> Open loop v. closed loop operations depend on the algorithm created and implemented by the user.

The first line should provide the number of points specified. The maximum number of points is 923. This line should not contain any other information. The subsequent lines (up to 923) should contain the consecutive set points. For example to input twenty points equally spaced in distance one can create a file called "example.trj" using any text editor as follows

```
20
5
10
15
20
25
30
35
40
45
50
55
60
65
70
75
80
85
90
95
100
```

The segment time, which is a time between each consecutive point, can be changed in the dialog box. For example if a 100 milliseconds segment time is selected, the above trajectory shape would take 2 seconds to complete ( $100 \times 20 = 2000$  ms). The minimum segment time is restricted to five milliseconds by the real-time controller. When Open Loop is selected, the units of the trajectory are assumed to be DAC bits (e.g. +16383 = 4.88 V, +16383 = -4.88 V) In Closed Loop mode, the units are assumed to be the position displacement units specified under User Units (Setup menu). The shape may be treated by the system as a discrete function exactly as specified, or may be smoothed by checking the Treat Data As Splined box. In the latter case the shapes are cubic spline fitted between consecutive points by the real-time controller. Obviously a user-defined shape may also cause an over-current condition in the drive if the segment time is too long or the distance between the consecutive points is too great.

2.1.6.3 The Execute dialog box (see Figure 2.1-7) is entered after the trajectories are selected. Here the user commands the system to execute the currently specified trajectory(s). The user may

select either Normal or Extended Data Sampling. Normal Data Sampling acquires data for the duration of the executed trajectory. Extended Data Sampling acquires data for an additional 5 seconds beyond the end of the maneuver. Both the Normal and Extended boxes must be checked to allow extended data sampling. (For the details of data gathering see Section 2.1.7.1, Setup Data Acquisition). Either *Trajectory 1*, or *Trajectory 2*, or both may be selected for execution, and a time delay between them may be specified as shown in the figure.

After selecting the trajectory and data gathering options, the user normally selects Run. The real-time controller will begin execution of the specified trajectory(s). Once finished, and provided the Sample Data box was checked, the data will be uploaded from the DSP board into the Executive (PC memory) for plotting, saving and exporting. At any time during the execution of the trajectory or during the uploading of data, the process may be terminated by clicking on the Abort button. If the process is aborted before the trajectory has completed, the associated *Commanded Position(s)* (reference input(s)) will be fixed at its current value(s). Finally, if one trajectory has a longer duration than the other does, the maneuver and data collection will continue until completion of the longer trajectory.

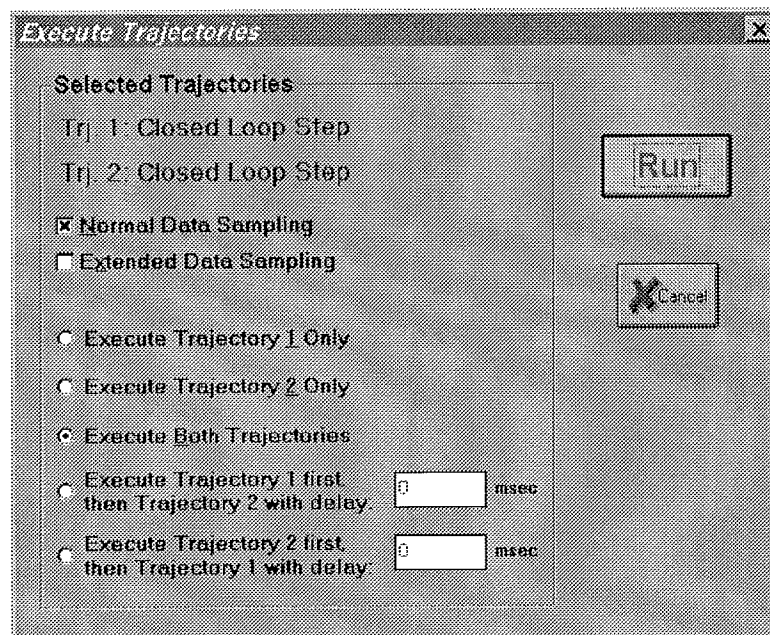


Figure 2.1-7. The Execute Dialog Box

### 2.1.7 Data Menu

The Data menu contains the following pull-down options

- Setup Data Acquisition
- Upload Data
- Export Raw Data

2.1.7.1 Setup Data Acquisition allows the user to select one or more of the following data items to be collected at a chosen multiple of the servo loop closure sampling period while running any of the trajectories mentioned above – see Figures 2.1-8 and 4.1-1:

- Commanded Position 1
- Commanded Position 2
- Sensor 1 Position
- Sensor 2 Position
- Control Effort 1 (output 1 to the servo loop or the open loop command)
- Control Effort 2 (output 2 to the servo loop or the open loop command)
- Variable Q10<sup>1</sup>
- Variable Q11
- Variable Q12
- Variable Q13

Here the user adds or deletes any of the above items by first selecting the item, then clicking on Add Item or Delete Item. The user must also select the data gather sampling period in multiples of the servo period. For example, if the sample time ( $T_S$  in the Setup Control Algorithm) is 0.00442 seconds and you choose 5 for your gather period here, then the selected data will be gathered once every fifth sample or once every 0.0221 seconds. Usually for trajectories with high frequency content (e.g. *Step*, or high frequency *Sine Sweep*), one should choose a low data gather period (say 4 ms). On the other hand, one should avoid gathering more often (or more data types) than needed since the upload and plotting routines become slower as the data size increases. The maximum available data size (no. variables x no. samples) is 33,586.

2.1.7.2 Selecting Upload Data allows any previously gathered data to be uploaded into the Executive. This feature is useful when one wishes to switch and compare between plotting previously saved raw data and the currently gathered data. Remember that the data is automatically uploaded into the executive whenever a trajectory is executed and data acquisition is enabled. However, once a previously saved plot file is reloaded into the Executive, the currently gathered data is overwritten. The Upload Data feature allows the user to bring the overwritten data back from the real-time controller into the Executive.

2.1.7.3 The Export Raw Data function allows the user to save the currently acquired data in a text file in a format suitable for reviewing, editing, or exporting to other engineering/scientific packages such as Matlab®.<sup>2</sup> The first line is a text header labeling the columns followed by bracketed rows of data items gathered. The user may choose the file name with a default extension of ".text" (e.g. `lqrstep.txt`). The first column in the file is sample number, the next is time, and the

---

<sup>1</sup> Q10 through Q13 are special real-time algorithm variables that may be specified for data acquisition. Any values (e.g. control constants or dynamic variables) may be acquired, exported, or plotted by assigning Q10 through Q13 to be equal to their value in the algorithm.

<sup>2</sup>The bracketed rows end in semicolons so that the entire file may be read as an array in Matlab by running it as a script once the header is stripped i.e. the script should be: `<array name>= [exported data file]`. Variable values over time are the columns of this array; the rows are the variable value set at successive sample numbers.

remaining ones are the acquired variable values. Any text editor may be used to view and/or edit this file.

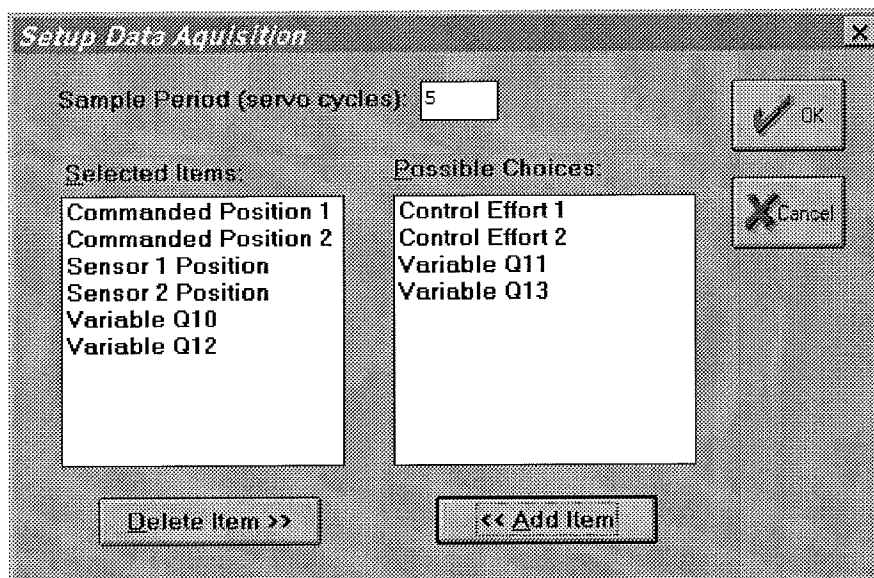


Figure 2.1-8. The Setup Data Acquisition Dialog Box

### 2.1.8 Plotting Menu

The Plotting menu contains the following pull-down options

- Setup Plot
- Plot Data
- Axis Scaling
- Print Plot
- Load Plot Data
- Save Plot Data
- Real Time Plotting

2.1.8.1 The Setup Plot dialog box (see Figure 2.1-9) allows up to four acquired data items to be plotted simultaneously – two items using the left vertical axis and two using the right vertical axis units. In addition to the acquired raw data, you will see in the box plotting selections of velocity and acceleration for the position and input variables acquired. These are automatically generated by numerical differentiation of the data during the plotting process. Simply click on the item you wish to add to the left or the right axis and then click on the Add to Left Axis or Add to Right Axis buttons. You must select at least one item for the left axis before plotting is allowed – e.g. if only one item is plotted, it must be on the left axis. You may also change the plot title from the default one in this dialog box.

Items for comparison should appear on the same axis (e.g. commanded vs. encoder position) to ensure the same axis scaling and bias. Items of dissimilar scaling or bias (e.g. control effort in volts and position in counts) should be placed on different axes.

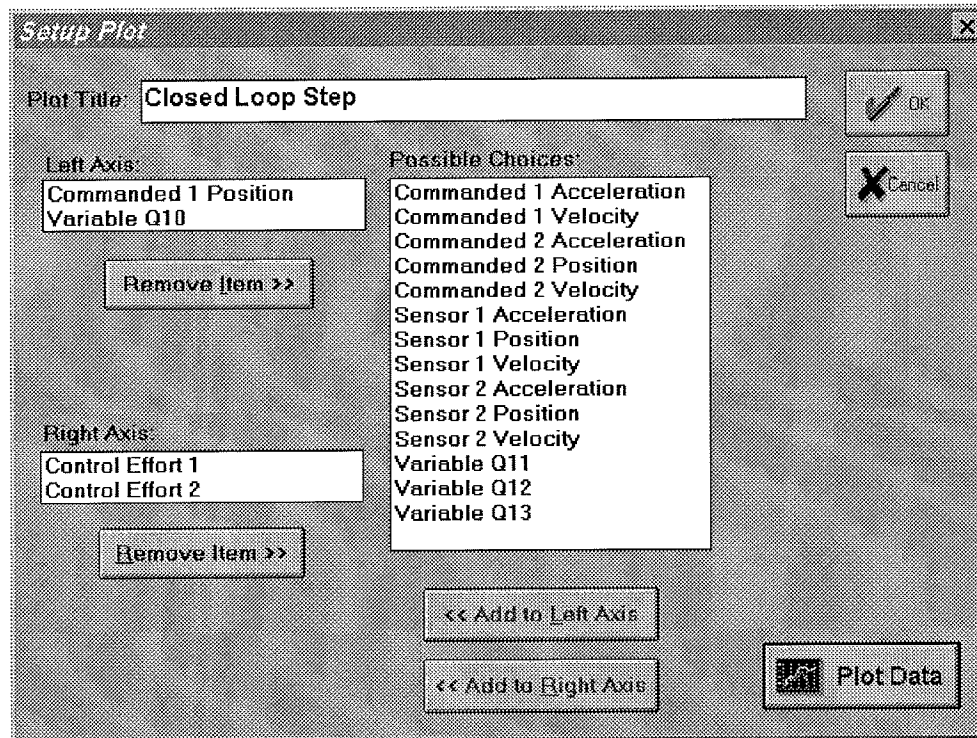


Figure 2.1-9 The Setup Plot Dialog Box

When the current data (either from the last test run or from a previously saved and loaded plot file) is from a Sine Sweep input, several data scaling/transformation options appear in the Setup Plot box. These include the presentation of data with horizontal coordinates of time, linear frequency (i.e. the frequency of the input) or logarithmic frequency. The vertical axis may be plotted in linear or Db (i.e.  $20 \cdot \log_{10}(\text{data})$ ) scaling. In addition, the Remove DC Bias option subtracts the average of the final 50 data points from the data set of each acquired variable. This generally gives a more representative view of the frequency response of the system, particularly when plotting low amplitude data in Db. Examples of sine sweep (frequency response) data plotted using two of these options are given later in Figure 3.2-3.

**Important Note:** The logic as to whether to include the Sine Sweep plotting options is driven by the currently selected shape under Trajectory 1. Sine Sweep must be selected in the Trajectory 1 Configuration dialog box in order for these options to be available in Setup Plot. E.g. if a sine sweep is desired for Trajectory 2 only, the user should also select Sine Sweep for Trajectory 1, and then select *Execute Trajectory 2 Only* under Execute – see Section 2.1.6.3. Conversely, if Trajectory 2 is not to be a sine sweep, then Sine Sweep should not be selected under Trajectory 1.

2.1.8.2 Plot Data generates a plot of the selected items. A typical plot as seen on screen is shown in Figure 2.1-10.

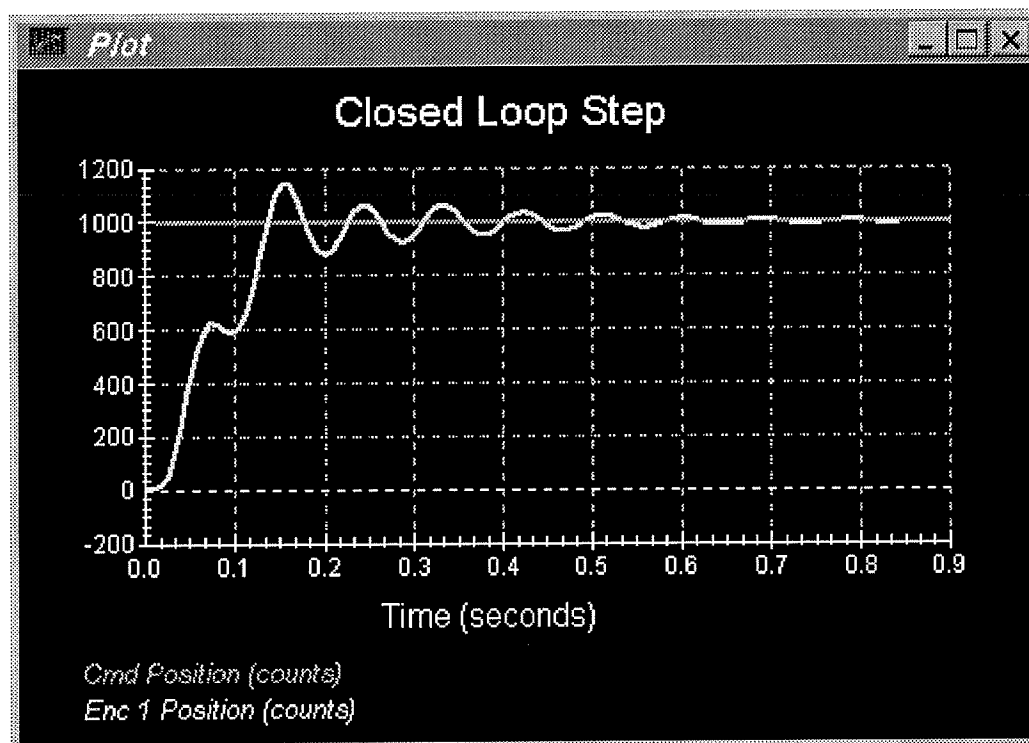


Figure 2.1-10. A Typical Plot Window

2.1.8.3 Axis Scaling provides for scaling or “zooming” of the horizontal and vertical axes for closer data inspection – both visually and for printing. This box also provides for selection or deselection of grid lines and data point labels. When Real-time Plotting is used (see Section 2.1.8.7), the data sweep / refresh speed and amplitudes may be adjusted via the Axis Scaling box.

2.1.8.4 The Print Data option provides for printing a hard copy of the selected plot on the current PC system printer. The plots may be resized prior to printing to achieve the desired print format

2.1.8.5 The Load Plot Data dialog box enables the user to bring into the Executive previously saved ".plt" plot files. Note that such files are not stored in a format suitable for use by other programs. For this purpose the user should use the Export Raw Data option of the Data menu. The ".plt" plot files contain the sampling period of the previously saved data. As a result, after plotting any previously saved plot files and before running a trajectory, you should check the servo loop sampling period  $T_s$  in the Setup Control Algorithm dialog box. If this number has been changed, then correct it. Also, check the data gathering sampling period in the Data Acquisition dialog box, this too may be different and need correction.



2.1.8.6 The Save Plot Data dialog box enables the user to save the data gathered by the controller for later plotting via Load Plot Data. The default extension is ".plt" under the current directory. Note that ".plt" files are not saved in a format suitable for use by other programs.

2.1.8.7 The Setup Real Time Plotting dialog box enables the user to view data in real time as it is being generated by the system. Thus the data is seen in an oscilloscope-like fashion. Unlike normal (off-line) plotting, real-time plotting occurs continuously whether or not a particular maneuver (via Execute, Command Menu) is being executed<sup>1</sup>. The setup for real-time plotting is essentially identical to that for normal plotting (see Section 2.1.8.1). Because the expected data amplitude is not known to the plotting routine, the plot will first appear with the vertical axes scaled to full scale values of 1000 of the selected variable units. These should be rescaled to appropriate values via Axis Scaling. The sweep or data refresh rate may also be changed via Axis Scaling when real-time plotting is underway. A slow sweep rate is suitable for slow system motion or when a long data record is to be viewed in a single sweep. The converse generally holds for a fast sweep rate.

The data update rate is approximately 50 ms and is limited by the PC/DSP board communication rate. Therefore, frequency content above about 5 Hz is not accurately displayed due to numerical aliasing. The real-time display however is very useful in visually correlating physical system motion with the plotted data. The data acquired via the data acquisition hardware (for normal plotting) may be sampled at much higher rates (up to 1.1 KHz) and hence should be used when quantitative high-speed measurements are desired.

### 2.1.9 Utility Menu

The Utility menu contains the following pull-down options:

- Configure Optional auxiliary DACs
- Jog Position
- Zero Position
- Reset Controller
- Rephase Motor
- Down Load Controller Personality File

2.1.9.1 The Configure Auxiliary DACs dialog box (see Figure 2.1-11) enables the user to select various items for analog output on the two optional analog channels in front of the ECP Control Box. Using equipment such as an oscilloscope, plotter, or spectrum analyzer the user may inspect the following items continuously in real time:

- Commanded Position 1
- Commanded Position 1

---

<sup>1</sup> In some cases, you will need to "drag" the Executing Input Shape box out of the way to see the plot during the maneuver. This is practical for longer duration maneuvers.

Sensor 1 Position  
 Sensor 2 Position  
 Control Effort 1  
 Control Effort 2  
 Variable Q10  
 Variable Q11  
 Variable Q12  
 Variable Q13

The scale factor which divides the item can be less than 1 (one). The DAC's analog output is in the range of +/- 10 volts corresponding to +32767 to -32768 counts. For example to output the commanded position for a sine sweep of amplitude 2000 counts you should choose the scale factor to be 0.061 ( $2000/32767=0.061$ ) This gives close to full +/- 10 volt reading on the analog outputs. In contrast, if the numerical value of an item is greater than +/- 32767 counts, for full-scale reading, you must choose a scale factor of greater than one. Note that the above items are always in counts (not degrees or radians) within the real time controller and since the DAC's are 16-bit wide, +32767 counts corresponds to +9.999 volts, and -32768 counts corresponds to -10 volts.

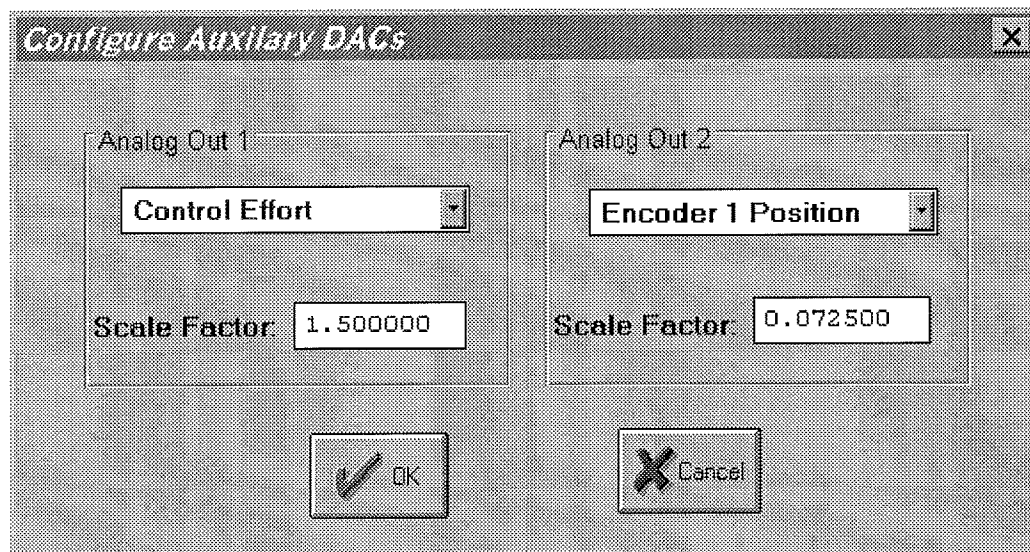


Figure 2.1-11. The Configure Auxiliary DACs Dialog Box

2.1.9.2 The Jog Position option is not used in the Model 730 system.

2.1.9.3 The Zero Position option is not used in the Model 730 system.

2.1.9.4 The Reset Controller option allows the user to reset the real-time controller. Upon Power up and after a reset activity, the loop is closed with zero gains and there it behaves in the same way as in the open loop state with zero control effort. Thus the user should be aware that even though the Control Loop Status indicates "closed loop", all of the gains are zeroed after a Reset. In order to implement (or re implement) a controller you must go to the Setup Control Algorithm box.

Important Note: If *Reset Controller* is selected the sensor mode is automatically set to *Raw Sensor Counts*. In order to use calibrated sensor values, the user must enter Setup Sensor Calibration and select *Calibrate Sensor* and then OK – see Section 2.1.5.2.

2.1.9.5 The Zero Position option is not used in the Model 730 system.

2.1.9.6 The Download Controller Personality File is an option that should not be used by most users. In a case where the real-time controller irrecoverably malfunctions, and after consulting ECP, a user may download the personality file if a ".pmc" file exists. In the case of Model 730, this file is named "m730xxx.pmc". This downloading process takes a few seconds.

## 2.2 Electromechanical Plant

### 2.2.1 Design Description

The plant, shown in Figure 2.2-1, consists of upper and lower drive coils that produce a magnetic field in response to a DC current. One or two magnets travel along a precision ground Pyrex<sup>®</sup> glass guide rod. By energizing the lower coil, a single magnet is levitated through a repulsive magnetic force. As current in the coil increases, the field strength increases and the levitated magnet height is increased. For the upper coil, the levitating force is attractive. Two magnets may be controlled simultaneously by stacking them on the glass rod. (See instructions later in this section). The magnets are of an ultra-high field strength rare earth (NeBFe) type and are designed to provide large levitated displacements to clearly demonstrate principles of levitation and motion control.

Two laser-based sensors measure the magnet positions. The lower sensor is typically used to measure a given magnet's position in proximity (8 cm. range) to the lower coil, and the upper one for proximity to the upper coil. This proprietary ECP sensor design utilizes light amplitude measurement and includes special circuitry to desensitize the signal to stray ambient light and thermal fluctuations. The sensor operation is described in detail in Section 4.5.

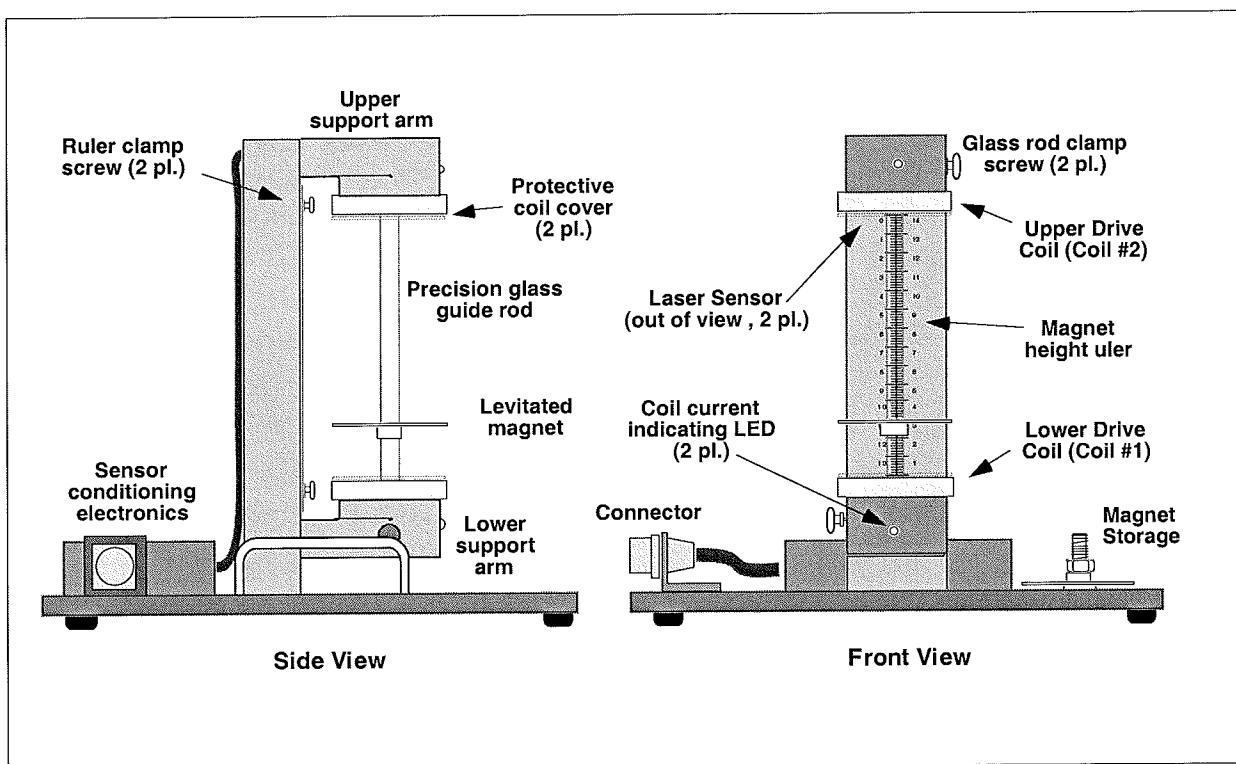


Figure 2.2-1. MagLev Apparatus

### 2.2.2 Instructions For Using & Changing Magnets

The following guidelines and procedures should be followed in using, changing, cleaning, and storing the magnets

#### **Important Notes:**

- 1) The high intensity magnets must be kept at least 20 cm. (8 in.) from each other and from other objects of ferromagnetic material. Failure to do so could cause the magnet and other body to be rapidly attracted and collide thereby damaging the magnet. It is highly recommended that the provided post for magnet storage be used when a magnet is not installed about the glass rod. It is particularly important to secure the magnets during the operation of installing and removing two magnets on the glass rod. (See instructions below)
- 2) The magnets should be kept a minimum of 40 cm. (16 in) from cathode ray tubes (CRT's, e.g. computer monitors and televisions) and from magnetic media such as floppy and hard disks. Failure to do so could result in permanent magnetic distortion and in the case of media, loss of data.
- 3) The white diffuse reflective surface of the magnets must be kept clean for proper function of the laser sensor. (See instructions below)
- 4) The glass rod must be kept clean to avoid contamination of the magnetic bushing dry lubrication. Do not handle the glass rod with bare hands – hand oils will lead to degradation of the lubrication. (See instructions below)
- 5) The magnets must be secured at all times either via installation on the glass rod or the magnet storage post.
- 6) The plastic safety clip should always be used to support the magnet prior to implementing attractive levitation via the upper coil / sensor. (See instructions below)

#### Magnet Orientation

- 1) For single magnet use, the magnetic north pole should be face up (see Figure 2.2-2)
- 2) For dual magnet use, the lower magnet should be as stated above, and the upper magnet should have its south pole facing upward.

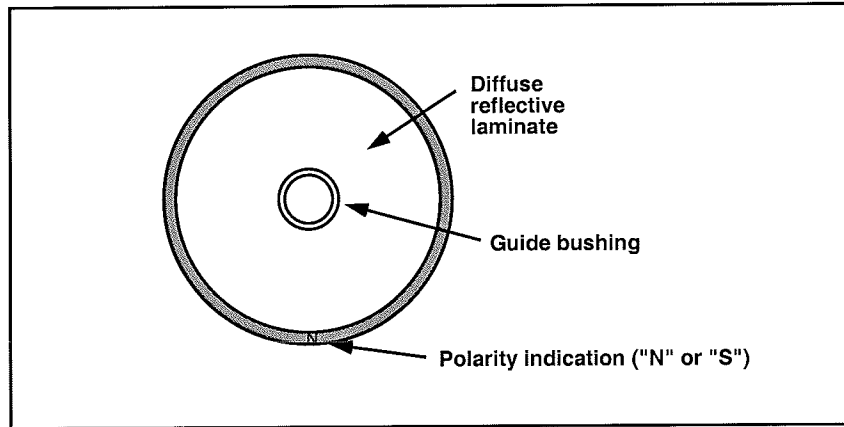


**Figure 2.2-2. Magnet Details**

### Changing The Magnets

- 1) Remove the glass rod by loosening the glass rod clamp screws and place it in a safe location. Use clean gloves or cloth to handle the glass rod.
- 2) Follow the above guidelines on magnet orientation.
- 3) If one magnet is to be installed, simply place it on the lower drive coil approximately centered. Lower the glass rod, threading it through the hole in the upper support arm, then through the magnet bushing and through the lower support arm. Make certain that the rod is securely held; it can be inadvertently chipped or broken if dropped or allowed to fall freely through the support arm holes. Lightly tighten the glass rod clamp screws
- 4) If two magnets are to be installed, it is advisable to have an assistant. One person should hold the magnets against the upper and lower support arms and approximately centered. The other person should gently lower the glass rod through the hole in the upper support arm and sequentially through each magnet. Be cautious in this step that the magnets are not free to suddenly become attracted and collide with each other. Be sure the magnet polarities are correct so that the magnets are repelling each other. Continue threading the glass rod through the lower support arm and lightly tighten the rod clamp screws. Gradually release the magnets verify that the upper magnet rests in equilibrium at approximately 8 cm above the lower one.

### Using The Safety Clip

- 1) The provided plastic safety clip should always be used to support the magnet prior to implementing attractive levitation via the upper coil/sensor – See Figure 2.2-3. It should also be kept at a location just beyond the anticipated travel range once levitation has been successfully implemented. The reason for using the clip is to position the magnet to within capture range for implementing closed loop control and to prevent excessive control effort due to the system attempting to levitate the magnet beyond its practical range.
- 2) Once a stable controller has been implemented and all intended trajectories have been successfully executed, the clip may be removed from the glass post if desired for demonstration purposes. It should be replaced whenever a controller is subsequently implemented or a different trajectory is executed.

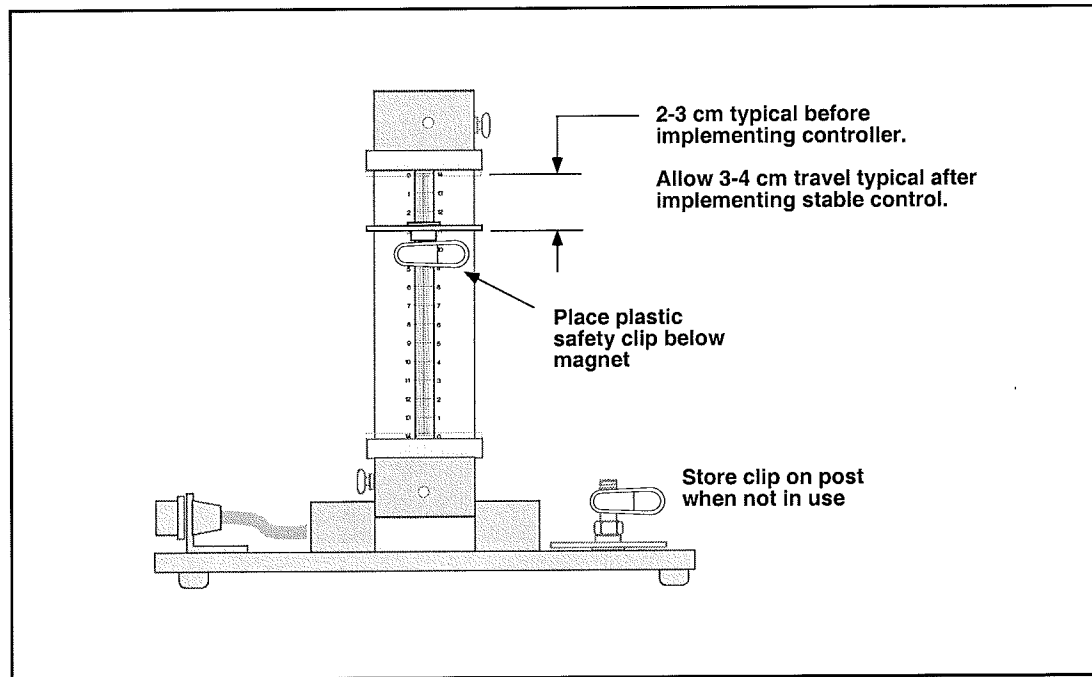


Figure 2.2-3. Using The Safety Clip

### Storing Magnets

- 1) Store any magnet not being used in the provided magnet storage area by placing it over the threaded bolt and tightening fully but lightly the 1/2-inch nut.
- 2) When storing two magnets, make certain that they are oriented with their north poles toward each other (See Figure 3.2-2). I.e. they should repel each other. Be cautious that the magnets are not free to suddenly become attracted and collide with each other.

### Handling and Cleaning Magnets

- 1) It is best to minimize handling of the magnets and thereby keep their optical and lubricated surfaces as clean as possible and avoid collision with other magnetically attracted objects. Magnets should be handled by their edges only with clean hands or by using clean non-contaminating gloves.
- 2) To clean the white laminate surface, use a clean soft white plastic eraser for “dry” contamination. Remove the eraser debris with a clean cloth or brush. For oily contamination, use alcohol or a non-foaming detergent such as window cleaner or household spray cleaner. Apply alcohol or cleaner to a clean cloth and wipe the white surface. Do not spray or soak the surface and make sure that no cleaner enters the center bushing. If cleaner is used, wipe afterwards using clean water.
- 3) The inner bushing surface should never require cleaning if properly handled. If this surface is inadvertently contaminated and friction between it and the glass rod has

measurably increased, clean the surface with a clean cotton swab and alcohol. Try to use a rolling motion between the swab and the bushing surface rather than a wiping one. This will minimize the removal of dry lubricant from the porous sintered bronze material.

#### Handling and Cleaning the Glass Rod

- 1) It is best to minimize handling of the glass rod and thereby keep it free of contaminants and avoid damage. The rod should never be handled with bare hands.
- 2) To clean the rod, use alcohol or window cleaner and a clean cloth to wipe the surface. If cleaner is used, wipe afterwards using clean water.



## 2.3 Safety

The following are safety features of the system and cautions regarding its operation. This section must be read and understood by all users prior to operating the system. If any material in this section is not clear to the reader, contact ECP for clarification before operating the system.

**Important Notice: In the event of an emergency, control effort should be immediately discontinued by pressing the red "OFF" button on front of the control box.**

### 2.3.1 Hardware

A relay circuit is installed within the Control Box that automatically turns off power to the Box whenever the real-time Controller (within the PC) is turned on or off. Thus for the PC bus version<sup>1</sup> of the real-time Controller the user should turn on the computer prior to pressing on the black ON switch. This feature is implemented to prevent uncontrolled motor response during the transient power on/off periods. The power to the Control Box may be turned off at any time by pressing the red OFF switch.

Although not recommended, it will not damage the hardware to apply power to the Control-Box even when the PC is turned off. However, doing so does not result in current activation as the motor current amplifier will be disabled. The *amplifier enable* signal input to the Control Box is connected to the real-time Controller via the 60-pin flat ribbon cable. This input operates in a normally closed mode. When power to the real-time Controller is off, this input becomes open which in turn disables the motor amplifier.

The recommended procedure for **start up** is as follows:

**First :** Turn on the PC with the real-time Controller installed in it.

**Second:** Turn on the power to Control Box (press on the black switch).

The recommended **shut down** procedure is:

**First:** Turn off the power to the Control Box.

**Second:** Turn off the PC..

**FUSES:** There are two 3.0A 120V slow blow fuses within the Control Box. One of them is housed at the back of the Control Box next to the power cord plug. The second one is inside the box next to the large blue colored capacitor.

---

<sup>1</sup>The majority of this section (2.3.1) pertains to the PC bus installation of the real-time controller. For the controller box/RS-232 version, the control box should generally be powered on before entering the executive software.

### 2.3.1.1 Energizing coils

The actuator coils designed to accommodate high drive currents momentarily but as any power dissipating device has limitations as to its long-term power dissipation capability. When purchase

**Important Note:**

**Do not exceed the following coil excitation durations for the current values given (each drive coil):**

**>10.0 Amperes: Never**

**≤10.0 Amperes: < 5 sec.**

**≤ 4.0 Amperes: <20 sec.**

**≤ 1.0 Amperes: indefinite**

When purchase as a complete system, the amplifiers are set to provide a maximum current of 4 amps.

### 2.3.2 Software

The Limit Exceeded indicator of the Controller Status display indicates that one or more of the following conditions have occurred:

High transient control effort (coil current)

High coil power over a sustained period (Excessive thermal build-up)

Servo time limit exceeded

The Limit Exceeded condition may occur whenever a non-stabilizing controller is implemented, an excessively large or rapid trajectory is executed, or the levitation distance is too great. The real-time Controller continuously monitors the above limiting conditions in its background routine (intervals of time in-between higher priority tasks). When one of these conditions occurs, the real-time Controller opens up the control loop with a zero current command sent to the actuator. The Limit Exceeded indicator stays on until a new set of (stabilizing) control gains are downloaded to the real-time Controller via the Implement Algorithm button of the Setup Control Algorithm dialog box, or a new trajectory is executed via the Command menu. Obviously the new trajectory must have parameters that do not cause the Limit Exceeded condition.

If the servo time limit is exceeded, the real-time computation burden has exceeded the capability of the processor. You should either increase the sampling period, reduce the complexity of the real-time algorithm, or reduce the computational requirements of the trajectory (i.e. sine sweep and sinusoidal are most complex).

Also included is a *watchdog timer*. This subsystem provides a fail-safe shutdown to guard against software malfunction and under-voltage conditions. The use of the watchdog timer is transparent to the user. This shutdown condition turns on the red LED on the real-time Controller card, and will cause the control box to power down automatically. You may need to cycle the power to the

PC in order to reinitialize the real-time Controller should a watchdog timer shutdown occur.

### 2.3.3 Safety Checking The Controller

While it should generally be avoided, in some cases it is instructive or necessary to manually contact the apparatus when a controller is active. This should always be done with caution and never in such a way that clothing or hair may be caught in the apparatus. By staying clear of the mechanism when it is moving or when a trajectory has been commanded, the risk of damage or injury is greatly reduced. Being motionless, however, is not sufficient to assure the system is safe to contact. In some cases an unstable controller may have been implemented but the system may remain motionless until perturbed – then it could react violently.

In order to eliminate the risk of injury in such an event, you should always safety check the controller prior to physically contacting the system. This is done by lightly grasping a slender, light object with no sharp edges (e.g. a ruler without sharp edges or an unsharpened pencil) and using it to lightly perturb the magnet up and down. If the magnet does not move rapidly or oscillate then it may be manually contacted – but with caution. This procedure must be repeated whenever any user interaction with the system occurs (either via the Executive Program or the Controller Box) if the mechanism is to be physically contacted again.

### 2.3.4 Warnings

**WARNING #1:** Stay clear of and do not touch any part of the mechanism while it is moving, while a trajectory has been commanded (via Execute, Command menu), or before the active controller has been safety checked – see Section 2.3.3.

**WARNING #2:** The following apply at all times except when motor drive power is disconnected (consult ECP if uncertain as to how to disconnect drive power):

- a) Stay clear of the mechanism while wearing loose clothing (e.g. ties, scarves and loose sleeves) and when hair is not kept close to the head.
- b) Keep head and face well clear of the mechanism.

**WARNING #3:** Verify that the magnets and glass rod are secured per section 2.2 of this manual prior to powering up the Control Box or transporting the mechanism.

**WARNING #4:** Do not take the cover off or physically touch the interior of the Control Box unless its power cord is unplugged (first press the "Off" button on the front panel) and the PC is unpowered or disconnected.

**WARNING #5:** The power cord must be removed from the Control box prior to the replacement of any fuses.

2.3.5 Important Notes:

- 1) The high intensity magnets must be kept at least 20 cm. (8 in.) from each other and from other objects of ferromagnetic material. Failure to do so could cause the magnet and other body to be rapidly attracted and collide thereby damaging the magnet. It is highly recommended that the provided post for magnet storage be used when a magnet is not installed about the glass rod. It is particularly important to secure the magnets during the operation of installing and removing two magnets on the glass rod. (See Section 2.2)
- 2) The magnets should be kept a minimum of 40 cm. (16 in) from cathode ray tubes (CRT's, e.g. computer monitors and televisions) and from magnetic media such as floppy and hard disks. Failure to do so could result in permanent magnetic distortion and in the case of media, loss of data.
- 3) The magnets must be secured at all times either via installation on the glass rod or the magnet storage post.
- 4) The plastic safety clip should always be used to support the magnet prior to implementing attractive levitation via the upper coil / sensor. (See Section 2.2)

### 3. Start-up & Self-guided Demonstration

This chapter provides an orientation "tour" of the system for the first time user. In Section 3.1 certain hardware verification steps are carried out. In Section 3.2 a self-guided demonstration is provided to quickly orient the user with key system operations and Executive program functions.

All users must read and understand Section 2.3, Safety, before performing any procedures described in this chapter.

#### 3.1 Hardware Setup Verification

At this stage it is assumed that

- a) The ECP Executive program has been successfully installed on the PC's hard disk (see Section 2.1.2).
- b) The actual printed circuit board (the real-time Controller) has been correctly inserted into an empty slot of the PC's extension (ISA) bus.
- c) The supplied 60-pin flat cable is connected between the J11 connector (the 60-pin connector) of the real-time Controller and the JMACH connector of the Control Box.
- d) The supplied 16-pin flat cable is connected between the J7 connector (the 16-pin connector near the center of the board) of the real-time Controller and the JANA connector of the Control Box.
- e) The other supplied cable is connected between the Control Box and the MagLev apparatus;
- f) The apparatus has a single magnet installed with the north magnet pole facing upward (small black "N" label facing upward). Use caution in handling the magnets and glass rod as per the instructions of Section 2.2.2.
- g) You have read the safety Section 2.3. All users must read and understand that section before proceeding.

Please check the cables again for proper connections.

##### 3.1.1 Hardware Verification (For PC-bus Installation)

**Step 1:** Switch off power to both the PC and the Control Box. Install one magnet on the glass rod with its *north* pole facing upward per the instructions of Section 2.2.2. Use caution when handling the magnets and rod per the notes in that section.

**Step 2:** With power still switched off to the Control Box, switch the PC power on. Enter the ECP program by double clicking on its icon. You should see the Background Screen (see Section 2.1.3). Turn on power to the control box - you should see its green LED illuminate<sup>1</sup>. Verify that the magnet is stationary (not levitated) and neither of the coil current LED's on the apparatus are

---

<sup>1</sup> It is necessary for the Control Box to be powered in order for the sensors to operate.

illuminated. The laser sensors should illuminate the magnet in a thin red line on both the upper and lower magnet surfaces.

Gently raise the magnet by hand (touch the edges only with clean hands and do not obstruct the laser beam). You should observe a change in the Sensor 1 counts. (The sensor is in an uncalibrated mode. The Sensor 1 value should equal  $30000 \pm 5000$  counts and decrease as you lift the magnet. The Sensor 2 value should equal  $0 \pm 2000$  counts and increase as you lift the magnet.) The Control Loop Status should indicate "OPEN" and the Drive 1 Status, Drive 2 Status, and Servo Time Limit should all indicate "OK". If this is the case skip Step 3 otherwise proceed to Step 3.

**Step 3:** If the ECP program cannot find the real-time Controller (a pop-up message will notify you if this is the case), try the Communication dialog box under the Setup menu. Select PC-bus at address 528, and click on the test button. If the real-time Controller is still not found, try increasing the time-out in increments of 5000 up to a maximum of 80000. If this doesn't correct the problem, switch off power to your PC and then take its cover off. With the cover removed check again for the proper insertion of the Controller card. Switch the power on again and observe the two LED lights on the Controller card. If the green LED comes on, all is well; if the red LED is illuminated, you should contact ECP for further instructions. If the green LED comes on, turn off power to your PC, replace the cover and turn the power back on again. Now go back to the ECP program and you should see the positions change on the background screen as you gently raise the magnet.

This completes the hardware verification procedure. Please refer again to Section 2.3 for future start up and shut down procedures.

## 3.2 Demonstration of ECP Executive Program

This section walks the user through the salient functions of the system. By following the instructions below you will actually implement controllers, maneuver the system through various trajectories, and acquire and plot data.

**Step 1: Loading A Configuration File.** It is assumed that you have completed the hardware verification of the previous section and that you have entered the Executive program and that the Controller Box is powered up. Now enter the File menu, choose Load Setting and select the file `default.cfg`. This configuration file is supplied on the distribution diskette and should have been copied into the ECP directory by now. In fact, it would have been loaded into the Executive automatically (see Section 2.1.4.1) upon startup. This particular `default.cfg` file contains the controller gain parameters and other trajectory, data gathering and plotting parameters specifically saved for the activities within this section.

Note again that this file has been created to operate with a plant with a single magnet, with its north pole facing upward)

**Step 2: Setting Up The Sensor.** Enter the Setup menu and choose Setup Sensor Calibration. You should see Calibrate Sensor and Apply Thermal Compensation selected. You should also see numerical values for the coefficients  $e, f, g,$  and  $h$  for both *Sensor #1* and *Sensor #2*. Exit by selecting OK. This effectively implements the sensor calibration. You should now see the Sensor 1 position equal to  $0 \pm 3000$  counts and see the position change in an approximately linear fashion as you raise the magnet (clean hands, edges only!) > the scale factor is nominally 10000 counts / cm.

**Step 2: Implementing The Controller.** Enter the Setup menu and choose Control Algorithm. You should see the sampling time  $T_s = 0.001768$  seconds, and the controller "SISO Comp Lower.alg" loaded. (The file name and its path should appear in the "User Code" field of the dialog box.) This controller was designed to compensate for the sensor and actuator nonlinearities, then close a simple linear control loop about the linearized plant<sup>1</sup> of the lower sensor/coil system.

Within the Setup Control Algorithm dialog box, select Implement Algorithm. The control law is now downloaded to the real-time Controller and immediately implemented. You should see the magnet levitate approximately 2 cm. above the lower limit of travel. If so congratulations! You have implemented closed loop magnetic levitation. Use a ruler or clean eraser end of a pencil to lightly perturb the magnet and verify that the control is stable. (see Sect. 2.3.3, "Safety Checking The Controller") If the magnet has not levitated, click on the Implement Algorithm button again until it is.

You may wish to view the real-time algorithm at this point. It contains a nonlinear actuator inversion function, the control law, and output formatting statements and follows the syntax and formatting protocols of the Executive USR routines as described in Section 2.1.5. You may do so by scrolling the viewer within Setup Control Algorithm. In order to get a closer view you may select Edit Algorithm. This brings you inside the editor in which you will later write real-time

---

<sup>1</sup> The furnished algorithm and `Default.cfg` files utilize nominal values of the sensor and actuator linearization/calibration parameters. For more accurate results, the user should calibrate these according to the instructions of Section 6.1.

routines. If you have entered the editor, select *Cancel* in the *File* menu to exit (do not select *Save Changes and Quit* in case some inadvertent change has been made that would adversely affect the routine).

**Step 3: Setting Up Data Acquisition.** Enter the Data menu and select Setup Data Acquisition. In this box make sure that the following four items are selected: *Commanded Position 1 & 2*, and *Variables Q10 & Q12*<sup>1</sup>. *Data sample period* should be 5 which means that data will be collected every fifth servo cycle (in this case every  $5 \times 0.001768 = 0.00884$  seconds).

**Step 4: Executing A Step Input Trajectory & Plotting.** Enter the Command menu and select Trajectory 1. In this box verify that *Unidirectional moves* is not checked; select Step and then Setup. You should see *Step Size* = 15000, *Dwell Time* = 1000 ms and *Number of Repetitions* = 2. If not, change the values to correspond to this parameter set. Exit this box and go to the Command menu. This time select Execute and with *Normal Data Sampling* and *Execute Trajectory 1 Only* selected, “Run” the trajectory. You should see a step move of approximately 1.5 cm, a dwell of 1 second, a return to nominal position, then a negative-going step of 1 second duration<sup>2</sup>. Wait for the data to be uploaded from the Real-time Controller to the Executive program running on the PC. Now enter the Plotting menu and choose Setup Plot. Select *Commanded Position 1* and *Variable Q10* as data to be plotted on the left axis, then select Plot Data.

You should see a plot similar to the one shown in Figure 3.2-1. There may be some differences in the details of the response for your particular system due to the use of nominal rather than unit-specific sensor and actuator nonlinearity compensation.

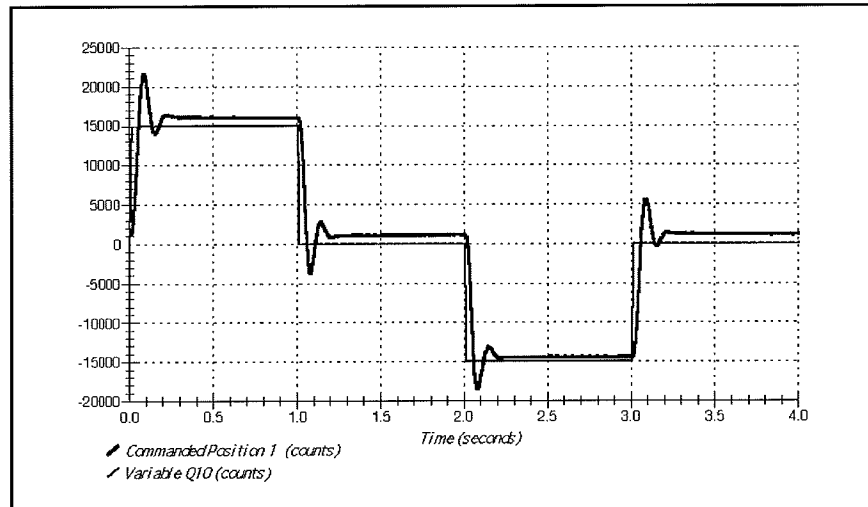


**Figure 3.2-1 Step Response at Lower Magnet (Repulsive levitation)**

**Step 5: Tracking Response.** Return to Trajectory 1, verify that *Unidirectional moves* is not checked, then select Ramp and then Setup to enter the *Ramp* dialog box. You should see *Distance* = 15000 counts, *Velocity* = 30000 counts/s, *Dwell Time* = 500 ms and *Number of Repetitions* = 2. If not, change the values to this set. Exit this box and go to the Command menu. Again select

<sup>1</sup> These variables are the sensor position data offset to the nominal levitated height of the magnet.

<sup>2</sup> The response has been made underdamped (significant overshoot) by design for the purposes of this demonstration.



Execute and with *Normal Data Sampling* and *Execute Trajectory 1 Only* selected, “Run” the trajectory. You should have noticed the ramp move (constant velocity) of 1.5 cm. followed by a dwell, a negative ramp return move and a second cycle of the same. Select Plot Data from the Plotting menu. You should see a plot similar to that of Figure 3.2-2. You may save the ramp response under `anyname.plt` using the Save Plot Data option. Any plot data thus saved may be reloaded from the disk using the Load Plot Data option for future inspection, plotting or printing. To print simply choose the Print Plot menu option. Alternatively, any set of collected data may be exported as an ASCII text file by the use of the Export Data option of the Data menu.

Now close all plot windows.

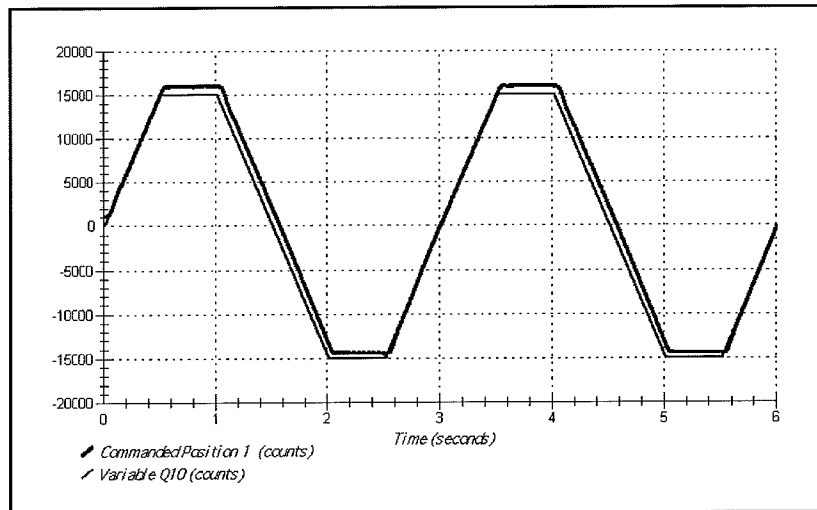


**Figure 3.2-2 Ramp Tracking Response at Lower Magnet**

**Step 7: Frequency Response.** Again enter Trajectory 1 and select Sine Sweep then Setup. You should see the *Amplitude = 5000 counts*, *End Frequency= 30 Hz*, *Start Frequency= 1 Hz*, *Sweep Time = 29.5 sec.*, and *Logarithmic Sweep* selected. Again, if different, change the values to correspond to this set. Again select Execute and with *Normal Data Sampling* and *Execute Trajectory 1 Only* selected, “Run” the trajectory.

While running this trajectory, you should notice sinusoidal motion with increasing frequency for about thirty seconds. At roughly 6 Hz you should see a resonance followed by high frequency attenuation. Now enter the Plotting menu and choose Setup Plot. This time select only *Variable Q10* for plotting (you may of course also view *Commanded Position 1* data if you wish). Choose Linear Time and Linear amplitude scaling for the horizontal and vertical axes; select *Remove DC Bias*; then plot the data. You should see a plot similar to the one shown in Figure 3.2-3a. Now return to Setup Plot and select *Logarithmic Frequency* and *Db* axis scaling with *Remove DC Bias* selected. Plot the data. Now the plots should appear similar to those shown in Figure 3.2-3b. (The vertical axis has been adjusted to a range of 30-80 Db via Axis Scaling in the Plotting menu)

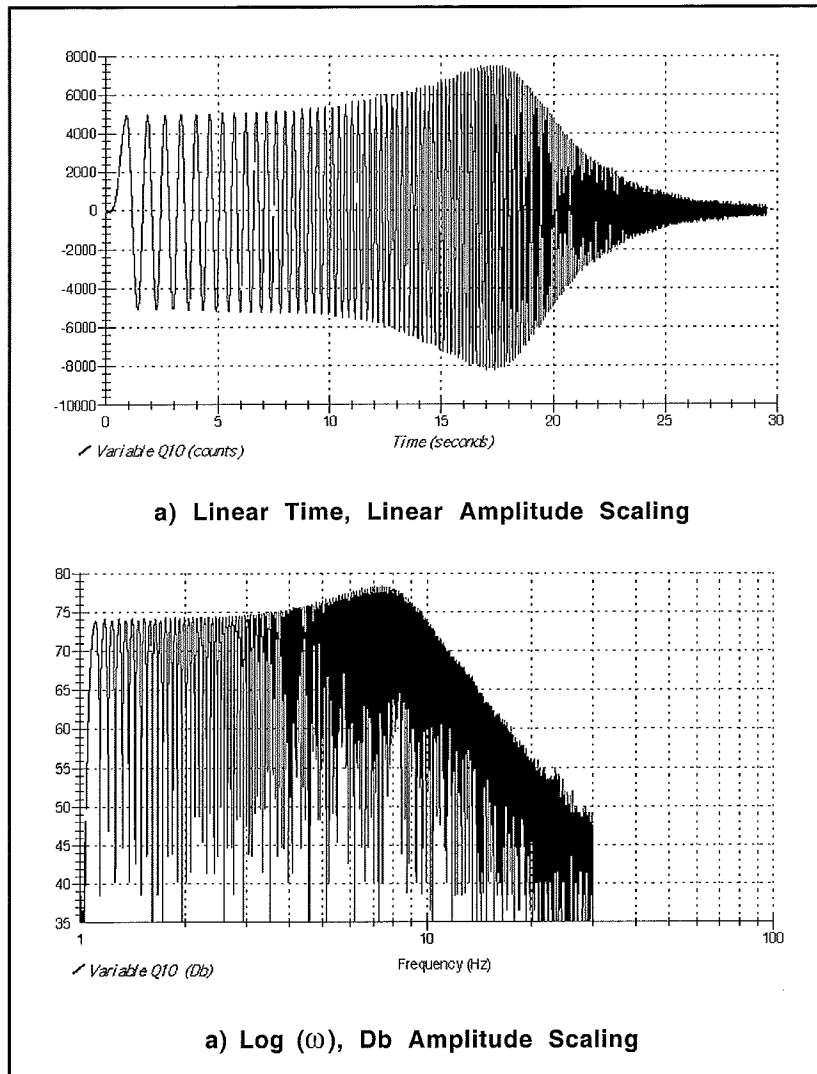


**Figure 3.2-3 Frequency Response at Lower Magnet**

The linear time / amplitude depiction shows the data in a manner that more directly represents the physical motion of the system as witnessed. The Log( $\omega$ ) / Db scaling presents the data in a way that gives students a physical understanding of the Bode magnitude plots commonly found in the literature. (The upper limit of the data curve is the experimental Bode magnitude plot.) The resonance at  $\omega_r$ , the low frequency constant amplitude and high frequency attenuation of  $-40$  Db/decade are clearly seen from the data.

**Step 8: Upper Magnet Control (Attractive Levitation).** Select Abort Control from the background screen to open the loop. The magnet should fall. Raise the magnet to a position of approximately 3 cm of travel distance below the upper limit of motion. Place the supplied plastic safety clip below the magnet so that the magnet rests in this approximate position. In the Executive, enter Setup Control Algorithm and Load the algorithm *SISO Upper SGD*. Now Implement this algorithm. You should see the magnet raise and be in stable regulation about the  $-2$  cm (2 cm below the upper support arm). If so, congratulations! You have successfully

implemented closed loop levitation on an open loop unstable plant. Lower the safety clip to the approximate  $-3.5$  cm position.

Go to Trajectory 1 Configuration and deselect *Sine Sweep* (e.g. select *Step*<sup>1</sup>. Go to Trajectory 2 Configuration and verify that *Unidirectional Moves* is not selected and that the trajectory is set up for a Step maneuver of 10000 count *Step Size*, 1000 ms *Dwell Time* and 2 *Repetitions*. Again select Execute and with *Normal Data Sampling* and *Execute Trajectory 2 Only* selected, "Run" the trajectory. You should see a series of upward and downward step responses similar to those of Figure 3.2-4. You may plot the *Variable Q10* (assigned to Sensor 2 compensated position minus offset) and *Commanded Position 2* data. You may also wish to run additional trajectories of other shapes. If you do, you should keep their amplitudes within  $\pm 10000$  counts ( $\sim 1.5$  cm.) Select Abort Control from the background screen to open the loop. The magnet should fall to the safety clip. You may now turn off power to the controller box.

This completes the basic self-guided tour of the Model 730 system. It is advised that you read all material in Chapters 2 and 3 before further operation of the equipment.

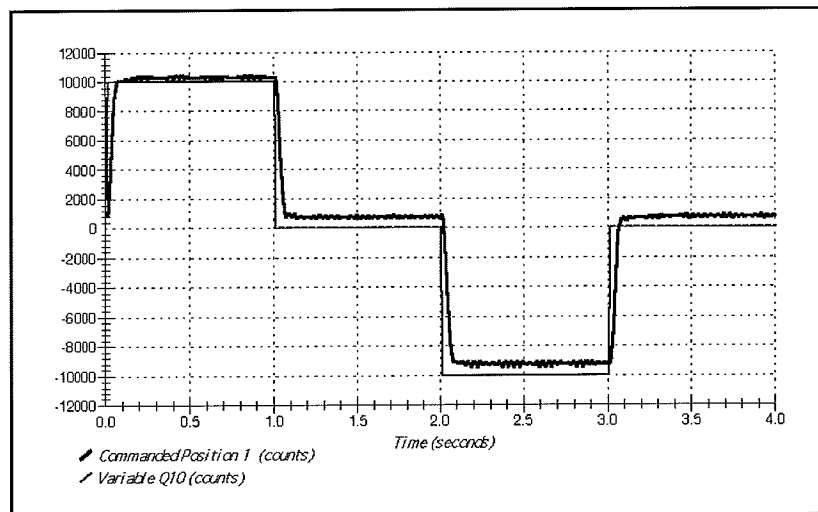


Figure 3.2-4 Step Response of Upper Magnet (Attractive Levitation)

### Step 9 (Optional): MIMO Operation.

Steps 1 through 6 above serve to fully verify the operation of the system. The following additional step may be of interest to some users. It provides an interesting demonstration of MIMO Control.

Setup the apparatus with two magnets as per the instructions of Section 2.2.2. Follow the instructions and cautionary notes in detail. Be extremely careful in handling the magnets so that they do not collide due to their mutual attraction and high field strengths. Gradually release the

<sup>1</sup> The logic as to whether to include the Sine Sweep plotting options is driven by the currently selected shape under Trajectory 1. See Sections 2.1.6.1 and 2.1.8.1.

magnets and verify that the upper magnet rests in equilibrium approximately 8 cm above the lower one.

In the Executive, enter Setup Control Algorithm and Load the algorithm *MIMO SGD*. Implement this algorithm. You should see the lower magnet raise to the 1 cm position and the upper one to the -2 composition. If so, congratulations again! You have successfully implemented MIMO control on a nonlinear MIMO system.

For Trajectory 1 select *Unidirectional Moves* and then *Impulse* and verify that the impulse is set up for a 15000 count *Amplitude*, 250 ms *Pulse Width*, 14 *Repetitions*, and 750 ms *Dwell Time*. For Trajectory 2 deselect *Unidirectional Moves* and then *Ramp* and verify that it is set up for a 15000 count *Amplitude*, 15000 counts/sec *Velocity*, 1000 ms *Dwell Time*, and 2 *Repetitions*.

Execute both these trajectories with Trajectory 2 beginning 500 ms before Trajectory 1. Note the motion of the magnets. The data may be plotted as *Commanded Position 1* and *Variable Q10* on the left axis and *Commanded Position 2* and *Variable Q12* on the right axis. Figure 3.2-5 shows a typical response where the axes are scaled (via Axis Scaling) so that the lower magnet data appears below that of the upper magnet. Although there is a strong magnetic force coupling between the magnets, the LQR based controller is effective at controlling them independently and reducing the cross-coupling effects!

Select *Abort Control* from the background screen to open the loop. The magnets should fall to their equilibrium positions. You may now turn off power to the controller box.

A variety of SISO, SIMO and MIMO control approaches are developed in the experiments of Chapter 6. Still an unlimited number of others remain to be invented! You should now have sufficient familiarity with the system to use its basic operational modes. It is advised that you read all material in Chapters 2 and 3 for a complete description of how to use the many system features before further operating it.

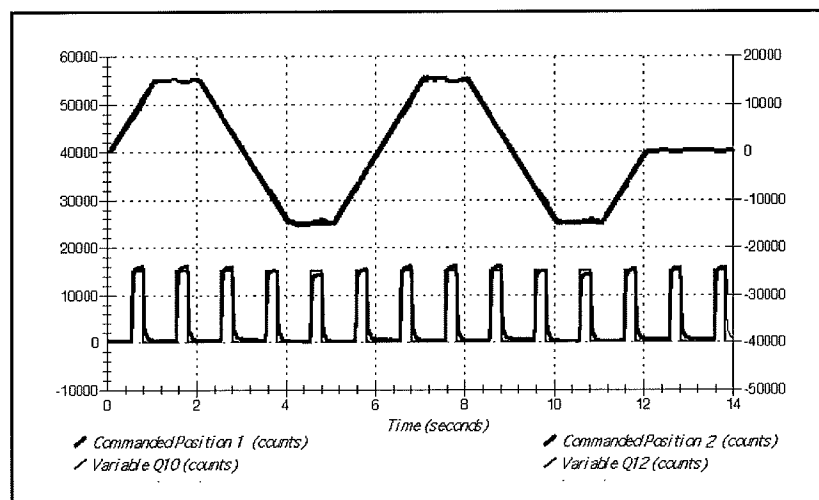
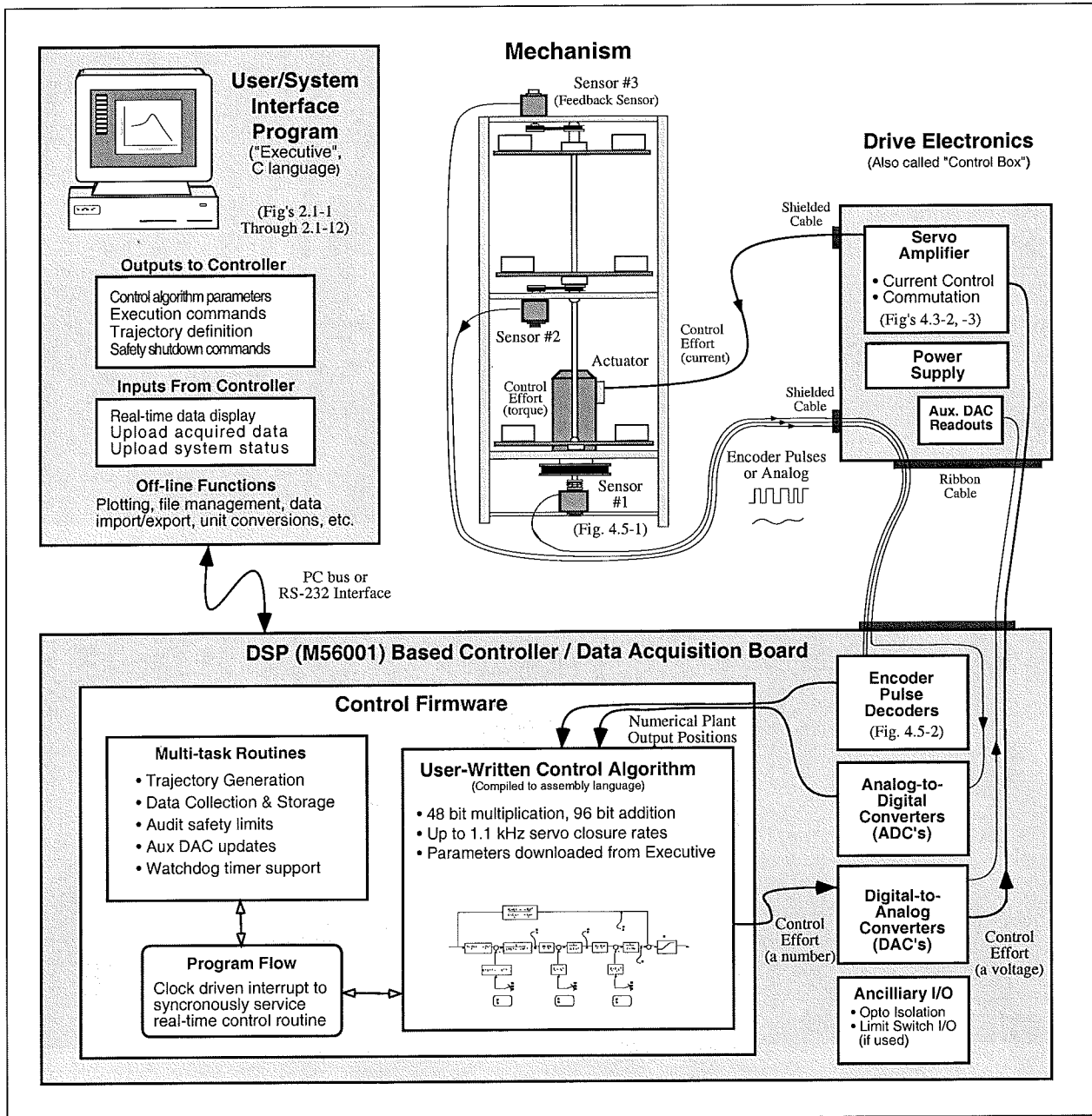


Figure 3.2-5 MIMO Tracking of Two Trajectories

## 4. Real-Time Control Implementation

A functional overview of a typical ECP control system is shown in Figure 4.0-1. The system is comprised of three subsystems: The mechanism including actuators and sensors, the real-time controller / drive electronics, and the user/system (“Executive”) interface software.



**Figure 4.0-1. Overview of Real-time Control System.**

This architecture is consistent with modern industrial control implementation.

A brief survey of the system architecture is afforded by tracing the data flow as the system is operated. (An analogous data flow structure exists in the case where the user's own controller/data acquisition hardware and software are utilized.) The user specifies the control algorithm in the Executive program and downloads it (via "Implement Algorithm") to the DSP based real-time controller board. The DSP immediately executes the algorithm at the specified sample rate. This involves reading the reference input<sup>1</sup> and feedback sensor values, computing the algorithm, and outputting the digital control effort signal to the digital-to-analog converter (DAC). In the case of the Model 730 system, there may be two such reference inputs and control effort outputs.

The DAC converts the resulting stream of digital words to an analog voltage which is transformed to a current by the servo amplifier and then to a force by the drive coil(s). The apparatus transforms the force to motion at the desired output according to the plant dynamics (i.e. equations of motion). These plant outputs are sensed by the laser sensors which in turn output analog signals. These signals are converted to digital words via an analog-to-digital converter (ADC). A laser temperature signal is also fed back and passed through the ADC for internal sensor temperature compensation. In the case of the optional turntable accessory, the rotor position is measured via an optical encoder. The encoder outputs a stream of pulses which are decoded by a counter on the DSP board. For all sensors, the sensed plant output is available as a digital word to the real-time control algorithm.

When the user specifies a trajectory and subsequently commands the system to "Execute" the maneuver, the trajectory parameters are downloaded to the controller board. The DSP generates corresponding reference input values for use by the real-time control algorithm. Throughout the maneuver, any data specified by the user is captured and stored in memory on the board. On completion of the maneuver, the data is uploaded to PC memory where it is available for plotting and storage.

Details of these and other significant system functions are given in the remainder of this chapter.

#### 4.1 Servo Loop Closure

Servo loop closure involves computing the control algorithm at the sampling time. The real-time Controller executes the user-specified control law at each sample period  $T_s$ . This period can be as short as 0.000884 seconds (approx. 1.1 KHz) or any multiple of this number. The Executive program's Setup Control Algorithm dialog box allows the user to alter the sampling period. All forms of control laws are automatically compiled by the Executive program into the M56000 assembly language prior to downloading ("implementing") to the Controller. The Controller immediately begins executing the algorithm. It uses 96-bit real number (48-bit integer and 48-bit fractional) arithmetic for computation of the control effort. The control effort is saturated in software at +/- 32768 to represent +/- 10 volts on the 16-bit DACs whose range is +/- 10 volts.

---

<sup>1</sup> Since no trajectory is being input at this point, the system is regulating about a reference input value of zero.

## 4.2 Command Generation

*Command generation* is the real-time generation of motion trajectories specified by the user. The parameters of these trajectories are downloaded to the real-time Controller through the Executive program via the Trajectory Configuration dialog box. This section describes the trajectories generated in the current control version.

### 4.2.1 Step Move

Figure 4.2-1a shows a step move demand. The desired trajectory for such a move can be described by

$$\begin{aligned}c_p(t) &= c_p(0) + C && \text{for } t > 0 \\c_v(t) &= 0 && \text{for } t > 0 \\c_v(0) &= \infty\end{aligned}$$

Where  $c_p(t)$  and  $c_v(t)$  represent commanded position and velocity at time  $t$  respectively and  $C$  is the constant step amplitude. Such a move demand generates a strong impulsive torque from the control actuator. The response of a mechanical system connected to the actuator would depend on the dynamic characteristics of the controller and the system itself. However, in a step move, the instantaneous velocity and its derivatives are not directly controllable. Usually step moves are used only for test purposes; more gentle trajectories are nearly always used for practical maneuvers.

### 4.2.2 Ramp Move

A ramp demand is seen in Figure 4.2-1b. The trajectory can be described by

$$\begin{aligned}c_p(t) &= c_p(0) + V * t && \text{for } t > 0 \\c_v(t) &= V && \text{for } t > 0 \\c_a(0) &= \infty\end{aligned}$$

where  $c_a(0)$  represents commanded acceleration at time zero and  $V$  is a constant velocity. Relative to a step demand, a ramp demand is more gentle, however the acceleration is still impulsive. The commanded velocity is a known constant during the maneuver.

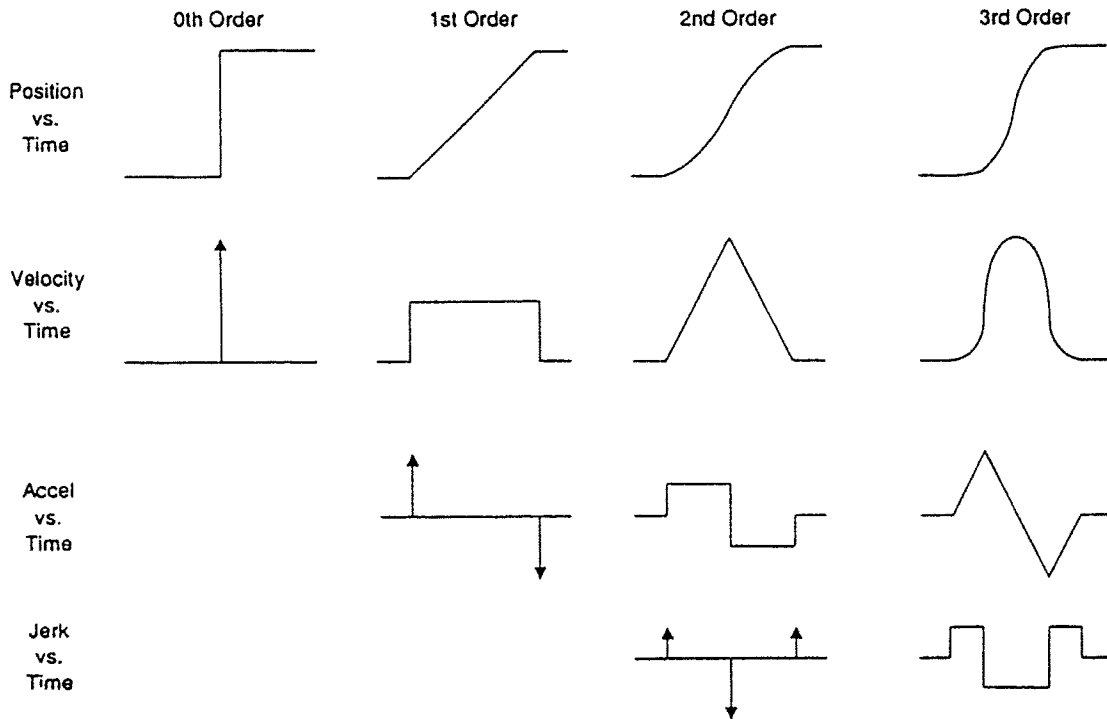


Figure 4.2-1. Geometric Command Trajectories Of Increasing Order

4.2.3 Parabolic Move

Figure 4.2-1c shows a parabolic move demand. Its trajectory can be expressed as:

$$\begin{aligned}
 c_p(t) &= c_p(0) + c_v(0) * t + 1/2 A * t^2 && \text{for } t > 0 < 1/2 t_f \\
 c_v(t) &= c_v(0) + A * t && \text{for } t > 0 < 1/2 t_f \\
 c_a(t) &= A && \text{for } t > 0 < 1/2 t_f \\
 c_j(0) &= \infty
 \end{aligned}$$

where  $c_j(t)$  represents commanded jerk at time  $t$  and  $A$  is a constant acceleration, and  $t_f$  is the final destination time. Relative to a ramp demand, a parabolic demand is more gentle, however the rate of change of acceleration (jerk) is still impulsive. Note that the commanded acceleration is a known constant during the maneuver. The second half of a parabolic demand uses  $-A$  for deceleration.

4.2.4 Cubic Move

Figure 4.2-1d shows a cubic demand which can be described by

$$\begin{aligned}
 c_p(t) &= c_p(0) + c_v(0) * t + 1/2 c_a(0) * t^2 + 1/6 J * t^3 && \text{for } t > 0 < 1/4 t_f \\
 c_v(t) &= c_v(0) + c_a(0) * t + 1/2 J * t^2 && \text{for } t > 0 < 1/4 t_f \\
 c_a(t) &= c_a(0) + J * t && \text{for } t > 0 < 1/4 t_f \\
 c_j(0) &= J
 \end{aligned}$$

where  $J$  represents a constant jerk. Relative to all the above demands, a cubic demand is more



gentle. The commanded acceleration is linearly changing during the three sections of the maneuver. The second half of a cubic demand uses  $-J$  and the third part uses  $J$  again for the jerk input.

#### 4.2.5 The Blended Move

Any time a ramp, a parabolic or a cubic trajectory move is demanded the real-time Controller executes a general blended move to produce the desired reference input to the control algorithm. The move is broken into five segments as shown in the velocity profile of Figure 4.2-2. For each section a cubic (in position) trajectory is planned. Five distinct cubic equations can describe the forward motion. After the dwell time, the reverse motion can be described by five more cubic trajectories. Each cubic has the form:

$$c_{p_i}(t) = c_{p_i}(0) + V_i * t + 1/2 A_i * t^2 + 1/6 J_i * t^3 \quad i = 1, \dots, 5$$

Using a known set of trajectory data (i.e. the requested total travel distance, acceleration time  $t_{acc}$ , and the maximum speed  $v_{max}$ , for each move), the constant coefficients  $V_i$ ,  $A_i$ , and  $J_i$  are determined for each segment of the move by the real-time Controller. This function is known as the "motion planning" task. Note that for a parabolic profile  $J_i=0$ , and for a ramp profile  $A_i$  is also zero which further simplifies the task. Having determined the coefficients for each section, the real-time Controller uses these values at the servo loop sampling periods to update the commanded position (reference input). For example if the segment is a cubic ( $J \neq 0$ ):

$$\begin{aligned} ca(k) &= ca(k-1) + J * Ts \\ cv(k) &= cv(k-1) + ca(k) * Ts \\ cp(k) &= cp(k-1) + cv(k) * Ts \end{aligned}$$

where  $Ts$  is the sampling period and  $ca(k)$ ,  $cv(k)$ ,  $cp(k)$  represent commanded acceleration, velocity and position at the  $k$ th sampling period.

Figure 4.2-2 Velocity Profile for General Blended Move

#### 4.2.6 Sinusoidal Move

The sinusoidal move is generated using the following equation:

$$c_p(k) = R * \sin(\theta(k))$$

where  $R$  is the amplitude,  $\theta(k) = \omega * k * T_p$  for  $k=0,1,\dots$ , and  $\omega$  is the commanded frequency in Hz.  $T_p$  is set to five milliseconds (i.e.  $k$  is incremented every 5 ms.). To further smooth out the trajectory, a cubic spline is fitted between the points as follows:

$$c_p'(k) = (c_p(k-1) + 4 * c_p(k) + c_p(k+1)) / 6$$

For the linear sine sweep,  $\omega(k) = \alpha * T_p$ , where  $\alpha$  is a constant determined by the difference between the maximum and the minimum frequency divided by the sweep time

$$\alpha = (\omega_{\max} - \omega_{\min}) / \text{sweep time}$$

For the logarithmic sweep

$$\omega = \omega_{\min} * 10^{(B-A)*(k*T_p)/\text{sweep time}}$$

where A and B are defined according to

$$A \triangleq \log_{10}(\omega_{\min}), B \triangleq \log_{10}(\omega_{\max})$$

### 4.3 Drive Coils, Brush Type DC Servo Motor, and Drive Amplifier

The control effort at the  $k^{\text{th}}$  sampling period is the input to a 16-bit DAC which provides an analog signal for the servo amplifier. The amplifier operates in a transconductance mode providing a current (as opposed to voltage) to the drive coil or motor (optional turntable) which in turn represents a proportional increase in magnetic field strength from the coil or a torque from the motor. To provide the current source capability an analog proportional plus integral (PI) controller is implemented within the servo amplifier for tracking the demanded current. Referring to the block diagram of Fig. 4.3-1, the transfer function between the motor current and the DAC output (control effort) is given by:

$$\frac{i(s)}{u(s)} = \frac{k_A k_c (k_p s + k_i)}{s(Ls + R + k_t k_b G(s)) + k_p s + k_i} \quad (4.3-1)$$

Here  $k_c$  is the DAC gain in volts/count (10 volts per 32767 counts),  $k_A$  is the amplifier forward gain which is dimensionless (V/V),  $R$  is the coil resistance or for the motor, the armature and brush resistance in ohms,  $L$  is the inductance in henrys,  $k_b$  is the motor back emf constant in  $v/(\text{rad/s})^1$ ,  $k_t$  is the motor torque constant in Nm/ampere,  $k_m$  is the mechanical advantage constant which is the gear ratio (Nm/Nm), and  $G(s)$  is the transfer function between current and the magnet velocity in the case of the basic apparatus and the motor velocity in the case of the turntable. In the current mode drive amplifier, both the proportional gain  $k_p$  and the integral gain  $k_i$  of the amplifier are chosen to be very high relative the inner back emf loop within the practical range of operation. As a result, the effect of the inner loop may be ignored and the transfer function may be simplified to:

<sup>1</sup> This term is generally negligible for the coil/magnetic system

$$\frac{i(s)}{u(s)} = \frac{k_A k_C (k_p s + k_i)}{s(Ls + R) + k_p s + k_i} \quad (4.3-2)$$

At steady state this transfer function becomes:

$$\frac{i(s)}{u(s)} = k_A k_C \quad (4.3-3)$$

The force generated on the magnet as a result of this current is described in Chapter 5. For the turntable, the torque delivered to the spin platter then becomes:

$$\frac{T(s)}{u(s)} = k_A k_C k_t k_m \quad (4.3-4)$$

In general, the analog PI controller gains of the amplifier are such that the dynamics of the current loop are much faster relative to the dynamics of the motor and mechanical plant. As a result the steady state value of current is achieved virtually instantaneously relative to changes in velocities and positions. Thus in this transconductance (current feedback) mode, the combined amplifier/ coil combination can be thought of as a force generator with instantaneous response.

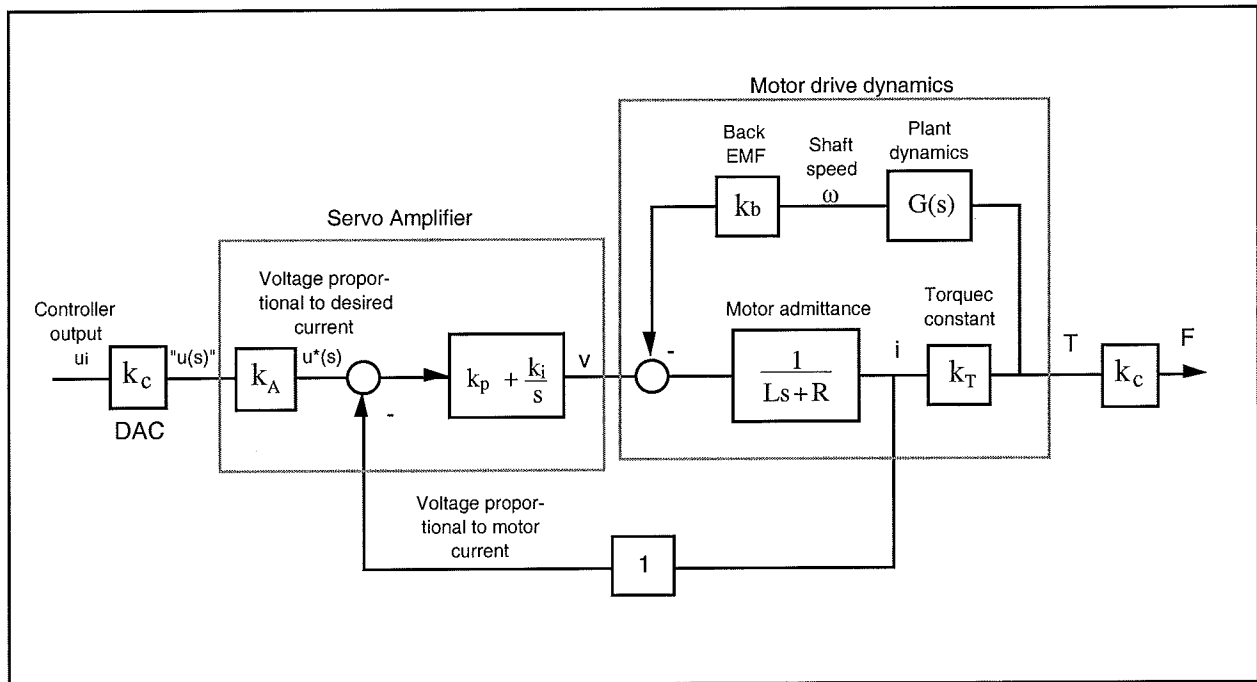


Figure 4.3-1. Mechanism Drive Block Diagram

#### 4.4 Multi-Tasking Environment

Digital control implementation is intimately coupled with the hardware and software that supports it. Nowhere is this more apparent than in the architecture and timing used to support the various

data processing routines. A well prioritized time multi-tasking scheme is essential to maximizing the performance attainable from the processing resources.

The priority scheme for the ECP real-time Controller's multi-tasking environment is tabulated in Table 4.4-1. The highest priority task is the trajectory update and servo loop closure computation which takes place at the maximum rate of 1.131 KHz (minimum sampling period is 0.000884 seconds). In this case, the user may reduce the sampling rate through the Executive Program via changes to  $T_s$  in the Setup Control Algorithm dialog box.

The trajectory planning task has the third highest priority and is serviced at a maximum rate of 377 Hz. Here the parameters for a new trajectory need not be calculated every time this task is serviced by the real-time Controller. Whenever a new trajectory is required (i.e. the current trajectory is near its completion) this task is executed. The lower priority tasks are system house keeping routines including safety checks, interface and auxiliary analog output.

**Table 4.4-1 The Multi-Tasking Priority Scheme of the Real-Time Controller**

<b>Priority</b>	<b>Task Description</b>	<b>Service Frequency</b>
1	Servo Loop Closure & Command Update	1.1 KHz
2	Trajectory Planning	377 Hz
3	Background Tasks including User Interface, Auxiliary DAC Update, Limit checks etc.	Background (In time between other tasks)

The higher priority tasks always prevail over lower ones in obtaining the computational power of the DSP. This multi-tasking scheme is realized by a real-time clock which generates processor interrupts.

### **4.5 Sensors**

The basic Model 730 apparatus uses laser light amplitude sensors for feedback while the optional turntable accessory uses an optical encoder.

The laser sensor is depicted functionally in Figure 4.5-1 and is a proprietary ECP design. The monochromatic, coherent laser beam is spread via a single hemicylindrical optical element into a fan shape. This beam is projected on the diffuse white surface of the magnet. A photodetector views the beam and generates a voltage proportional to the amount of beam power incident on it. The white surface properties and laser/detector view factors and geometries are designed to maximize the sensor gain slope (change in output v. change in position) through the sensor operational range of 5.cm.

Because of the fan beam shape and the fact that the reflected light is a combination of specular and diffuse, the power on the detector diminishes with the inverse and inverse square of the magnet distance. Additionally, the geometry of the laser, detector, and magnet and the resulting cutoff of the detector's view of the beam as a function of magnet height give rise to a linear dependency at

small magnet distance. These relationships are used to motivate the general form of the sensor linearization function as discussed in Chapters 5 and 6.

Proprietary electronic circuitry makes the design immune to stray light noise, such as turning room lights on and off, and rejects most induced electronic disturbances. Thus a relatively low noise signal is output to the analog-to-digital converter (ADC) located in the Control Box. The resulting digital word, scaled at  $2^{15}$  (32,768) counts = 10 V is made available to the DSP board for subsequent real-time processing. A laser temperature signal is also output to the ADC and subsequently to the DSP board. This is used to compensate for the laser's inherent reduction in emitted power as a function of temperature (approx. 15% maximum for the operational temperatures of the Model 730 apparatus). This compensation is accomplished in background processing and is transparent to the user.

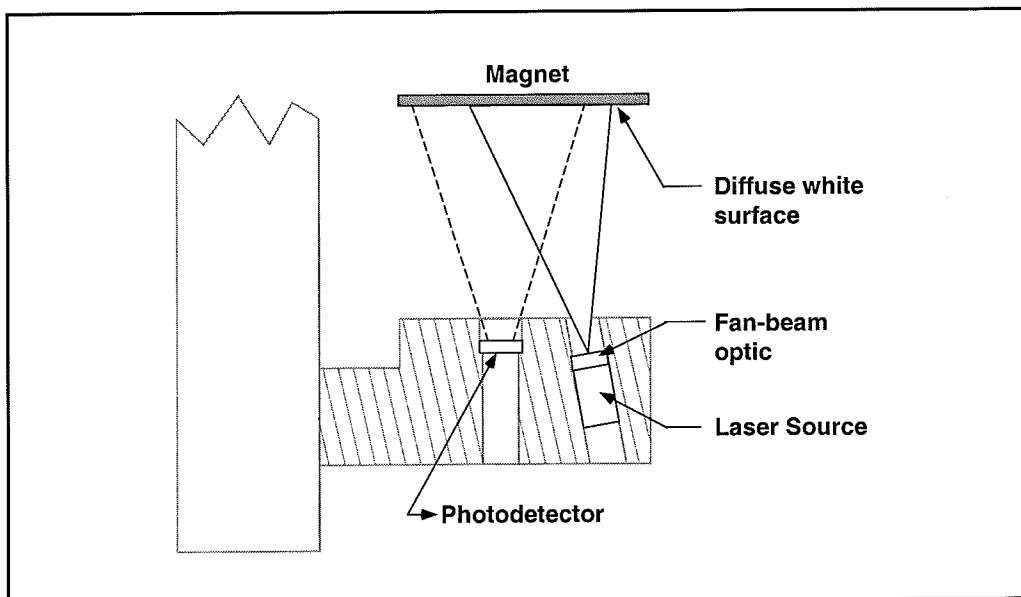


Figure 4.5-1. Laser Sensor Functional Diagram

For the optional turntable, the feedback is via an optical encoder whose principle of operation is depicted in Figure 4.5-2. A low power light source is used to generate two 90 degrees out of phase sinusoidal signals on the detectors as the moving plate rotates with respect to the stationary plate. These signals are then “squared up” and amplified in order to generate quadrate logic level signals suitable for input to the programmable gate array on the real-time Controller. The gate array uses the A and B channel phasing to decode direction and detects the rising and falling edge of each to generate 4x resolution – see Figure 4.5-3. The pulses are accumulated continuously within 24-bit counters (hardware registers). The contents of the counters are read by the DSP once every servo (or commutation) cycle time and extended to 48-bit word length for high precision numerical processing. Thus the accumulation of encoder pulses provides an angular position measurement (signal) for the servo routines.

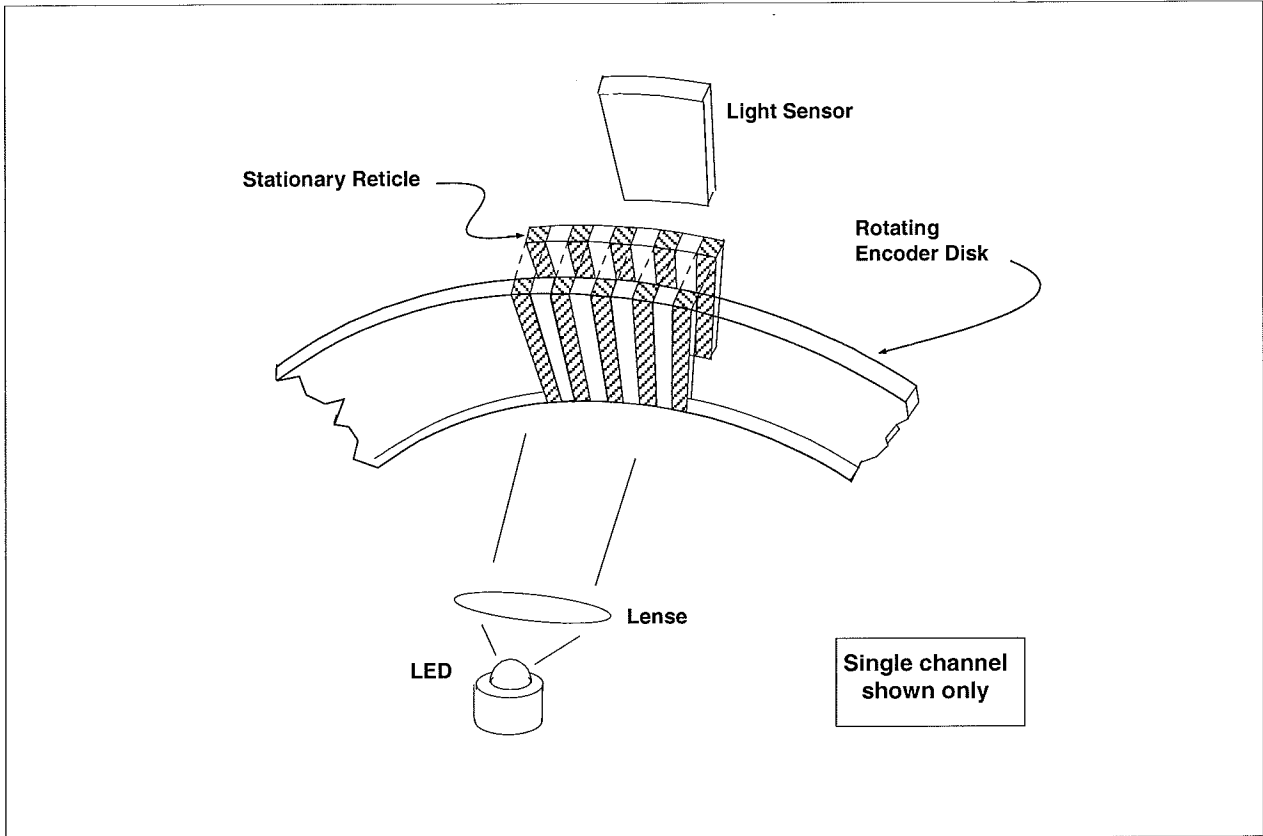


Figure 4.5-2 The Operation Principle of Optical Incremental Encoders

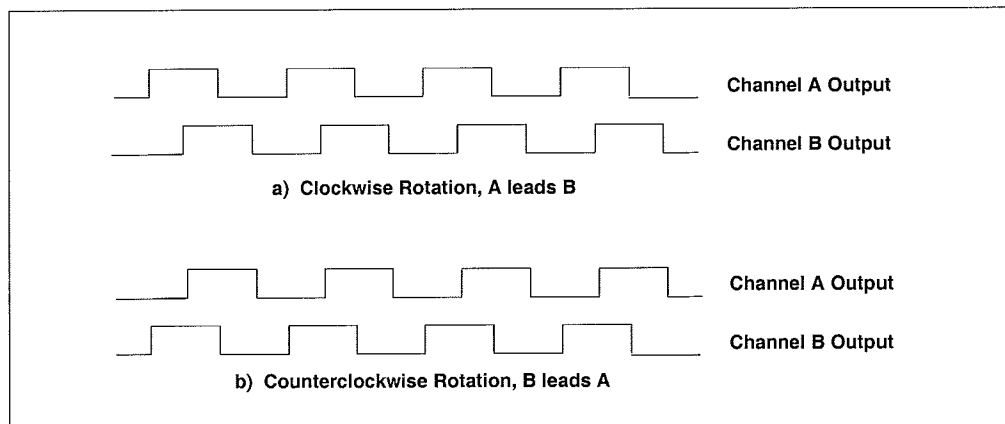


Figure 4.5-3. Optical Encoder Output

## 4.6 Auxiliary Analog Output (System Option)

A system option provides two analog output channels in the Control Box which are connected to two 16-bit DACs that physically reside on the real-time Controller. Each analog output has the range of +/- 10 volts (-32768 to +32767 counts) with respect to the analog ground. The outputs on these DACs are updated by the real-time Controller as a low priority task. However, for virtually all trajectories (e.g. for sine sweep up to approx. 25 Hz) the update rate is sufficiently fast for an oscilloscope or other analog equipment to inspect the various internal Controller signals. See the section on the Executive Program's Utility menu for the available signals to output on these DACs.

## 5. Plant Dynamic Models

This chapter provides time domain dynamical expressions in nonlinear and linear forms useful for control implementation and for use in the experiments described later in this manual. An overview of the principles of magnetism and magnetic levitation is given in Appendix A. The appendix gives the motivation for and form of the magnetic force terms used in this chapter.

### 5.1 Full Order Nonlinear Model

A free body diagram of two suspended magnets in the Model 730 apparatus is shown in Figure 5.1-1. Either magnet is acted on by forces from either drive coil, from the other magnet, from gravity, and from friction (modeled as viscous).

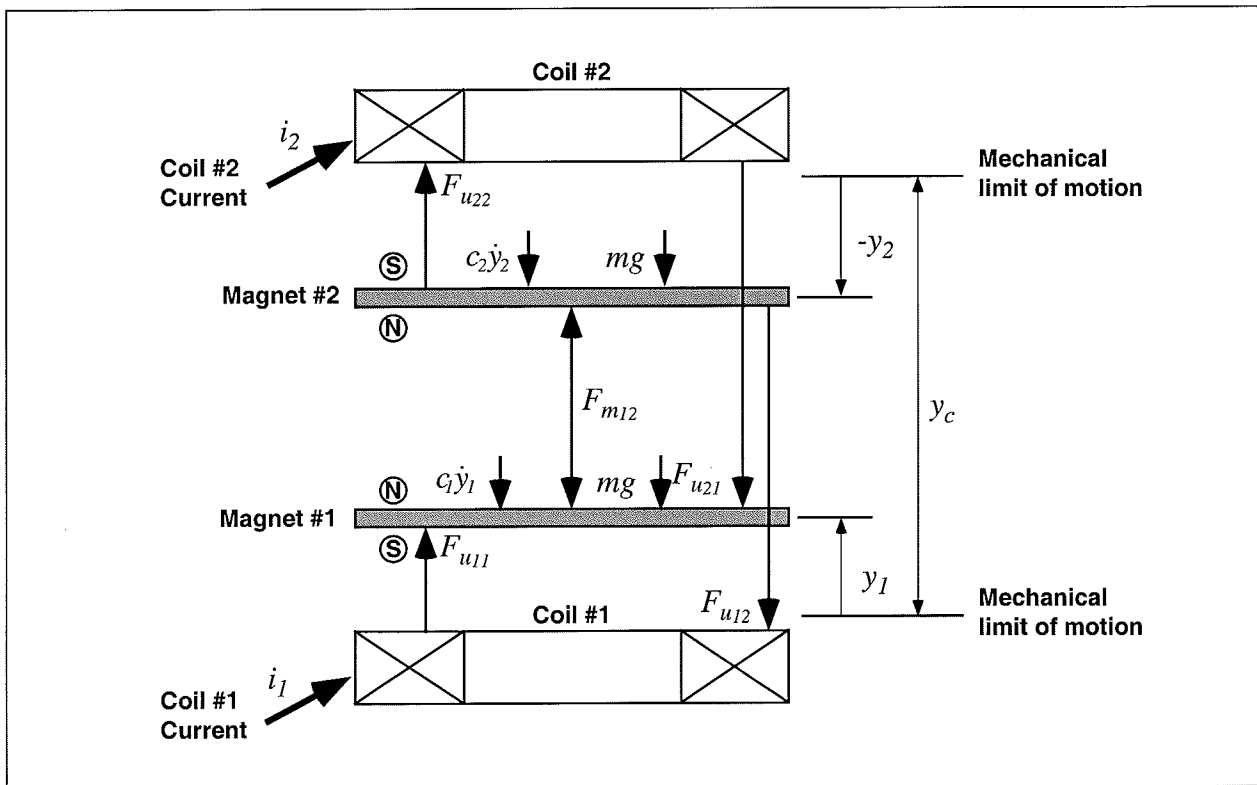


Figure 5.1-1. Free Body Diagram & Dynamic Configuration



From Figure 5.1-1, we have for the first magnet

$$m\ddot{y}_1 + c_1\dot{y}_1 + F_{m12} = F_{u11} - F_{u21} - mg \quad (5.1-1)$$

Similarly for the second magnet

$$m\ddot{y}_2 + c_1\dot{y}_2 - F_{m12} = F_{u22} - F_{u12} - mg \quad (5.1-2)$$

The magnetic force terms are modeled as having the following forms (see Appendix A for details)

$$F_{u11} = \frac{i_1}{a(y_1 + b)^N} \quad (5.1-3)$$

$$F_{u12} = \frac{i_1}{a(y_c + y_2 + b)^N} \quad (5.1-4)$$

$$F_{u21} = \frac{i_2}{a(y_c - y_1 + b)^N} \quad (5.1-5)$$

$$F_{u22} = \frac{i_2}{a(-y_2 + b)^N} \quad (5.1-6)$$

$$F_{m12} = \frac{c}{(y_{12} + d)^N} \quad (5.1-7)$$

where

$$y_{12} = y_c + y_2 - y_1 \quad (5.1-8)$$

and  $a$ ,  $b$ ,  $c$ ,  $d$ , and  $N$  are constants which may be determined by numerical modeling of the magnetic configuration or by empirical methods. Typically  $3 < N < 4.5$ .

## 5.2 Simplified Equations of Motion

The cross magnet/actuator forces,  $F_{u12}$  and  $F_{u21}$  are generally small compared to  $F_{u11}$  and  $F_{u22}$  for typical values of coil current and for the magnets in their normal operating range. For the Model 730 apparatus, the friction forces are also typically small. In addition, a value of four for the power of the denominator terms in Eq's (5.1-3 through -7) has been shown empirically to yield a

close approximation of the force/distance relationships – see Figure 5.2-1<sup>1</sup>. The following simplified model is therefore valid for many control design and analysis purposes.

$$m\dot{y}_1 + F_{m12} = F_{u11} - mg \tag{5.2-1}$$

$$m\dot{y}_2 - F_{m12} = F_{u22} - mg \tag{5.2-2}$$

where

$$F_{u11} = \frac{u_1}{a(y_1+b)^4} \tag{5.2-3}$$

$$F_{u22} = \frac{u_2}{a(-y_2+b)^4} \tag{5.2-4}$$

$$F_{m12} = \frac{c}{(y_{12}+d)^4} \tag{5.2-5}$$

The coil current,  $i_i$ , has been replaced with the more general term of *control effort* denoted as  $u_i$ . The control effort may be a digital word, voltage, or current and is presumed to be linearly proportional to the coil current. The coefficient  $a$  must of course be consistently scaled with the units of  $u_i$ . The above equations may be modified to describe the SISO and SIMO systems by obvious deletion of the appropriate terms.

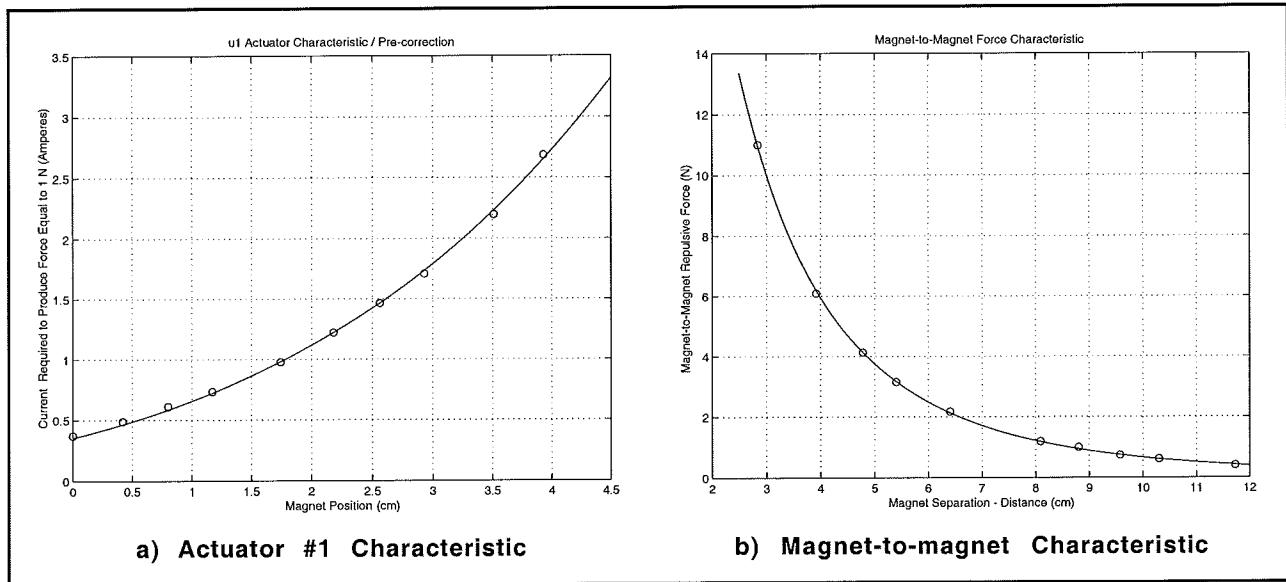


Figure 5.2-1. Fourth Order Fit for Actuator and Magnet-to-magnet Force Terms<sup>2</sup>

<sup>1</sup> This characteristic is measured experimentally in Chapter 6.

<sup>2</sup> The actuator curve shown is fourth order. It depicts the coil current required to generate 1 N of force at a given magnet distance. The corresponding force term  $F_{u11}$  is the inverse of this relationship. The magnet-to-magnet data is shown fitted with an inverse fourth power curve which directly corresponds with the term  $F_{m12}$ .

### 5.4 Linearized Equations of Motion

For small motions, the system may be modeled as being linear. The linearized equations of motion are found by the customary method of solving for the zeroeth and first order terms of the Taylor's Series expansion of the respective equations about the operating point. Calling the expression of Eq. (5.2-1)  $\alpha$ , for example, the linearized equation of motion is found by calculating

$$\alpha(y_{1o}, y_{2o}, u_{1o}, t) + \frac{\partial \alpha}{\partial y_1} \Big|_{y_{1o}, y_{2o}, u_{1o}} *(y_1 - y_{1o}) + \frac{\partial \alpha}{\partial y_2} \Big|_{y_{1o}, y_{2o}, u_{1o}} *(y_2 - y_{2o}) + \frac{\partial \alpha}{\partial u_1} \Big|_{y_{1o}, y_{2o}, u_{1o}} *(u_1 - u_{1o}) \quad (5.3-1)$$

Where  $y_{1o}$ ,  $y_{2o}$ , and  $u_{1o}$  are the respective magnet positions and control effort that define the operating point. For the purposes of control design, we shall choose the operating point to be at an equilibrium so that

$$(F_{m_{12}} - F_{u_{11}} + mg) \Big|_{y_{1o}, y_{2o}, u_{1o}} = 0 \quad (5.3-2)$$

Evaluating Eq. (5.3-1) and using Eq. (5.3-2) we have

$$m\ddot{y}_1 + \left( \frac{4c}{(y_{12o} + d)^5} + \frac{4u_{1o}}{a(y_{1o} + b)^5} \right) (y_1 - y_{1o}) - \frac{4c}{(y_{12o} + d)^5} (y_2 - y_{2o}) = \frac{1}{a(y_{1o} + b)^4} (u_1 - u_{1o}) \quad (5.3-3)$$

which may be rewritten as:

$$m\ddot{y}_1^* + (k_1' + k_{12}') y_1^* - k_{12}' y_2^* = k_{u_1}' u_1^* \quad (5.3-4)$$

Similarly for Eq. (5.2-2)

$$m\ddot{y}_2^* + (k_{12}' - k_2') y_2^* - k_{12}' y_1^* = k_{u_2}' u_2^* \quad (5.3-5)$$

where

$$y_i^* = y_i - y_{i_o} \quad , \quad i=1,2 \quad (5.3-6)$$

$$u_i^* = u_i - u_{i_o} \quad , \quad i=1,2 \quad (5.3-7)$$

$$k_1' = \frac{4u_{1o}}{a(y_{1o} + b)^5} \quad (5.3-8)$$

$$k_2' = \frac{4u_{2o}}{a(-y_{2o} + b)^5} \quad (5.3-9)$$

$$k_{12}' = \frac{4c}{(y_{12o} + d)^5} \quad (5.3-10)$$

$$k_{u_1}' = \frac{1}{a(y_{1o} + b)^4} \quad (5.3-11)$$

$$k'_{u_2} = \frac{1}{a(-y_{2o}+b)^4} \tag{5.3-12}$$

From Eq.(5.3-2) we may solve for the equilibrium control effort values

$$u_{1o} = a(y_{1o}+b)^4 \left( \frac{4c}{(y_{12o}+d)^5} + mg \right) \tag{5.3-13}$$

$$u_{2o} = a(y_{2o}+b)^4 \left( \frac{4c}{(y_{12o}+d)^5} + mg \right) \tag{5.3-14}$$

Thus for small motions, the salient dynamics are identical in form to those of the linear discrete system shown in Figure 5.3-1. Note in the figure that  $k'_2$  is a “negative spring” and that the magnets in this case are configured so that they repel each other. If they are set to attract each other,  $k'_{12}$  becomes negative.

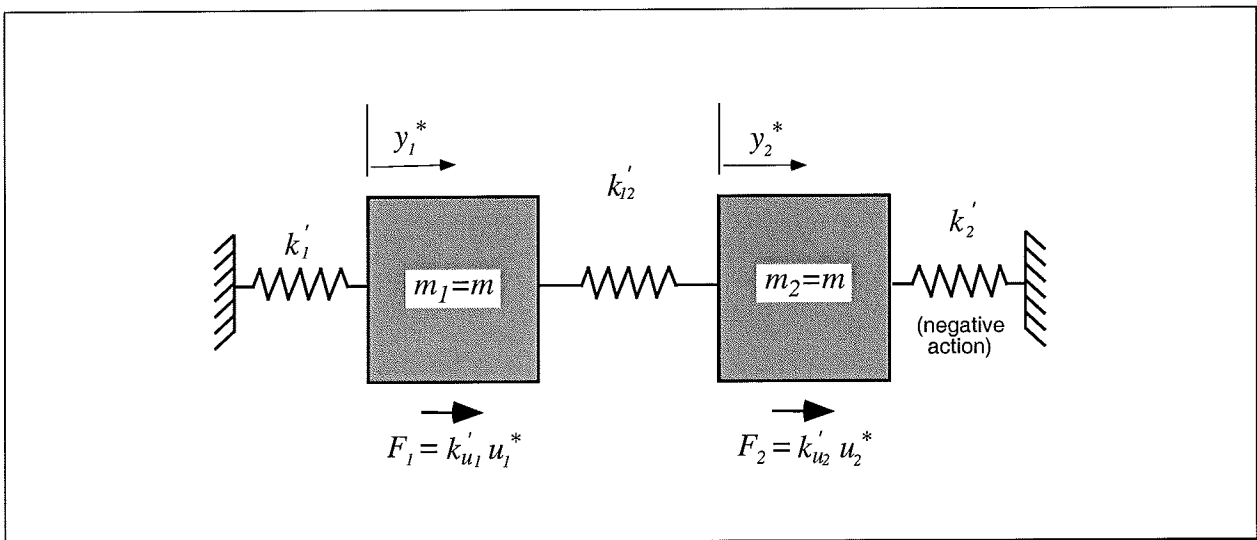


Figure 5.3-1. Equivalent Simplified/Linearized Plant

Again, the Model 730 apparatus is easily configured for SISO, MISO, and SIMO operation by removing one magnet and/or exciting only one coil. The linearized models for such systems may be found by neglecting the appropriate terms in Eq's (5.3-4, -5). A state space realization of this system is:

$$\begin{aligned} \dot{x} &= Ax + BU(t) \\ Y &= Cx \end{aligned} \tag{5.3-15}$$

where

$$x = \begin{bmatrix} y_1^* \\ \dot{y}_1^* \\ y_2^* \\ \dot{y}_2^* \end{bmatrix}, \quad A = \begin{bmatrix} 0 & 1 & 0 & 0 \\ -(k_1' + k_{12}')/m & 0 & k_{12}'/m & 0 \\ 0 & 0 & 0 & 1 \\ k_{12}'/m & 0 & (k_2' - k_{12}')/m & 0 \end{bmatrix}, \quad B = \begin{bmatrix} 0 & 0 \\ k_{u1}'/m & 0 \\ 0 & 0 \\ 0 & k_{u2}'/m \end{bmatrix},$$

$$C = \begin{bmatrix} C_1 & 0 & 0 & 0 \\ 0 & C_2 & 0 & 0 \\ 0 & 0 & C_3 & 0 \\ 0 & 0 & 0 & C_4 \end{bmatrix}, \quad U(t) = \begin{bmatrix} u_1^*(t) \\ u_2^*(t) \end{bmatrix}$$

and  $C_i = 1$  ( $i=1,2,3,4$ ) when  $X_i$  is an output and equals 0 otherwise.

#### 5.4 Sensor Model & Linearized System Using Raw Sensor Data

The sensor output characteristic as described in Section 4.5, is nonlinear. The following equation is motivated by examining the optical design and geometry of the laser / detector / magnet system.

$$y_{ical} = \frac{e_i}{y_{iraw}} + \frac{f_i}{\sqrt{y_{iraw}}} + g_i + h_i y_{iraw}, \quad i = 1, 2 \quad (5.4-1)$$

where  $y_{ical}$  is the linearized/calibrated output of the sensor, and  $y_{iraw}$  is the raw sensor output.<sup>1</sup> The coefficients,  $e$ ,  $f$ ,  $g$ , and  $h$  are found by calibrating the sensor according to the instructions of Section 6.1. A default set of coefficients that provide nominal measurement accuracy is furnished with each unit. A depiction of typical sensor data fitted with a curve of the form of Eq.(5.4-1) is shown in Figure 5.4-1 (The discrete data points correspond to physical  $y_i$  positions of the magnet; the continuous curve is  $y_{ical}$ ). Note that the sensor#2 plot has negative values of  $y_2$  and  $y_{2cal}$ .

<sup>1</sup> The “raw” output is net of the laser thermal compensation done in the background (transparent to the user) unless “Apply Thermal Compensation” is not checked in the Setup Sensor Calibration dialog box. It is recommended that thermal compensation be applied in all cases. If thermal compensation is not applied, the coefficients  $e$ ,  $f$ ,  $g$ , and  $h$  in Eq. (5.4-1) should be evaluated with the thermal compensation turned off and at the anticipated steady state operating temperature of the coil/sensor block(s).

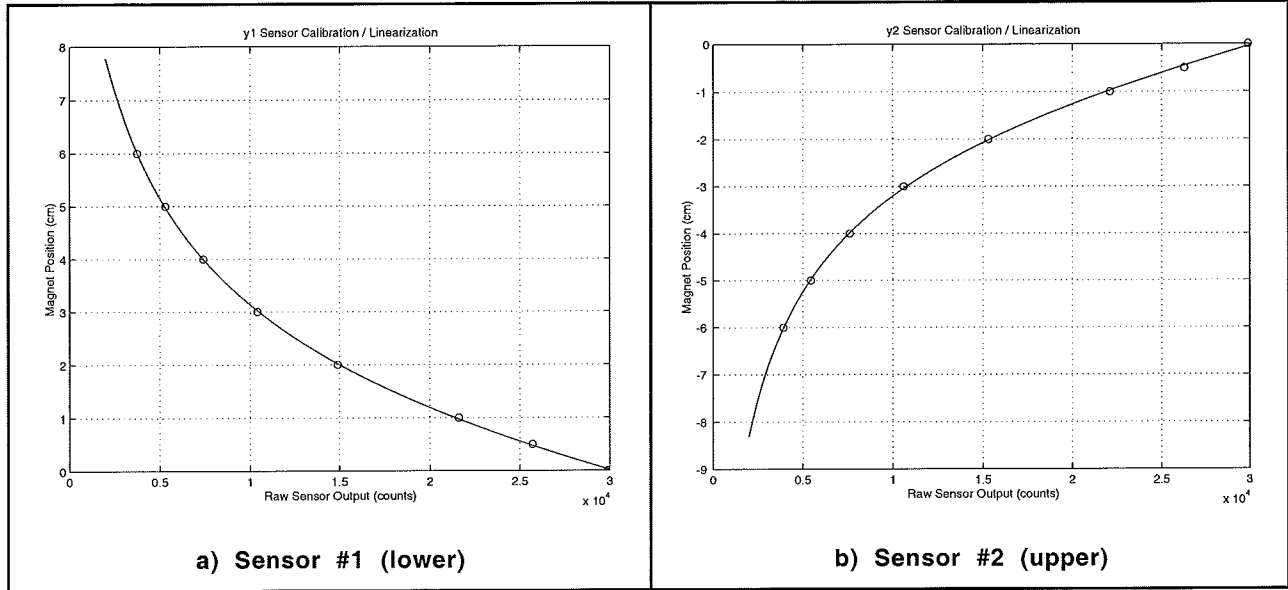


Figure 5.4-1. Nonlinear Sensor Input/Output Characteristic

For certain control approaches, the raw sensor output may be used as the feedback signal. In general, the control designer will linearize the sensor output in such a case. Assuming  $y_{ical}$  is a sufficiently accurate approximation of  $y_i$ , the linearized form of such a system is found by replacing  $y_i$  with  $y_{ical}$  in Eq. (5.3-4) and using the chain rule of differentiation where the derivative is taken with respect to  $y_{iraw}$ , i.e.

$$\frac{\partial \alpha}{\partial y_{iraw}} = \frac{\partial \alpha}{\partial y_i} \frac{\partial y_i}{\partial y_{iraw}} \approx \frac{\partial \alpha}{\partial y_i} \frac{\partial y_{ical}}{\partial y_{iraw}}, \quad i = 1, 2 \quad (5.4-2)$$

The resulting equations of motion are:

$$mk_{y1r} \ddot{y}_{1raw}^* + (k_1' + k_{12}') k_{y1r} y_{1raw}^* - k_{12}' k_{y2r} y_{2raw}^* = k_{u1}' u_1^* \quad (5.4-3)$$

$$mk_{y2r} \ddot{y}_{2raw}^* + (k_{12}' - k_2') k_{y2r} y_{2raw}^* - k_{12}' k_{y1r} y_{1raw}^* = k_{u2}' u_2^* \quad (5.4-4)$$

where

$$k_{yir} = \left. \frac{\partial y_{ical}}{\partial y_{iraw}} \right|_{y_{irawo}} = \frac{-e_i}{(y_{1rawo})^2} - \frac{-f_i}{(y_{1rawo})^{3/2}} + h_i, \quad i=1, 2 \quad (5.4-5)$$

$$y_{iraw}^* = y_{iraw} - y_{irawo}, \quad i=1, 2$$

and  $y_{irawo}$  is the raw sensor output corresponding to  $y_{io}$  ( $\approx y_{icalo}$ ). Note that the gain slope of  $y_{1raw}$  has reversed polarity from that of  $y_{1cal}$  (e.g. as the magnet #1 position increases,  $y_{1raw}$  decreases). Thus  $k_{y1}$  is always negative.

## 6. Experiments

This chapter outlines experiments which identify the plant characteristics and parameters, implement a variety of control schemes, and demonstrate many important control principles. The versatility of the software / hardware system allows for a much broader range of experimental uses than will be described here and the user is encouraged to explore whatever topics and methodologies may be of interest. The safety portion of this manual, Section 2.3, must be read and understood by any user prior to operating this equipment.

The instructions in this chapter begin at a high level of detail so that they may be followed without a great deal of familiarity with the apparatus and the Executive program's system interface and become more abbreviated in details of system operation as the chapter progresses. To become more familiar with these operations, it is strongly recommended that the user read Chapter 2 in its entirety prior to undertaking the operations described here. Remember here, as always, it is recommended that the user save data and control configuration files regularly to avoid undue work loss should a system fault occur. The graphical description of the MagLev apparatus, Figure 6.1-1, should be referred to in following the instructions of this section.

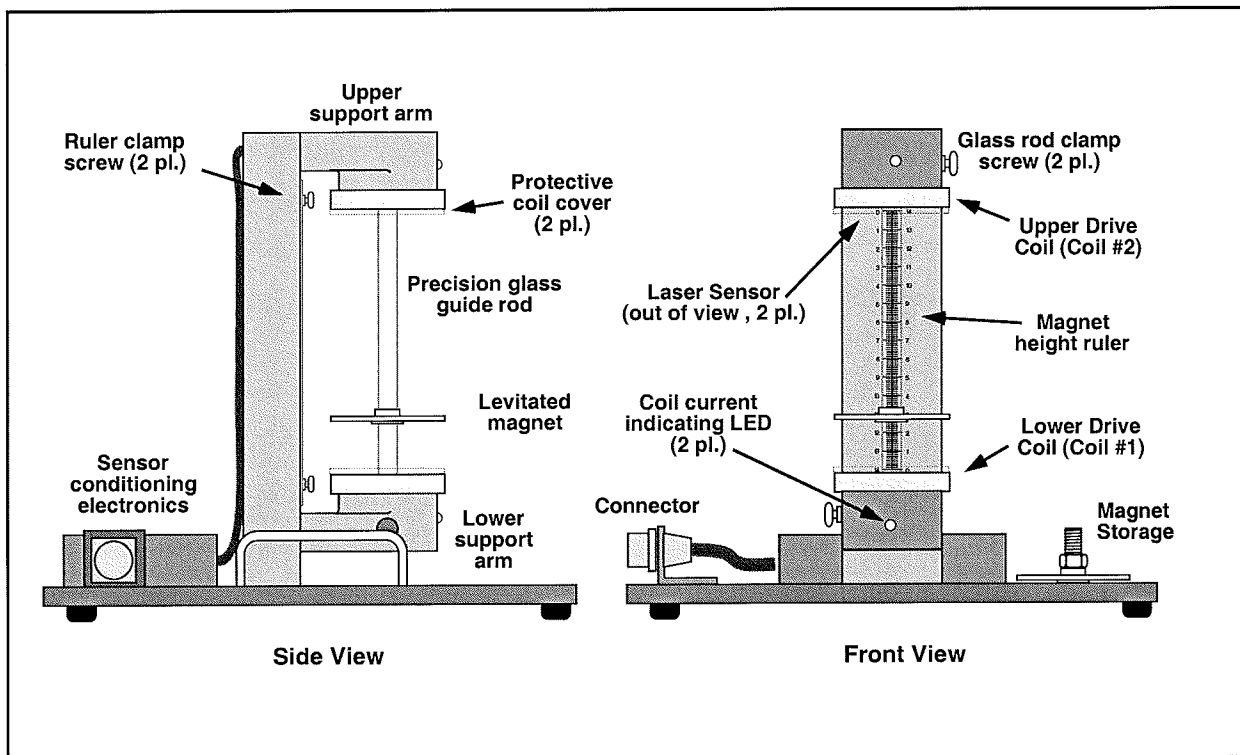


Figure 6.1-1. MagLev Apparatus

## 6.1 System Identification

This section gives a procedure for identifying the plant parameters and nonlinear characteristics given in Chapter 5. The approach will be to measure the specific input/output characteristics of the laser sensor and magnet/coil actuators and the magnet/magnet interactions as they vary with relative position. The laser position nonlinearity results from the nature of the change of light intensity on the detector with magnet position and is associated with the particular sensor used. The strong magnetic field nonlinearities, however, are inherent in this class of magnetic systems.

### 6.1.1 Sensor Characteristic

#### Procedure

1. Setup the mechanism with one magnet only resting on the lower drive coil (See Section 2.2 regarding installing the magnets and cleaning the white diffuse reflective surfaces if necessary). Make certain that your hands are clean at all times when touching the magnet - avoid touching the white surface. Power to the Control Box should be off. Construct tables similar to of Table 6.1-1, -2 to record data.
2. Enter the Setup Sensor Calibration box via the Setup menu, and verify that *Use Raw Sensor Counts* and *Apply Thermal Compensation* are selected. Select *OK* to exit to the background screen. Select *Abort Control* to make sure that no real-time controller is active. Turn on power to the Control Box. You should see the laser light beam on the upper and lower magnet surfaces. Move the magnet manually up and down to verify that the sensor counts displayed on the Background Screen are changing.
3. Sight along the top of the magnet and adjust the ruler height so that the 0 cm. position precisely matches the plane of the top of the magnet.
4. Record the raw sensor output at the 0 cm. position as read from the *Sensor 1* display on the Background Screen. Refer to the notes below regarding moving the magnet to the desired calibration positions and reading the sensor counts. Manually move the magnet to the 0.50 cm position and read and record the raw sensor output. Continue moving and recording the sensor data according for the magnet positions in Table 6.1-1.
5. Repeat Steps 1 through 3 for the upper sensor. Here you will need to sight off the bottom surface of the magnet. In this case "Magnet Position" is the distance below its uppermost travel. Note that by convention, the displacements of the upper magnet are negative-going as the magnet moves downward.

#### Notes on taking sensor calibration data:

- 1) Hold the magnet only by the edges and do not block the laser light.
- 2) Apply light finger pressure radially inward so that the magnet bushing is snug against one side of the glass rod. This will assure that the magnet is not cocked relative to the rod and is approximately horizontal. It should



also assure that the magnet does not move during the measurement. Any movement can lead to inaccurate results. Further enhancement in the accuracy of results of this and the next section may be obtained by taping a ruler (cm./mm. graduations) along side of the upper and lower sensor/coil support arms with the ruled edge very close to the magnet travel zone. In this way the magnet height may be more reliably read.

- 3) When the magnet is at the close end of travel relative to the sensor (at the bottom for sensor #1, at the top for sensor #2) you should rotate it and find the clocking position where the sensor output is approximately the average of the highest and lowest values. There may be as much as  $\pm 1000$  counts difference between the highest and lowest values (if there is more than this you should clean the white surface per the instructions of Section 2.2.2). This amounts to an equivalent position measurement error of less than 1 mm and becomes much less for positions further away from the coil. You should try to maintain this approximate clocking for the remainder of the magnet positions at which you take sensor data in Step 4 (e.g. keep the magnet polarity "N" label pointed in the same direction).

There will be some noise in the sensor reading; you should "visually average" the values displayed. You need only read the sensor to three significant digits for the purposes here.

**Table 6.1-1. Sensor Calibration / Linearization Data**

Magnet Position For Sensor #1 (cm)	$Y_{1raw}$ (Sensor 1, counts)	Magnet Position For Sensor #2 (cm)	$Y_{2raw}$ (Sensor 2, counts)
0.00		0.00	
0.50		-0.50	
1.00		-1.00	
2.00		-2.00	
3.00		-3.00	
4.00		-4.00	
5.00		-5.00	
6.00		-6.00	

6.1.2 Actuator Characteristic

The mechanism should be in the same configuration as in the last section. Assure that the north pole of the magnet is facing upward. The ruler should again be adjusted to measure off the upper surface of the magnet when it is resting in its lowermost position.

Procedure

1. Write a simple real-time algorithm to activate actuator coil #1 (i.e. put control effort values on the DAC) with a constant control effort of 5000 counts.<sup>1</sup> Review the algorithm with your instructor or laboratory supervisor before proceeding to the next step.
2. Implement this algorithm using the following steps:
  - a) Enter Setup Control Algorithm via the Setup menu and select *Edit Algorithm*. You are now in the control algorithm editor. If the editor contains any text select *New* under *File*.
  - b) Type in your algorithm. Select *Save As...* and choose an appropriate name and directory to save this algorithm in. Close the editor by either selecting *Save Changes and Quit* or simply clicking on the upper right hand button.
  - c) Stay well clear of the apparatus when initially performing the next step. Select *Implement Algorithm* to begin immediate execution of your algorithm. You should see the lower magnet levitate roughly 1 cm.
3. Record the height of the magnet corresponding to 5000 counts in a table similar to Table 6.1-2. You may wish to spin the magnet (again touching only its edge) to reduce the effects of friction so that the true equilibrium height is observed.
4. Re-enter the algorithm editor via *Edit Algorithm*, reduce the control effort to 4000 counts, select *Save Changes and Quit*, and *Implement Algorithm*. You should notice the magnet height become lower. Record the magnet height.
5. Repeat step 4 to find the control effort value at which the magnet is lifted only a very slight amount above the support pads (i.e. the 0<sup>+</sup> position). Again, you may wish to spin the magnet to reduce the effects of friction.
6. Repeat step 4 for the remaining control effort values of Table 6.1-2. Select *Abort Control* immediately after measuring magnet height to minimize heat build-up in the coil and servo amplifiers during exposure to the higher control effort values (those greater than 10,000 counts) Do not exceed 22,000 counts of control effort.

---

<sup>1</sup> These counts are converted to a voltage via a digital-to-analog converter (DAC), then to a current via the servo amplifier, to a magnetic field via the coil, and finally to a force by repulsion of the magnet's magnetic field. The scaling of all of these transformations affect the system gain and will be examined in more detail in the sections that follow. See also Chapter 4 for a description of the control hardware and software functionality.

Table 6.1-2. Actuator Calibration / Linearization Data

Magnet Position (cm)	$u_{I_{raw}}$ (Uncompensated Control Effort, counts)
0.00	
	4000
	5000
	6000
	8000
	10000
	12000
	14000
	18000
	22000

### 6.1.3 Magnet-to-magnet Force Characteristic

The interaction of the two magnets has a nonlinear force characteristic. When two magnets are used in the MagLev apparatus, they are typically stacked with like poles facing each other so that they repel. When the lower magnet is stationary, the upper magnet comes to rest in equilibrium between the upward repulsive magnet force and downward gravitational force. The magnetic force characteristic may be measured by adding and subtracting weight from the upper magnet and measuring the equilibrium height. The measurement technique is similar to that of the previous section. For Model 730 this characteristic does not vary appreciably from system to system. Results of a typical test are shown in Table 6.1-3.

The student is not required to repeat these measurements. The student may however wish to install the second magnet and witness the remarkably strong magnet-to-magnet repulsion of these rare-earth magnets and the effective spring (nonlinear) that is created with the force of gravity acting downward and the repulsive magnetic force acting upward. Be careful when handling the magnets in this process. The procedures of Section 2.2.2 must be followed closely to avoid damaging the magnets.

Table 6.1-3. Magnet-to-magnet Force Interaction Data

Weight at Magnet #2 ( $f_{m_{12}}$ , N)	Magnet #2 Position Relative to Magnet #1 At Equilibrium ( $y_{12}$ , cm)
0.402	11.73
0.612	10.30
0.735	9.57
0.998	8.80
1.190	8.09
2.171	6.72
3.152	5.90
4.133	4.78
6.095	4.25
11.00	2.74

#### 6.1.4 Mass of Magnet

The final salient properties of the magnet in the MagLev apparatus and its dynamic environment are its inertia (or mass) and the associated force (weight) due to the earth's gravitational field.

#### Procedure

1. Determine the mass and weight of the magnet (including the bronze bushing). You may use the "free" magnet stowed at the magnet storage post and assume both magnets to be equal. Mass should be measured to the nearest gram.

#### Questions / Exercises:

- A. Plot the sensor #1 output ( $y_{I_{raw}}$ ) as a function of magnet height. Plot the inverse of this function (magnet height as a function of  $y_{I_{raw}}$ ). Use curve fitting techniques to find a set of coefficients  $\{e^*, f^*, g^*, h^*\}$ <sup>1</sup> in Eq.(6.1-1) that yields values of  $y_{I_{cal}}^*$  that closely match your data

<sup>1</sup> The inverse and inverse square terms in Eq. 6.1-1 are physically motivated by the inverse and inverse square relationships obtained by optical analysis of the fan-beam laser light scattered and reflected off the diffuse white surface of the magnet and incident in the detector (see Section 4.5). The constant and linear terms give additional degrees of freedom in the curve fitting to accommodate the various affects of masking of the reflected light from the detector at close magnet distances and other non-nominal optical geometric and surface reflectance factors.

(within 1 mm for the 0 and 0.5 cm position and within 0.5 mm for all other points) at the locations measured in Table 6.1-1. Using these coefficients, plot  $y_{1cal}^*$  ( $y_{1raw}$ ) on the same plot as the test data to show the closeness of the match. Repeat this procedure for the Sensor #2 output.

$$y_{1cal}^* = \frac{e^*}{y_{1raw}} + \frac{f^*}{\sqrt{y_{1raw}}} + g^* + h^* y_{1raw} \quad (6.1-1)$$

Scale the coefficients such that the new set  $\{e, f, g, h\}$  result in values of  $y_{1cal}$  having units 10,00 times smaller. I.e. the new calibration is

$$y_{1cal} = \frac{e}{y_{1raw}} + \frac{f}{\sqrt{y_{1raw}}} + g + h y_{1raw} \quad (6.1-2)$$

with  $y_{1cal}$  having resolution of 10,000 counts per cm. This finer resolution will be used to reduce computational quantization effects during subsequent digital processing. Find the same scaling for sensor #2.

- B. The experiments in Section 6.1.2 found the equilibrium height of the magnet for a given control effort (in controller counts or, proportionally, current in the coil). Equivalently, the same information establishes the control effort  $u_{1test}$ , required to produce a constant force on the magnet  $F_w$  (equal to the magnet's weight) as a function of magnet height. Plot your data from 6.1.2 showing this required control effort,  $k^*_{u_{cor}} (= u_{1raw})$  as a function of magnet height. Solve for coefficients  $\{a, b\}$  to fit this data with a function<sup>1</sup>

$$F_w = \frac{u_{1test}}{a(y_1 + b)^4} \quad (6.1-3)$$

within a tolerance of  $\leq 400$  counts at a given height. From the closeness of the fit of Eq. (6.1-3) to your data, is the form of this equation a reasonably close approximation of the coil-magnet force term in Eq.(5.1-3?) (As a point of reference, typical servo amplifier nonlinearities are on the order of 2-10%) What are the units of the denominator in the right hand side of Eq.(6.1-3)?

In certain control schemes, we shall later invert (approximately) the actuator nonlinearity in a real-time algorithm according to

<sup>1</sup> The fourth power form is used because it is shown to yield a sufficiently close approximation of the empirical data (the student should verify this) and is less computationally intensive to implement in real-time processing than non-integer forms.

$$\underbrace{(a_c(y_{1cal} + b_c)^4)}_{\text{control effort compensation}} \underbrace{\left(\frac{1}{a(y_1 + b)^4}\right)}_{\text{plant actuator nonlinearity}} \triangleq K_{u_1} F_{u_1} \stackrel{\Delta}{=} 1 \tag{6.1-4}$$

where  $y_{1cal}$  is the available measurement or estimate of the magnet position, and  $F_{u_1}$  is the force on the magnet. For convenience of notation, we define

$$K_{u_1}(y_{1cal}) \triangleq (a_c(y_{1cal} + b_c)^4) \tag{6.1-5}$$

with  $K_{u_1}$  being the nonlinear control effort compensation routine. (In real-time processing, the values sent to the DAC will be  $u_1 K_{u_1}$ ). Solve for the coefficients  $\{a_c, b_c\}$  with scaling such that when  $u_1 = 10,000$  counts, a force of 1 N is exerted on the magnet.

The attractive magnetic characteristic (force v. distance) of the upper coil/magnet is essentially the same as the repulsive one of the lower coil/magnet. Assuming that the upper actuator is configured so that a positive control effort imparts an attractive force on the magnet, what are  $a_c$  and  $b_c$  for the upper actuator?

- C. From the data of Table 6.1-3, find a set of coefficients  $\{c, d\}$  in the relationship

$$F_{m_{12}} = \frac{c}{(y_{12} + d)^4} \tag{6.1-6}$$

so that the inter-magnet force  $F_{m_{12}}$  for a given magnet-to-magnet separation  $y_{12}$  is within 300 N of the data values in the table. From the closeness of the fit of Eq. (6.1-6) to your data, is the form of this equation (fourth order denominator) a reasonably close approximation of the coil-magnet force term in Eq. (5.1-7)?

- D. State the measured value of the weight of the magnet in Section 6.1.4. Can you think of a simple way to physically manipulate the MagLev apparatus to obtain the measured magnet separation for weights less than this value as shown in Table 6.1-3?

### 6.1.5 Verification of Calibration / linearization Results

In this section we verify through real-time implementation that the derived calibration and linearization expressions from the previous sections are valid.

### Preparation

1. Generate a real-time algorithm that operates on the raw sensor data (this is the global variable `sensor1_pos` in the real-time environment<sup>1</sup>) and outputs the linearized position measurement,  $y_{I_{cal}}$ . Assign the variable `q10` to the values of  $y_{I_{cal}}$ . (this is one of four variables, `q10` through `q13`, available for general plotting - see Section 2.1.7). Assign both `control_effort1` and `control_effort2` equal to zero to assure that no current is driven through the coils.
2. Generate a second algorithm that applies a constant force to the magnet equal to one half the weight of the magnet. The algorithm should use the linearized position routine ( $y_{I_{cal}}$ ) from the previous step and generate a constant control effort as per the relationship of Eq. (6.1.4). The output of this algorithm assigns the appropriate real-time value to the variable `control_effort1`. (Recall that `control_effort1` is a special variable whose value gets written to the DAC for voltage output to the servo amplifier and subsequent current output to the coil)
3. Have your laboratory supervisor check and approve both algorithms before proceeding.

### Procedure

4. Implement the algorithm of Step 1 as per the process of Step 2 of Section 6.1.2 with  $T_s=0.00442s$ . selected. Save this in a file for later use.
5. Go to Trajectory 1 Configuration under the Setup menu and enter Step. Specify a *Step Size* of 0 counts, a *Dwell Time* of 15000 ms, and 1 *repetition* (this prepares the system to execute a zero valued input for a total duration of 30 sec while data may be acquired) Select *OK*, successively and enter Setup Data Acquisition (Setup menu). Specify *Sensor 1 Position* and *Q10* as data to be acquired with a *Sample Period* of 5 servo cycles. Verify that the sensor calibration is set up as described in Step 2 of Section 6.1.1. (In the future, the sensor calibration will be specified via this dialog box for convenience).
6. Go to Execute (Command menu) and specify *Normal Data Sampling* and *Execute Trajectory 1 only*. Prepare to manually move the magnet (clean hands, edges only!) incrementally in steps of 1 cm. from 0 to 6 cm. as measured visually via the ruler. You should wait for about a second, then move the magnet to the 1 cm position and hold it there for one or two seconds, then move on to the next whole centimeter position. Practice doing this so you can complete all seven positions within 30 seconds while holding it still briefly at each position. Select *Run* and perform the described procedure.
7. Go to Setup Plot (Plotting menu), and plot the *Sensor 1* (raw) data on the left vertical axis and *q10* on the right. You may want to rescale the plot axes via *Axis Scaling*. The plot should show the nonlinear characteristic of the raw sensor data and the linear nature of the corrected output. You may repeat Step 6 if you are dissatisfied with your result. Print and save (Plotting menu) your plot. You may repeat this process for the upper sensor if you wish.

---

<sup>1</sup> In subsequent experiments we shall enter the calibration coefficients via the Setup Sensor Calibration when the calibrated sensor option is selected. The global variable `sensor1_pos` then becomes the calibrated/linearized sensor data.

8. Implement the algorithm generated under Step 2 above. In this and all subsequent procedures, do not move the magnet beyond 4.0 cm. height. This will cause excessive current to flow through the actuator coils and could damage the equipment. Slowly move the magnet through the 0 to 4 cm. *operational range*. Can you feel it's apparent weight being approximately half its true weight? Observe the Control Effort 1 value displayed on the Background Screen. How does it vary with position of the magnet? Modify the algorithm so that the upward force is approximately equal to the magnet weight. Hold on to the edge of the magnet and implement the algorithm. Does the magnet feel approximately weightless through the operational range? Again observe the change in control effort with position. You may make another trial with the control effort equal to 1.2x the magnets weight. (This time do not exceed a height of 3 cm.). In this case do not move the magnet beyond 3.5 cm & make sure that you hold on to the magnet when you implement the algorithm! Save the algorithm to a file for later use.

#### Questions / Exercises:

- E. Submit your plot of the sensor output v. position from Step 7. Describe the salient differences between the raw and corrected sensor signals.
- F. Describe the change in control effort with magnet position from Step 8. Explain briefly. Does the effective force on the magnet change appreciably? Explain briefly.
- G. Figure 6.1-2 is a control block diagram for a single magnet (at the lower position, sensor/actuator #1) showing the nonlinear elements of the magnetic field and sensor and the effect of gravity acting on the magnet. It also contains a forward path Controller block and the linear portion of the plant dynamics,  $G(s)$ . Expand on this block diagram to show where the compensation algorithms developed in Sections 6.5.1&2 (i.e.  $y_{I_{cal}}$  ( $y_{I_{raw}}$ ) and  $K_{uI}$  ( $y_{I_{cal}}$ )) may be introduced to effectively remove the nonlinearities. Include the signal flow from the position measurement to the control effort compensation. Indicate which elements would be implemented in real-time processing and which are part of the "natural" system. Show also where a feedforward signal may be introduced to negate the effects of gravity. When introduced in the proper location in the signal flow, this signal can compensate for gravity for all  $y_I$  in the operational range. Are the nonlinearity compensation and gravity feedforward algorithms static (time independent) or dynamic in nature? Describe how would this block diagram be changed to depict the system of a magnet in the upper position (sensor/actuator #2)?
- H. Draw a simplified block diagram of the system assuming that the sensor and control effort algorithms are effective at linearizing the respective nonlinearities. For later control design purposes, the system gain must be evaluated. For a system of this type<sup>1</sup>, the forward path gain – which

<sup>1</sup> The description of gain applies to a rectilinear translating lumped inertia type plant with position feedback.



we will call  $k_u$ , - is the amount of force imparted on the plant per unit of control effort. The return path gain – which we will call  $k_s$  - is the position measurement signal value per unit length of motion at the plant output. For purposes of calculating the gains, all physical properties should be evaluated in terms of consistent SI units. On your block diagram, show the value of the gains net of the sensor and control effort compensation algorithms as  $k_s$  and  $k_u$  respectively and indicate their value and units.

What is the expression for  $k_u$  in the case that control effort nonlinearity compensation is not included? What is the expression for  $k_s$  in the case that the sensor nonlinearity compensation is not included?

What are their units?

The system gain,  $k_{sys}$ <sup>1</sup> is defined as follows

$$k_{sys} \triangleq \text{the product of all the gains in the loop except the controller} \quad (6.1-7)$$

What is the value of  $k_{sys}$  for the fully compensated system? What are its units? In general terms, how does the system gain change with position for the uncompensated sensor and actuator?

I. For control modeling purposes, the system gain should be lumped with the plant model (e.g. as a factor in the numerator of a SISO transfer function). Based on your parameter values obtained in this section and the appropriate equations in Chapter 5, construct the numeric plant models for three cases for the lower (sensor/actuator #1) SISO plant. Express your answer in transfer function and state space forms.

- 1) A system using the raw sensor counts as feedback and no compensation of the actuator nonlinearity. The plant should be linearized about the operating point  $y_{1o} = 2.0$  cm and  $u_{1o} =$  control effort required to maintain static equilibrium at  $y_{1o}$ .
- 2) The same as 1 above except the sensor nonlinearity is compensated for.
- 3) The same as 2 except the actuator nonlinearity is compensated for and the system may operate throughout its range (i.e. the model is not linearized about any particular operating point).

Repeat steps 1 through 3 above for the upper sensor/coil location where the equilibrium point (where applicable) is about  $y_{2o} = -2.0$  cm and  $u_{2o}$

<sup>1</sup> The measurements of sensor and actuator characteristic contain the gains of the various system components such as the sensor analog output, the ADC, the DAC, the servo amplifier, and the coil-magnet force field. They also of course contain the gains specified for scaling.

is the control effort required to maintain this equilibrium.

- J. Construct the numerical plant model for the MIMO system with the magnets stacked so that they repel each other. Construct both the transfer matrix and state space models for each of the three nonlinear compensation approaches (no compensation, sensor compensation, sensor & actuator compensation) described in Exercise I. The equilibrium positions are  $y_{1o} = 1.0$  cm,  $y_{2o} = -2.0$  cm. In the case of the fully compensated plant, the magnet-to-magnet interaction force,  $F_{m_{12}}$  will remain as a nonlinear term. You may use the linearized term,  $k'_{12}$  for this force where linearization is about the equilibrium positions above. You may assume that the available magnet travel distance,  $y_c = 13.3$  cm.

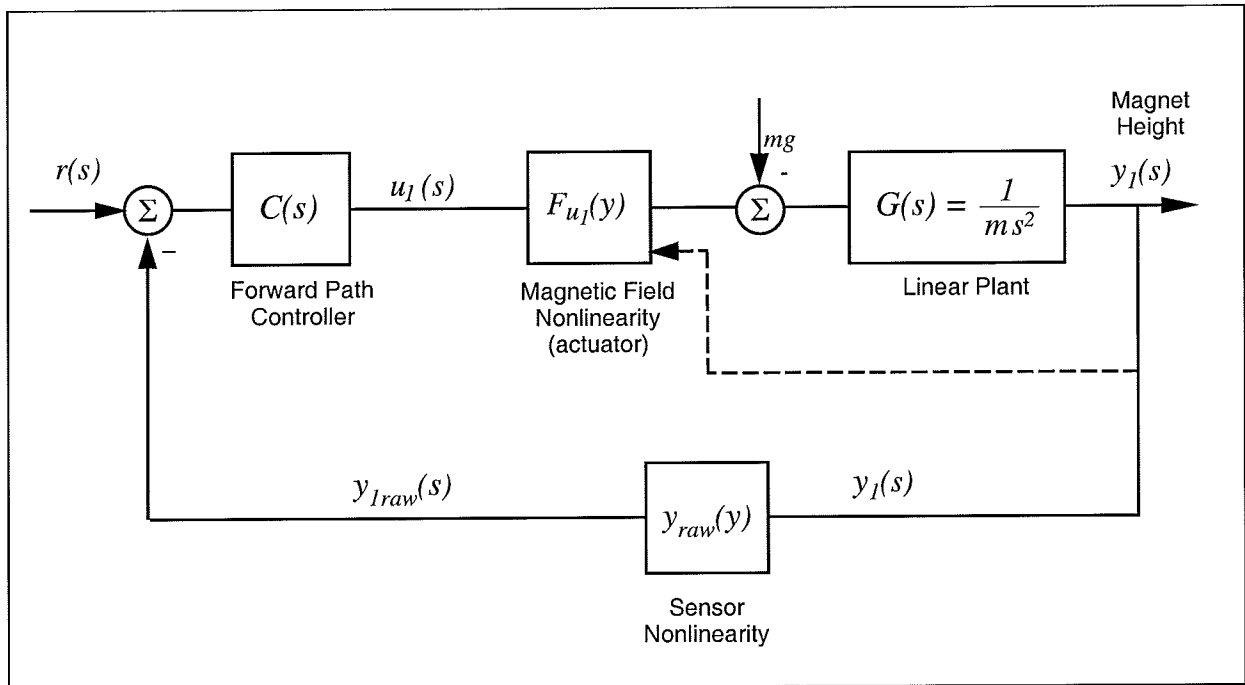


Figure 6.1-2. Block Diagram of SISO System Showing Nonlinear Elements

### 6.2 Nonlinear Plant Control: Linearization About Operating Point

This section implements a simple linear proportional plus rate feedback controller about the nonlinear plant. It uses the uncompensated plant and associated model developed in the last section. The control effort to offset gravity at the operating point is fed forward. The block diagram of the closed loop system is shown in Figure 6.2-1.

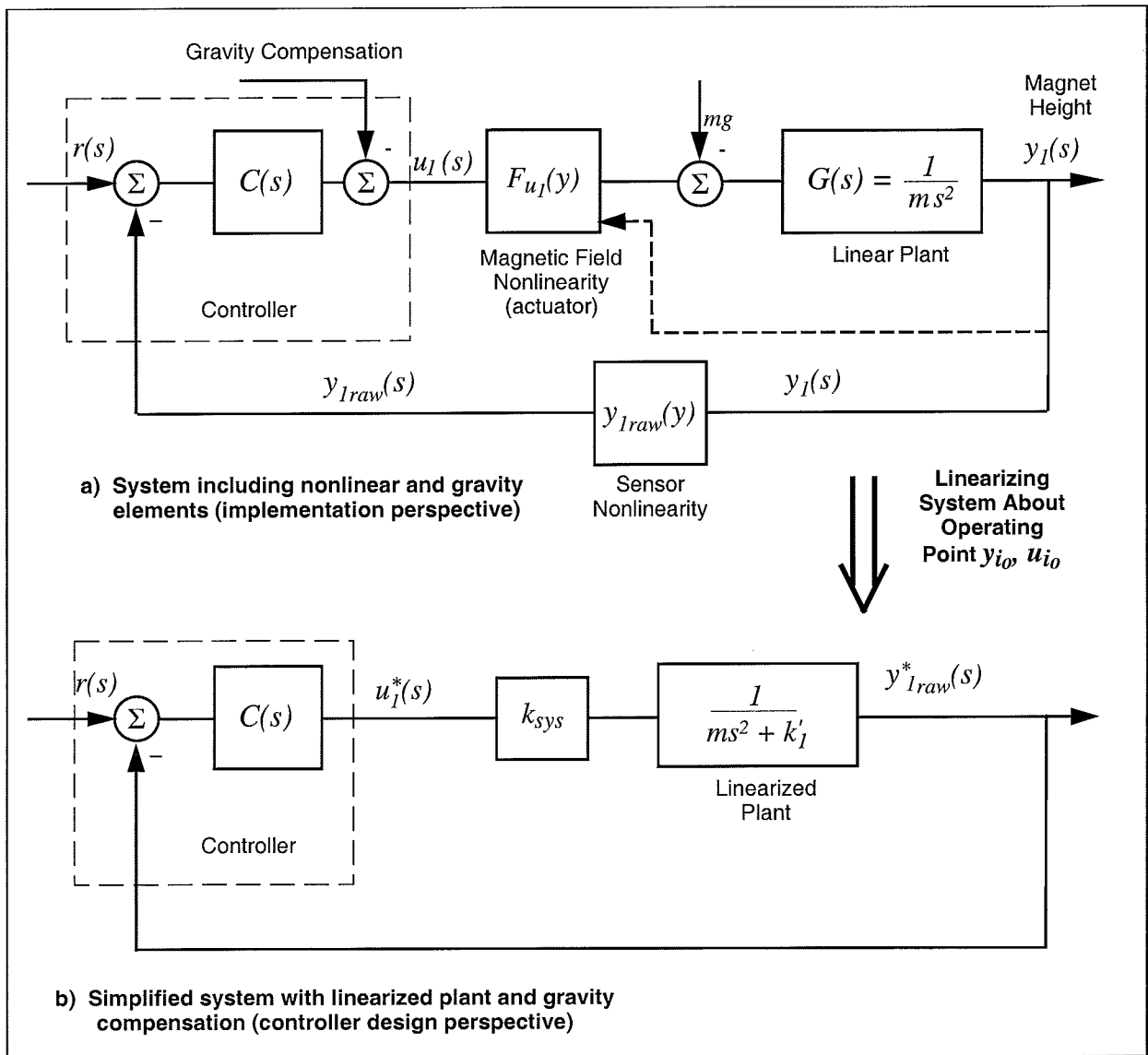


Figure 6.2-1. Reduction of System to Linearized Form

In the procedures that follow, we will design a controller for the linearized system model and measure the effectiveness of the control system for small and large motions about the operating point. We will also investigate the stability (and instability) of the plant and its implication to closed loop stability.

The closed loop block diagram using proportional plus rate feedback control is shown in Figure 6.2-2.<sup>1</sup> It incorporates the linearized plant model and assumes the gravity feedforward  $u_{i0}$  offsets the effect of gravity on the magnet at equilibrium.

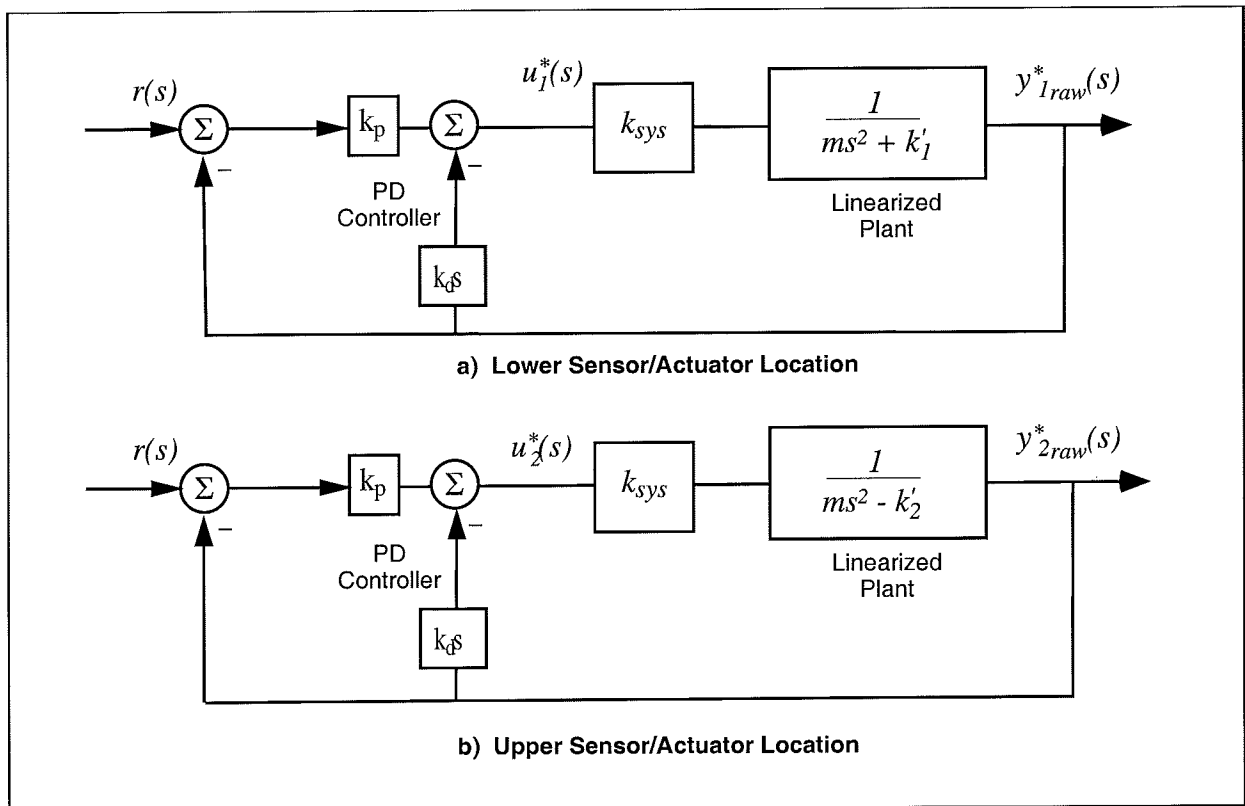


Figure 6.2-2. Control Design Block Diagrams

From Figure 6.2-2, the closed loop transfer functions for the lower (repulsive) and upper (attractive) systems are respectively:

$$\frac{y_{1raw}^*(s)}{r(s)} = \frac{(k_p k_{sys1})/m}{s^2 + (k_d k_{sys1}/m)s + (k_p k_{sys1} + k'_1)/m} \tag{6.2-1}$$

<sup>1</sup> The controller incorporates the derivative action  $k_d s$  in the return path rather than using the forward path PD form:  $C(s) = k_p + k_d s$ . This is to more clearly demonstrate certain fundamental properties of this class of control systems in this and subsequent experiments. The characteristic equation and hence stability of the two system forms is identical, but their responses to dynamic inputs is different.

$$\frac{y_{2raw}^*(s)}{r(s)} = \frac{(k_p k_{sys2})/m}{s^2 + (k_d k_{sys2}/m)s + (k_p k_{sys2} - k_2')/m} \quad (6.2-2)$$

Considering the lower plant and defining:

$$\omega_n \triangleq \sqrt{\frac{k_p k_{sys1} + k_1'}{m}} \quad (6.2-3)$$

$$\zeta \triangleq \frac{k_d k_{sys1}}{2m \omega_n} \quad (6.2-4)$$

we may express:

$$T(s) = \frac{\omega_n^2}{s^2 + 2\zeta\omega_n s + \omega_n^2} \quad (6.2-5)$$

This form also holds for the upper plant where

$$\omega_n \triangleq \sqrt{\frac{k_p k_{sys1} - k_2'}{m}} \quad (6.2-6)$$

$$\zeta \triangleq \frac{k_d k_{sys2}}{2m \omega_n} \quad (6.2-7)$$

### Procedure :

#### PD Control Design

1. Using the appropriate numerical models of the previous section and the expressions above, design controllers (i.e. find  $k_p$  &  $k_d$ ) for a system natural frequency  $\omega_n = 4$  Hz, and  $\zeta = 0.5$  for both the lower (repulsive levitation) and upper (attractive levitation) locations. Design also the gains required for  $\omega_n = 6$  Hz and  $\zeta = 0.5$  in each case.
2. Generate a real time control routine that implements the block diagram of Figures 6.2-1a and 6.2-2a for the lower coil/sensor system and includes the following. The equilibrium operating point should be at  $y_{I_o} = 2.0$  cm.
  - a) execution of the real-time PD algorithm shown in Figure 6.2-2.
  - b) feedforward of the equilibrium gravity offset control effort  $u_{I_o}$
  - c) subtraction of the equilibrium position,  $y_{raw_o}$ , from the feedback sensor signal  $y_{raw}$  to provide  $y_{raw}^*$  for control law execution and plotting.
  - d) use of the backwards difference transformation to implement discrete time differentiation according to

$$s \approx \frac{1-z^{-1}}{T_s} \quad (6.2-8)$$

to approximate the rate feedback signal with a sample period of 0.884 ms.

- e) use of `cmd1_pos` as the reference input to the controller.
- Repeat Step 2 for the upper system. Have your laboratory supervisor review and approve your algorithms before proceeding. Your control gains should be in the range of  $-2 \leq k_p < 0$ ,  $-0.1 \leq k_d \leq -0.02$  for the lower magnet/coil system and  $1 \leq k_p \leq 4$ ,  $0.02 \leq k_d \leq 0.1$  for the upper system. You may wish to use `cmd2_pos` as the reference input signal. The equilibrium should be calculated for  $y_{2_0} = -2.0$  cm.

#### PD Control Implementation – Lower Magnet Position

- Set-up the plant with a single magnet with the north pole facing upward (See Section 2.2.2; handle magnets by edges only and do not touch the glass rod with bare hands [e.g. use a clean cloth]). Verify that *Use Raw Sensor Counts* and *Apply Sensor Calibration* are selected under Setup Sensor Calibration.
- Turn on power to the Control Box. Enter the Control Algorithm box under Setup and set  $T_s = 0.000884$  s. Implement your algorithm from Step 2 above. The magnet should levitate to the 2 cm. position. Use a clean non-sharp object such as the eraser end of a pencil to lightly perturb the magnet to assure that the control system is stable.
- Set-up to collect Sensor #1 information via the Set-up Data Acquisition box in the Data menu with data acquisition sample period of 5 servo cycles ( $T_s$ 's). Set up a *Step* trajectory of 10000 counts, dwell time = 1000 ms, and 2 repetitions (Trajectory 1 Configuration box in the Command menu). Set this for a set of bidirectional steps (one up, one down) by deselecting *Unidirectional moves*.
- Execute* the bidirectional step maneuver and plot the Sensor 1 data. Save your plot. Note the shape of the response and the relative magnitudes of the upward and downward going curves. Note also the polarity of the plotted magnet motion v. the direction the magnet actually moved during the maneuver.
- Increase the step amplitude to 15000 counts and repeat the step maneuver. Continue increasing the amplitude in increments of 5000 counts until the magnet contacts the lower limit of travel (mechanical stop) during the downward portion of the maneuver.<sup>1</sup> Plot and save the case prior to this where the magnet does not contact the bottom. Record the input trajectory amplitude. Note the shape of the positive and negative going system step responses.
- Repeat Steps 5 through 8 for the 6 Hz control gains from Step 1 except perform the first step maneuver with an input amplitude of 3000 counts. (This yields roughly the same output amplitude as 10000 counts for the 4 Hz system. You should verify this from the results and be prepared to explain why this is the case.) Increase the amplitude in increments of 2000 counts to find the limiting amplitude without contacting the mechanical stop.

#### Control Implementation—Upper Magnet Position

- Set the plastic clip on the glass rod (See Section 2.2.2) so that the magnet cannot fall below 4 cm from the upper mechanical stop. Prepare to implement

<sup>1</sup> You may have to modify your real-time algorithm by multiplying `cmd1_pos` by a constant to provide sufficient amplitude. It should not be necessary to use a constant greater than 4. Make sure that you properly compensate for this factor in specifying the step amplitude via the Trajectory dialog box. (The trajectory input amplitude is limited in software to impede inadvertent over-driving of the system. With the present control scheme however the output is substantially less than the reference input due to the relatively low net gains.)

your 4 Hz algorithm for the upper magnet position from Step 3. While holding the magnet at the approximate  $y_2 = -2$  cm position, implement the algorithm.

11. Execute a 1500 count bidirectional step (set this up via “Trajectory 2 if `cmd2_pos` is used in the control routine for the upper location) and plot and save the Sensor 2 data. Slowly increase the amplitude (e.g. use roughly 500 count increments initially, then smaller ones) and find the limiting case where the magnet remains levitated during the downward step but falls to the plastic safety clip<sup>1</sup> during this leg of the maneuver for any greater amplitude input trajectory. Plot and save this limiting case.
12. Repeat Steps 10 and 11 for the 6 Hz controller.

#### Questions:

- A. Consider the “linearized plant” for the repulsive levitation system in Figure 6.2-2a. Is this plant stable or unstable? Assuming  $k_p k_{sys}$  and  $k_d k_{sys}$  are positive, are there any conditions on these gains for the system of Eq. (6.2-1) to be stable?
- B. Does the polarity of the physical motion of the magnet agree with that of the plotted data (i.e. does the plotted data increase with upward motion of the magnet)? Explain. Describe the symmetry of the positive-going v. the negative-going (physical magnet motion) step responses for the lower position 4 Hz control system for the initial 10000 count trajectory. Describe this for the large amplitude steps (i.e. the largest case measured without contacting the mechanical stop). As will be studied later, the degree of overshoot and oscillation in the step response correspond to the effective damping ratio  $\zeta^2$ . Explain the differences in symmetry for each case in terms of the differences in  $k_{sys}$  at the various positions of the magnet during the maneuvers, and its effect on damping ratio [Eq. (6.2-4)] and steady state position error [via Eq. (6.2-1)].
- C. Repeat Exercise B for the case of the 6 Hz system in the lower magnet position. Compare the 4 Hz and 6 Hz responses. How do their symmetries of response (upward v. downward motion) compare with respect to their apparent damping. How do they compare with respect to steady state error (for a given reference input or trajectory amplitude)?
- D. Consider the “linearized plant” in Figure 6.2-2b for the upper magnet position. Is this plant stable or unstable? Assuming  $k_p$ ,  $k_{sys}$  and  $k_d$  are positive, are there any conditions on these gains for the system of Eq. (6.2-2) to be stable? If so what are they?
- E. Does the polarity of the physical motion of the magnet agree with that of the plotted data? Explain. Describe the symmetry of the positive-going

<sup>1</sup> You may consider the magnet to have fallen away from the controllable range even if it returns under control on the final leg of the trajectory. It would have fallen completely away if not for the safety clip.

<sup>2</sup> For  $\zeta < 1$  there is overshoot and are oscillations during settling that increase with decreased  $\zeta$ . For  $\zeta > 1$  the response becomes more heavily damped with no overshoot. You may not always see overshoot in the in the nominal design case of  $\zeta = 0.5$  for the present controller due to the effects of friction and the relatively low gains used.

v. the negative-going step responses for the upper position 4 Hz control system for the initial 2000 count trajectory. Describe this for the large amplitude steps (the largest without the magnet falling to the safety clip). Explain the differences in symmetry for each case in terms of the differences in  $k_{sys}$  at the various positions of the magnet during the maneuvers, and its effect on damping ratio and steady state position error [via Eq. (6.2-2)]. For a fixed position gain,  $k_p$ , there is a position at which reduction in the system gain results in instability. Find an expression for this position.

- F. Repeat Exercise E for the case of the 6 Hz system in the upper magnet position. Compare the 4 Hz and 6 Hz responses. How do their symmetries of response (upward v. downward motion) compare with respect to their apparent damping. How do they compare with respect to steady state error (for a given reference input or trajectory amplitude)? Which system has greater range of downward motion before the magnet falls away (system becomes unstable). Explain.

### 6.3 Control of Nonlinear Compensated SISO Systems

In this experiment, we shall employ the real-time algorithms established in Section 6.1 to compensate for the sensor and actuator nonlinearities and reduce the control design to that involving a simple rigid body plant. The detailed diagram showing the nonlinear compensation blocks that reduce to the form of Figure 6.3-1 was given as an exercise in Section 6.1

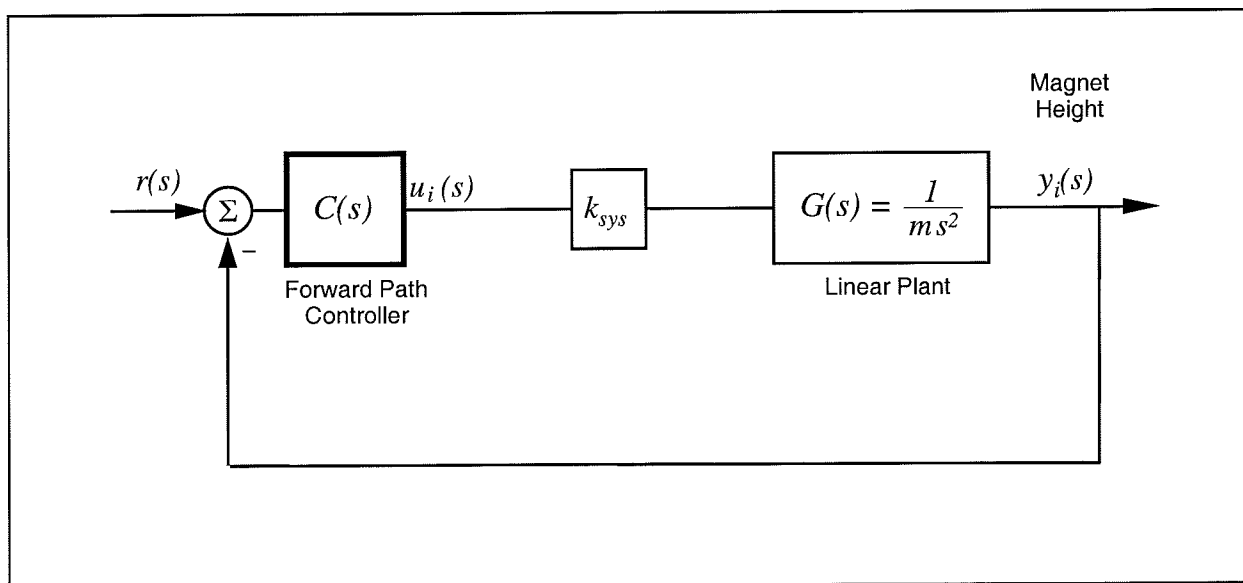


Figure 6.3-1. Block Diagram Model for System with Nonlinear Compensated Plant

We shall employ PD control and begin by reviewing some basic characteristics of PID controlled



rigid body plants. The block diagrams for forward and return path derivative action are shown in Figure 6.3-2. The corresponding transfer functions are for the respective subfigures “a” and “b”:

$$T(s) \equiv \frac{y(s)}{r(s)} = \frac{(k_{sys}/m)(k_d s^2 + k_p s + k_i)}{s^3 + (k_{sys}/m)(k_d s^2 + k_p s + k_i)} \tag{6.3-1a}$$

$$T(s) \equiv \frac{y(s)}{r(s)} = \frac{(k_{sys}/m)(k_p s + k_i)}{s^3 + (k_{sys}/m)(k_d s^2 + k_p s + k_i)} \tag{6.3-1b}$$

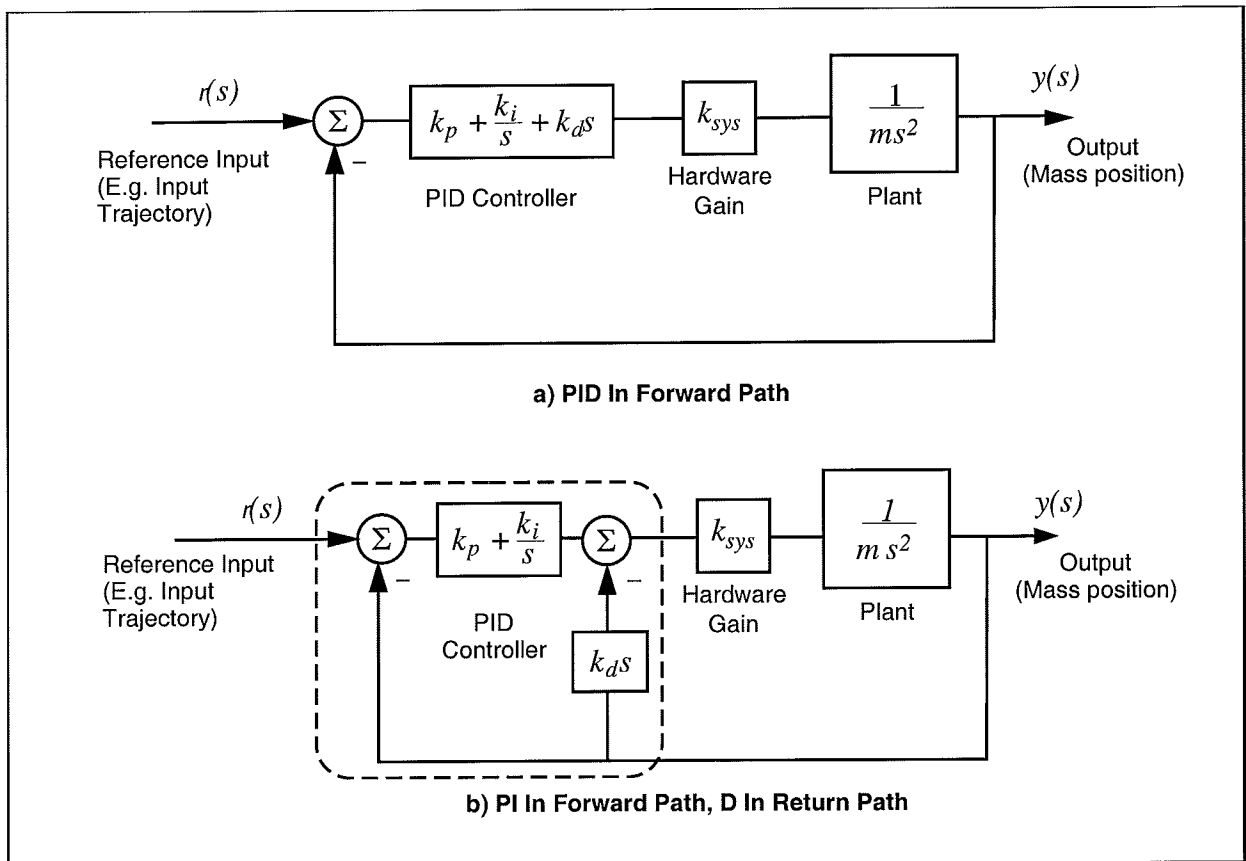


Figure 6.3-2. Rigid Body PID Control – Control Block Diagram

For the present experiments, we shall consider PD control only ( $k_i=0$ ). For the case of  $k_d$  in the return path the closed loop transfer function reduces to:

$$T(s) = \frac{k_p k_{sys}/m}{s^2 + (k_{sys}/m)(k_d s + k_p)} \tag{6.3-2}$$

By defining:

$$\omega_n \triangleq \sqrt{\frac{k_p k_{sys}}{m}} \quad (6.3-3)$$

$$\zeta \triangleq \frac{k_d k_{sys}}{2m \omega_n} = \frac{k_d k_{sys}}{2\sqrt{m k_p k_{sys}}} \quad (6.3-4)$$

we may express:

$$T(s) = \frac{\omega_n^2}{s^2 + 2\zeta\omega_n s + \omega_n^2} \quad (6.3-5)$$

We shall implement PD control structures on the nonlinear compensated plant in this section. In the next section we shall demonstrate the salient properties of the above class of system and study the effect of changing  $k_p$  and  $k_d$ .

### Procedure :

#### Control Design

1. Using the appropriate numerical model of Section 6.1 and the expressions above, design controllers (i.e. find  $k_p$  &  $k_d$ ) for a system natural frequency  $\omega_n = 6$  Hz, and damping ratio  $\zeta = 0.707$  for both the lower (repulsive levitation) and upper (attractive levitation) locations.
2. Generate a real time control routine that implements the block diagram of Figures 6.3-2b and your detailed block diagram from Exercise G of Section 6.1 for nonlinear compensation. You may use the routines developed in Section 6.1 for the nonlinear control effort compensation. You may use the dialog box Setup Sensor Calibration to implement the sensor compensation coefficients (the global variable `sensor1_pos` then linearized). This routine should be for the lower (repulsive) system with the operating point set at  $y_{1o} = 2.0$  cm and include the following:
  - b) feedforward of the equilibrium gravity offset control effort  $u_{1o}$  (recall that in this case  $u_{1o}$  is scaled in units of N/10000 counts)
  - c) subtraction of the equilibrium position,  $y_{1o}$ , from the sensor signal  $y_1$  to provide  $y^*_1$  for control law execution
  - d) assign the global variable `q10 = y^*_1` (this makes  $y^*_1$  available for plotting)
  - d) use of the backwards difference discrete time differentiation to approximate the rate feedback signal with a sample period of 1.768 ms.
  - e) use of `cmd1_pos` as the reference input to the controller.
3. Repeat Step 2 for the case of the upper (attractive) system using `cmd2_pos` as the reference input, the nominal position as  $y_{2o} = -2.0$  cm., and making all other appropriate changes in notation of the parameters and variables.

### Procedure :

#### Control Implementation

4. Set-up the plant with a single magnet with the north pole facing upward (See Section 2.2.2, handle magnets by edges only and do not touch the glass rod with bare hands [e.g. use a clean cloth])
5. Turn on power to the Control Box. Enter the Control Algorithm box under Set-up and set  $T_s=0.001768$  s. Implement your algorithm from Step 2 above. The magnet should levitate to the 2 cm. Position. Use a clean non-sharp object such as the eraser end of a pencil to lightly perturb the magnet to assure that the control system is stable.
6. Set-up to collect Variable Q10 ( $y_1^*$ ), Commanded Position 1, and Control Effort 1 information via the Set-up Data Acquisition box in the Data menu with the data acquisition sample period set for every 5 servo cycles. Set up a *Step* trajectory of 15000 counts, dwell time = 1000 ms, and 2 repetitions. Set this for a set of bidirectional steps by deselecting *Unidirectional moves*.
7. *Execute* the step maneuver and plot the Variable Q10 and Commanded Position 1 data. Plot a second graph showing the control effort (use right hand plot axis) Save your plots.

#### Control Implementation—Upper Magnet Position

8. Set the plastic clip on the glass rod (See Section 2.2.2) so that the magnet cannot fall below 4 cm from the upper mechanical stop. Prepare to implement your algorithm for the upper magnet position from Step 3. While holding the magnet at the approximate  $y_2 = -2$  cm position, implement the algorithm.
9. Set-up to collect Variable Q10 ( $y_2^*$ ), Commanded Position 2, and Control Effort 2 data. Execute a 10000 count bidirectional step and plot the Variable Q10 and Commanded Position 2 data. Plot a second graph showing the control effort (use right hand plot axis) Save your plots.

#### **Questions:**

- A. Compare the responses obtained in this section with those of the previous section. Specifically, how do the symmetry of response and steady-state errors compare? Is the upper position (attractive levitation) response substantially different than the lower one? Explain.
- B. Consider the control effort data from the maneuvers of this section. Visually average the data (approximate its mean value) through each step segment. Describe the relative change in control effort with magnet position (i.e. its absolute position relative to the coil) for both the upper and lower magnets. What is the relationship between control effort and dissipated power (hence heat) in the drive coil? What is the approximate ratio of power dissipated in the lower coil between the lower and higher levitated heights of the step maneuver? Does the control effort exhibit more or less noise than the position sensor signal? Why?

## 6.4 Fundamental Properties Of Second Order Systems

This experiment demonstrates some key concepts associated with proportional plus derivative (PD) control and subsequently the effects of adding integral action (PID). This control scheme, acting on plants modeled as rigid bodies finds broader application in industry than any other. It is employed in such diverse areas as machine tools, automobiles (cruise control), and spacecraft (attitude and gimbal control). The block diagram for forward path PID control of a rigid body was shown in Figure 6.3-2a where friction is neglected.<sup>2</sup> Figure 6.3-2b shows the case where the derivative term is in the return path. Both implementations are found commonly in application and –as the student should verify – have identical characteristic roots. They therefore have identical stability properties and vary only in their response to dynamic inputs.

The S-domain equations that describe these systems were presented in the previous section. In this section the effect of  $k_p$  and  $k_d$  on the roots of the denominator (damped second order oscillator) of Eq (6.3-5) is studied and the associated transient and frequency responses are demonstrated.

### Procedure :

#### Proportional & Derivative Control Actions

1. Set-up the plant with a single magnet with the north pole facing upward (See Section 2.2.2, handle magnets by edges only and do not touch the glass rod with bare hands [e.g. use a clean cloth])
2. Edit your control algorithm from the previous section to set the proportional gain,  $k_p$ , equal to zero and the derivative gain,  $k_d$  unchanged. Verify that sampling time is set to  $T_s = 0.001768 \text{ sec}$ .
3. Hold the magnet (edges only) at the approximate 2 cm. position and implement the algorithm. Move the magnet back and forth briskly through a range of roughly 0 to 3 cm. (do not exceed 3.5 cm.) Move it slowly at first and then more rapidly. Do not move the magnet so rapidly as to set up a large control force (i.e. no greater than approximately 2x the magnet weight). What is the nature of the resistive force imparted by the control system?
4. Double the value of  $k_d$  and repeat Step 3. Can you feel the control force increase?
5. Edit your algorithm to set  $k_p$  equal to the same value as used in the previous section and  $k_d$  equal to zero. Hold the magnet (edges only) at the approximate 2 cm. position and implement the algorithm. Move the magnet through a range of  $\pm 0.5 \text{ cm}$ . What is the nature of the resistive force imparted by the control system?

---

<sup>2</sup>The student may want to later verify that for the relatively high amount of control damping in the scheme that follows – induced via the parameter  $k_d$  – that the plant damping is very small.

6. Edit your algorithm to double the value of  $k_p$ . Repeat Step 5 and note the change in force characteristic.

### PD Control Design

7. From Eq's (6.3-3,-4) design controllers (i.e. find  $k_p$  &  $k_d$ ) for two systems, one with a system natural frequency  $\omega_n = 4$  Hz, and damping ratio  $\zeta = 0.05$  and one with  $\omega_n = 8$  Hz and  $\zeta = 0.25^1$ .
8. Design a controller with  $\omega_n = 6$  Hz and three damping cases: 1)  $\zeta = 0.2$  (under-damped), 2)  $\zeta = 1.0$  (critically damped), 3)  $\zeta = 2.0$  (over-damped).

### Step Response

9. Edit your algorithm to set the initial offset to  $y_{I_0} = 15000$  counts (nominally 1.5 cm.) Implement the 4 Hz design from Step 7 and set up a trajectory of 10000 count amplitude with 1000 ms dwell time and 1 repetition.
10. Execute the *Step* command and plot the *Commanded Position* and *Q10* ( $y^*1$ ) data. Note the frequency of oscillations (number of cycles divided by the corresponding time) in the response. Save your plot.
11. Repeat Step 10 for the 8 Hz design of Step 7.
12. Implement the three controllers of Step 8 and execute and plot the step response. Note the effect of changing damping in each case. Save your plots.

### Frequency Response

Review the discussion at the end of this section regarding the use of various sine sweep data scaling options prior to completing Step 13.

13. Edit your algorithm to set the initial offset to  $y_{I_0} = 20000$  counts<sup>2</sup> and set the gains for the  $\omega_n = 6$  Hz,  $\zeta = 0.2$  design from Step 8. Implement this algorithm and check the *Sensor 1* display on the background screen. If not within  $20000 \pm 100$  counts, adjust the gravity offset in your algorithm so that the *Sensor 1* value falls within this range. (This helps keep the magnet position from drifting during high frequency excitation.)
14. Setup a *Sine Sweep* trajectory with 5000 count *Amplitude*<sup>3</sup>, a *Start Frequency* of 0.1 Hz, *End Frequency* of 30 Hz, *Sweep Time* of 30 sec. and *Logarithmic Sweep* checked.
15. Setup to collect *Variable Q10* and *Commanded Position 1* data every 4 *Servo Cycles*.
16. Execute the sine sweep and plot the *Variable Q10* and *Commanded Position 1* data using *Linear Time* and *Linear amplitude* for the horizontal and vertical axes (*Remove DC Bias* checked). The data will reflect the system motion seen as the

<sup>1</sup> These controllers are used to implement lightly damped systems for physical measurement of natural frequency. The very low damping ratio for the 4 Hz system is to provide an oscillatory response in spite of the effect of magnet/glass rod friction which becomes exaggerated in this low gain case.

<sup>2</sup> This greater height is necessary to assure that the magnet does not strike the mechanical stop during the frequency response tests. You may need to reduce the amplitude slightly in the underdamped system sine sweep if it contacts the stops during resonance.

<sup>3</sup> You may need to reduce the amplitude slightly in the underdamped system sine sweep if it contacts the stops during resonance

sine sweep was performed. Now plot the same data using Logarithmic Frequency and Db amplitude. By considering the amplitude (the upper most portion of the data curve) you will see the data in the format commonly found in the literature for Bode magnitude plots. Can you easily identify the resonance frequency and the high frequency (>5 Hz) and low frequency (< 0.8 Hz) gain slopes? (i.e. in Db/decade).

17. Repeat Step 16 for the critically damped and overdamped control gains. You may need to reduce the upper frequency on the sine sweep (to say 10 Hz) in the overdamped case if the high frequency response is irregular (does not diminish smoothly with frequency). Such an irregular response is due to system noise propagation, which results from differentiation of the laser sensor signal.

#### Adding Integral Action

18. Modify your algorithm to reduce the gravity force offset,  $u_o$ , by 20%. This will cause a steady state error in the PD controlled system. Also modify your algorithm to introduce integral action according to Figure 6.3-2b. You may use the backwards difference approximation of  $s$  (Eq. (6.2-8)) or other transformation as suggested by your instructor. Set the position offset to  $y_{1o} = 15000$  counts. Have your laboratory instructor or supervisor check your algorithm before proceeding.
19. Set the integral term in your algorithm equal to zero and  $k_p$  and  $k_d$  to values for the case of  $\omega_n = 6$  Hz,  $\zeta = 1.0$ . Perform a 15000 count unidirectional step of 2000 ms duration. Plot and save the *Variable Q10* and *Commanded Position 1* data. Note the steady state error in the response.
20. Compute the integral term such that  $k_i k_{sys} = 800$  N/(m-s) and implement you algorithm containing this value. Execute the trajectory of Step 19 and plot and save your data. Note the shape of the curve and the steady state error. Grasp the magnet by the edges and lightly apply a upward or downward force. Do not allow the force to build up more than twice the magnet weight. Can you feel the nature of the restoring force – i.e. that it grows over time for a given error (proportional to the integral of the error over time)?
21. Repeat Step 20 for  $k_i k_{sys} = 2000$  N/(m-s). Note the change in the shape of the response.

#### **Questions:**

A. What is the effect of the system gain,  $k_{sys}$ , the inertia,  $m$ , and the control gains,  $k_p$  and  $k_d$  on the natural frequency and damping ratio? Derive the transfer function for the spring/mass/damper system shown in Figure 6.4-1. How do the viscous damping constant,  $c$ , and the spring constant  $k$  correspond to the control gains  $k_d$  and  $k_p$  in the PD controlled rigid body of Figure 6.3-2b? What are the units of  $k_d k_{sys}$  and  $k_p k_{sys}$  and how do these relate to the units of the corresponding parameters of Figure 6.4-1.

B. Describe the effects of natural frequency and damping ratio on the

characteristic roots of Eq's 6.2-1. Use an S-plane diagram in your answer to show the effect of changing  $\zeta$  from 0 to  $\infty$  for a given  $\omega_n$ .

- C. Compare the step response and frequency response plots for the under-, critical, and overdamped cases ( $k_i = 0$ ). Discuss how the resonance (if present), and *bandwidth*<sup>1</sup> seen in the frequency response data correlate with features of the step responses.
- D. What is the general shape of the frequency response amplitude (i.e. amplitude vs. time) of the three plots obtained in Steps 16 and 17 (linear time / linear amplitude) at amplitudes well below and above  $\omega_n$ ? What is the shape when viewing the same data plotted with  $\log(\omega)$  / Db scaling? Explain your answer in terms of the asymptotic properties of the closed loop transfer functions as  $\omega$  tends to zero and infinity.
- E. Review the two step response plots obtained by adding integral action (Steps 20 & 21) with the first response obtained without integral action damped plot ( $k_i = 0$ ) of Step 19. What is the effect of the integral action on steady state error?

Static or Coulomb friction may be modeled as some disturbance force acting on the output as shown in Figure 6.4-2. Assume that this force to be a constant<sup>2</sup>, and use the final value theorem to explain the effect of the disturbance on the PD controlled system with and without the addition of integral action.

In what way does integral action effect overshoot in the step response (again, compare with the critically damped plot of Step 19)? Why?

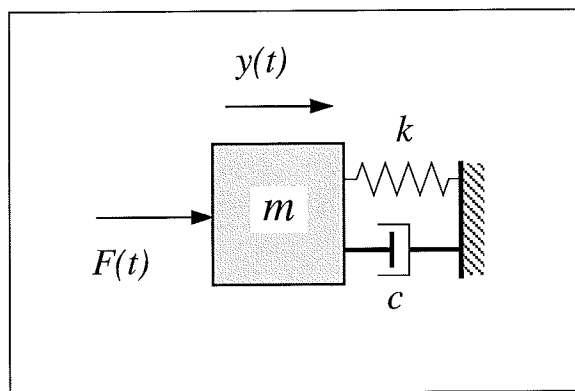


Figure 6.4-1. Classical Second Order Damped Oscillator

<sup>1</sup> For the purposes here, consider *bandwidth* to be the frequency in the sine sweep data at which the system attenuates below 1/2 (-6Db) of its low frequency amplitude

<sup>2</sup> In practice, friction and its effect on system response are much more complex. This assumption however is valid in discussing the effect of the integrating term.

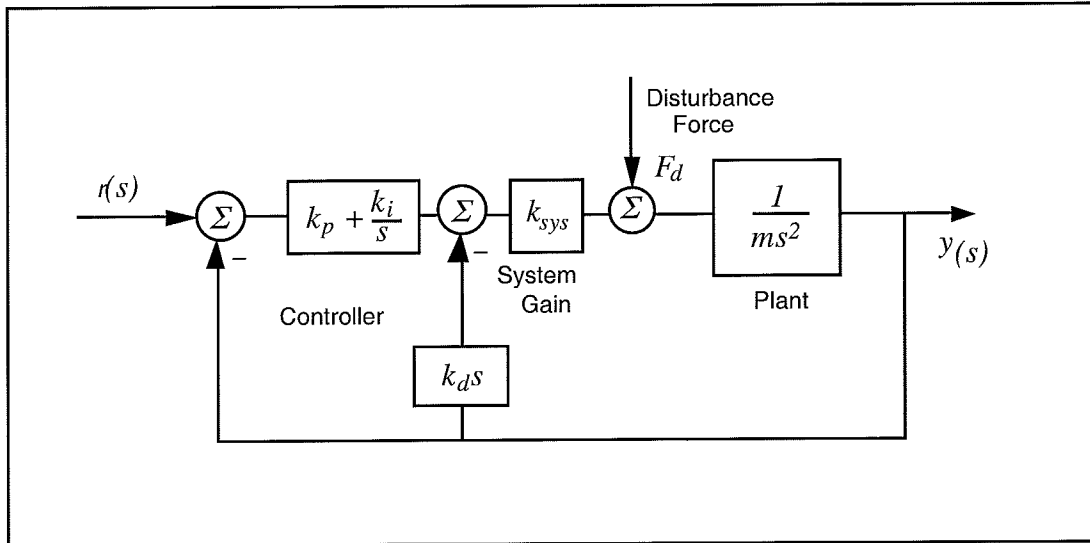


Figure 6.4-2. System With Disturbance Force at Output

Viewing Sine Sweep (Frequency Response) Plots

Much insight into frequency response behavior is afforded by viewing the sine sweep plots in the various data scaling functions available in the Setup Plot dialog box. By viewing data in the Linear Time - Linear Amplitude modes, the curve appears as the system motion is viewed during the sine sweep. Note the large range in amplitudes as frequency changes. In Linear Frequency - Linear Amplitude mode, the amplitude is as before but the data is shown in with frequency of oscillation as the horizontal coordinate so that amplitude may be associated with a particular frequency.

In Logarithmic Frequency - Linear Amplitude mode the frequency is distributed logarithmically (the sine sweep was executed this way in our case). This is an appropriate frequency scaling function in many cases because magnitude changes of linear systems occur as powers (e.g.  $\omega$ ,  $\omega^{-1}$ ,  $\omega^{-2}$ , etc.) of the excitation frequency and hence often occur over a large dynamic range of frequency. For example the change in output between 0.1 and 0.2 Hz may be greater than that between 9 and 10 Hz but would be difficult to ascertain in a linear frequency distribution between say 0.1 and 10 Hz because they would constitute only 1% of the plot length. Similarly, phase changes are symmetrically shaped in a logarithmic frequency distribution.

In Logarithmic Frequency - Db mode the frequency is distributed logarithmically and the magnitude is in Db. This method of data presentation, once the user is familiar with it, quickly affords much information about the system. The response magnitude asymptotically tends toward straight lines whose slope is associated with the salient system dynamics (i.e. the powers of  $\omega$  mentioned above).

In ECP systems, the Db magnitude (see Eq. 6.2-6) of each data point is taken so that the upper bound of the trace represents the cycle-to-cycle maximum amplitude. In virtually all other plots that the engineer may encounter, peak Db magnitude is shown as a pure function of frequency - i.e. it is a single curve on the plot. Thus the mapping of actual test data into the frequency-Db format, as done here, affords physical insight into the meaning of these important analytical and design tools.

$$Db(y) = 20 \log(y) \tag{6.4-1}$$



The methods of  $\text{Log}(\omega)$  - Db Magnitude scaling, and  $\text{Log}(\omega)$  - Linear Phase scaling are widely used in industrial and academic practice.

The Remove DC bias check box subtracts the average of the last 50 data points from all points on the curve to provide results that are centered about zero at high frequency. It generally provides better appearance to plots that have low amplitude in the high frequency section (e.g. all  $y_1$  and  $y_2$  sine sweeps in this manual) and is necessary in many cases to obtain useful Db data at high frequency. It may provide misleading results, however, if the bias of the original data or the amplitude in the final 50 points is large.

## 6.5 Disturbance Rejection of Various 1 DOF Plant Controllers

In this experiment, we consider the performance of three distinct controller designs in rejecting low and higher frequency disturbances. A disturbance is easily imparted using the Model 730 Apparatus by controlling the position of one magnet (The upper one in this case) and measuring the effect of the resulting changes in force on the other magnet. It is important to keep in mind while running this experiment that the upper magnet motion is simply imparting a disturbance force to the lower one. It is the study of the effectiveness of various control schemes (applied to the lower magnet) at rejecting this disturbance force that is the focus of this experiment.

The plant should be setup with two magnets so that the north pole of the lower magnet points upward and that of the upper magnet points downward. Take great care in handling the magnets to avoid sudden collision of the magnets by virtue of their high attractive forces. Follow the instructions and precautions of Section 2.2

### Procedure :

#### Setup Disturbance Apparatus

1. The three controllers to be studied are as follows:
  - a) PD control with  $\omega_n \approx 3$  Hz and  $\zeta \approx 0.5$ , and feedback at Encoder #1.
  - b) Same as "a" plus added integral action:  $k_i k_{sys} = 1000$ .
  - c) Same as "a" plus a cascaded lead/lag filter with the following specifications: Zero at 0.25 Hz, Pole at 1.5 Hz, DC gain = 1.

Design the lead/lag filter for controller "c". [Hence find  $n_o$ ,  $n_l$ ,  $d_o$ , and  $d_l$  in  $F(s) = (n_o + n_l s)/(d_o + d_l s)$ ] Use  $T_s = 1.768$  ms. in each case.

2. Modify your algorithm to include both PD control of the upper magnet and a control algorithm for the lower magnet that is capable of implementing the three controllers above<sup>1</sup>. The combined routine should incorporate the following.

---

<sup>1</sup> It is recommended that you merge the appropriate portions of the upper magnet controller from Section 6.3 and the lower magnet PID controller from the previous section – then modify the result to add the lead/lag filter.

- a) Set the offset positions to  $y_{1o} = 15000$ ,  $y_{2o} = -20000$ .
- b) Use for the gravity offsets:  $u_{1o} = 18800$ ,  $u_{2o} = 4800$ <sup>1</sup>
- c) Use the following gains for the upper magnet controller:  $k_p = 3.1$ ,  $k_d = 0.1$ .<sup>2</sup>
- d) Use `cmd2_pos` as the reference input for the upper magnet controller

Have your instructor or laboratory supervisor approve your algorithm before proceeding.

3. Set up a *Sinusoidal* trajectory of 0.1 Hz frequency, 10000 count amplitude and 3 repetitions for the upper magnet. (You should reduce the data acquisition sampling frequency to once every 10-20 servo cycles to avoid an unnecessarily large data file. You need only collect *Variable Q10* and *Variable Q12* data). Input your routine set up to implement Controller “a” above using  $T_s = 0.001768$  sec. Execute the above trajectory selecting *Execute Trajectory 2 Only* in the Execute dialog box. This drives the upper magnet at 0.1 Hz while the lower magnet (the focus of this experiment) remains under regulation. Plot and save the *Variable Q10* and *Variable Q12* (i.e. the regulated system and disturbance) data. Scale your plot so that the disturbance and the response of the regulated system appear separately (one above and one below) on the plot. Repeat this disturbance regulation test for controllers “b” and “c”
4. Repeat this procedure for controllers “a”, “b”, and “c” for a disturbance frequency of 3.0 Hz and of the same amplitude as above. You should increase the number of cycles to 30 or more so that the total duration of the plots is of the same order as that of the 0.1 Hz plots. You may also want to increase the data acquisition sampling frequency somewhat.

**Questions:**

- A. Consider the block diagram of Figure 6.5-1. Derive the open loop transfer function

<sup>1</sup> Here the lower magnet gravity offset must be increased by the intermagnet force at the nominal separation distance. The upper magnet offset is reduced by this amount. You should be prepared to explain this and to show that these values are consistent with the intermagnet force relationship derived in Section 6.1.

<sup>2</sup> You should verify that these result in  $\omega_n = 8$  Hz,  $\zeta = 0.5$  for the upper system. This provides a relatively “stiff”, *high bandwidth* control so that the magnet follows the desired trajectory closely. This provides for a well-controlled disturbance force as seen by the lower magnet for the frequencies tested.

$$\frac{N_{ol}(s)}{D_{ol}(s)} = K(s) k_{sys} P(s) \quad (6.5-1)$$

and closed loop transfer function  $y_1(s) / F_d(s)$  for each controller.

- B. Plot the Bode response for the open and closed loop transfer functions in each of the three controller cases. Explain the disturbance attenuation characteristics of each controller in terms of their Bode response.

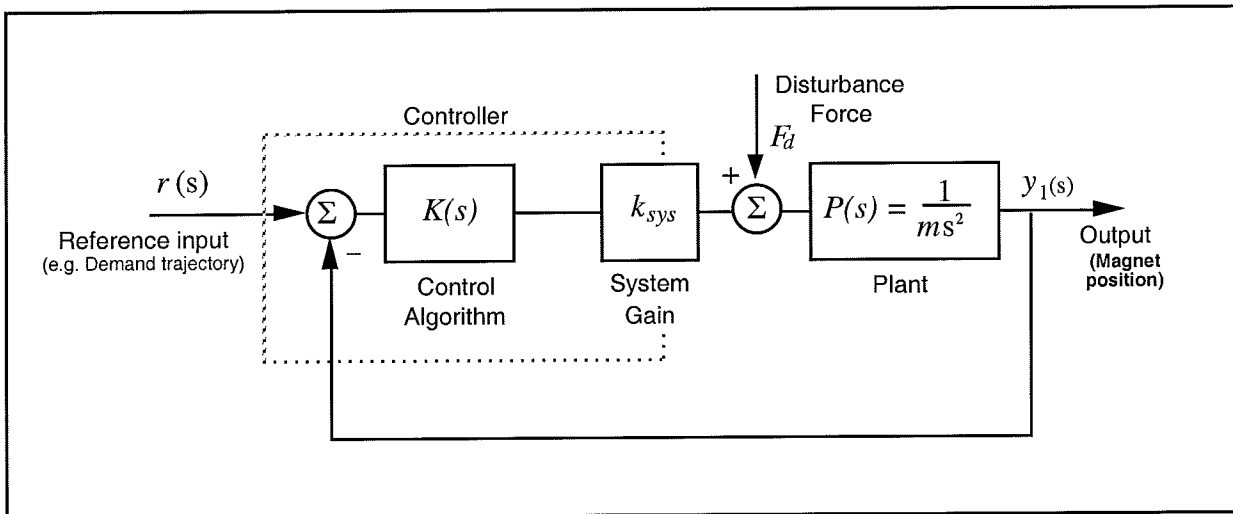


Figure 6.5-1 Disturbance Force Input To Rigid Body Control Scheme

## 6.6 Collocated Control of SIMO Plant

In this experiment we consider the plant configured with two magnets stacked on the glass rod and utilize only the lower coil/magnet actuator. In mechanical systems when the primary feedback sensor is rigidly coupled to the actuator, the system is referred to as being *collocated*. When some flexible structural member exists between the actuator and the sensor<sup>1</sup>, the system is referred to as being *noncollocated*. Systems with flexibly coupled inertia occur commonly in the industry. Examples include flexible drive shafts, conveyor belts, and other mechanical linkages. An example of collocated control in such cases is when the feedback sensor is integral with the drive motor even though there may be flexible elements that are driven by the motor. An example of noncollocated control is when a flexible conveyor belt position is fed back for closed loop control.

<sup>1</sup> There may be multiple sensors used including ones that are both collocated and noncollocated relative to the actuator. If the location of objective control is not collocated with the actuator, then the plant is typically referred to as being noncollocated.

The open loop system is analogous to that of Figure 6.6-1 which reflects the effective use of the nonlinear control effort, gravity feedforward, and sensor compensation routines used in previous sections. The effective “spring” is the linearized term resulting from the forces of gravity and magnetic repulsion acting on the second magnet. Recall however that this term is in fact quite nonlinear. Recall also that we have neglected the interaction of the second magnet with the magnetic field of the drive coil.

The addition of the spring and second inertia to the rigid body case studied above increases the plant order by two and adds an oscillatory mode to the plant dynamics. This may be thought of, in a sense, as a dynamic disturbance to the rigid body plant. The collocated PD control implemented in this section is the approach most commonly used in industry. It may be practically employed when there is flexibility between the actuator and some inertia, and the location of objective control is near the actuator. If the location of objective control is at the distant inertia, however, this method has its limitations.

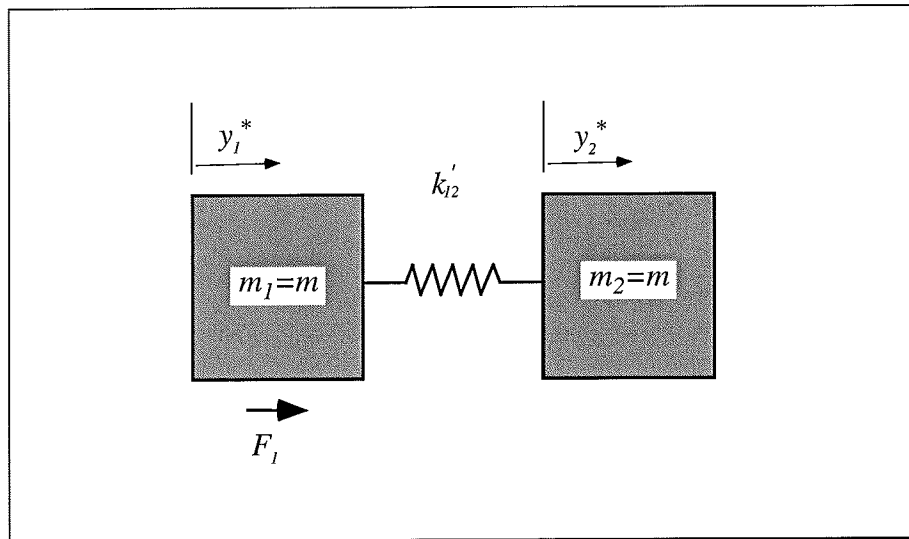


Figure 6.6-1 Analogous System to Idealized SIMO Plant (Net of Nonlinear Compensation)

In examining this system we shall use the notation:

$$\frac{y_1(s)}{u_1(s)} = \frac{N_1(s)}{D(s)}, \quad \frac{y_2(s)}{u_1(s)} = \frac{N_2(s)}{D(s)} \quad (6.6-1)$$

The approach in this experiment will be to design the controller by interactively changing the PD gains and observing their effect on the physical system. The control block diagram is shown in Figure 6.6-2

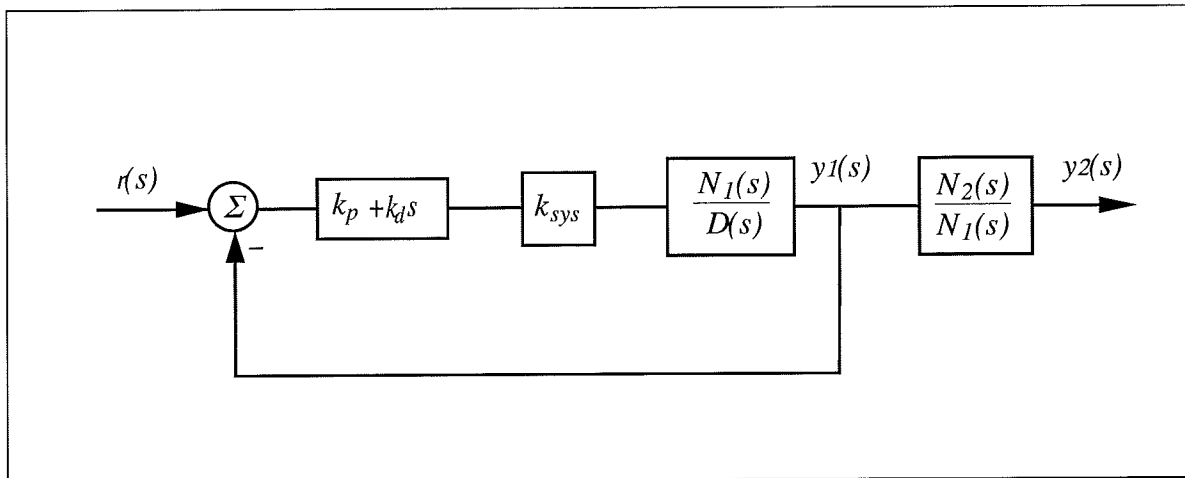


Figure 6.6-2. Control Block Diagram for Collocated Control Experiment

#### Collocated Control – Procedure :

1. Set-up the system with two magnets in repulsion according to the instructions of Section 2.2.2.
2. Use your real time algorithm from the previous section and modify it as follows:
  - a. Set the offset in  $y_1$  to  $y_{1o}=10,000$ . It is very important in this configuration to keep this offset small. Do not exceed  $y_{1o}=10000$ . In this configuration, the weight of both magnets plus the control actuation force is supplied by the lower coil. The required current increases dramatically with height of the lower magnet. Excessive amplitude for sustained duration will overheat the coil and damage the apparatus
  - b. Adjust the gravity feedforward,  $u_{1o}$ , to compensate for the support of the weight of two magnets through the bottom coil.
  - c. Add a provision so that the second reference input, `cmd2_pos`, is output on the second DAC (`control_effort2`). This will be used to apply a disturbance force to the upper magnet.
  - d. Use a sampling rate of  $T_s=0.001768$  s.

Have your laboratory supervisor or instructor review and approve your algorithm before implementing it.

3. Set the input trajectory to a unidirectional *Step* of 15000 count (nominally 1.5 cm.) amplitude and 1000 ms duration. Set initial gain values to  $k_p = 1$ ,  $k_d = 0.05$ . Implement and obtain the step response of the upper and lower magnets. If the plotted position offsets are large, you may want to adjust them as follows. First increase or reduce the gravity offset to obtain *Sensor 1 Position*  $\approx 10000$  counts as seen on the background screen (you may want to spin the magnets in this process to release any Coulomb friction). Next, adjust the upper magnet position offset equal to the *Sensor 2 Position* as read from the background

Iteratively adjust the gains  $k_p$  &  $k_d$ , to obtain a rise time  $\leq 200$  ms (0-90% amplitude) in the lower magnet with overshoot less than 10%. Make your gain

adjustments gradually (not more than 50% at a time) and note the effects of increasing or reducing each of them. Do not input  $k_p > 5$  or  $0.02 < k_d < 0.12$ . If the system becomes noisy (“rumbling” sound and erratic movement of the lower magnet) reduce  $k_d$ . If it becomes too oscillatory as seen at the lower magnet, increase  $k_d$  (within the above bounds)<sup>1</sup>. Save your best step response plot. Manually displace the upper and lower magnets (touch edges only!) and note their relative stiffness. (The lower magnet stiffness is entirely due to the control system.

4. For your last iteration in Step 3, plot and save the step response of the two magnets. What is the predominant characteristic of the top magnet motion? Can you give an explanation for the difference in the responses of the two magnets in terms of their closed loop transfer functions?

Apply a disturbance to the upper magnet of magnitude 20000 counts in the downward direction using *Trajectory 2*. Select a unidirectional *Impulse* of 1000 ms pulse width, 2 repetitions, and 1000 ms dwell time. It is recommended that you change your *Trajectory 1* Step input to a duration (dwell time) of 2000 ms, 1 repetition, zero amplitude. *Execute* both trajectories (remember in this case that Trajectory 2 is simply imparting a disturbance force) with a delay of 500 ms for Trajectory 2 after Trajectory 1. Assure that the 20000 count control effort to the upper coil is applied only momentarily. Plot the result and note the relative effect of the disturbance on each magnet.

5. Now using the existing values of  $k_p$  &  $k_d$  as starting points, iteratively reduce gains and plot results to provide a well-behaved step response in the upper magnet displacement,  $y_2^*$ , with  $\leq 10\%$  overshoot in both directions, without excessive oscillation, and as fast a rise time as possible. Save your final plot and record the corresponding gains. Manually displace the lower and upper magnets and note their stiffness. Are they generally more or less stiff than for the controller of Step 3? How does the steady state error compare with the high gain controller from Step 3? Repeat the disturbance input test of Step 4.

#### Questions:

A. Calculate the poles of the closed-loop transfer functions:  $y_1(s)/r(s)$  and  $y_2(s)/r(s)$  for your final controllers in Steps 3 & 5 respectively assuming effective nonlinear compensation, linearity in the “spring  $k_{12}$ ”, and negligible friction. How close to the imaginary axis (and right half plane) are the most lightly damped poles in each case? How close are the complex poles of  $y_1(s)/r(s)$  to its zeros in each case? Explain your answer in terms of the root loci for this system for gain ratios of  $k_d/k_p = 0.05, 0.10, 0.17, \text{ and } 0.25$ .

B. Calculate the closed loop transfer function in the form:

$$\frac{y_2(s)}{r(s)} = \frac{(N(s))_{\text{forward path}} / D_{ol}(s)}{1 + N_{ol}(s) / D_{ol}(s)} \quad (6.6-1)$$

Use the open loop numerator and denominator,  $N_{ol}$  and  $D_{ol}$ , to obtain the open loop Nyquist or Bode responses resulting from your high and

<sup>1</sup> An oscillatory response may also result from excessively high gain in both  $k_p$  and  $k_d$  due to low gain margin (in the real, not idealized, system). In this case you should reduce both gains.

low gain controllers from Steps 3 & 5 respectively. What are the associated phase and gain stability margins? What are these margins for  $y_I(s)/r(s)$ ? Explain.

C. Referring to Figure 6.6-3, the transfer function between the disturbance force and the first magnet position is:

$$\frac{y_1(s)}{F_d(s)} = \frac{N_1(s)}{D(s) + k_{h_{sys}}(k_p + k_d s) N_1(s)} \quad (6.6-2)$$

Use the final value theorem to find this expression for a constant disturbance force. The inverse of this expression is called the *static servo stiffness*. What is the static servo stiffness of your final controllers from Steps 3 & 5 for the first magnet? What is the equivalent expression for the second magnet (i.e. defining static stiffness at the second magnet as the force required to displace it one meter). What is its value for the second controller at each location? Explain the results of your disturbance response tests (latter parts of Steps 3 and 5) as to the relative responses at each location for the low and high gain controllers. Recalling Section 6.5, what is the static stiffness with integral action in the controller (i.e.  $k_i \neq 0$ )?

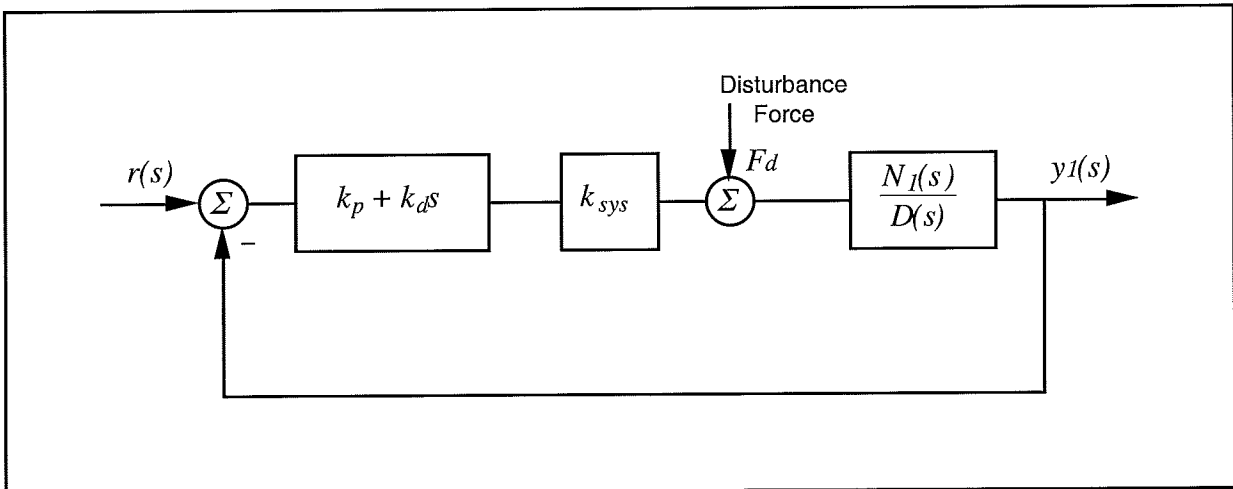


Figure 6.6-1. Disturbance Forces On PD Controlled 2-DOF Plant

### 6.7 Noncollocated SIMO Control: Successive Loop Closure

In this experiment we explore noncollocated control where the actuator is at the lower magnet, and we are attempting to control the upper magnet using the upper sensor as the primary feedback. In our approach, we first close a position loop about the collocated ( $y_1$ ) position with a relatively high bandwidth (close tracking) control. We then make the assumption that the lower magnet closely follows its internal demand  $r^*(s)$  so that for designing a controller for  $y_2$ , the "plant" is approximated by the transfer function  $y_2(s)/y_1(s)$  (i.e.  $N_2/N_1(s)$ ). The block diagram for this approach is given in Figure 6.7-1.

The design and control implementation in this section proceeds as follows

1. High bandwidth PD control of  $y_1$
2. Outer loop control via pole placement methodology

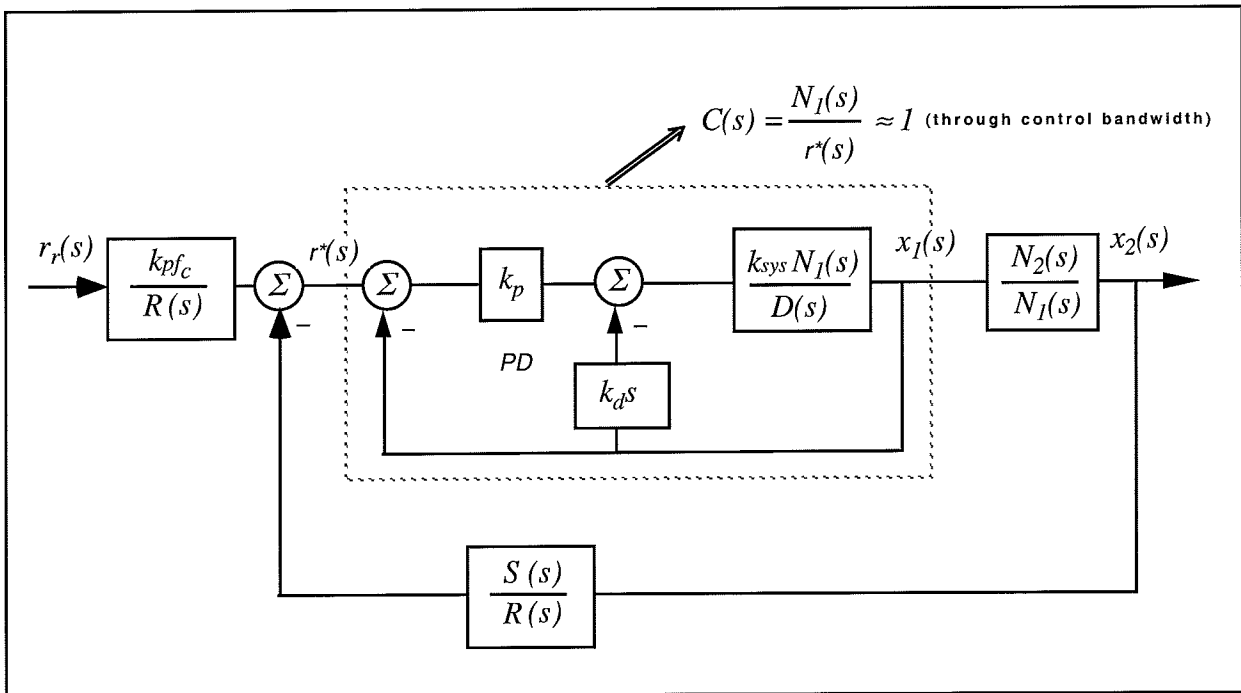


Figure 6.7-1. Control Structure For Successive Loop Closure with High Gain Inner Loop

#### 6.7.1 PD Control Of The Lower Magnet

1. Setup the plant with two magnets as in the configuration of the previous experiment.



### PD Control Design & Implementation

2. Design the PD control gains such that  $\omega_n = 8$  Hz, and  $\zeta = 0.707$  when considering only the lower magnet acting as a rigid body.
3. Set the sampling rate to  $T_s = 0.001768$  seconds and implement your control design using your algorithm of the previous section. Make certain that the offset,  $y_{10}$ , is set to 10000 (not greater!). Verify that the system is stable and gently perturb the upper and lower magnets to feel their relative stiffness.

#### 6.7.2 Pole Placement Control of $y_2(s)$

Having closed a relatively high bandwidth ( $\approx 8$  Hz) loop about the lower magnet, we utilize the fact that the transfer function of Eq. 6.3-2 has near unity input/output gain (and relatively small phase lag) through the bandwidth ( $\approx 4$  Hz) that we will attempt to attain in the overall control of  $y_2$ . Thus for the control of  $y_2$  we consider the outer loop in the block diagram of Figure 6.6-1.

Now the plant to be controlled is:

$$\frac{y_2(s)}{y_1(s)} = \frac{N_2}{N_1} \triangleq \frac{N^*(s)}{D^*(s)} \quad (6.7-2)$$

The numerical values of the parameters in this expression were determined in Section 6.1. For convenience we restate

$$N_1 = ms^2 + c_2s + k'_{12} \quad (6.7-3)$$

$$N_2 = k'_{12} \quad (6.7-4)$$

Here we have included the damping term to represent the friction at the upper magnet<sup>1</sup>. Using this simplified model, the dynamics of the outer loop system become identical to those of the base motion controlled system shown in Figure 6.7-2.

---

<sup>1</sup> Friction at the upper magnet (modeled as viscous) is included here because the actuation force acting on this magnet must pass through  $k'_{12}$  – a rather weak “spring”. Thus the friction effects present a non-negligible portion of the force acting on the magnet. In cases where the upper coil drives the upper magnet (e.g. the MIMO control of the next section) the control forces can be made strong such that friction may be neglected.

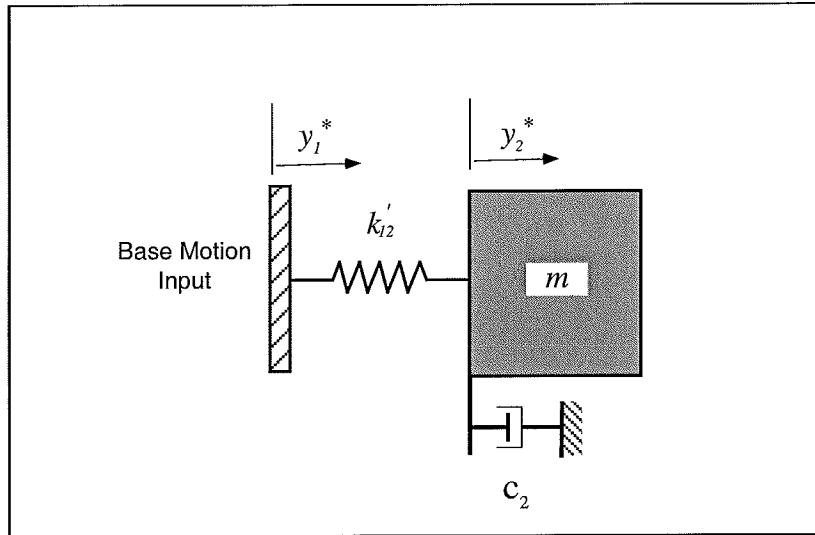


Figure 6.7-2. Equivalent Idealized “Plant” For Control of Outer Loop

We now seek to find a controller  $S(s)/R(s)$  which will result in a prescribed set of closed loop poles. The closed loop denominator will have the form:

$$D_{cl}(s) = D^*(s)R(s) + N^*(s)S(s) \tag{6.7-3}$$

which may be expressed as

$$D_{cl}(s) = (d_2s^2 + d_1s + d_0)(r_1s + r_0) + (n_0)(s_1s + s_0) \tag{6.7-4}$$

where the  $d_i$ 's and  $n_i$ 's are the respective coefficients of the denominator and numerator of the right hand side of Eq. (6.7-2). Their values are known from the plant model of Section 6.1 (except  $c_2$  which will be approximated in this experiment).

By linear system theory, for coprime  $N^*(s), D^*(s)$  with  $N^*(s)/D^*(s)$  proper, there exists an  $(n-1)$ <sup>th</sup> order  $S(s), R(s)$  which when convolved as per Eq. (6.7-3) form an arbitrary  $(2n-1)$ <sup>th</sup> order  $D_{cl}(s)$  where  $n$  is the order of  $D^*(s)$ .

Here we shall solve for the desired denominator:

$$D_{cl}(s) = \left( s + 8\pi \frac{(1+j)}{\sqrt{2}} \right) \left( s + 8\pi \frac{(1-j)}{\sqrt{2}} \right) (s + 16\pi) \tag{6.7-5}$$

I.e. closed loop poles at  $-2.8 \pm j2.8$  Hz. and  $-8$  Hz <sup>2</sup>

---

<sup>2</sup> This has two poles of magnitude  $|s| = 4$  Hz that lie at 135 and 225 deg and an additional real pole at  $-8$  Hz.

Pole Placement Design

4. Determine the coefficients of the controller polynomials  $S(s)$  and  $R(s)$  by equating coefficients in the expanded forms of Eq's 6.6-4 and 6.6-5 or other numerical methods. Assume  $c_2/m = 8$  initially.
5. Calculate the scalar prefilter gain  $k_{pf}$  by referring to Figure 6.6-1. The goal is to have the output  $y_2(s)$  scaled equal to the input  $r_r(s)$ . Hint: Consider the system in static equilibrium. Set  $y_2 = 1$  and  $r_r = 1$  and solve for  $k_{pf}$  using only the constant terms in all control blocks.

Control Implementation

6. Modify your algorithm from Step 3 above to include the following.
  - a) Implement the outer loop of Figure 6.7-1 incorporating the control terms  $S(z)$  and  $R(z)$ . You may use a bilinear (Tustin) or backwards difference transformation in converting your design from continuous to discrete. You should move  $R(z)$  into the equivalent forward path location (from its location in both the return path and prefilter) to avoid calculating it twice in the real-time algorithm.
  - b) Use `cmd1_pos` as your reference input.
  - c) As in the previous section, add a provision so that the second reference input, `cmd2_pos`, is output on the second DAC (`control_effort2`). This will be used to apply a disturbance force to the upper magnet.

Have your laboratory supervisor or instructor review and approve your algorithm before implementing it.

7. Implement your algorithm and verify that the system is stable. If so, lightly perturb the upper magnet and verify that the lower one moves in opposition to your disturbance in an attempt to regulate it. If this occurs congratulations! You have just implemented noncollocated control! Perform a 15000 count step input and plot the magnet 1 and magnet 2 positions.

If there is significant overshoot, ( $>15\%$ ) in the  $y_2$  position trace, increase the damping  $c_2/m$ <sup>2</sup> in your model by say 20%, recalculate the coefficients of the outer controller (via Eq. 6.7-4), convert to discrete time form and re-implement. If this increases the overshoot, then reduce  $c_2/m$  in your model and re-implement. Repeat this process if necessary to produce a well-behaved response in the  $y_2$  trace. Notice the shape of the  $y_1$  trace as its response compensates for the flexibility between it and the upper magnet. (Bear in mind that our objective here is to control the position of the upper magnet.) Save your final plot.

As in the latter part of Step 4 of Section 6.6, add a disturbance to the upper magnet of magnitude 20000 counts in the downward direction. Assure that the 20000 count control effort to the upper coil is applied only momentarily. Plot the result and note the relative effect of the disturbance on each magnet. Save

<sup>1</sup>You may also select Control Effort if you wish to later observe this value .

<sup>2</sup>The damping will vary from one apparatus to the next and is also dependant on the cleanliness and condition of the glass rod and magnet bushing surfaces. A damping mismatch between the model and the actual system can result in excessive overshoot if the model damping is either too high or too low.

your plot. Note the change in both the step response and disturbance attenuation at the upper magnet as compared with the previous collocated design.

**Questions:**

- A. Report your calculated values for  $s_0$ ,  $s_1$ ,  $r_0$ ,  $r_1$ , and  $k_{pf}$ . Submit your real-time algorithm
- B. Determine an expression for the closed-loop transfer function  $y_2(s)/r_1(s)$  including all elements in the block diagram of Figure 6.6-1. You may express this in terms of the polynomials  $D(s)$ ,  $N_1(s)$ ,  $R(s)$ , etc. rather than expanding each term fully. Determine  $y_2(s)/r_1(s)$  using the assumption  $C(s)=1$ . Compare the simulated frequency response of the full and reduced order transfer functions. In which regions are the two similar in magnitude and phase and in which are they different? Are they similar throughout the final system closed loop bandwidth? Is the assumption of unity gain in  $C(s)$  valid for the purposes here?
- C. Determine the phase and gain margins for the outer loop considering the full expression for the closed inner loop  $C(s)$  (i.e. consider  $C(s)$  to be a single block in the outer loop block diagram). Determine the phase and gain margins of the outer loop using the  $C(s) = 1$  assumption. How do the two compare?
- D. For this design, determine the static stiffness at  $y_1$  and  $y_2$  for  $F_{d1}$  and  $F_{d2}$  applied at  $y_1$  and  $y_2$  respectively (i.e.  $F_{d1}/y_1$  and  $F_{d2}/y_2$ ). What are the “cross” static stiffnesses (i.e.  $F_{d2}/y_1$  and  $F_{d1}/y_2$ )? How do the relative stiffness of the upper and lower magnet compare in each case?

## 6.8 MIMO Control

In this experiment, full MIMO control is implemented on the two magnet system. The physical plant configuration is again that of the previous two sections except that now we apply inputs at both the upper and lower magnet locations. We shall implement a linear quadratic regulator using full state feedback where the states are defined to be the position and velocity of each magnet (i.e. those of Eq.(5.3-15)). The outputs are taken as  $y_1$  and  $y_2$ ; i.e. the output matrix is

$$C = \begin{bmatrix} 1 & 0 & 0 & 0 \\ 0 & 0 & 1 & 0 \end{bmatrix} \quad (6.7-1)$$

Here we employ the sensor and actuator nonlinearity compensation of the previous sections. The plant model was previously generated in Section 6.1. Recall that the underlying assumption in this model is that the sensor and actuator nonlinearity compensation functions are sufficiently near the inverse of the underlying plant nonlinearities that the new “plant” may be modeled as being

linear for control design purposes. Recall also that there is no nonlinear compensation for the effective “spring”  $k_{i2}$ . It is modeled as a linear spring whose value was derived by linearization about the operating point  $\{y_{10}, y_{20}\}$ .

In the experiment that follows, we shall first implement SISO controllers (from previous sections) for the upper and lower magnets simultaneously and compare the resulting system performance with that of the MIMO design. Block diagram depictions of the full state feedback multivariable system is shown in Figure 6.8-1.

#### LQR Design:

1. Construct a state space model of the plant using the realization form of Eq (5.3-15) for the plant with nonlinear sensor and actuator compensation. Be sure to include the system gain,  $k_{sys}$ , in your model. (You may have already generated this model as an exercise in Section 6.1)
2. The following notation shall be used for LQ optimization:

Feedback law:

$$u = -Kx \quad (6.7-2)$$

where

$$K = \begin{bmatrix} k_{11} & k_{12} & k_{13} & k_{14} \\ k_{21} & k_{22} & k_{23} & k_{24} \end{bmatrix} \quad (6.7-3)$$

Perform LQR synthesis via the Riccati equation solution<sup>1</sup> or numerical synthesis algorithms to find the controller  $K$  which minimizes the cost function:

$$J = \int (x'Qx + u'Ru)dt \quad (6.7-4)$$

In this synthesis choose  $Q=C'C$  so that the error at the intended outputs,  $y_1$  and  $y_2$ , is minimized subject to the control effort cost  $R$ . Because of symmetry of the system choose  $R=rI$  where  $I$  is the  $2 \times 2$  identity matrix and  $r$  is scalar. Perform synthesis for control effort weight values:  $r = 10, 1.0, 0.1, \text{ and } 0.01$ . Calculate the closed loop poles for each case as the eigenvalues of  $[A-BK]$

- 3) From this data, select a control effort weight to put the lowest pole frequency between 5.75 and 6.25 Hz. Use one of the above obtained  $K$  values if it meets this criteria, or interpolate between the appropriate  $r$  values and perform one last synthesis iteration.<sup>2</sup>

<sup>1</sup>See for example Kwakernaak and Sivan, "Linear Optimal Control Systems", Wiley & Sons, 1972.

<sup>2</sup> $k_{i1}$  and  $k_{i3}$  ( $i=1,2$ ) scale control effort proportional to the respective positions,  $k_{i2}$  and  $k_{i4}$  scale control effort proportional to the respective velocities. Excessive values of  $K_1$  or  $K_3$  can lead to low stability margin and in the

- 4) Generate a real-time routine that implements the above LQR design and includes the following.
  - a) Nominal operating points  $y_{1o}$  and  $y_{2o}$  at 1.0 and  $-2.0$  cm respectively.
  - b) Sample period  $T_\sigma=0.001768$  s.
  - c) For tracking, the prefilter gain  $k_{pfl}$  must be set equal to  $k_{11}+k_{13}$  and  $k_{pfl2}$  set equal to  $k_{21}+k_{23}$ .

### Control Implementation

#### Simultaneous SISO

- 5) Consider the simultaneous implementation of the two PD controllers with sensor and actuator nonlinearity compensation from Section 6.3. This identical configuration was used in Section 6.5 to control the upper magnet and thereby impart a disturbance to the lower one for the study of disturbance rejection. Modify this routine as follows:
  - a) Set the nominal operating points to  $y_{1o} = 1.0$  cm and  $y_{2o} = -2.0$  cm.
  - b) Adjust the gravity offset parameters  $u_{1o}$  and  $u_{2o}$  to account for the constant force due to  $k_{12}$  imposed on each magnet at the nominal separation distance  $y_{12o}$ .
  - c) Calculate and enter control gains such that  $\omega_n = 6$  Hz and  $\zeta=0.707$  for each sensor/actuator/magnet system.
  - d) Use `cmd1_pos` for the lower magnet reference input and `cmd2_pos` for the upper.
  - e) Set the variables  $q_{10} = y_1^*$  and  $q_{12} = y_2^*$  for later data collection and plotting.

Have your laboratory supervisor or instructor review your algorithm before proceeding.
- 6) Use the plastic safety clip so that the magnet rests at approximately  $-2.5$  cm. Implement this routine and if the controller is stable and functioning properly (e.g. the magnets are levitating at roughly their proper heights) remove the plastic clip. Setup the following multivariable input: *Trajectory 1: Step input, 15000 count amplitude, 1000 ms dwell, 4 repetitions, unidirectional*; *Trajectory 2: Step input, 15000 count amplitude, 1000 ms dwell, 4 repetitions, bidirectional* (deselect *unidirectional*).

Execute these two trajectories with a 500 ms delay of Trajectory 1 after Trajectory 2. Notice the response of the magnets and the *cross coupling* between them (e.g. how much the stationary magnet moves as the moving one changes position). Plot your commanded position and  $y_i^*$  ( $i=1,2$ ) data for each axis. (You may want to use the *Axis Scaling* function so that the upper magnet

---

presence of time delays, instability. Large  $K_2$  or  $K_4$  cause excessive noise propagation and lead to "twitching" of the system. Generally, it is desirable to obtain the highest performance possible (e.g. best tracking, regulation, and disturbance rejection) through high gain subject to the above gain limitations. For the present system, gains that provide approximately 6 Hz closed loop bandwidth represent a reasonable trade between performance and noise and stability.

commanded and output positions are shown above those of the lower one on the plot.) Notice the cross coupling in the output and in which magnet positions it is most pronounced.

#### Full State Feedback MIMO

- 7) Repeat Step 6 for the LQR based controller of Step 4. Check that the system is providing stable regulation of each magnet. If so congratulations! You have successfully implemented multivariable control! How does the cross-coupling compare with that of the independent SISO controllers? You may wish to input other trajectories such as impulses or ramps and view/plot the system response. Do not input amplitudes greater than 15000. Also, note that a bidirectional trajectory  $>10000$  for the lower magnet will cause it to hit the mechanical stop in the negative direction and should not be executed.

#### **Questions / Exercises:**

- A. Report your calculated values of the closed loop poles for the various values of  $r$  in Step 2 and for your final design. Report the values of  $K$ , for your final design.
- B. Describe the motion of the two magnets under independent SISO controllers from your step series response in terms of their relative interference when the two magnets are closest together and when they are furthest apart. Compare the response to the same series from the multi-variable LQRT based design. Which has the greater cross coupling? Can you see the nonlinear effect of the spring in the outputs? Explain.

## Appendix A. Magnetic Levitation Principles

This appendix gives a brief overview of key concepts in magnetism in general and magnetic levitation in particular. It includes equations and illustrations that show how magnetic fields and forces are generated within the Model 730 apparatus and turntable accessory and concludes with a reference section. For a more rigorous treatment of these topics, the reader is referred to the literature listed at the end of the appendix.

### A.1 Introduction

Magnetic fields are used to describe forces at a distance from electric currents. These currents are of two types: (1) free, or Amperian, currents as drawn from a battery pack, power supply, or an electrical outlet and (2) bound currents as in permanent magnet materials. The forces come in three variations: a. An electrical current feels a force from another current, b. a current feels a force from a permanent magnet, and c. a permanent magnet feels a force from another permanent magnet. This action at a distance is described by saying a magnetic field exists created by one of the bodies at the location of the other body. The magnetic field is the medium by which the force is transferred.

In this section, a brief discussion concerning the magnetic fields caused by magnetized materials (i.e., permanent magnets) is presented. By demonstrating that magnetic materials can be reduced to effective current distributions, this discussion forms the basis for calculating the forces on permanent magnets. The magnetic fields due to free current distributions are calculated next. These fields are used to calculate the forces felt by current-carrying conductors. Time-varying currents cause time-varying magnetic fields. These changing magnetic fields induce electric currents that, in turn, experience a force.

Maglev systems utilize the fundamental physics of electric currents experiencing forces-at-a-distance. These systems are most often described in terms of the interaction of electrical current with magnetic fields. Because the masses of the vehicles are large, large forces are required for magnetic suspension. These large forces are provided by the high magnetic fields of either large superconducting currents or small air gaps in normal ferromagnetic circuits.

A dictionary of common terms is provided at the end of the section and a reference list is included featuring books, Maglev studies and Maglev URLs.

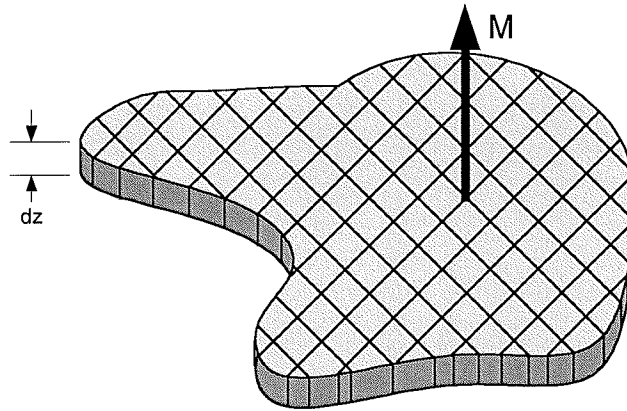
### A.2 Magnetic Fields & Forces

#### A.2.1 Magnetic Fields Caused by Magnetized Materials

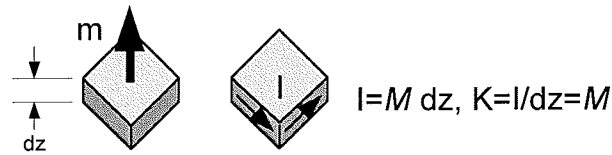
Electron spin is a quantum mechanical phenomenon. Its significance here is the fact that there is associated with the electron spin a magnetic moment of fixed magnitude. To determine the forces on magnetic materials, we use the fact that the magnetic moment of the electron spin *acts as if* it is a current loop.



A volume of magnetized material contains a very large number of aligned electron spins. This is illustrated schematically in the figure below. A grid pattern was superposed onto the material to indicate small volumes of materials which can be analyzed discretely.

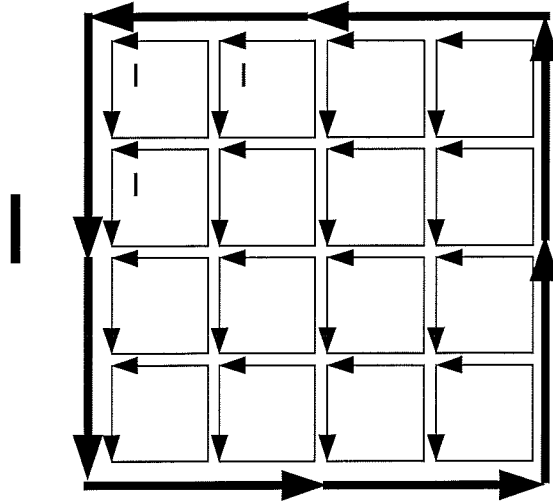


The figure below isolates two small volumes. The one on the left generates a magnetic field due to its magnetic moment,  $m$ . The one on the right generates a magnetic field by virtue of the current wrapping the volume (this is commonly referred to as a “*current sheet*.”), and otherwise ignores the presence of the magnetic material. **The two magnetic fields are entirely equivalent** (external to the material). The material property  $M$  describes the strength of the magnetic material and the amount of current required per unit distance of height. The parameter  $K$  describes the current per unit height within the current sheet. For modern high performance neodymium-iron-boron permanent magnets,  $K \sim 900,000$  amps/meter.

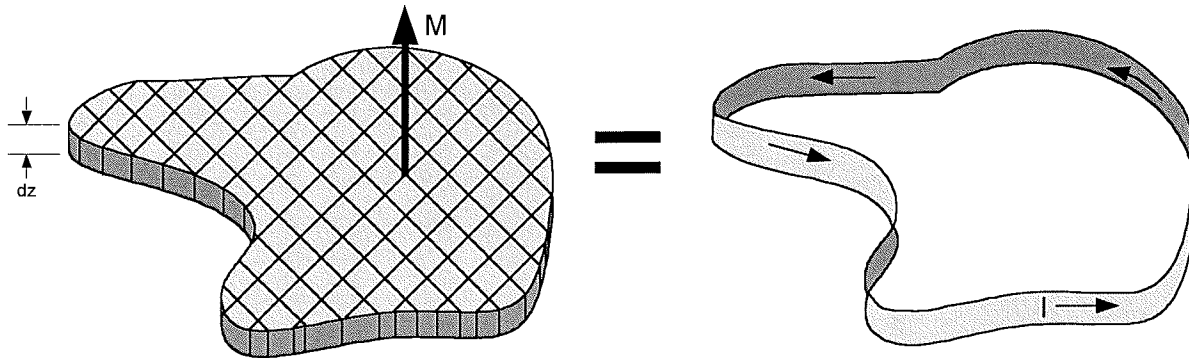


Equivalent as sources  
of magnetic field

Assembling many small volumes in juxtaposition, one can see in the figure below the result of substituting the current loop for the magnetic material; the internal currents cancel while the surface currents do not cancel. Hence, no matter the shape of the material, the external magnetic field can be exactly reproduced by a current stripe along the material perimeter. (This is true if the magnetization is uniform. If the magnetization is uniform then the currents are equal and cancel. If the magnetization is not uniform, then the equivalent current distribution can be calculated by  $J = \text{curl } M$ , where  $J$  is the volume current density.)



In summary, the magnetic field of a uniformly magnetized permanent magnet can be exactly reproduced by a current sheet along the perimeter. This equality is indicated graphically in the figure below. The magnitude of the current is proportional to the material thickness with the constant of proportionality dependent upon the material itself. This equivalence of magnetic fields is commonly exploited to calculate the forces on permanent magnet materials.



A.2.2 Calculating Magnetic Fields

The Biot-Savart Law is the fundamental relationship between current and magnetic field:

$$d\vec{B} = \frac{\mu}{4\pi} \frac{I d\vec{l} \times \vec{r}}{r^3}, \quad (1)$$

- where,
- $dB$  = differential magnetic field, tesla,
- $\mu$  = permeability, Henry/m,
- $I$  = current, amps,
- $dl$  = differential length of current-carrying element, m,

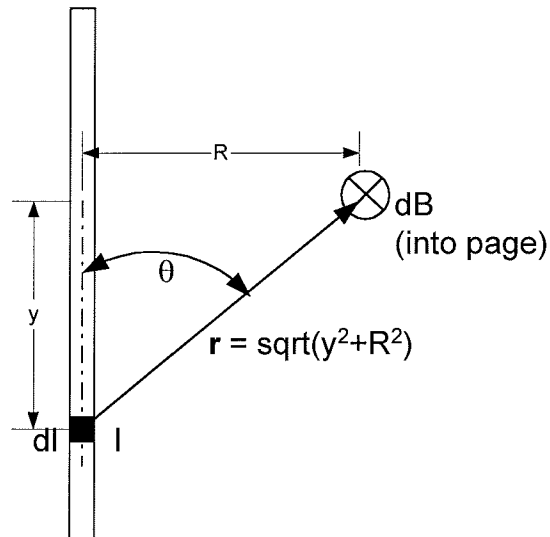
$r$  = vector distance from current element to field point, m.

Two simple geometries for calculating the magnetic field are an infinitely long, straight conductor and a circular loop of conductor.

### A.2.2.1 Straight Conductor

For the straight conductor carrying current upwards along the y-direction, the magnetic field can be calculated at any point due to a differential current element as:

$$dB = \frac{\mu}{4\pi} \frac{I dl \sin \theta}{r^2} \quad (2)$$



By integrating along  $y$  from  $\pm$  infinity, the result is:

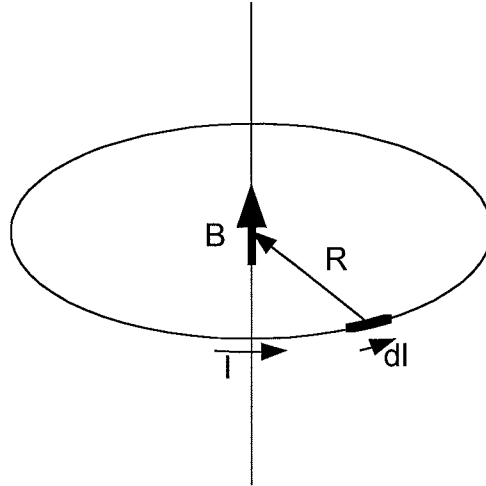
$$B = \frac{\mu I}{2\pi R},$$

where the direction of the magnetic field is determined by the right hand rule (point the thumb of the right hand along the direction of current and the fingers curl in the direction of the magnetic field).

### A.2.2.2 Circular Loop @ Center

The magnetic field at the center of a circular loop of wire can also be calculated from the Biot-Savart Law. In this case, the angle between the current element and field point is a constant ( $90^\circ$ ) so the vector cross product always yields unity. Then the magnetic field is:

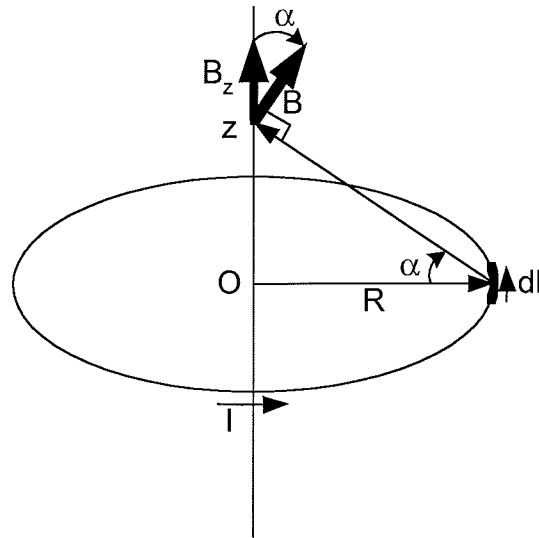
$$dB = \frac{\mu}{4\pi} \frac{I 2\pi R}{R^2} = \frac{\mu I}{2R}. \quad (3)$$



### A.2.2.3 Circular Loop Anywhere Along Axis

The magnetic field along the axis of a circular loop of wire can also be calculated from the Biot-Savart Law. In this case, the angle between the current element and field point is still a constant ( $90^\circ$ ) so the vector cross product always yields unity. The net magnetic field from any current element has vertical and horizontal components. However, as the current element follows the conductor path, the horizontal components of the field cancel while the vertical components add. Then the axial magnetic field is:

$$B_z = \frac{\mu}{4\pi} \frac{I 2\pi R}{z^2 + R^2} \cos \alpha = \frac{\mu I R}{2(z^2 + R^2)} \frac{R}{\sqrt{z^2 + R^2}} = \frac{\mu I R^2}{2(z^2 + R^2)^{3/2}}. \quad (4)$$



Due to the common occurrence of circular coils, this relationship is very important. Along the axis the magnetic field is purely vertical. For values of height,  $z$ , above the plane of the coil, which are small compared to the radius,  $R$ , ( $z \ll R$ ) the vertical magnetic field is insensitive to  $z$ . This is due to the finite radius of the coil. For heights  $z$  much larger than  $R$  ( $z \gg R$ ) the axial field decreases as the reciprocal third power of height. Off-axis, the radial magnetic field decreases as the reciprocal fourth power of height.

### A.2.3 Calculating Magnetic Forces

The force between current carrying conductors is given by the Lorentz Law:

$$d\vec{F} = I d\vec{l} \times \vec{B}, \quad (4)$$

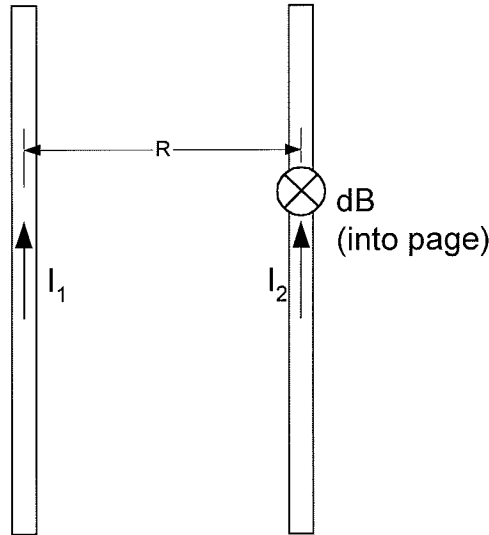
where,

$dF$  = differential force, Newtons.

One simple geometry for calculating the magnetic force per unit length is two infinitely long, straight conductors parallel to each other.

$$\frac{F}{l} = -\frac{\mu I_1 I_2}{2\pi R}.$$

The negative sign means the two parallel currents attract one another. If the direction of one of the currents were to be reversed (anti-parallel currents), the force would also reverse, and the currents would repel. Reversing *both* currents, of course, once again produces an attractive force.



To evaluate the magnetic field at off-axis points, the same formula (1) can be used. The mathematics quickly becomes intractable and the solution is usually implemented numerically. Alternatively, specialized computer aided design software can be used to calculate the magnetic field at arbitrary points in space. The two methods approach the calculation differently (the former is the idealized magnetic field numerically approximated while the other is the high fidelity numerical model of the detailed system). Either method will, of course, yield the same result.

The force due to a current-field interaction off-axis can be calculated according to (4). Thus, in the case of a Neodymium Iron Boron permanent magnet positioned above a coil, the magnet can be modeled as a current sheet of thickness equal to that of the magnet. This “current” creates a magnet field at the location of the coil conductors. The force on the coil and, by Newton’s third law, the force on the magnet is simply the product of the magnetic field, current and conductor path length.

Since the equivalent current of the permanent magnet is in the theta direction (circumferential around the magnet), the vector cross product in the force equation suggests that to get an axial force,  $F_z$  we must have a radial magnetic field,  $B_r$  ( $-\hat{z} = \hat{\theta} \times \hat{r}$ ). In developing the control system, it is convenient to express the radial magnetic field equation in the following form.:

$$B_r = \frac{C1}{(z + C2)^N},$$

where,

$C1$  and  $C2$  are constants depending upon the geometry of the permanent magnets and  $N$  is a parameter describing the decrease in magnetic field with increasing axial distance. For the case of the axial magnetic field, we saw above  $C1$  is the surface current density multiplied by the magnet thickness,  $C2$  is related to the square of the magnet radius, and  $N$  is three or less, depending upon the relative axial distance. The radial magnetic field decreases more rapidly

with distance than the axial magnetic field by approximately one more power of the denominator:  $3 < N < 4$ .<sup>1</sup>

In order to suit the control law, the following form of the force equation for a magnet-coil interaction is sought:

$$F = \frac{K}{(z + D)^N} \cdot \frac{I}{I_{\max}}$$

The various magnet-coil interactions have been analyzed and the appropriate constants have been determined. Because of the inherent non-linearity of magnetic fields, these *constants* can vary when the excursion from the calculated system is large, i.e., the equations have been approximated by constant parameters in the region of interest. That is, at very large axial heights or very low heights the constants will differ from those calculated.

The form of the force is the same for interactions between permanent magnets due to the equivalent current concept discussed above. In this case, however, the current is not a free parameter for control but is determined by the geometry.

#### A.2.4 Calculating Induced Currents

A time-varying magnetic field induces voltages in a closed loop according to Faraday's Law:

$$V = -N_t \frac{\partial \phi}{\partial t},$$

where,

V is the induced voltage around a closed loop,

$N_t$  is the number of turns of conductor around the loop, and,

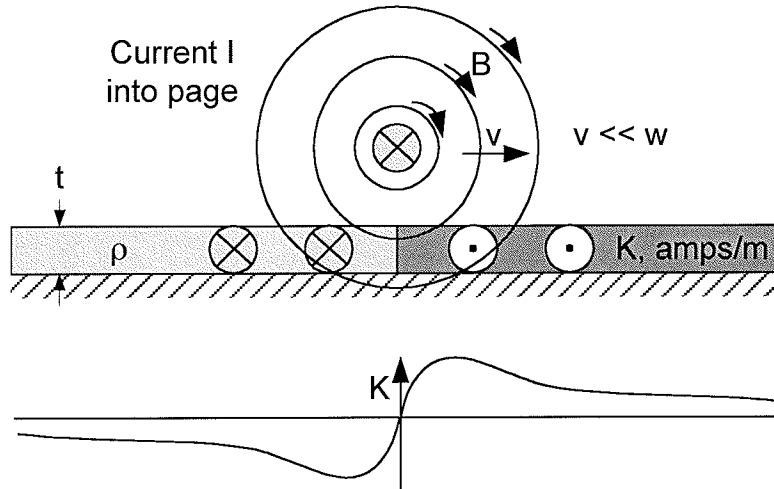
$\partial \phi / \partial t$  is the flux rate of change through that loop.

The negative sign in Faraday's Law is the manifestation of Lenz's Law. Lenz's Law states that when currents are induced in bodies due to a changing magnetic field, the currents are in such a direction as to cancel the change in magnetic field experienced by the body. For instance, if no field is present and suddenly a field is applied, the induced currents tend to circulate to cancel the magnetic field. If, however, the magnetic field has previously existed, removal of the magnetic field causes currents to flow in an attempt to maintain the field.

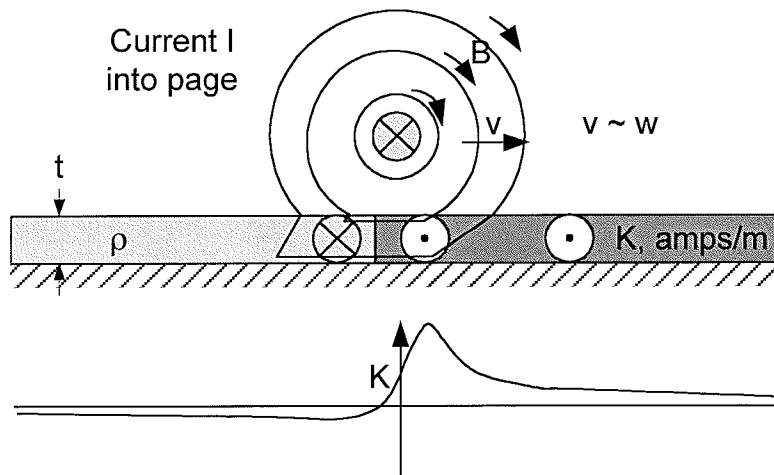
Consider a single current-carrying conductor moving relative to a conductive sheet. It can be shown [Magneto-Solid Mechanics, p. 339 ff] that there is a characteristic velocity of the motion,  $w$ :  $w = \frac{2\rho}{\mu_0 t}$ , where,  $\rho$  is the sheet material resistivity,  $t$  is the thickness of the sheet and  $\mu_0$  is the permeability of free space. At standstill, the magnetic field of the current will fully permeate the

<sup>1</sup> In evaluating specific geometries and using numerical curve fitting, exponents of value  $N > 4.0$  can result. For the Model 730 Apparatus,  $N \leq 4.3$ .

sheet conductor. The magnetic field lines will be perfect circles about the current center. At very low speeds, ( $v \ll w$ ) the field still permeates the sheet and the field lines will still be very nearly circular. This situation is shown in the figure below, the induced current in the sheet is  $K$  amps/meter.



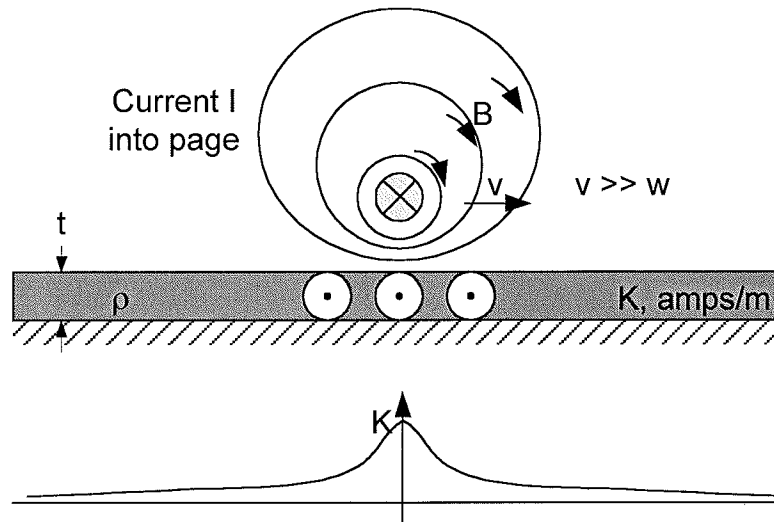
As the conductor speed is increased to approximately the characteristic velocity ( $v \sim w$ ), the movement of the magnetic field through the sheet causes induced currents to flow. According to Lenz's Law, these currents flow in such a manner so as to cancel the effect of the approaching field. Nevertheless, due to finite resistance, the magnetic field will still penetrate the conductive sheet to an extent and as the conductor leaves the region of magnetic field additional currents are induced to maintain the presence of the field. This situation is shown in the figure below. Notice the shear effect of the motion on the magnetic field.



When the speed is increased to substantially above the characteristics velocity, the conductivity of the sheet prevents the magnetic field from any significant penetration. The conductor is moving sufficiently fast that significant resistive dissipation does not occur. Each section of



sheet generates the exact required current to perfectly shield the interior of the conductive sheet from the magnetic field. This situation is shown in the figure below. Notice that the magnetic field lines do not enter the sheet.



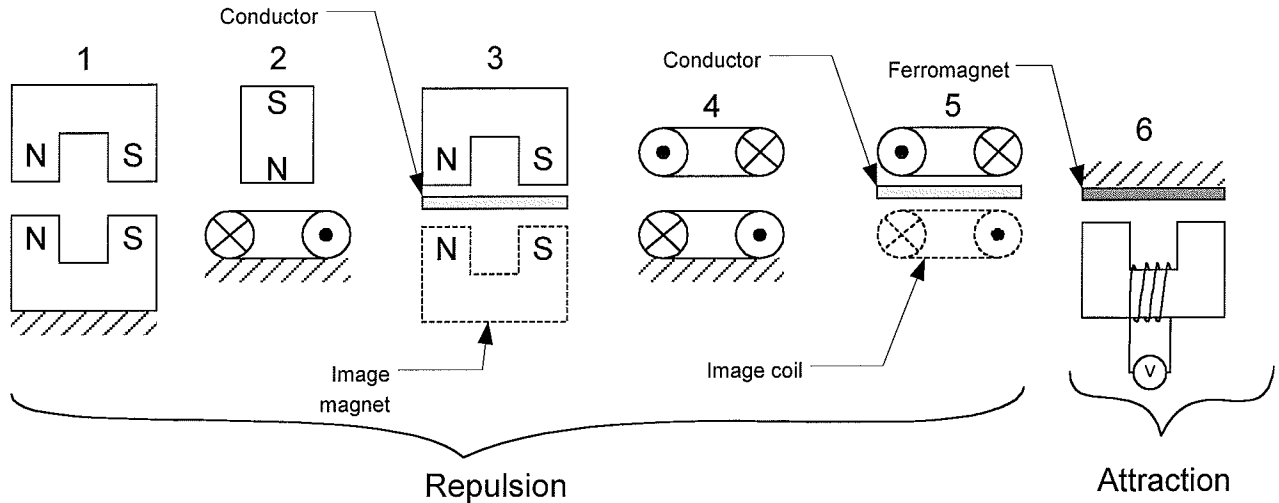
For application to the demonstration unit, the current element is the equivalent current of the permanent magnet edge. The permanent magnet flying above a rotating conductive sheet introduces several details different from that described above. The physical principle remains the same; that is, the currents are induced in the sheet in response to the apparent change in magnetic field, and these currents tend to cancel the change in magnetic field. The interaction of the (magnetic field from) the induced currents and the original permanent magnetic field produce a repulsion force which levitates the magnet. These fundamentals are the basis of several different configurations of Maglev systems.

### A.3 Maglev Applications

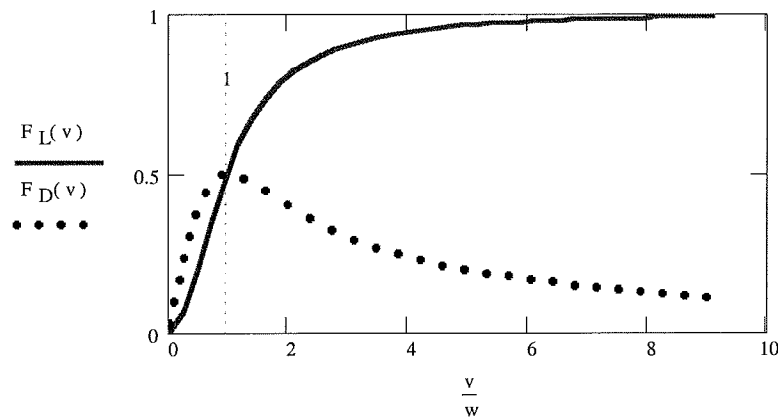
The figure below shows six arrangements used in magnetic levitation of moving vehicles. Five of the arrangements rely on repulsive forces. The lower elements are fixed (say, with respect to the earth) and the upper elements levitate. The first arrangement (permanent magnet like poles) is the common one for demonstrating like magnetic poles repel. The second and fourth arrangements (permanent magnet and/or superconducting magnet flying over a normal copper lower coil) is similar to that used for the Japanese superconducting Maglev system. The third and fifth systems are similar to the Magneplane system where permanent magnets or superconducting coils fly over normal sheet conductor. Notably, this has been variously proposed as an inexpensive method to attain levitation.

The sixth arrangement (electromagnet under a ferromagnet) is quite different and is the basis for the German Transrapid Maglev system. The fixed element is the upper ferromagnetic material and the lower electromagnet is actively controlled. If the current in the electromagnet is too large, the electromagnet feels a net upward force until it contacts the ferromagnetic material. If

the current is too small, then insufficient force is available and the electromagnet falls. Hence, the current in the electromagnet must be continuously adjusted to enable levitation without contact.



For applications involving moving vehicles, all maglev designs share a common trait: while generating magnetic lift (in the direction perpendicular to travel) there is also generated magnetic drag (opposing the direction of travel). The details of the lift and drag forces, of course, depend upon the configuration, but the following figure (calculated for the conductor moving over the sheet, configuration 5 above) gives an idea of the variation in magnetic lift and drag with speed. The figure shows the drag peak and the reduction in drag as speed increases—in marked contrast to aerodynamic drag. The figure also shows the monotonic increase in lift force with increasing relative speed. Note that the lift force equals the drag force when the relative speed is equal to the characteristic velocity,  $w$ . Note also that this lift force is equal to 50% of the maximum lift force.



## A.4 Reference

News Item: 14 April 1999 Japanese Maglev vehicle demonstrates top speed of 552 km/hr (345 mph).

### A.4.1 Current Status of Maglev in the United States & Internationally

Superconducting Maglev technology was initiated in the late 1960's and early 1970's in the United States in 1969 when Drs. James Powell and Gordon Danby of New York's Brookhaven National Laboratory invented the concept of a repulsive magnetic suspension using superconducting magnets. In the mid-1970's the US stopped Maglev development due to funding problems. Other countries, however, continued to develop Maglev and today have viable systems. In the early 1990's Maglev research was rekindled at a Federal government level. At various times, the Department of Transportation's Federal Railroad Administration and Federal Transit Administration, NASA, Department of the Air Force, and Department of the Navy have joined resources for the purpose of developing Maglev and Linear Motor technology. Although each agency had its own specific application in mind, a loose consortium seemed to provide the best bang for the buck. The situation has progressed where today there are several high speed (~300 mph) and low speed (~100 mph) regions in this country where Maglev is thought to be a viable alternative means of rapid public transportation—yet it is still unproven in the United States.

Germany's Transrapid vehicle has been extensively tested and has been proposed for use on several projects in this country. The Germans are presently constructing a Transrapid route from Hamburg to Berlin.

Japan is developing a system that uses superconducting magnets and is currently constructing a major test route that will ultimately be incorporated into a revenue-producing route. Approximately 80% of this system will be in tunnels cut into mountains. This has greatly increased the construction cost but has decreased the cost of land acquisition for the Maglev right-of-way.

### A.4.2. Glossary

<b>Term</b>	<b>Definition</b>
Eddy Currents	Induced currents in conductors by changing magnetic fields. Since the currents flow in closed paths within the materials, they are similar to eddies in rivers. In accordance with Lenz's Law, these currents flow in such a manner as to oppose the change in magnetic field inducing them. Frequently, eddy currents are undesirable, but they can be desired in cases of induction and microwave heating for industrial and consumer purposes.
EDS	Electrodynamic System
Electrodynamic System	Magnetic forces based upon repulsion from induced currents. Inherently stable can be lightly damped or even negatively damped at sufficiently high frequencies.

Electromagnetic System	Magnetic forces based upon attraction from applied currents. Inherently unstable and currents must be controlled.
EMS	Electromagnetic System
HSST	High Speed Surface Transportation (not as “high speed” as the name sounds). Japanese EMS Maglev.
Maglev	Generic term for magnetic suspension. Sometimes refers to both levitation(vertical forces) and guidance (side-to-side forces).
Magnetic Drag	Magnetic force opposing propulsion, due to resistive dissipation. Units are Newtons.
Magnetic Field, $\mathbf{H}$	Three-dimensional vector used to calculate the enclosed current as used in Ampere’s Law. $\nabla \times \mathbf{H} = \mu_0 \mathbf{J}_{free}$ . This parameter is independent of the material properties. Units are Amperes/meter, A/m.
Magnetic Flux Density, $\mathbf{B}$	Three-dimensional vector used to calculate the force on conductors and magnetic materials. Units are $\text{Wb}/\text{m}^2$ or Tesla, T. $\nabla \times \mathbf{B} = \mu_0 (\mathbf{J}_{free} + \mathbf{J}_{bound})$ . Recall also $\mathbf{F} = I \, d\mathbf{l} \times \mathbf{B}$ .
Magnetic Flux, $\phi$	$\phi = \iint \vec{\mathbf{B}} \cdot d\vec{\mathbf{A}}$ , the integral of the vector dot product of the flux density and area. Units are Webers, Wb.
Magnetic Lift	Magnetic force opposing gravity.
Permeability	$\mu = \mathbf{B}/\mathbf{H}$ , Ratio of flux density to magnetic field. Units are Henries/meter, H/m.
Reluctance	Ratio of total magnetomotive force to total flux through a circuit. Units are inverse Henries, $\text{H}^{-1}$ .
RTRI	Railway Technical Research Institute Japanese research arm to develop EDS Maglev
Superconductivity	The material property of the complete lack of electric resistance, obtained for special materials only under conditions of refrigeration. Two classes of materials are low critical temperature superconductors ( $T \leq 10\text{K}$ ) and high critical temperature superconductors (HTSC) ( $T \leq 77\text{K}$ ).
Transrapid	German EMS Maglev, Hamburg to Berlin route under construction.
Inductance, L	$L = N_t \phi / I$ , Total flux linked per unit current. Units are Henries, H.
Magnetomotive force, mmf	$MMF = \oint \vec{\mathbf{H}} \cdot d\vec{\mathbf{l}} = N_t I$ . Intermediate quantity used for magnetic circuits. Conceptually similar to the electromotive force or voltage of an electric circuit. Units of mmf are Ampere-turns.
Lenz’s Law	A law stating that induced currents resulting from a change in magnetic field are in such a direction as to oppose the change in magnetic field. Hence, if a magnetic field is increased, current is induced to cancel it. If the magnetic field is decreased, current is induced to preserve it.

### A.4.3 Reference Literature:

#### Books

1. Superconducting Levitation: Applications to Bearings and Magnetic Transportation, Francis Moon, Wiley & Sons, New York, 1994.
2. Case Studies in Superconducting Magnets: Design and Operational Issues, Yukikazu Iwasa, Plenum Press, New York, 1994.
3. Magneto-Solid Mechanics, Francis Moon, Wiley & Sons, New York, 1984.
4. Electromagnetic Levitation and Suspension Techniques, B.V. Jayawant, Edward Arnold Publishers, London, 1981.
5. Electromagnetics, J.D. Kraus, McGraw Hill Companies, New York, 1992, p. 288.
6. Electricity & Magnetism, E. Purcell, McGraw-Hill Book Companies, New York, 1965.

#### Maglev Studies

7. "Study of Japanese Electrodynamic Suspension Maglev Systems", J.L. He, D.M. Rote, H.T. Coffey, Argonne National Lab, Argonne, IL, 60439, April 1994.
8. "New York State Technical and Economic Maglev Evaluation," Michael Proise, Grumman Space and Electronics Division, New York, June 1991.
9. "Electrodynamic Suspension and Linear Synchronous Motor Propulsion for High Speed Guided Ground Transportation," David Atherton, Canadian Maglev Group, CIGGT Report No. 77-13, September 1977.
10. "Conceptual Design and Analysis of The Tracked Magnetically Levitated Vehicle Technology Program Repulsion Scheme, Volume I – Technical Studies," Ford Motor Co., US DOT/FRA, Report PB247931, Feb. 1975.

#### Maglev Web Sites:

11. <http://bmes.ece.utexas.edu/~jcamp/physics/index.html> Descriptive link of Maglev technologies and basic physics.
12. <http://eb-p5.eb.uah.edu/maglev/maglev.html> Univ. of Alabama Huntsville College of Engineering WWW Archive and Information service for High Speed and Automated Transportation Technologies. (This site is relatively new and has unfinished links.)
13. <http://www.rtri.or.jp/> RTRI Home page. Japanese EDS Maglev.
14. <http://www.mvp.de/english.htm> Transrapid Official Homepage. German EMS Maglev.
15. <http://weber.u.washington.edu/~jbs/itrans/hsst.htm> HSST unofficial descriptive page.
16. <http://www.meitetsu.co.jp/chsst/mecha.html> Mechanism of HSST. Japanese EMS.
17. <http://popularmechanics.com/popmech/sci/9805STTRP.html> "Track to the Future" article. Descriptive article of one recent Maglev approach.
18. <http://www.llnl.gov/str/Post.html> "A New Approach to Levitating Trains - and Rockets." Elaboration of the previous link for a Maglev approach.



## **6i. Instructor's Supplement To Experiments**

This is the instructor's supplement to the experiments described in Chapter 6 of the main manual. It contains the expected experimental results and solutions to exercises as well as additional optional experiments and exercises.

This supplement is organized with section numbers consistent with those of the seven experiments in the main manual body. In addition to describing experimental results, Section 6.1i contains numerical models of three plant configurations. Appendix Ai lists MATLAB® scripts and real time routines that are provided with the system and are useful in building numerical plant models and performing the experiments.

### On The Nature & Scope of Experiments

The experiments are designed to provide sufficient detail that the students may, for the most part, follow the instructions without undue burden in laboratory supervision. Such supervision is of course required however. Also, the material may not be presented precisely in a manner consistent with the desired content or time constraints of a particular course. It is therefore important that the instructor read ahead of each lesson to tailor the content if necessary. In particular, some preparation and homework on the part of students in advance of the experiments will significantly reduce the time required in the laboratory.

There are many control systems topics that relate to this system and these experiments which are not explored in the manual, but which the instructor may wish to bring out. The methodologies presented here demonstrate some fundamental principles and behaviors, but are not represented to be necessarily superlative practical control solutions. They do in the least however, give the undergraduate student a hands-on introduction to control implementation. The more advanced user is provided a working orientation to the system from which more general topics may be explored.

### Note to instructors and advanced users:

If you or your students synthesize and implement a control structure that is of particular academic or instructional interest, please share it with us! Pending ECP review and your approval, it may be included in a future revision of this manual with credits of course to the inventor. For all earnest submittals, you will receive a complementary software and manual upgrade!

### 6.1i System Identification

The procedure given is for verifying the nonlinear forms of the magnetic fields and identifying the raw sensor characteristic. The resulting models of these nonlinear effects are used in control analysis and for real-time compensation of the nonlinearities. The latter part of this section demonstrates the effectiveness of the nonlinear compensation<sup>1</sup> and shows how these can be used to reduce the control design to that of a simple rigid body plant. A quick procedure for generating the nonlinear characteristics and plant models is given at the end of this chapter.

#### Expected Experimental Results:

1. In 6.1.1: Representative data of the sensor characterization tests are shown in Table 6.1-1i. These may vary by as much as 10% from system to system for a given position.

**Table 6.1-1. Representative Sensor Calibration / Linearization Data**

Magnet Position For Sensor #1 (cm)	$Y_{1_{raw}}$ (Sensor 1, counts)	Magnet Position For Sensor #2 (cm)	$Y_{2_{raw}}$ (Sensor 2, counts)
0.00	30,000	0.00	29,900
0.50	25,700	-0.50	26,300
1.00	21,600	-1.00	22,100
2.00	14,900	-2.00	15,300
3.00	10,400	-3.00	10,600
4.00	7400	-4.00	7600
5.00	5300	-5.00	5450
6.00	3750	-6.00	3920

2. In 6.1.2: Representative data of the actuator characterization tests are shown in Table 6.1-2i. These may vary by as much as 5% from system to system; this is largely due to differences in the servo amplifier gains. For most control design purposes, the upper and lower actuator characteristics may be assumed to be identical. There will be some differences due to amplifier gain, but the nonlinear characteristic is primarily due to the shape of the magnetic field which does not vary appreciably. If precise characterization of the upper actuator input/output characteristic is needed, the unit may be inverted and the described procedure repeated. (This must of course be done in such a way to protect and not damage the apparatus – e.g. support the baseplate by blocks at its corners that are taller than the vertical column of the apparatus.)

<sup>1</sup> Here the “nonlinear compensation” refers to a non-dynamic (position dependent only) inversion of the nonlinear characteristic.



**Table 6.1-2i. Representative Actuator Calibration / Linearization Data**

Magnet Position (cm)	$u_{I_{raw}}$ (Uncompensated Control Effort, counts)
0.00	3050
0.49	4000
0.88	5000
1.22	6000
1.83	8000
2.28	10000
2.69	12000
3.03	14000
3.60	18000
4.05	22000

3. In 6.1.3: The simple real-time algorithm for putting control effort values on the DAC is

```
begin
control_effort1=5000
end
```

Representative data of the magnet-to-magnet force characteristic is shown in Table 6.1-1i. This data is provided to the students and is repeated here for convenience.

**Table 6.1-3i. Magnet-to-magnet Force Interaction Data**

Weight at Magnet #2 ( $f_{m_{12}}$ , N)	Magnet #2 Position Relative to Magnet #1 At Equilibrium ( $y_{12}$ , cm)
0.402	11.73
0.612	10.30
0.735	9.57
0.998	8.80
1.190	8.09
2.171	6.72
3.152	5.90
4.133	4.78
6.095	4.25
11.00	2.74

4. In 6.1.4: The mass of the magnet should be  $120 \pm 4$  g. The corresponding weight is  $1.18 \pm 0.04$  N.

### Questions / Exercises

- A. The curve fitting may be done by iteration starting with the inverse term with the inverse square root term equal to zero and adjusting the bias and slope (coefficients  $c$  and  $d$ ) for a best fit. The inverse square root term may be strengthened and again the bias and slope adjusted. By iterating with adjustments of  $a$  and  $b$  while setting the best slope and bias in each case, a close fit can be found within roughly 10 to 15 passes.

A more rigorous and efficient method however is to use regression-based curve fitting of the function  $y^*_{I_{cal}}$  which is linear in the coefficients. A Matlab™ script for this is given in Appendix Ai and yields for the values of Table 6.1-1i :

$$\begin{aligned} \text{Sensor \#1:} \quad e^* &= -10720 \\ f^* &= 692 \\ g^* &= -2.27 \\ h^* &= -0.0000448 \end{aligned}$$

$$\begin{aligned} \text{Sensor \#2} \quad e^* &= 5600 \\ f^* &= -555 \\ g^* &= 1.195 \\ h^* &= 0.0000595 \end{aligned}$$

Note that the sign of the coefficients is reversed for sensor #2 v. #1. A comparison of the test data and the correction function is shown in Figure 6.1-1 where the discrete data points are shown as circles and the fitted function is a continuous line. The above yield  $y^*_{I_{cal}}$  in units of 1 count per cm. When scaled in units of 10,000 counts per cm, these become

$$\begin{aligned} \text{Sensor \#1:} \quad e &= -107200000 \\ f &= 6920000 \\ g &= -22700 \\ h &= -0.448 \end{aligned}$$

$$\begin{aligned} \text{Sensor \#2} \quad e &= 56000000 \\ f &= -5550000 \\ g &= 11950 \\ h &= 0.595 \end{aligned}$$

- B. Again the curve fitting for the actuator correction can be found by “manual iteration”, but is more efficiently derived with the help of linear regression. Here several trials of the parameter  $b$  must be made while the algorithm solves for  $a$  in each case. The Matlab™ script for this is again given in Appendix Ai and yields the following using the data of Table 6.1-2i.

$$a = 1.65$$

$$b = 6.2$$

The data and fitted curve are shown in Figure 6.1-2i. The closeness of the fitted curve appears to justify the use of the fourth power approximation of the magnetic force term in Eq. (5.2-3). (The differences between the data points and the fitted curve are generally less than 1% of full scale which corresponds to a relatively minor nonlinearity in the net control effort. Other nonlinearities such as friction and those in the servo amplifier itself are typically of greater magnitude).

The units of the denominator in the right hand side of Eq.(6.1-3) are DAC counts per Newton. In order for  $K_{u_l} F_{u_l}$  to have units of  $N/10,000$ ,  $a$  must be divided by 10,000; i.e.

$$a_c = 0.000165$$

$$b_c = 6.2$$

The characteristic for the upper actuator (#2) is the same as that of the lower one except the sign of  $b$  is reversed.

- C. The Matlab™ script for fitting the intermagnet force data is again given in Appendix Ai and yields the following using the data of Table 6.1-3i.

$$c = 2.69$$

$$d = 4.2$$

The data and fitted curve are shown in Figure 6.1-3i. The closeness of the fitted curve appears to justify the use of the fourth power approximation of the magnetic force term in Eq. (5.1-7).

- D. The weight of the magnet should be reported to be  $1.18 \pm 0.04 N$ . The values of magnet separation for weights less than this were obtained by tilting the apparatus so that the glass rod is oriented at various angles from the vertical. The force is the projection of the magnet weight onto the direction of the glass rod and the separation distance is measured as before. The data for weight = 0.612 N for example was taken with the glass rod nearly 60 degrees from vertical. (This procedure is facilitated by spinning the magnet to release the bushing/rod friction at high tilt angles)

The weight at magnet two is equal to the repulsive force at equilibrium.

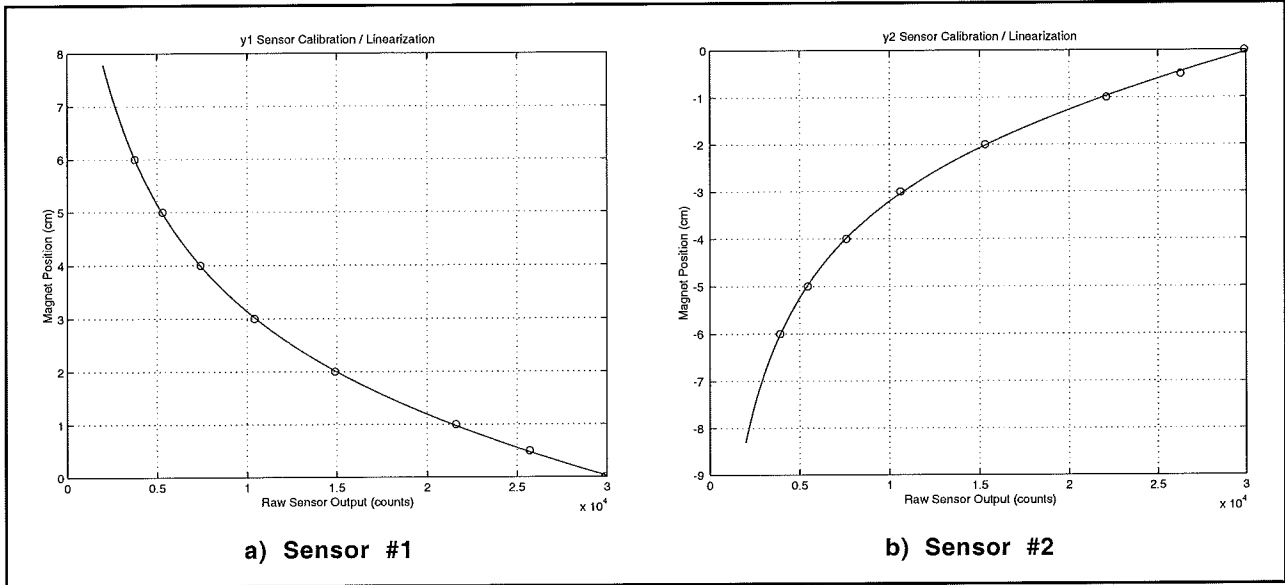


Figure 6.1-1i. Curve Fit for Sensor Calibration / Compensation

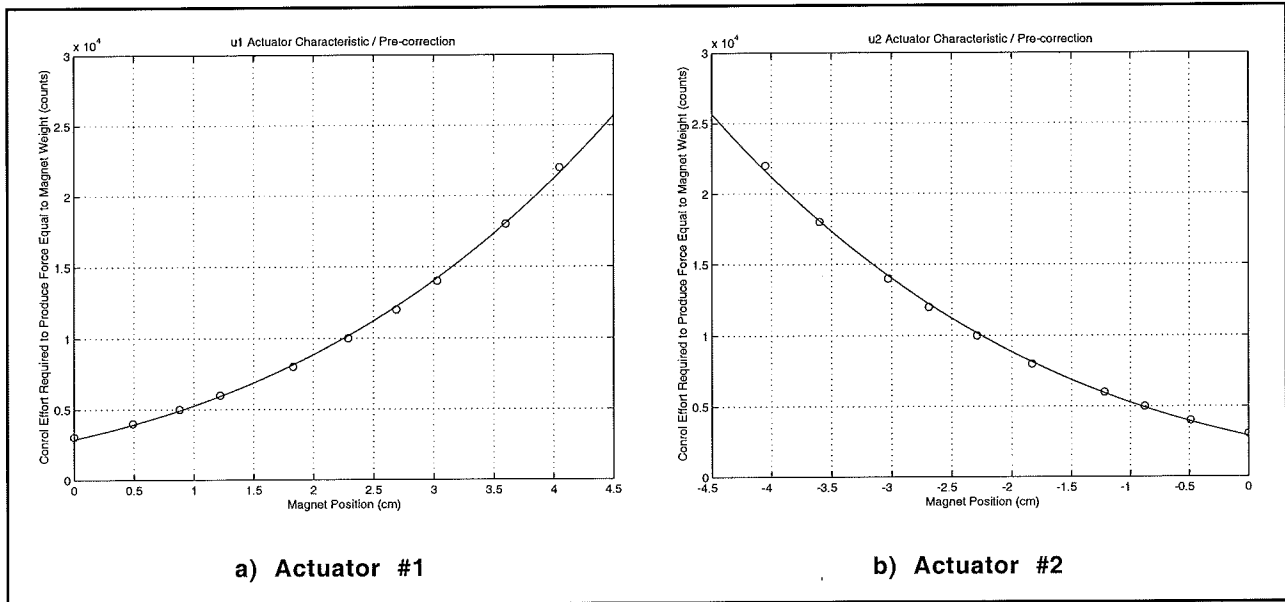


Figure 6.1-2i. Curve Fit for Actuator Calibration / Compensation

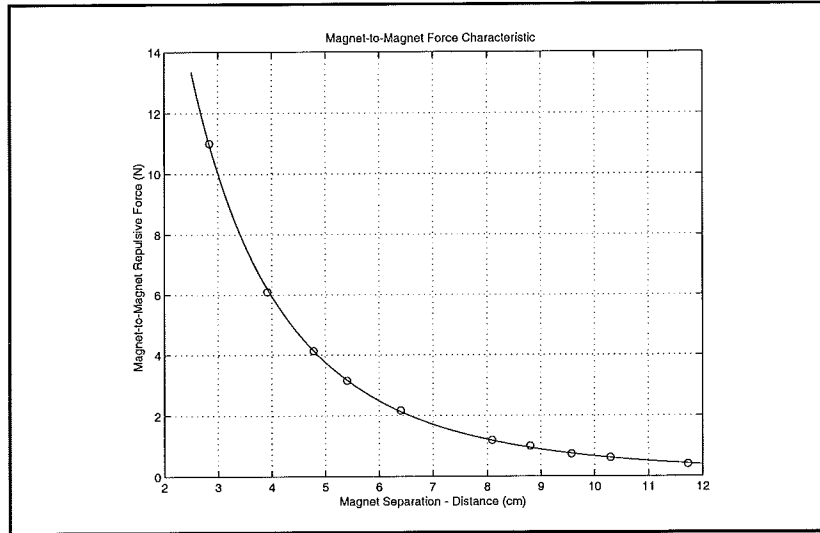


Figure 6.1-3i. Curve Fit of Intermagnet Repulsion Characteristic

5. In 6.1.5: The real-time algorithm for sensor nonlinearity correction should be consistent with the following recommended one where the coefficients of  $y_{Ical}$  are those given above.

```

;*****Declare variables*****
#define ylcal q5
#define ylrw q6
;*****Initialize*****
ylcal = 0
control_effort1=0
control_effort2=0
;*****Begin Real-time Algorithm*****
begin
ylrw=sensor1_pos; Choose "Use Raw Sensor Data" in Setup Sensor Calibration dialog
box
ylcal=-107200000/sensor1_pos+6920000/sqrt(sensor1_pos)-22700-0.448*sensor1_pos
q10=ylcal
q11=ylrw
end

```

**Important Note:** There may be slight differences between the version of any real-time routine shown in this manual and those on the diskette furnished with the system. The diskette contains the latest version of these routines and should be used for actual implementation.

The algorithm for constant force (position independent) should be consistent with the following:

```

;*****Declare variables*****
#define ylcal q4
#define ylrw q5
#define magwt q6
#define gravityoffset q7
#define uterm1 q8
#define uterm2 q9

```

```

;*****Initialize*****
control_effort1=0
control_effort2=0
magwt=11800 ;Newtons
gravityoffset=magwt/1 ;One half the magnet weight

;*****Begin Real-time Algorithm*****
begin
ylraw=sensor1_pos; Select "Use Raw Sensor Counts" in Setup Sensor Calibration
dialog box
ylcal=-10720000/ylraw+6920000/sqrt(ylraw)-22700-0.448*ylraw
uterm1=6.2+ylcal/10000
uterm2=uterm1*uterm1
control_effort1=0.000165*uterm2*uterm2*gravityoffset
end

```

**Important Note:** Students should understand the need for induced drive saturation in the real-time processing. The two's complement DAC will abruptly change output polarity at full amplitude once its range ( $2^{15}=32768$ ) has been exceeded. This is obviously an undesirable condition that could lead to a large amplitude limit cycle and equipment damage. To avoid this, a saturation routine is always included in the ECP firmware to so that its amplitude saturates at full scale. Such a routine should be implemented whenever the user provides his/her own control processing resources (e.g. the system was purchased in the "Plant Only" form). The saturation routine has the following logic. This code may be implemented within the real-time routine if, for example, the user desires to reduce the saturation limits.

```

if (u1>30000)
u1=30000
endif
if (u1<-30000)
u1=-30000
endif
control_effort1=u1

```

Here `u1` is the output of the control algorithm and `control_effort1` is (as always) the number put on DAC #1.

#### Questions / Exercises

- E. The plot of the raw and linearized sensor outputs is shown in Figure 6.1-4i. The raw signal is highly nonlinear with much greater change in output with position (i.e. gain) near zero position (approximately 30,000 counts) than at 6 cm. Its value decreases with increasing position. The linearized sensor data shows equal change of output with actual position through the range tested and increases with increased position. Some errors in the plot will result from the manual operation of positioning the magnet at the incremental (1 cm.) positions.
- F. The student should feel an approximately constant force during the trials. In the trial with the force specified as one magnet weight the magnet should (of course) feel approximately weightless. Some variations in force will occur due to errors in the curve fit and friction and servo amplifier nonlinearities.
- G. The expanded closed loop block diagram including nonlinearity and gravity

feedforward compensation is shown in Figure 6.1-5i. The elements to be implemented in the real time algorithm are shown in bold outline. The nonlinearity compensation and gravity feedforward algorithms are static (i.e. are constant or depend only on the position, [e.g. not velocity or acceleration] of the system). The subscript "c" in  $(mg)_c$  denotes the magnet weight in controller output units (N/10000). For a magnet in the upper position with positive displacement of  $y_2$  being upward, the block diagram as shown would be identical except of course that the subscripts indicating location 1 v. 2 would be changed. The polarities of the magnet and coil are assigned so that positive control effort results in a repulsive force in the lower actuator and an attractive one in the upper. The underlying plants are qualitatively different in that the lower one is open loop stable and the upper is unstable. That they appear identical in the closed loop diagram is due to the control effort nonlinearity compensation which approximately negates the magnetic field force/position characteristic (the source of the instability in the upper plant). The inherent stability / instability of these systems is addressed in the next section.

- H. The equivalent simplified block diagram is shown in Figure 6.1-6i which includes the values of the gains  $k_s$  and  $k_u$ . The system gain,  $k_{sys}$ , is the product  $k_s k_u$  and has the value of 100 N/m. When the control effort nonlinearity is not compensated, the actuator gain is

$$k_{u1} = \frac{1}{a(y_1+b)^4}, \quad k_{u2} = \frac{1}{a(-y_2+b)^4} \quad (\text{N / count}) \quad (6.1-1i)$$

where the *counts* are counts on the DAC. The sensor gain is the change in raw sensor counts with position. I.e. it is the inverse of the right hand side of Eq.(5.4-5)

$$k_{si} = 100 \left( \frac{-e_i}{(y_{i_{raw}})^2} - \frac{f_i}{(y_{i_{raw}})^{3/2}} + h_i \right)^{-1} \quad i = 1, 2 \quad (\text{sensor counts/m}) \quad (6.1-2i)$$

where the *counts* are counts on the ADC and the factor of 100 is needed for length units of meters. The above gains are dependent on position. The actuator gain decreases with the inverse fourth power of position, and the sensor gain magnitude decreases with position (it increase in magnitude with  $y_{i_{raw}}$ ). Thus the system will display relatively high gain for small coil/magnet separation and much lower gain when the separation is large.

- I. The numerical plant models are given below. These are easily generated using the Matlab™ script *SISOplant.m* whose routines follow directly from the equations of Chapter 5. In solving for case 1 in the exercise, the raw sensor output,  $y_{1_{raw}}$ , at  $y_{1o} = 2.0$  cm is needed – similarly for the upper output. These may be found by solving Eq.(5.4-1) numerically or by reading off the plots of Figure 6.1-1i. For the specific parameters given in this section, the raw outputs are  $y_{1_{rawo}} = 15000$  counts,  $y_{2_{rawo}} = 15400$  counts for  $y_{1o} = 2.0$  cm and  $y_{2o} = -2.0$  cm respectively.
- J. The numerical multi-variable plant models are also given below. These are easily generated using the Matlab™ script *MIMOplant.m*. The state space forms derive directly from the equations of Chapter 5. The transfer matrix expressions require solving the appropriate equation of motion pairs (e.g. Eq's 5.3-4, -5) to isolate the independent variables and solve for the characteristic denominator.

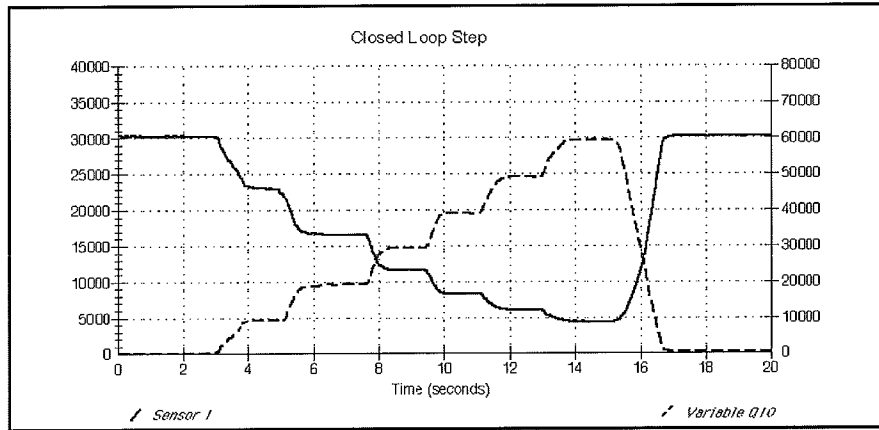


Figure 6.1-4i. Typical Plot From Sensor Compensation Verification Test

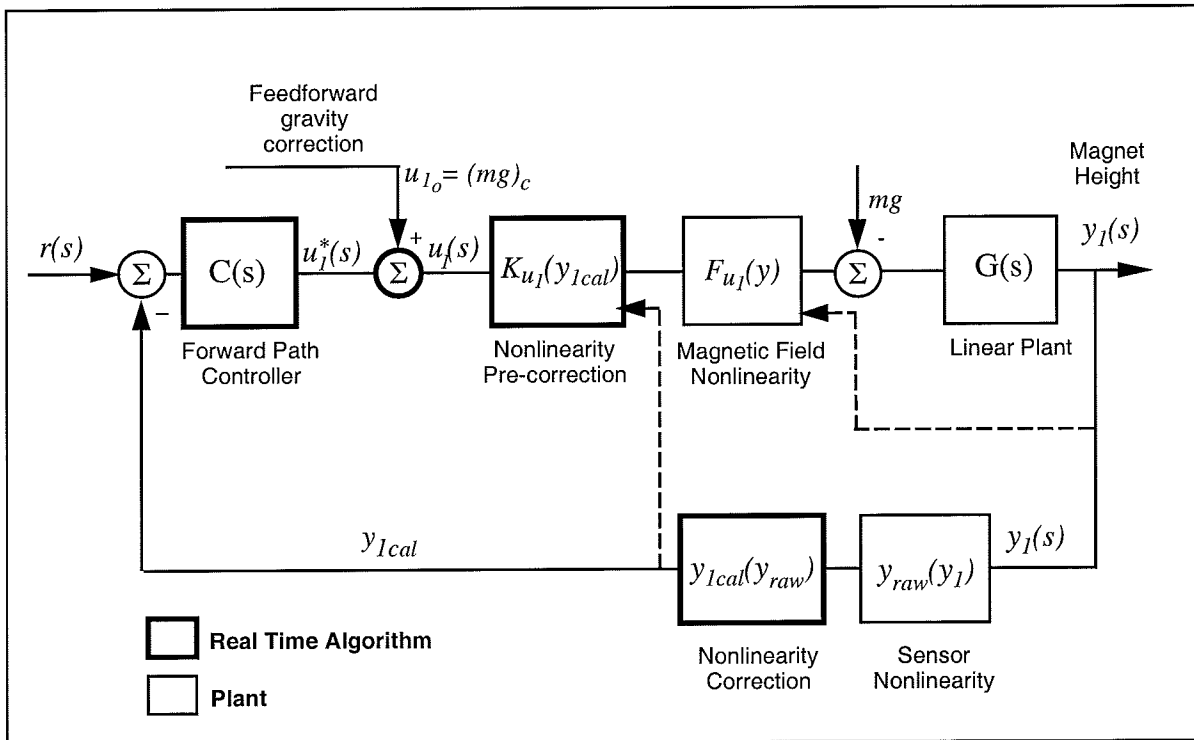
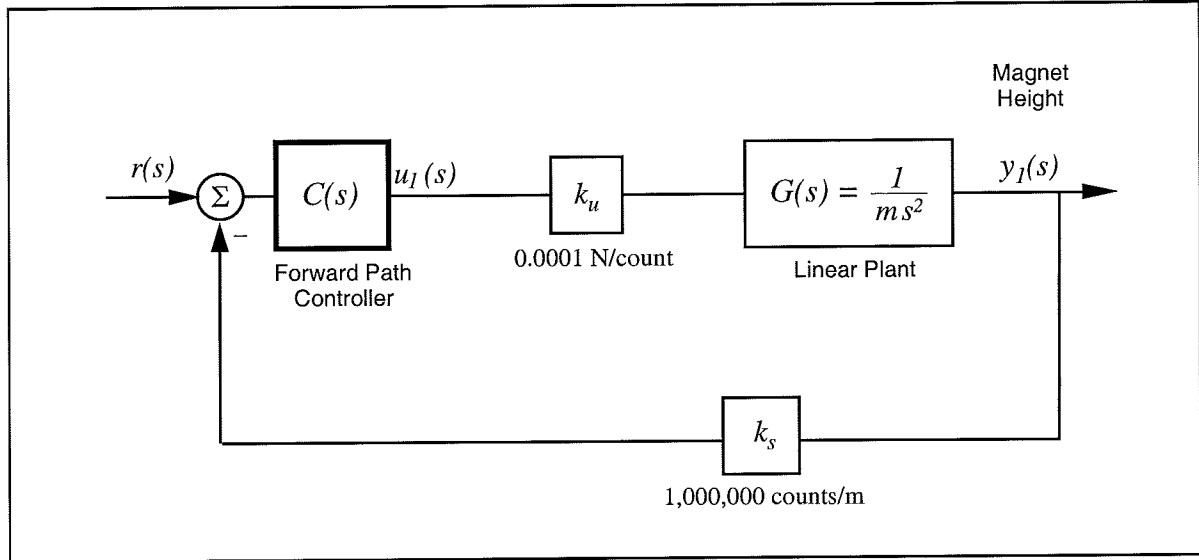


Figure 6.1-5i. Block Diagram of Closed Loop System Including Nonlinear and Gravity Compensation Elements





**Figure 6.1-6i. Equivalent Block Diagram Assuming Effective Nonlinear and Gravity Compensation**

Note to Instructor: Exercises I&J do not need to be completed in their entirety to complete the experiments of this manual. In this manual, only plant types listed under 1a, 1b, 3a, 3b, and 6 below are used. (All are quickly generated using *SISOplant.m* and *MIMOplant.m*) The exercises may of course be reduced in scope at the discretion of the instructor. – It’s a lot of homework!

Numerical Plant Models:

The following numerical plant models are consistent with the parameters of a particular apparatus as given elsewhere in this chapter. They are nominally representative of any Model 730 system. For more accurate modeling, the specific parameters of a given system should be measured as per the instructions given in the student’s section or using the “Quick Steps” below. The expressions below were generated using the Matlab™ scripts *SISOplant.m* and *MIMOplant.m* given in Appendix Ai.

1a) SISO, Location #1, Nonlinear Actuator & Sensor, Plant Linearized About  $y_I = 2.0$  cm.

$$\frac{y_{1_{raw}}^*(s)}{u_1^*(s)} = \frac{-597}{s^2 + 479} \tag{6.1-3i}$$

$$X = \begin{bmatrix} y_{1_{raw}}^* \\ \dot{y}_{1_{raw}}^* \end{bmatrix}, A = \begin{bmatrix} 0 & 1 \\ -479 & 0 \end{bmatrix}, B = \begin{bmatrix} 0 \\ -597 \end{bmatrix}, C = [ 1 \ 0 ] \tag{6.1-4i}$$

2a) SISO, Loc. #1, Nonlin. Actuator, Linearized Sensor, Plant Linearized About  $y_I = 2.0$  cm.

$$\frac{y_1^*(s)}{u_1^*(s)} = \frac{1110}{s^2 + 479} \tag{6.1-5i}$$

$$X = \begin{bmatrix} y_1^* \\ \dot{y}_1^* \end{bmatrix}, A = \begin{bmatrix} 0 & 1 \\ -479 & 0 \end{bmatrix}, B = \begin{bmatrix} 0 \\ 1110 \end{bmatrix}, C = [1 \ 0] \quad (6.1-6i)$$

3a) SISO, Location #1, Linearized Actuator, Linearized Sensor

$$\frac{y_1^*(s)}{u_1(s)} = \frac{826}{s^2} \quad (6.1-7i)$$

$$X = \begin{bmatrix} y_1^* \\ \dot{y}_1^* \end{bmatrix}, A = \begin{bmatrix} 0 & 1 \\ 0 & 0 \end{bmatrix}, B = \begin{bmatrix} 0 \\ 826 \end{bmatrix}, C = [1 \ 0] \quad (6.1-8i)$$

1b) SISO, Location #2, Nonlinear Actuator & Sensor, Plant Linearized About  $y_2 = -2.0$  cm.

$$\frac{y_{2_{raw}}^*(s)}{u_2^*(s)} = \frac{611}{s^2 - 478} \quad (6.1-9i)$$

$$X = \begin{bmatrix} y_{2_{raw}}^* \\ \dot{y}_{2_{raw}}^* \end{bmatrix}, A = \begin{bmatrix} 0 & 1 \\ 478 & 0 \end{bmatrix}, B = \begin{bmatrix} 0 \\ 611 \end{bmatrix}, C = [1 \ 0] \quad (6.1-10i)$$

2b) SISO, Loc. #2, Nonlin. Actuator, Linearized Sensor, Plant Linearized About  $y_2 = -2.0$  cm.

$$\frac{y_2^*(s)}{u_2^*(s)} = \frac{1110}{s^2 - 479} \quad (6.1-12i)$$

$$X = \begin{bmatrix} y_2^* \\ \dot{y}_2^* \end{bmatrix}, A = \begin{bmatrix} 0 & 1 \\ 479 & 0 \end{bmatrix}, B = \begin{bmatrix} 0 \\ 1110 \end{bmatrix}, C = [1 \ 0] \quad (6.1-13i)$$

3b) SISO, Sensor/Actuator #2, Linearized Actuator, Linearized Sensor

$$\frac{y_2^*(s)}{u_2(s)} = \frac{826}{s^2} \quad (6.1-14i)$$

$$X = \begin{bmatrix} y_2^* \\ \dot{y}_2^* \end{bmatrix}, A = \begin{bmatrix} 0 & 1 \\ 0 & 0 \end{bmatrix}, B = \begin{bmatrix} 0 \\ 826 \end{bmatrix}, C = [1 \ 0] \quad (6.1-15i)$$

4) MIMO, Nonlinear Actuators & Sensors, Plant Linearized About  $y_1 = 1.0$  cm,  $y_2 = -2.0$  cm.

$$\begin{bmatrix} y_{1_{raw}}^*(s) \\ y_{2_{raw}}^*(s) \end{bmatrix} = \begin{bmatrix} \frac{-1412s^2 - 871800}{D(s)} & \frac{-116500}{D(s)} \\ \frac{142700}{D(s)} & \frac{611.5s^2 + 418100}{D(s)} \end{bmatrix} \begin{bmatrix} u_1^*(s) \\ u_2^*(s) \end{bmatrix}, \quad D(s) = s^4 + 13010s^2 + 402830 \quad (6.1-16i)$$

$$X = \begin{bmatrix} y_{1_{raw}}^* \\ \dot{y}_{1_{raw}}^* \\ y_{2_{raw}}^* \\ \dot{y}_{2_{raw}}^* \end{bmatrix}, A = \begin{bmatrix} 0 & 1 & 0 & 0 \\ -683.8 & 0 & -190.5 & 0 \\ 0 & 0 & 0 & 1 \\ -101.1 & 0 & -617.3 & 0 \end{bmatrix}, B = \begin{bmatrix} 0 & ? \\ -1412 & 0 \\ 0 & 0 \\ 0 & 611.5 \end{bmatrix}, C = \begin{bmatrix} 1 & 0 & 0 & 0 \\ 0 & 0 & 1 & 0 \end{bmatrix} \quad (6.1-17i)$$

5) MIMO, Nonlinear Actuator & Lin. Sensors, Plant Linearized About  $y_1=1.0, y_2=-2.0$  cm.

$$\begin{bmatrix} y_1^*(s) \\ y_2^*(s) \end{bmatrix} = \begin{bmatrix} \frac{1864s^2+1151000}{D(s)} & \frac{153800}{D(s)} \\ \frac{258700}{D(s)} & \frac{1108s^2+757700}{D(s)} \end{bmatrix} \begin{bmatrix} u_1^*(s) \\ u_2^*(s) \end{bmatrix}, D(s) = s^4 + 1301s^2 + 402800 \quad (6.1-18i)$$

$$X = \begin{bmatrix} y_1^* \\ \dot{y}_1^* \\ y_2^* \\ \dot{y}_2^* \end{bmatrix}, A = \begin{bmatrix} 0 & 1 & 0 & 0 \\ -683.8 & 0 & 138.8 & 0 \\ 0 & 0 & 0 & 1 \\ 138.8 & 0 & -617.3 & 0 \end{bmatrix}, B = \begin{bmatrix} 0 & ? \\ 1864 & 0 \\ 0 & 0 \\ 0 & 1108 \end{bmatrix}, C = \begin{bmatrix} 1 & 0 & 0 & 0 \\ 0 & 0 & 1 & 0 \end{bmatrix} \quad (6.1-19i)$$

6) MIMO, Linear Actuators & Sensors,  $k_{I2}$  Linearized About  $y_1=2.0$  cm,  $y_2=-2.0$  cm.

$$\begin{bmatrix} y_1^*(s) \\ y_2^*(s) \end{bmatrix} = \begin{bmatrix} \frac{826.4s^2+114700}{D(s)} & \frac{114700}{D(s)} \\ \frac{114700}{D(s)} & \frac{826.4s^2+114700}{D(s)} \end{bmatrix} \begin{bmatrix} u_1(s) \\ u_2(s) \end{bmatrix}, D(s) = s^4 + 277.5s^2 \quad (6.1-20i)$$

$$X = \begin{bmatrix} y_1^* \\ \dot{y}_1^* \\ y_2^* \\ \dot{y}_2^* \end{bmatrix}, A = \begin{bmatrix} 0 & 1 & 0 & 0 \\ -138.7 & 0 & 138.7 & 0 \\ 0 & 0 & 0 & 1 \\ 138.7 & 0 & -138.7 & 0 \end{bmatrix}, B = \begin{bmatrix} 0 & ? \\ 826.4 & 0 \\ 0 & 0 \\ 0 & 826.4 \end{bmatrix}, C = \begin{bmatrix} 1 & 0 & 0 & 0 \\ 0 & 0 & 1 & 0 \end{bmatrix} \quad (6.1-21i)$$

**Instructors & Advanced Users: Quick Steps For Developing the Plant Models**

- 1) Perform the sensor and actuator characterization tests as described in the student's section 6.1.1 and 6.1.2
- 2) Run the scripts: *Sensorcal.m*, *Actuatorcal.m*, and *Magnet2Magnetcal.m* to establish the parameters of the nonlinear characteristics.<sup>1</sup>
- 3) Run the script *SISOplant.m* or *MIMOPlant.m*
- 4) To generate calibrated/linearized real-time sensor data enter the sensor calibration coefficients from *Sensorcal.m* in Setup Sensor Calibration (Setup menu)

**This section covered:**

1. Characterization of the nonlinear sensor characteristic and development of a linearizing / calibrating algorithm.
2. Characterization of the nonlinear actuator characteristic (largely due to the magnetic field properties) and development of a linearizing / calibrating algorithm.
3. Characterization of the intermagnet nonlinearity.
4. Development of the closed loop system block diagram including that of the nonlinear system, the nonlinear compensated system, and the resulting simplified system (assuming effective nonlinear compensation). The system gain and gravity compensation approach were also established.
5. Development of numeric SISO and MIMO plant models for cases of the nonlinear plant being linearized about an operating point and when the nonlinear terms are compensated for in the real-time algorithms. In the latter case, "plant" refers to the open loop system net of the nonlinear compensation routines.

**6.2i Nonlinear Plant Control: Linearization About Operating Point**

This section demonstrates that the linearized view of the system is valid for small motions about the equilibrium but yields qualitatively asymmetric results for large displacements about the operating point. For the case of the attractive levitation system, a minimum gain is required to stabilize the system at the equilibrium operating point and large displacements from the equilibrium can result in instability.

---

<sup>1</sup> For plants where the raw sensor output is used, the equilibrium positions in raw sensor counts must be determined from these results- generally they may be found by inspection of the plots generated in *Sensorcal.m*

Expected Results<sup>1</sup>:

- 1) In Step 1, for the 4 Hz system in the lower (repulsive) position and consistent with the specific plant parameters above:  $k_p = -0.26$ ,  $k_d = -0.042$ . For the 6 Hz system:  $k_p = -1.6$ ,  $k_d = -0.063$ .

For the upper (attractive) location at 4 Hz:  $k_p = 1.8$ ,  $k_d = 0.041$ . At 6 Hz:  $k_p = 3.1$ ,  $k_d = 0.062$ .

These are readily solved for via the script *PDdesigner.m*

- 2) In Step 2, an acceptable real-time algorithm for PD control of the bottom magnet is as follows:

```
;Set Ts=0.000884 s
;*****Declare variables*****
#define ylcal q2
#define ylrwo q3
#define kp q4
#define kd q5
#define kdd q6
#define Ts q7
#define ylstr q8
#define pos_last q15
#define ulstr q16
#define ulo q17
#define ul q18
;*****Initialize*****
Ts=0.000884 ;for local use only must set Ts in dialog box for sample period
control_effort1=0
control_effort2=0
;Specify Parameters
ulo=8850 ;gravity feedforward
ylrwo=15000
kp=-0.26
kd=-0.042
;kp=-1.8
;kd=-0.063
kdd=kd/Ts ;Discrete time derivative term, division by Ts here saves real-time
computation

;*****Begin Real-time Algorithm*****
begin
ylstr=sensor1_pos-ylrwo ;Use raw sensor counts, i.e. sensor1_pos=ylrwo
ulstr=kp*(cmdl_pos-ylstr)-kdd*(ylstr-pos_last) ;CONTROL LAW
pos_last=ylstr
ul=ulstr+ulo ;Add gravity offset
control_effort1=ul
ql0=-ylstr ; reverse polarity for plotting (compensates for neg sensor gain)
ql1=-cmdl_pos ; reverse polarity for plotting (compensates for neg sensor gain)
end
```

- 3) In Step3, an acceptable real-time algorithm for PD control of the top magnet position is as follows:

---

<sup>1</sup> These may vary according to a particular system's  $k_{sys}$ .

```

;Set Ts=0.000884 s
;*****Declare variables*****
#define y2rawo q3
#define kp q4
#define kd q5
#define kdd q6
#define Ts q7
#define y2str q8
#define pos_last q15
#define u2str q16
#define u2o q17
#define u2 q18
;*****Initialize*****
Ts=0.000884 ;for local use only must set Ts in dialog box for sample period
control_effort1=0
control_effort2=0
;Specify Parameters
u2o=8400 ;gravity feedforward
y2rawo=15400
kp=1.8
kd=0.041
;kp=3.1
;kd=0.062
kdd=kd/Ts ;Discrete time derivative term, division by Ts here saves real-time
computation
;*****Begin Real-time Algorithm*****
begin
y2str=sensor2_pos-y2rawo ;Use raw sensor counts, i.e. sensor2_pos=y2raw
u2str=kp*(cmd2_pos/3.2-y2str)-kdd*(y2str-pos_last) ;CONTROL LAW
pos_last=y2str
u2=u2str+u2o ;Add gravity offset
control_effort2=u2
q10=y2str
end

```

- 4) In Steps 7 and 8, the low and high amplitude step responses of the 4 Hz system are shown in Figure 6.2-1ia and 6.2-1ib. The rough symmetry in the low amplitude and asymmetry in the large amplitude maneuvers is clearly seen. The input amplitudes for the various low amplitude tests are varied in the instructions to the students to provide roughly equal output amplitudes. The students should refer to the specific input amplitudes for each test however when considering the steady state errors of the various systems in the exercises.
- 5) In Step 9, the low and high amplitude step responses of the 6 Hz system are shown in Figure 6.2-1ic and 6.2-1id. Again, the rough symmetry in the low amplitude and asymmetry in the large amplitude maneuvers is seen. The large amplitude steady state displacements are more symmetrical than for the 4 Hz system, but the differences in the damping characteristic are present and possibly greater than in the prior case.
- 6) In Steps 10, 11, and 12, the responses for the upper magnet position are shown in Figure 6.2-2i. The asymmetry of response is greater for the high amplitude maneuvers than for the low amplitude ones and for the 4 Hz system than for the 6 Hz one. In both the large amplitude plots shown, the magnet nearly fell away before being captured by the control system yielding an irregular trace for the negative step position.

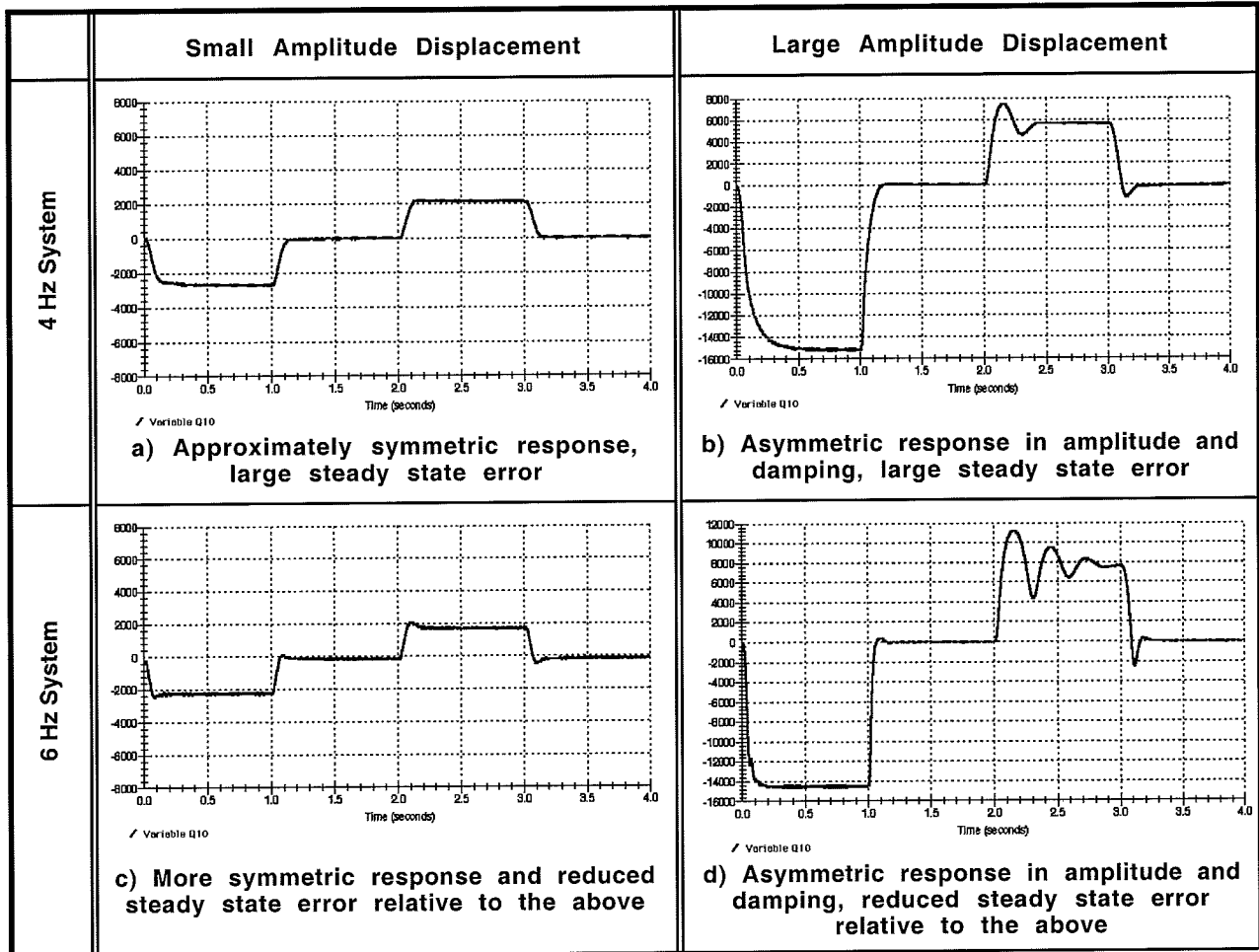


Figure 6.2-1i Typical Experimental Results Show Dependence of Step Response on Gain and Tracking Amplitude – Lower Repulsive System

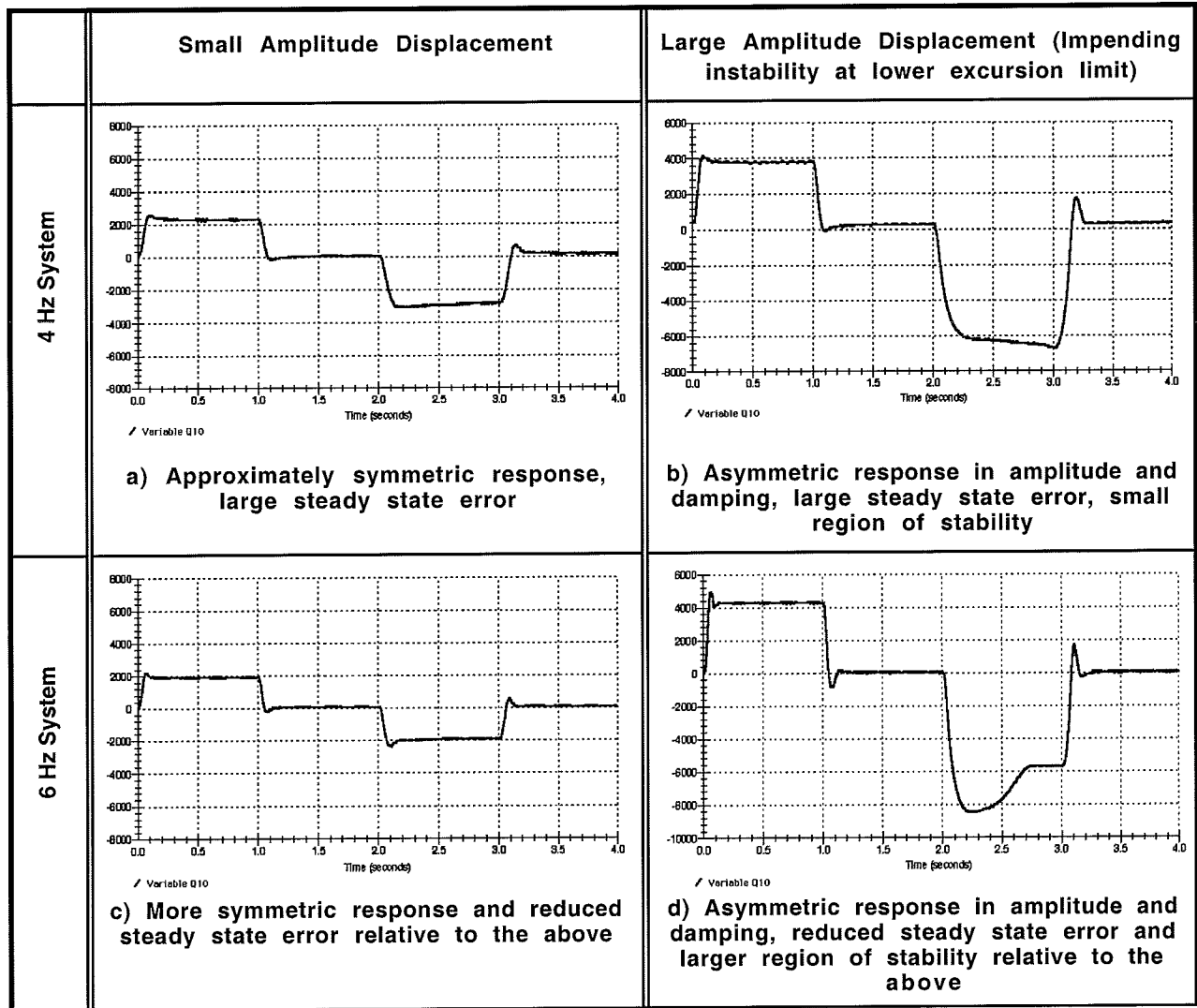


Figure 6.2-2i Typical Experimental Results Show Dependence of Step Response on Gain and Tracking Amplitude, and Spatial Region of Stability – Attractive Levitation

**Answers to Questions**

- A. From the denominator of Eq. (6.2-1), the lower repulsive linearized (and nonlinear) plant is stable and the closed loop system is stable for all positive  $k_p k_{sys}$  and  $k_d k_{sys}$ .
- B,C. The polarity of the plotted data is opposite to the physical motion. This is because the raw sensor signal decreases with increased position of the magnet in the lower system. The output of the 4 Hz system is roughly symmetrical for positive and negative excursions of low amplitude about the operating point. For large amplitude, the negative-going response is of much greater amplitude and damping ratio than the positive going one (the actual appearance of the plot will vary from apparatus to apparatus due to the relatively low gain of the controller and unmodeled effects). These characteristics are explained in terms of the system gain,  $k_{sys} = k_s k_u$  which increases dramatically with decreased position of the magnet according to Eq's (6.1-1i,-2i). The



increased damping ratio with increased  $k_{sys}$  (and hence lower position) is shown in Eq. (6.2-4). The position changes result in much smaller system gain changes for the small amplitude maneuvers than for the large amplitude ones. From Eq. (6.2-1) the steady-state error to a constant position reference input of amplitude  $a$  is (type 0 system):

$$E_{ss1} = a \frac{k_1'}{k_p k_{sys1} + k_1'} \quad (6.2-1i)$$

Hence the steady state error is reduced in the 6 Hz system v. the 4 Hz one due to the higher proportional gain and is reduced for both systems at large negative-going amplitude due to the higher system gain.

- D. From the denominator of Eq. (6.2-2), the upper (attractive) linearized plant is unstable and the closed loop system is stable for all

$$k_p k_{sys} > k_2' \quad (6.2-2i)$$

E,F. The polarity of the plotted data is the same as the physical motion in the attractive levitation case. The raw sensor signal increases with increased position of the magnet. The output of the 4 Hz system is roughly symmetrical for positive and negative excursions of low amplitude about the operating point. For large amplitude, the negative-going response is of much greater amplitude and reduced damping ratio than the positive going one. (The effect on damping ratio may be masked by friction in the for the negative-going excursions due to the low effective gain and hence relatively high friction) These characteristics are due to changes in the system gain,  $k_{sys} = k_s k_u$  which increases dramatically with increased position of the magnet according to Eq's (6.1-1i,-2i). The increased damping ratio with increased  $k_{sys}$  (and hence higher position) is shown in Eq. (6.2-7). The position changes result in much smaller system gain changes for the small amplitude maneuvers than for the large amplitude ones. From Eq. (6.2-2) the steady-state error to a constant position reference input of amplitude  $a$  is (type 0 system) for a stable system:

$$E_{ss2} = -a \frac{k_2'}{k_p k_{sys2} - k_2'} \quad (6.2-3i)$$

The negative sign in the error indicates that the steady state value is greater than the reference input (this is one reason why the relative response amplitudes were greater for the upper system than for the lower one). From Eq. (6.2-3i), the steady state error is reduced in the 6 Hz system v. the 4 Hz one due to the higher proportional gain. This is one reason why the 6 Hz system maintains attractive levitation of the magnet at a greater negative distance than the 4 Hz one. Another reason is that the requirement on stability given by Eq. (6.2-2i) is maintained over a larger range. The steady-state error is reduced for both systems at large positive-going amplitude due to the higher system gain.

Suggested Additional Exercise: Show that for the full nonlinear plant model, the lower repulsive system is (ideally) stable for all positive  $k_p k_{sys}$  and  $k_d k_{sys}$  and give the conditions on stability for the upper system.

**This section showed:**

1. That the lower repulsive system is open loop stable and the upper attractive one is open loop unstable. The upper system may be stabilized with sufficiently high control gain.
2. That in both cases, the linearized model / constant control gains yield well-behaved (approximately linear) results for relatively small excursions about the equilibrium operating point but poor, asymmetrical, control characteristics for large excursions.
3. The nonlinear nature of the system results in instability for the upper system for sufficiently large downward motion.
4. The region of approximately linear behavior, and the region of stability (upper system) are increased with increased control gain and the steady state error is reduced. (It should of course be pointed out to students that there is a practical limit to the amount of control gain one may employ due to system stability issues and noise propagation, and drive saturation effects).

### 6.3i Control of Nonlinear Compensated SISO Systems

This section demonstrates that the system when compensated for the nonlinear magnetic field (actuator) and sensor yields results that are practically the same as those for a simple second order double integrator (rigid body) plant. The section that follows this one uses this equivalent system to demonstrate fundamental properties of second order systems. It may be skipped if the course content is of a more advanced nature.

Expected Results:

- 1) In Step 1, for both the upper and lower system the control gains are:  $k_p = 1.72$ ,  $k_d = 0.065$ . These are readily solved for via the script *PDdesigner.m*

- 1) In Steps 2 and 3, suitable real-time algorithms for the lower and upper systems are (the lower system routine also contains the integral term used in the next section)

Lower

```
;Set Ts=0.001768 s

;*****Declare variables*****
#define ylcal q2
#define ylawo q3
#define kp1 q4
#define kd1 q5
#define kddl q6
#define Ts q7
#define ylstr q8
#define comp_effort q9
#define pos_last q15
#define ulstr q16
#define ulo q17
#define ul q18
#define laser1 q19
#define ylo q20
#define uterm1 q21
#define uterm2 q22
#define error q23
#define kil q24
#define kid1 q25
#define ui q26
#define ui_last q27
#define delta_y1 q28
;*****Initialize*****
Ts=0.001768 ;for local use only must set Ts in dialog box for sampling period
;Specify Parameters
ulo=11800 ;gravity offset in N/10000
ylo=20000
kp1=1.72
kd1=0.065
;kil=8
kil=0
kddl=kdl/Ts ;Discrete time terms, compute here to save real-time computation
kid1=kil*Ts
ui_last=0
control_effort2=0
;*****Begin Real-time Algorithm
begin
ylstr=sensor1_pos-ylo ; Use calibrated sensor, sensor1_pos=ylcal
error=cmd1_pos-ylstr
delta_y1=ylstr-pos_last
ui=kid1*error+ui_last
;CONTROL LAW
ulstr=kp1*error-kddl*delta_y1+ui
;OUTPUT
ul=ulstr+ulo ;Add gravity offset
uterm1=6.2+sensor1_pos/10000 ;nonlinear actuator compensation in three steps
uterm2=uterm1*uterm1
comp_effort=0.000165*uterm2*uterm2*u1
control_effort1=comp_effort
;UPDATE
pos_last=ylstr
ui_last=ui
q10=ylstr
end
```

Upper

```

;Set Ts=0.001768 s
;*****Declare variables*****
#define y2cal q2
#define y2rawo q3
#define kp2 q4
#define kd2 q5
#define kdd2 q6
#define Ts q7
#define y2str q8
#define comp_effort q9
#define pos_last q14
#define u2str q15
#define u2o q16
#define u2 q17
#define y2o q18
#define uterm1 q19
#define uterm2 q20
#define error q21
#define delta_y2 q22
;*****Initialize*****
Ts=0.001768 ;for local use only must set Ts in dialog box for sampling period
control_effort1=0
;Specify Parameters
u2o=11900 ;gravity feedforward
y2o=-20000
kp2=1.72
kd2=0.065
kdd2=kd2/Ts ;Discrete time derivative term, division by Ts here saves real-time
computation
;*****Begin Real-time Algorithm*****
begin
y2str=sensor2_pos-y2o ; Use calibrated sensor, sensor2_pos=y2cal
error=cmd2_pos-y2str
delta_y2=y2str-pos_last
;CONTROL LAW
u2str=kp2*error-kdd2*delta_y2
;OUTPUT
u2=u2str+u2o ;Add gravity offset
uterm1=-6.2+sensor2_pos/10000 ;nonlinear actuator compensation in three steps
uterm2=uterm1*uterm1
comp_effort=0.000165*uterm2*uterm2*u2
control_effort2=comp_effort
;UPDATE
pos_last=y2str
q10=y2str
end

```

- 3) In Steps 7 and 9, typical step response results for the upper and lower systems are shown in Figure 6.3-1i The responses including control effort data are shown in Figure 6.3-2i.

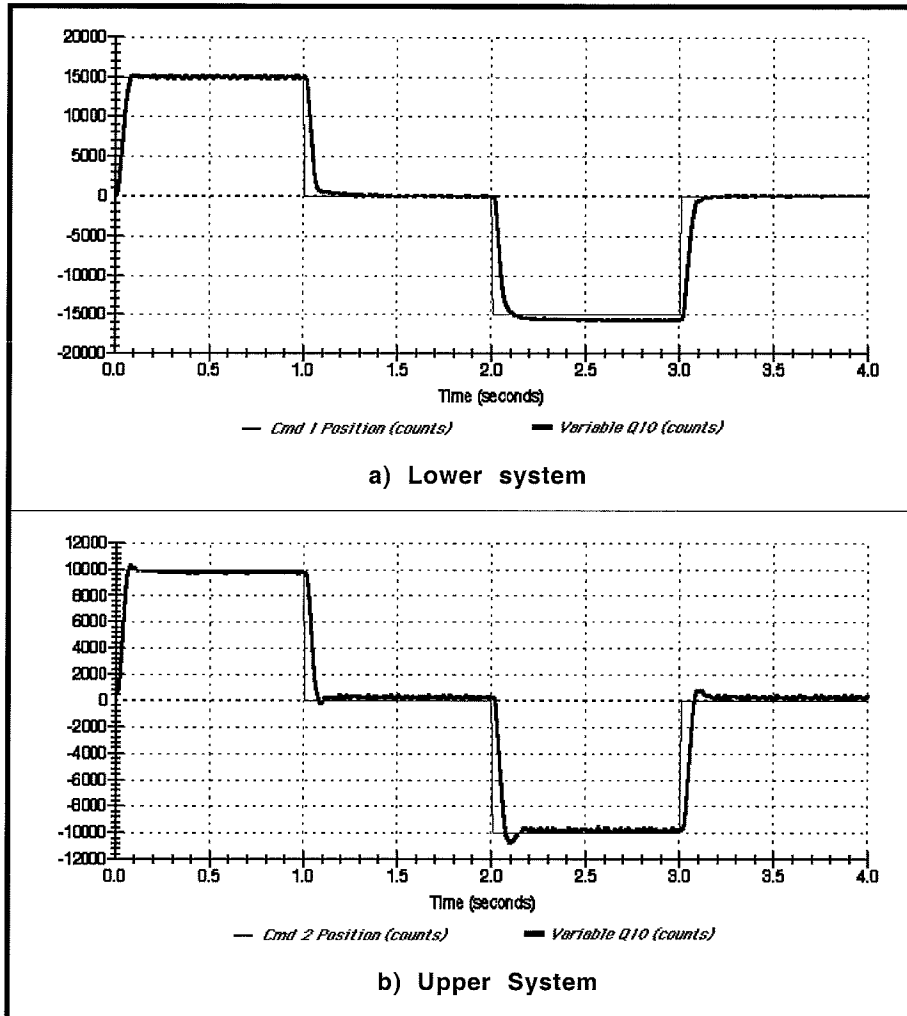


Figure 6.3-2i Step responses At lower & Upper Locations Show Good Symmetry and Relatively Small Steady State Error

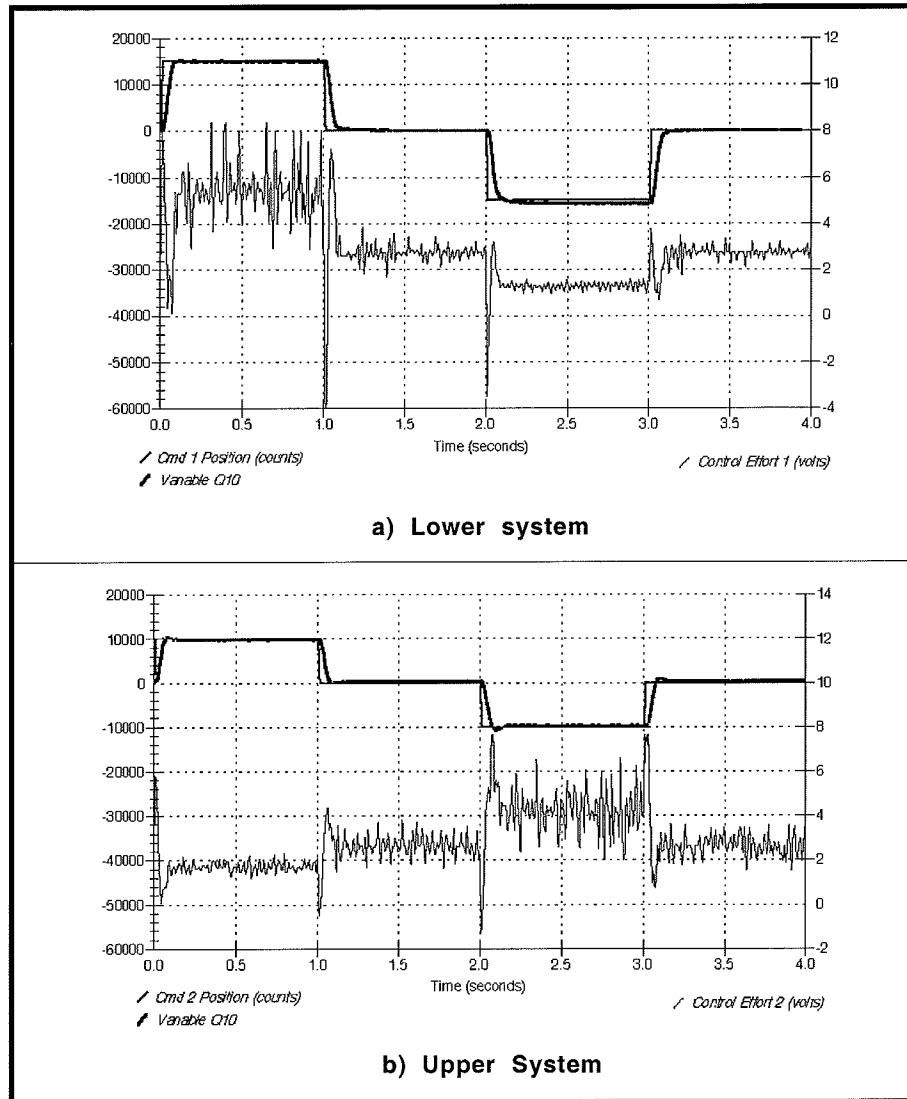


Figure 6.3-2i Step Responses Show Asymmetric Control Effort Characteristic

#### Answer to Question

- A. The responses shown are significantly better controlled than those of the previous section. The responses are essentially symmetric and with relatively small steady state error. The upper and lower responses are similar.
- B. For the lower system, the change in control effort in going from the nominal to the +15000 position is approximately twice the amount in going from the -15000 position to the nominal. This is because the control routine inverts the nonlinear actuator (magnetic field, inverse fourth power) characteristic to cause the system to behave in a linear fashion. I.e. it is generating an approximately linear input/output position characteristic at the expense of control effort. In the upper system the same holds except that the larger control effort is required for negative excursions. The lower position required three times as much control effort and hence current ( $I$ ) in the coil for

the positive excursion (from nominal) as for the negative one. The associated power is  $I^2R$  where  $R$  is the coil resistance. Hence the power dissipation is nearly a factor of 10 greater in the highly levitated state. This is why it is important not to leave the system in a condition of high levitation of the magnet for sustained periods.

The control effort is much noisier than the position sensor signal because it includes the differentiated sensor signal. Signal differentiation amplifies high frequency noise. The system naturally low pass filters much of this noise. The noise is greater at the distant locations from the sensor because the raw sensor signal has a rapidly reducing gain slope (change in signal / change in position) with position. In cases where the noise becomes an issue, a low pass filter such as that shown in the solution in Section 6.7 (Optional Exercise A) may be included in the real-time routine. There is of course a practical lower bound to the filter cutoff frequency due to the attendant phase lag and hence adverse affect on stability.

#### **This section showed:**

1. That the nonlinear compensation algorithms are effective in inverting the plant nonlinearities so that it behaves similar to a simple double integrator. (This approximate inversion of the nonlinearities has limitations of course of motion range, accuracy of inversion, and attainable system bandwidth.)
2. That the linear system linear input/output behavior results in a nonlinear control effort characteristic which dramatically increases drive power as levitation distance increases.
3. The control effort signal for this and many other control systems is much noisier than the sensor signal due to differentiation (or other high frequency amplification) of the sensor data.

### **6.4i Fundamental Properties of Second Order Systems**

This section first demonstrates the relationship of  $k_p k_{sys}$  and  $k_d k_{sys}$  to the natural frequency and damping ratio of the closed loop system. Parameters are selected to implement under-, over-, and critically damped systems and characteristic step responses are plotted. Integral action is then added and its effect on response, steady-state error, and stability are studied.

#### Expected Results<sup>1</sup>:

---

<sup>1</sup> The gains given will be identical for systems scaled to  $k_{sys} = 100$  N/m.

- 1) In Steps 3 and 4,  $k_d = 0.065$  and  $0.13$  respectively. The control action of the derivative term has force proportional to and in the opposite direction of the speed of motion, i.e. it is effectively viscous damping.
- 2) In Steps 5 and 6,  $k_p = 1.7$  and  $3.4$  respectively. The control action of the proportional term has force proportional to and in the opposite direction of the displacement, i.e. it is effectively a spring.
- 3) In Step 7, the gains for the respective 4 and 8 Hz systems are  $k_p = 0.76$ ,  $k_d = 0.003$ , and  $k_p = 3.1$ ,  $k_d = 0.03$ . The step responses of these systems are shown in Figure 6.4-1i from which the damped natural frequency,  $\omega_d$  ( $\approx \omega_n$  for low damping) is seen to be near the design values.
- 4) In Step 8, gains for the respective under-, critical, and over-damped cases are  $k_p = 1.7$ ,  $k_d = 0.018$ ,  $0.091$ , and  $0.18$ . Their step responses are shown in Figure 6.4-2i. The oscillation in the underdamped case and slower rise time with increased damping are clearly seen.
- 5) Sine sweeps for the three damping cases are shown in Figure 6.4-3i, which shows the identical data plotted using the Linear time / Linear amplitude, and log( $\omega$ ) / Db scaling options. (The overdamped case was limited to 10 Hz due to irregularities associated with differentiated signal noise – see “Note On Running Sine Sweep Tests” below.) The resonance in the underdamped case and reduced bandwidth with increased damping are obvious.
- 6) Figure 6.4-4i shows critically damped case with added integral terms  $k_i k_{sys} = 800$  N/(m-s) [ $k_i = 8$ ] and  $k_i k_{sys} = 1200$  N/(m-s) [ $k_i = 12$ ]. The where the characteristic overshoot and zero steady state error are evident. The PID algorithm was given in the solutions of the last section.

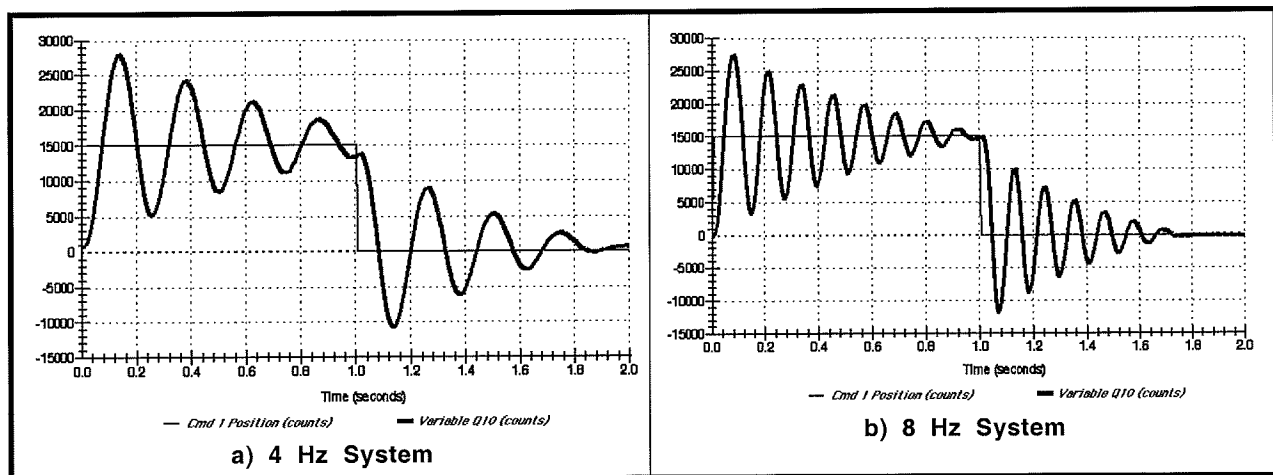


Figure 6.4-1i. Lightly Damped System Responses Show Damped Natural Frequency



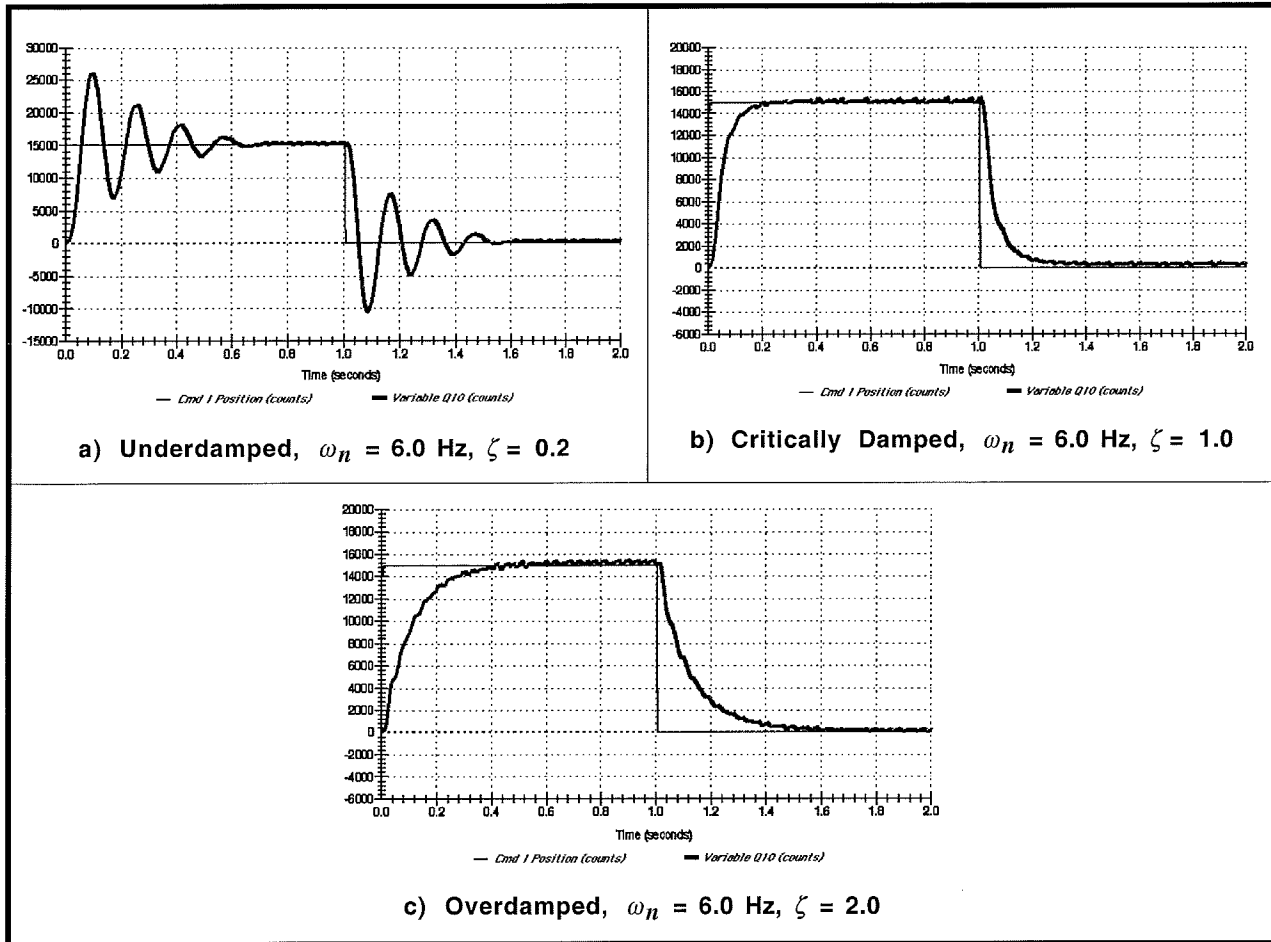
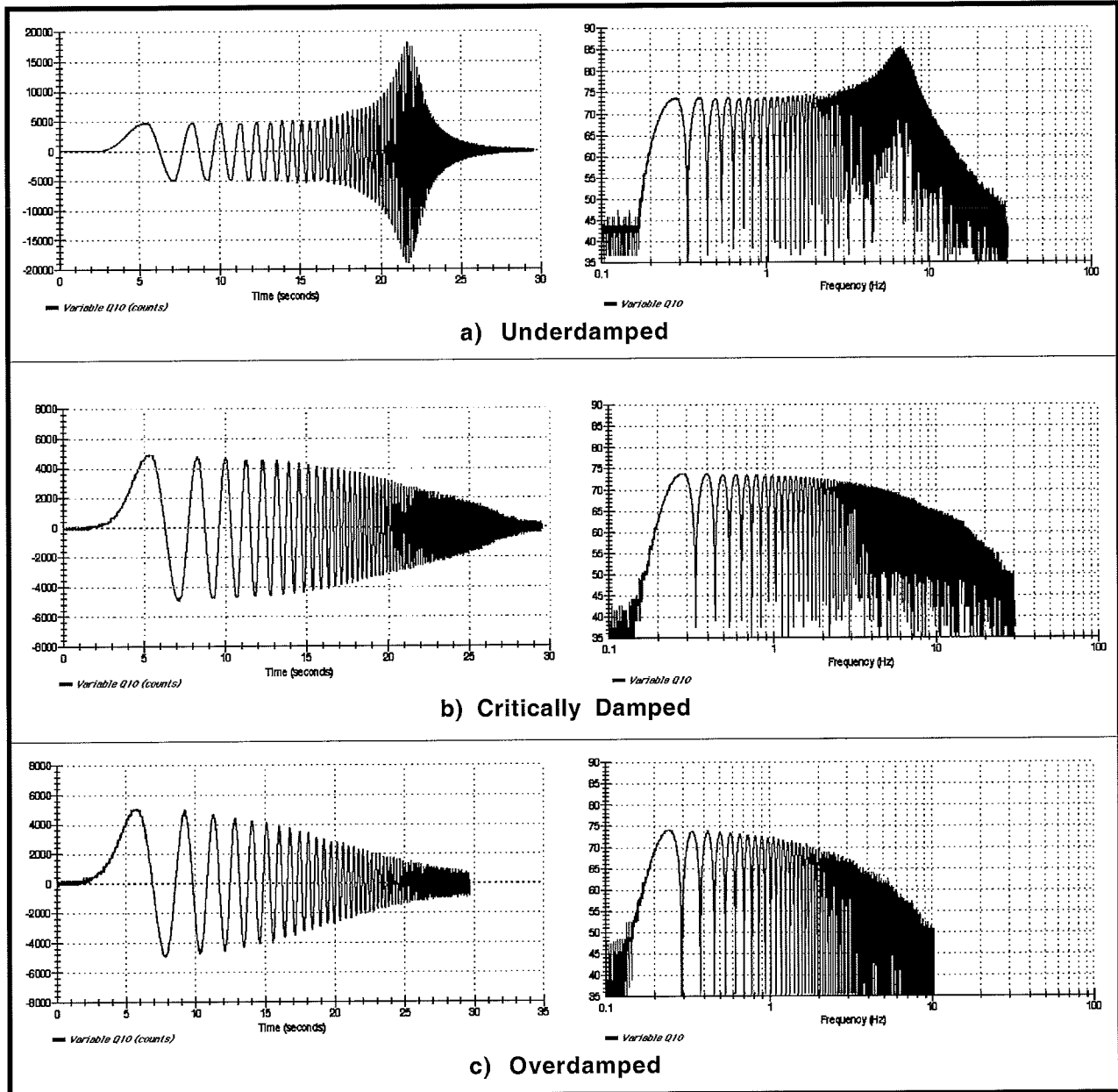


Figure 6.4-2i Typical Results of Step Response Tests Show Classical Second Order Transient Characteristics

Note On Running Sine Sweep Tests. When running sine sweep trajectories, the output may be seen to drift or be biased at high frequency. This is normal and is associated with: a) offsets between the nominal position offset,  $y_o$ , and the gravity offset,  $u_o$ ; b) system noise from differentiation of the position signal (particularly at high damping values); and c) actuator nonlinearities. It is often most apparent in the Db plots because the low amplitudes are graphically amplified due to the logarithmic scaling. The following should be considered in plotting experimental data.

1. If a bias is seen, this may usually be eliminated by selecting Remove DC Bias in the Setup Plot window.
2. If there is wandering or drift in the high frequency data, open the loop, then adjust the value of  $u_o$  in the real-time algorithm so that Sensor 1 value shown in the background display matches the  $y_o$  value used in your algorithm.
3. Bias and wander is essentially eliminated in viewing velocity and acceleration data. This data of course differs from the position data by  $\omega$  and  $\omega^2$  (+20 and +40 Db/decade).
4. For irregularities caused by differentiated signal noise, the problem may be mitigated through

increased sample period (as long as stability is not significantly affected) or by reducing the upper frequency of the sweep.



**Figure 6.2-2i Representative Frequency Response Test Data Plotted With Linear Time / Amplitude & Log( $\omega$ ) / Db Amplitude Scaling**

Linear scaling best represents the data as students witness the test. The low frequency constant amplitude and  $1/\omega^2$  high frequency roll-off are evident. With  $\log(\omega)$  / Db scaling, the amplitude of the system motion traces out the familiar Bode magnitude characteristics, thereby bridging from test results to theoretical concepts. Here the underdamped resonance frequency is read directly from the plot

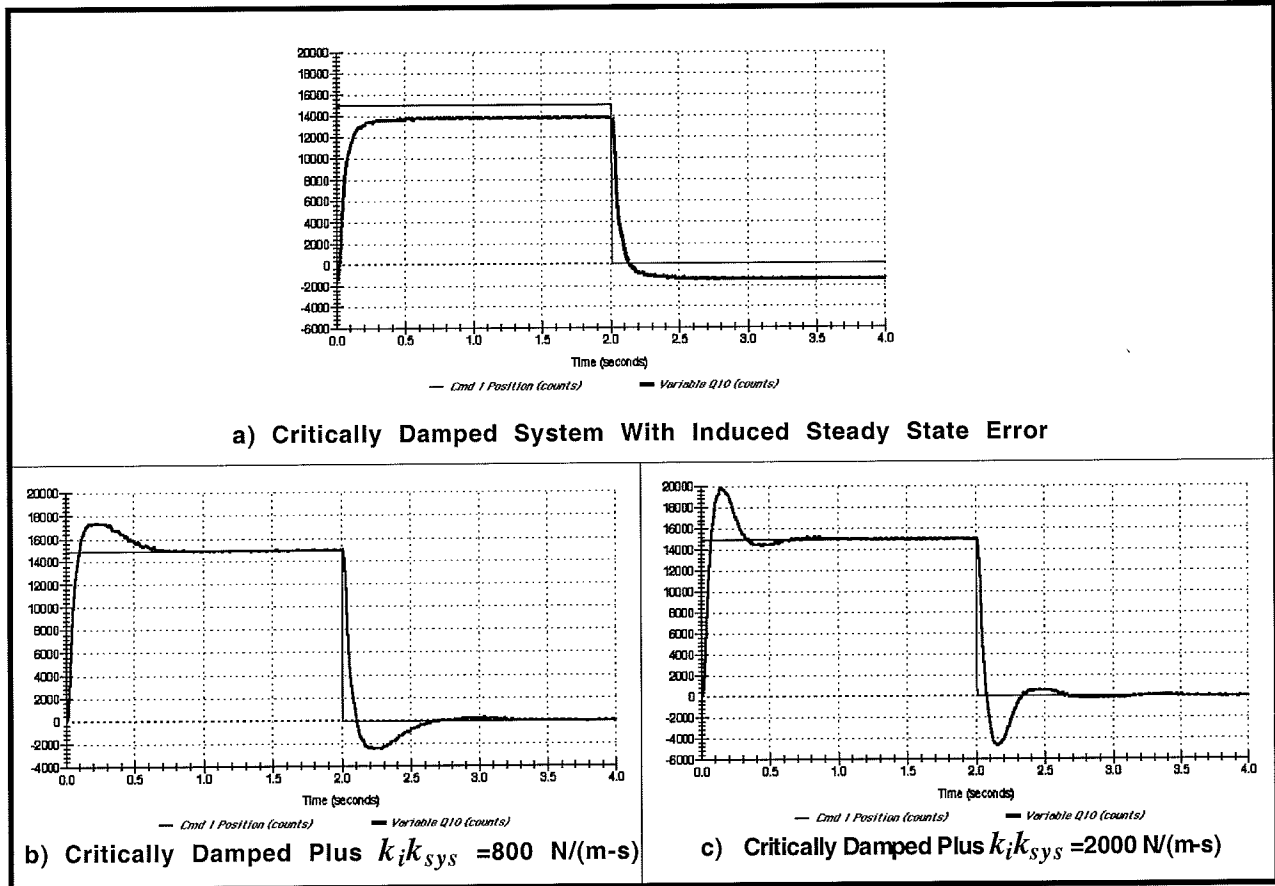


Figure 6.4-4i. Added Integrator Results in Overshoot & Zero Steady State Error

**Answers to Questions**

- A. Increased  $k_{sys}$  increases both  $\omega_n$  and  $\zeta$  by  $\sqrt{k_{sys}}$ . “ $m$ ” reduces both  $\omega_n$  and  $\zeta$  by  $\sqrt{1/m}$ . “ $k_p$ ” increases  $\omega_n$  by  $\sqrt{k_p}$  and decreases  $\zeta$  by  $\sqrt{1/k_p}$ . “ $k_d$ ” does not affect  $\omega_n$  but increases  $\zeta$  proportionally. By replacing  $k = k_p k_{sys}$  and  $c = k_d k_{sys}$ , the transfer function of the plant of Fig. 6.4-1 is identical to Eq. 6.3-2 except that the numerator is equal to  $1/m$  rather than  $k_p k_{sys}/m$ . Thus the PD controlled rigid body is dynamically the same as the spring/mass/damper except for a scaling constant. It may be pointed out to students that the system shown in Figure 6.4-5i, where the input is the position of the base of the spring, is in fact dynamically identical to the PD controlled system of Figure 6.3-2b ( $k_i=0$ ). (If the damper connects between  $r(t)$  and the mass rather than between inertial ground and the mass, the system becomes that of the forward path differentiated PD form.) “ $k_p k_{sys}$ ” has units of N/m and  $k_d k_{sys}$  has units of N/(m/s) which correspond to appropriate unit sets for  $k$  and  $c$  respectively.
- B. The S-plane diagram of the roots of Eq. 6.2-1 is shown in Fig. 6.4-6i. The roots are purely imaginary for  $\zeta=0$  corresponding to a pure oscillator. They become complex and lie along the circle  $|s| = \omega_n$  becoming more damped as  $\zeta$  increases. For  $\zeta \geq 1$  the roots are purely negative real corresponding to an exponential decay with no oscillation. As  $\zeta$  increases beyond 1, the response becomes slow as governed by the

smaller magnitude root. The relative location of the roots in the s-plane is determined by  $\zeta$  while their dilation about the origin (time scaling) is determined by  $\omega_n$ .

- C. The oscillation in the underdamped step response has frequency  $\approx 6$  Hz corresponding to the approximate resonance in the frequency response. The overdamped and critically damped cases have no oscillations nor resonances. The bandwidth is greatest for the underdamped system and least for the overdamped one. This corresponds to the fastest and slowest rise times respectively.
- D. For all damping cases, the amplitude is constant and nominally equal to the input amplitude at low frequency. At high frequency, the shape is  $k/m\omega^2$  in the linear time and amplitude scaling and -40 Db/decade in the Log( $\omega$ )/Db scaling. These properties are shown by taking the steady-state frequency response amplitude found from  $|T(j\omega)|$  (Eq. 6.3-5) and evaluating as  $\omega$  tends to zero and infinity.
- E. Integral action eliminates steady state error to a step input. The transfer function between the disturbance and the output when the integrator is present is

$$\frac{y(s)}{T(s)} = \frac{s/m}{s^3 + (k_{sys}/m)(k_d s^2 + k_p s + k_i)} \quad (6.4-1i)$$

The final value for  $y$  is <sup>1</sup>

$$\lim_{s \rightarrow 0} y(s) = \lim_{s \rightarrow 0} \left( \frac{s/m}{s^3 + (k_{sys}/m)(k_d s^2 + k_p s + k_i)} u \right) = 0 \quad (6.4-2i)$$

where  $u$  is the step magnitude. Without the integrator, the final value is

$$\lim_{s \rightarrow 0} y(s) = \lim_{s \rightarrow 0} \left( \frac{s/m}{s^3 + (k_{sys}/m)(k_d s^2 + k_p s)} \right) u = \frac{u}{k_p k_{sys}} \quad (6.4-3i)$$

which is reduced according to the size of the proportional gain but never zero.

The integral term always results in an overshoot (linear, second order system) due to the integration of error during the period before the output initially reaches the step demand amplitude.

<sup>1</sup> It may be useful to point out to students the concept of *static servo* stiffness which is the inverse of the final value of the unit step response of Eq. (6.4-1i). Here, the static servo stiffness is infinite with the integral control term and is  $k_p k_{sys}$  without that term.

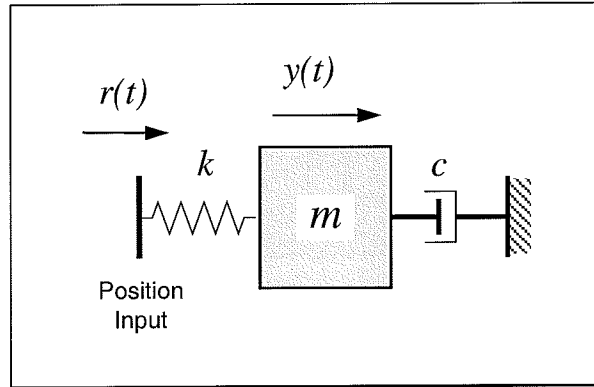


Figure 6.4-5i. Dynamically Equivalent System to PD Controlled RIGID Body

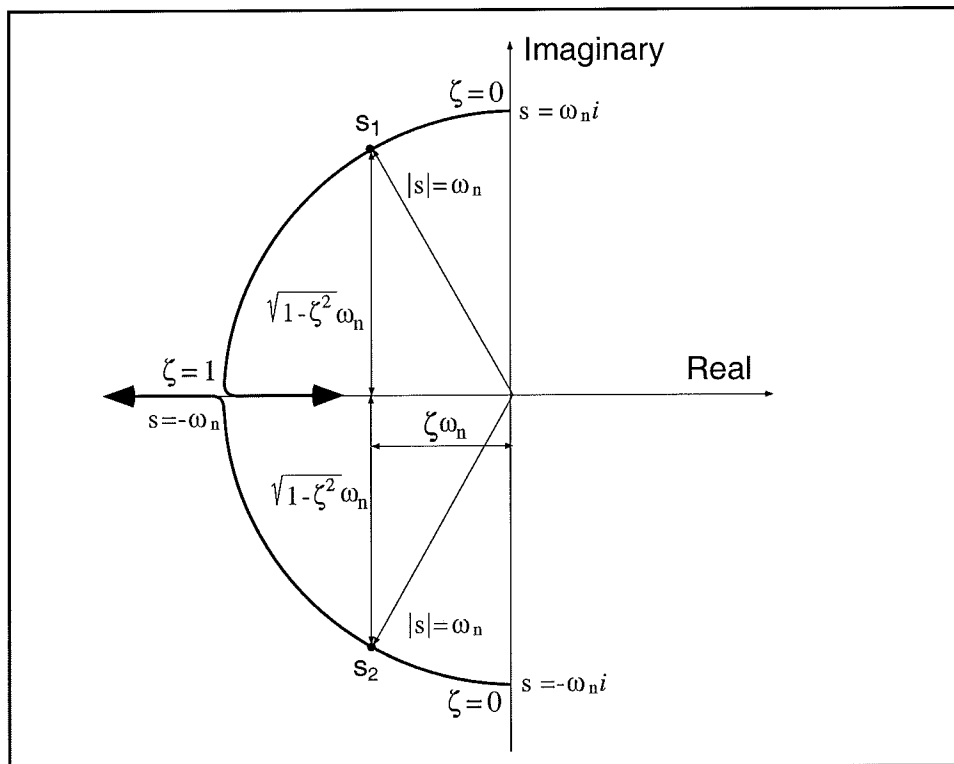


Figure 6.4-6i. Loci of Roots of Second Order Characteristic Equation

### Optional Exercises & Solutions

A. What are the phase and gain margins under PD control?

*ans.:* Gain margin is ideally infinite, however as the ratio  $k_p/k_d$  increases to large values, phase margin becomes vanishingly small. In practical systems, there are time delays and nonlinearities which lead to instability when the ratio  $k_p/k_d$  is large. There are also discretization issues which affect the stability of all sampled data systems. For sufficiently large  $T_s$  the associated time delay leads to instability. (Conversely if  $T_s$  is too small, excessive noise is propagated due to numerical differentiation with finite sensor (and numerical processor-internal) quantization.

B. Discuss via root locus arguments, the stability of the PID controlled rigid body when  $k_i \neq 0$ . In constructing the loci, assume that  $k_p$ ,  $k_i$  &  $k_d$  all increase proportionally.

*ans.:* The locus of roots where  $k_p$ ,  $k_i$  &  $k_d$  all increase proportionally, begins at the triple integrator with one root tending toward  $-\infty$  and the other two toward the roots of  $(s^2 + (k_p/k_d)s + k_i/k_d)$ . The angles of departure of the three loci from the triple pole are 60, 180, and 300 deg and therefore the system is unstable at sufficiently low gains for all relative ratios of  $k_p$ ,  $k_i$  &  $k_d$ . Via the Routh-Hurwitz criterion, the requirement for closed loop stability is  $K_s k_p k_d > k_i$  where  $K_s$  is the gain  $k_{sys}/m$ . Thus sufficient increase in relative magnitude of  $k_i$  leads to instability.

C. Determine the sensitivity of the closed loop PD controlled system (assume reverse path  $k_d$ ) to changes in  $m$ . Plot the magnitude of this sensitivity as a function of frequency using the following control gain sets:<sup>1</sup>

$$\begin{aligned} k_p &= 0, & k_d &= 0 \text{ (same as open loop)} \\ k_p &= 0.1, & k_d &= 0.022 \\ k_p &= 1.0, & k_d &= 0.070 \\ k_p &= 10, & k_d &= 0.22 \end{aligned}$$

Use the classical definition of the sensitivity of some function  $T(\alpha)$  to the parameter  $\alpha$ , i.e.

$$S_{\alpha}^{T(\alpha)} = \frac{d \ln T(\alpha)}{d \ln \alpha} = \frac{d T(\alpha)}{d \alpha} \frac{\alpha}{T} \quad (6.4-4i)$$

How does feedback control effect the sensitivity of the closed loop system to parameter changes? How does the magnitude of the control gains affect the sensitivity?

*ans.:* Applying Eq.(6.4-4i) to Eq.(6.3-2) yields

$$S_m^{T(m)} = \frac{-ms^2}{ms^2 + k_{sys}(k_d s + k_p)} \quad (6.4-5i)$$

<sup>1</sup> These values correspond to incremental increases in  $\omega_n$  by  $\sqrt{10}$  with constant damping ratio ( $=1.0$ ) for the parameters used in this manual). The student should be able to show this.

The magnitude of  $S_i^{(0)}(j\omega)$  is plotted for the specified control gains in Figure 6.4-7i. The open loop system has a sensitivity of 1 (0 Db) at all frequencies. The low and medium frequency sensitivity (up to the neighborhood of the closed loop system bandwidth) is reduced by feedback control<sup>1</sup>. The sensitivity is increasingly reduced and brought to higher frequencies with increase in control gain. At frequencies beyond the neighborhood of the closed loop bandwidth, sensitivity is unchanged by feedback control. (i.e. the high frequency closed loop attenuation characteristic is essentially the response of the inertia itself rather than that of the control action: hence the sensitivity to changes in  $J$  at these high frequencies is 1.)

### Optional Experiments

#### A. Frequency response phase measurements

The important concept of frequency response phase behavior is easily demonstrated with the experimental system. By exciting the system at a particular frequency<sup>2</sup> and plotting the Commanded Position and Q10 data, the phase is found from the expression

$$\phi = -360^\circ \frac{t_{\omega_o}}{t_{\omega_i}} \quad (6.4-6i)$$

where  $t_{\omega_o}$  and  $t_{\omega_i}$  are measured from the data according to Figure 6.4-8i. Typically 5-10 cycles of sinusoidal input is sufficient to establish steady state. The students should “zoom” in to view a cycle of the data near the end of the maneuver. Typical test results for the three PD damping cases are shown in Figure 6.4-9i. These clearly demonstrate the effect of damping ratio on the output phase.

#### B. Tracking and frequency response with $k_d$ in forward vs. return path

It is instructive for students to compare the response of the system to a dynamic input with the derivative control term in the forward and return paths. Shown in Figure 6.4-10i is the response of the critically damped system under these two control types to a ramp input. From the figure it is seen that the derivative in the forward path provides closer tracking but requires higher peak control effort due to the derivative action acting on the reference input. This difference is slight for the present system, but can be large where inertial force dominates the control effort. These results may be correlated with experimental frequency responses of the two systems where the forward path  $k_d$  system is seen to have higher bandwidth and a reduced high frequency attenuation of -20 Db/dec. vs. -40 Db/dec. for the return path case.

A useful exercise for students is to find the steady state error ( $e_{ss}$ ) of each system to a ramp input. It is readily shown that

$$\begin{aligned} e_{ss} \text{ for ramp input with } k_d \text{ in reverse path} &= Rk_d/k_p \\ e_{ss} \text{ for ramp input with } k_d \text{ in forward path} &= 0 \end{aligned}$$

<sup>1</sup> It may be brought to students attention that the system bandwidth is typically the “useful” frequency range for practical systems. I.e. it is in this frequency band that sensitivity reduction is usually most important.

<sup>2</sup> The phase measurements may also be made from the frequency response (sine sweep) data but generally yields less accurate results due to the transient behavior associated with the changing input frequency.

where  $R$  is the ramp constant.

- C. The results described in Optional Exercise B above regarding instability with increased  $k_i$  may be shown by slowly and successively increasing its value and implementing the resulting PID controller on the system. The system will become increasingly oscillatory and then unstable. Be certain that  $k_i$  is increased slowly and that the safety instructions of Section 2.3 are followed strictly during this procedure.

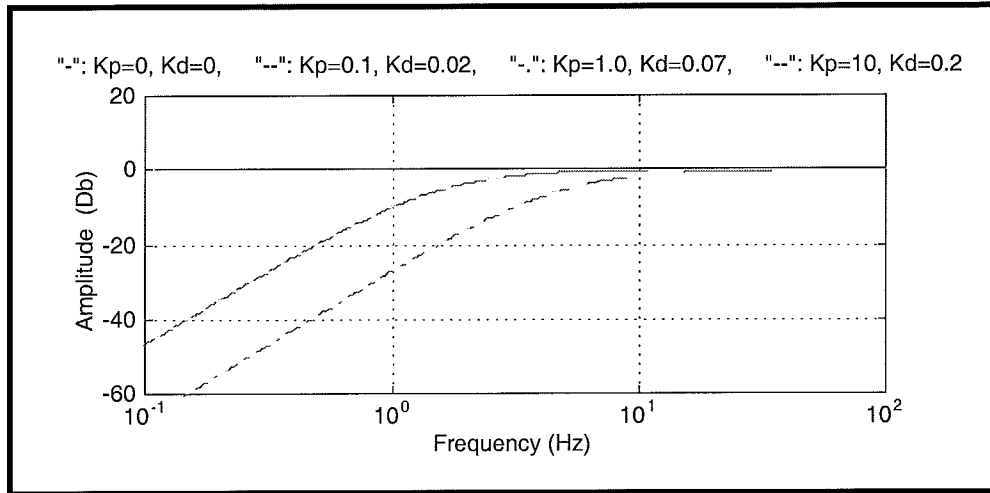


Figure 6.4-7i. Effect of Feedback Gain on Sensitivity To Inertia Changes

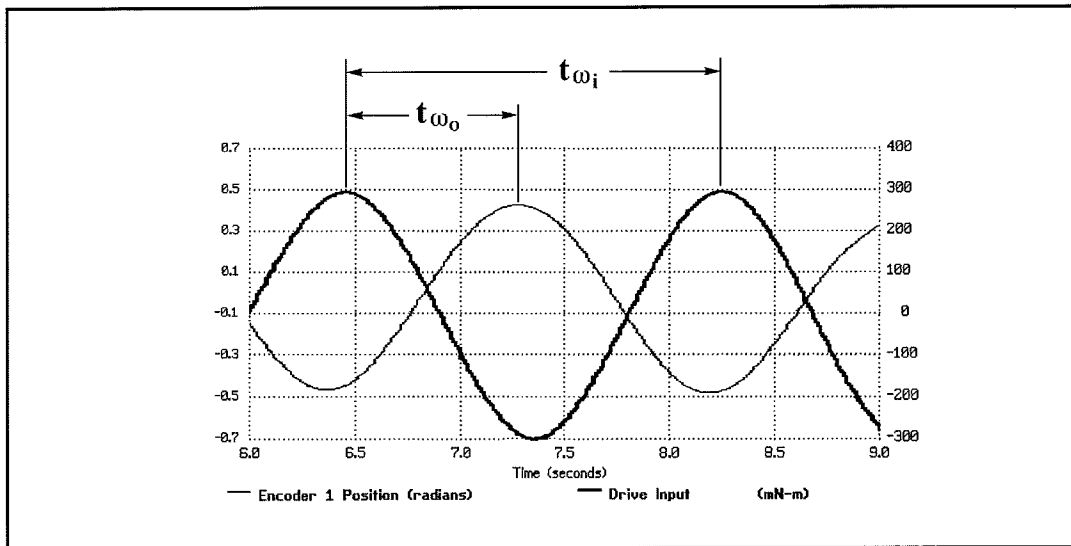


Figure 6.4-8i Phase Measurement Method<sup>1</sup>

<sup>1</sup> See also Eq. (6.2-4i)



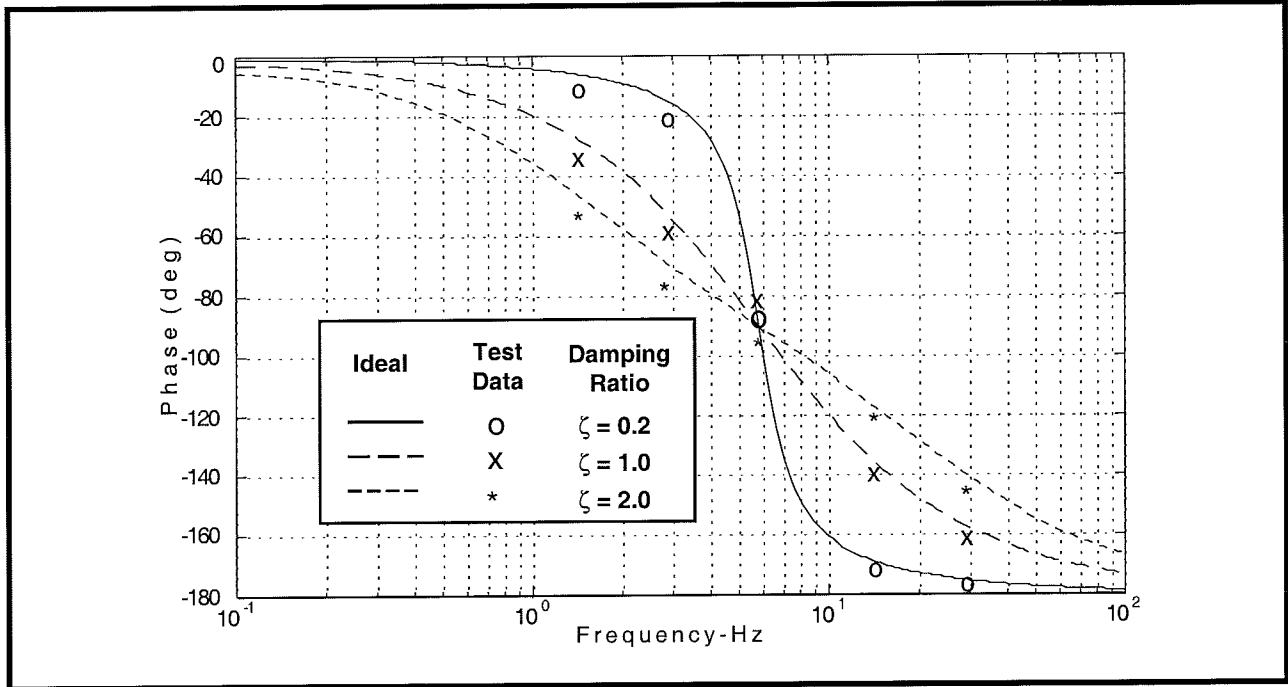


Figure 6.4-9i. Typical Phase Measurement Test Results Show Effect of Damping

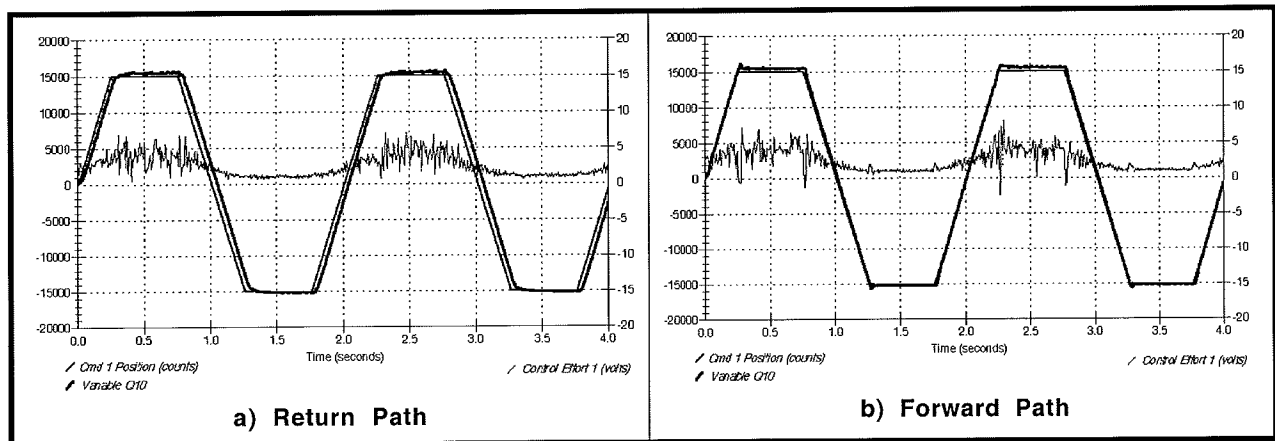


Figure 6.4-10i. Tracking Response Using Forward and Return Path Derivative Terms

**This section showed:**

1. The distinct actions of proportional and derivative control terms and their equivalence to mechanical springs and viscous dampers.
2. The effect of proportional and derivative control terms on the S-plane closed loop roots.
3. Pole Placement PD control design.
4. The effect of integral action and elimination of steady state error. (Static servo stiffness)
5. The characteristic under- critical, and overdamped PD step responses.
6. The frequency response magnitude shapes for the various damping cases and the characteristic low and high frequency gain slopes.
7. The frequency response phase characteristic of second order systems and the effect of damping ratio. (optional experiment)
8. The stability characteristics of the second order PD controlled systems and the effect of adding integral action. (optional exercise)
9. The difference between forward and reverse path derivative control and the effect on tracking performance, frequency response, and required control effort. (optional experiment)
10. Correlation between step (transient, time domain) and sine sweep (frequency domain) characteristics
11. The role of feedback control in reducing sensitivity to parameter changes. (optional exercise)

**6.5i Disturbance Rejection of Various 1 DOF Controllers**Expected Results:

1. In Step 1a:  $k_p = 0.43$ ,  $k_d = 0.023$
2. In Step 1b: The integral gain is:  $k_i = 1000/k_{sys} = 10$
3. In Step 2c: The filter is in the s-domain :  $F(s) = \frac{9.42 + 6s}{9.42 + s}$

The script *Disturbode.m*, given in Appendix Ai solves for the discrete coefficients of the filter and provides the numerical transfer functions and Bode plots used in the solutions to Exercises A and B below. A suitable real-time routine is as follows where the parameter values are set to implement the lead/lag filter and not the integrator.

```
;Set Ts=0.001768 s
;*****Declare variables*****
#define ylcal q2
#define ylrawo q3
#define kp1 q4
#define kd1 q5
#define kdd1 q6
#define Ts q7
#define ylstr q8
#define comp_effort q9
#define pos_last q15
#define ulstr q16
#define ulo q17
#define ul q18
#define laser1 q19
#define ylo q20
#define uterm1 q21
#define uterm2 q22
#define error q23
#define kil q24
#define kid1 q25
#define uil q26
#define uil_last q27
#define delta_y1 q28
#define y2cal q30
#define y2rawo q31
#define kp2 q32
#define kd2 q33
#define kdd2 q34
#define y2str q35
#define pos_last2 q36
#define u2str q37
#define u2o q38
#define u2 q39
#define laser2 q40
#define y2o q41
#define ulstrstr q42
#define ulstrstr_last q43
#define ulstr_last q44
#define n0d q435
#define n1d q46
#define d1d q47
;*****Initialize*****
Ts=0.001768 ;for local use only must set Ts in dialog box for sampling period
;Specify Parameters
ulo=18300 ;gravity offset
ylo=15000
u2o=4800 ;gravity offset
y2o=-20000
kp1=.43
kd1=0.023
;kil=10; Integral term
kil=0; Use this line to eliminate integrator
n0d=6; Lead/lag coeff's
n1d=-5.984
d1d=-0.984
;n0d=1; Use the these three coeff's to eliminate lead/lag
```

```

;nld=0
;dld=0
kp2=3.06
kd2=0.061
kdd1=kd1/Ts ;Discrete time terms, compute here to save real-time computation
kid1=ki1*Ts
kdd2=kd2/Ts
uil_last=0

;*****Begin Real-time Algorithm*****
begin
ylstr=sensor1_pos-y1o
error=cmd1_pos-ylstr
delta_y1=ylstr-pos_last
uil=kid1*error+uil_last
ulstrstr=kp1*error-kdd1*delta_y1+uil ;CONTROL LAW sans lead/lag
ulstr=n0d*ulstrstr+nld*ulstrstr_last-dld*ulstr_last; Lead/lag
ulstrstr_last=ulstrstr
ulstr_last=ulstr
pos_last=ylstr
uil_last=uil
u1=ulstr+ulo ;Add gravity offset
uterm1=6.2+sensor1_pos/10000 ;nonlinear actuator compensation in three steps
uterm2=uterm1*uterm1
comp_effort=0.000165*uterm2*uterm2*u1
control_effort1=comp_effort
q10=ylstr

;Simple PD Control of Upper Magnet to Provide Disturbance
y2str=sensor2_pos-y2o
u2str=kp2*(2*cmd2_pos-y2str)-kdd2*(y2str-pos_last2) ;CONTROL LAW
pos_last2=y2str
u2=u2str+u2o ;Add gravity offset
uterm1=-6.2+sensor2_pos/10000 ;nonlinear actuator compensation in three steps
uterm2=uterm1*uterm1
comp_effort=0.000165*uterm2*uterm2*u2
control_effort2=-comp_effort;Polarity reversed due to magnet N/S orientation
q12=y2str
end

```

4. The plots of the disturbance magnet motion and regulated magnet response are shown in Figure 6.5-1i. From the plots, it is seen that the PD controller had similar response amplitude at both low and high frequency. The PID system, was effective the at attenuating low frequency disturbances, but actually had an amplified response at the higher frequency. The PD+lead/lag controller had similar response as the PD system at low frequency, but was effective at attenuating the high frequency disturbance.

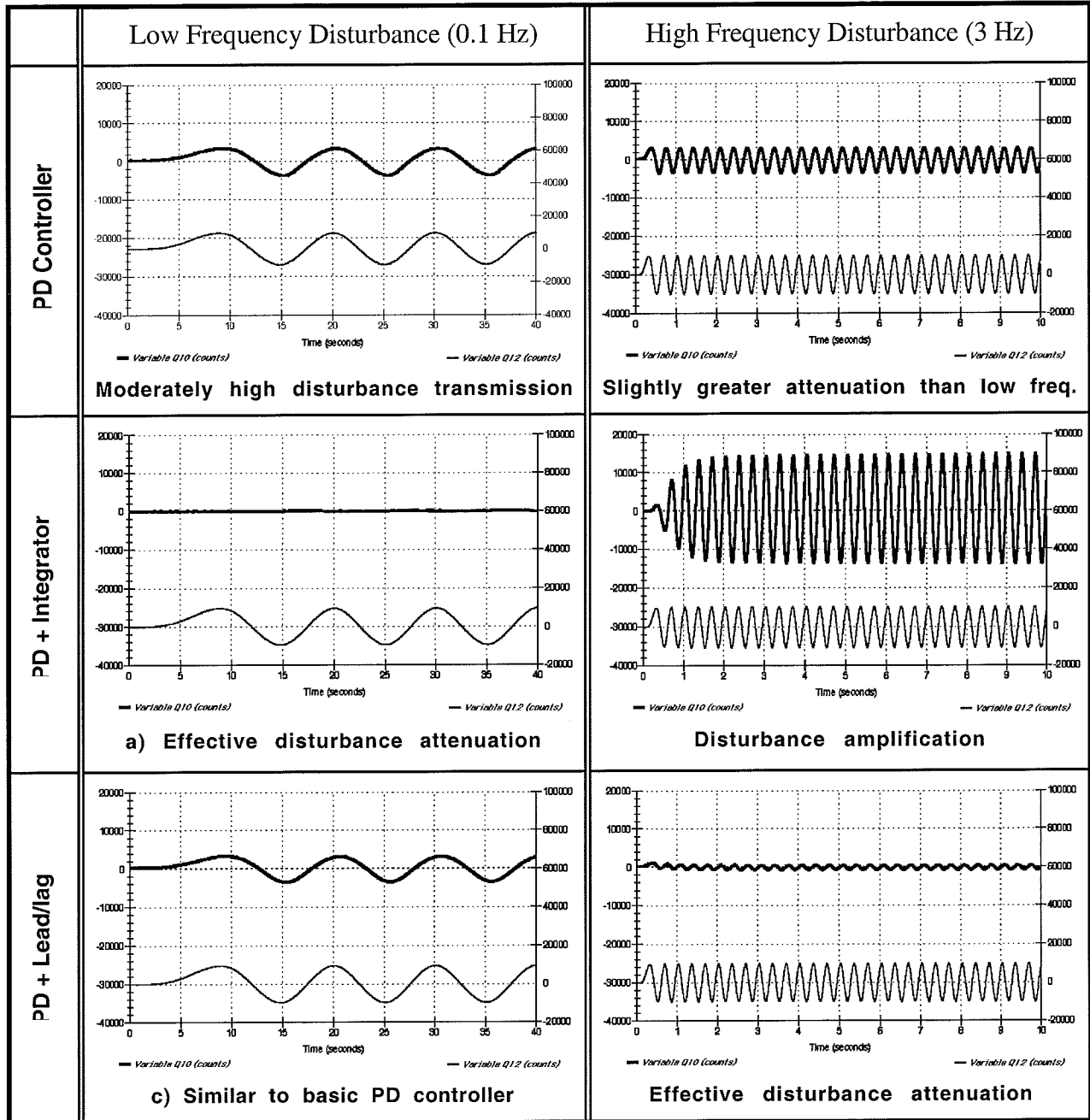


Figure 6.5-1i Experimental Results Show Frequency Dependence of Disturbance Attenuation For Three Controllers

**Answers to Exercises**

A. The open loop transfer functions for Controllers “a” and “b” are:

$$\frac{N_{ol}(s)}{D_{ol}(s)} = \frac{k_d s^2 + k_p s + k_i}{s} \frac{k_{sys}}{m s^2} \quad (6.5-1i)$$

$$= \frac{826(0.023s+0.43)}{s^2} \quad (\text{Controller "a"})$$

$$= \frac{826(0.023s^2+0.43s+10)}{s^3} \quad (\text{Controller "b"})$$

For Controller "c", the expression is:

$$\begin{aligned} \frac{N_{ol}(s)}{D_{ol}(s)} &= (k_d s + k_p) \frac{N_f(s)}{D_f(s)} \frac{k_{sys}}{m s^2} & (6.5-2i) \\ &= \frac{826(0.023s+0.43)(6s+9.42)}{s^2(s+9.42)} \end{aligned}$$

where  $N_f(s)$  and  $D_f(s)$  are the numerator and denominator respectively in  $F(s)$ .

For the closed loop expressions,  $y_1(s)/F_d(s)$ :

Controllers "a" & "b":

$$\frac{y_1(s)}{F_d(s)} = \frac{s}{m s^3 + k_{sys}(k_d s^2 + k_p s + k_i)} \quad (6.5-3i)$$

$$= \frac{8.26}{s^2 + 826(0.023s+0.43)} \quad (\text{Controller "a"})$$

$$= \frac{8.26s}{s^3 + 826(0.023s^2+0.43s+10)} \quad (\text{Controller "b"})$$

Controller "c":

$$\begin{aligned} \frac{y_1(s)}{F_d(s)} &= \frac{D_f(s)}{m s^2 D_f(s) + k_{sys} (k_d s + k_p) N_f(s)} & (6.5-4i) \\ &= \frac{8.26(s+9.42)}{s^3 + 151s^2 + 284s + 335} \end{aligned}$$

B. The Bode magnitude of the above transfer functions is given in Figure 6.5-2i. The correlation between the closed loop gain and the experimentally obtained disturbance attenuation at the two test frequencies is clear. The integrator in controller "b" provides large low frequency attenuation but has a high gain peak between three and four Hz making it ineffective at these frequencies. The lead-lag filter made no improvement over the PD controller at very low frequencies but was effective in the higher frequencies as predicted in the closed loop Bode response.

The correlation between the open and closed loop gains is also clear. The integrator is manifested as the -60 Db/dec. low frequency slope and provides complete static disturbance attenuation (zero DC gain) in the closed loop. The low open loop gain slope near crossover correlates with the closed loop resonance near three Hz. The added gain from the lead-lag filter for frequencies beyond 0.1 Hz yields higher frequency attenuation in the closed loop.

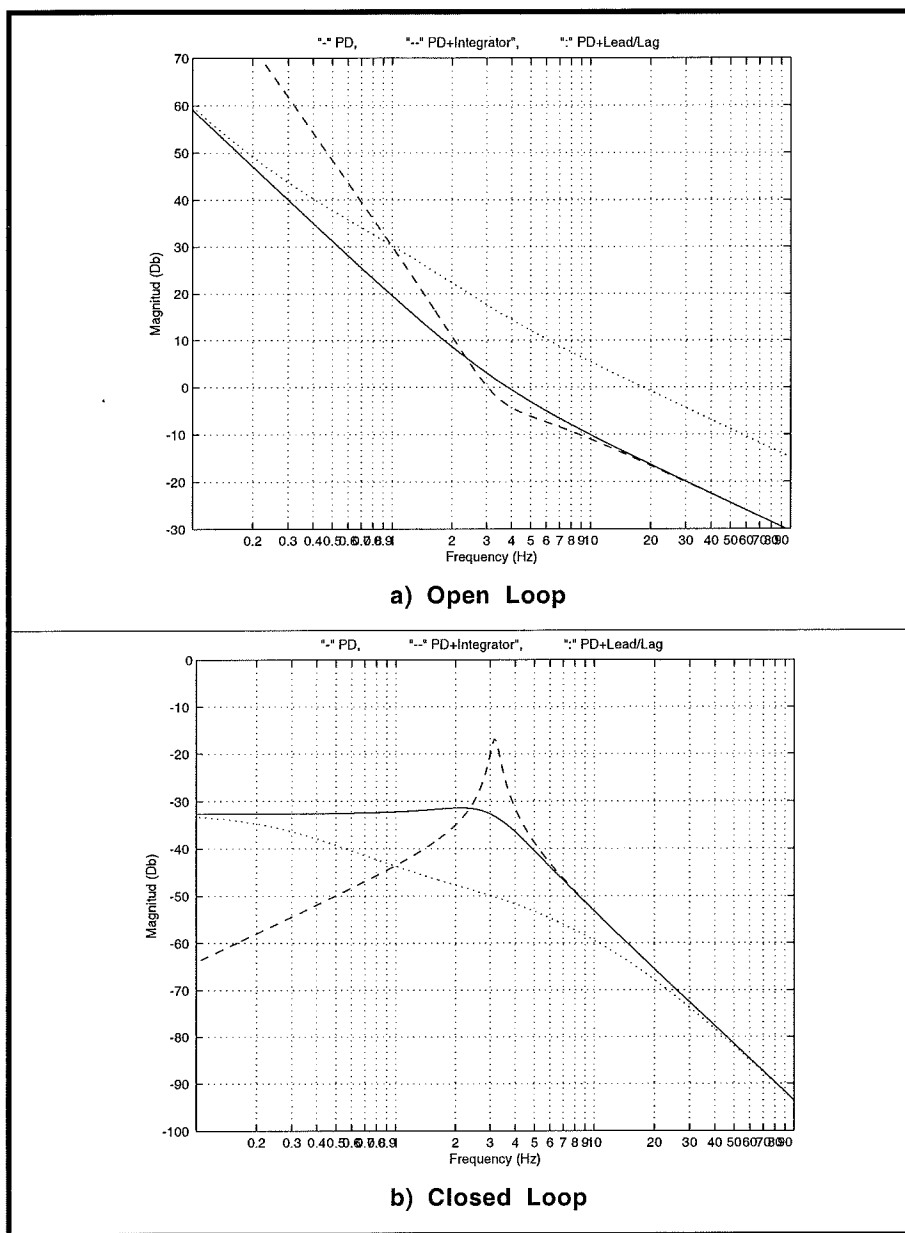


Figure 6.5-2i Transfer Functions of Disturbance to Output Give Underlying Basis For Experimental Results

**This section showed:**

1. An integrator in the controller can be an effective way to attenuate disturbances at low frequencies due to the attendant infinite DC gain. It can however be deleterious for higher frequency disturbance attenuation.
2. Providing high open loop gain in the expected disturbance frequency band of interest is an effective attenuation approach (subject of course to the requirement for closed loop stability).
3. Disturbance attenuation properties may generally be predicted from the open loop frequency response. (The open loop frequency response also indicates other important properties such as bandwidth, stability, sensitivity to parameter changes and static stiffness.)
4. That the effectiveness of a particular control design depends on the control objective. For example a controller may be very effective at attenuating low frequency disturbances but ineffective (even deleterious) for attenuating high frequency ones.

**6.6i Collocated Control of SIMO Plant**

This experiment illustrates the affect of dynamic coupling on the plant, characteristic differences between collocated and noncollocated dynamics, and the inherent controllability difficulties in the use of a collocated scheme when point of objective control is not at the sensor/actuator collocation.

Expected Results:

- 1) In Step 2, a suitable algorithm is as follows:

```

;Set Ts=0.001768 s

;*****Declare variables*****
#define y1cal q2
#define y1rawo q3
#define kp1 q4
#define kd1 q5
#define kddl q6
#define Ts q7
#define y1str q8
#define comp_effort q9
#define pos_last q15
#define u1str q16
#define u1o q17
#define u1 q18
#define laser1 q19
#define y1o q20
#define uterm1 q21
#define uterm2 q22
#define y2o q23
#define y1_delta q25
;*****Initialize*****

```



```

Ts=0.001768 ;for local use only must set Ts in dialog box for sampling period
;Specify Parameters
ulo=11800*2 ;gravity feedforward
ylo=10000
y2o=-43000
kp1=3
kd1=0.1
kdd1=kd1/Ts
pos_last=0
cmd1_pos_last=0
;*****Begin Real-time Algorithm*****
begin
ylcal=sensor1_pos
ylstr=ylcal-ylo
yl_delta=ylstr-pos_last
;CONTROL LAW
ulstr=kp1*(cmd1_pos-ylstr)-kdd1*(yl_delta);
ul=ulstr+ulo ;Add gravity offset
uterm1=6.2+ylcal/10000 ;nonlinear actuator compensation in three steps
uterm2=uterm1*uterm1
comp_effort=0.000165*uterm2*uterm2*ul
control_effort1=comp_effort
;INCREMENT VALUES
pos_last=ylstr
q10=ylstr
q11=control_effort1
q12=sensor2_pos-y2o
control_effort2=cmd2_pos
end

```

- 2) Step responses at  $y_1$  and  $y_2$  in Step 3 are shown in Figure 6.4-1ia where  $k_p = 3.0$ ,  $k_d = 0.1$  were selected.
- 3) In Step 4, the predominant feature in  $y_2$  is the damped oscillation @ roughly 2.5 Hz. The relatively high PD gains have brought the closed loop poles near the collocated zeros (roots of  $N_1(s)$ ); thus the oscillations are largely attenuated in  $y_1$ . Note this response will vary widely from apparatus-to apparatus due to the sensitivity of the response to friction. If friction is so high that very little overshoot is obtained, clean the glass rod (and possibly magnet bushing surfaces) according to the instructions of Section 2.2.

The disturbance affects the upper magnet considerably more [roughly 8x] than the lower one. (If a bilateral disturbance is used, the amplitude should be decreased to avoid attracting the upper magnet out completely up to the mechanical stop (approx. 4 cm.). This difference in displacement results from the nonlinearity in the magnet-to-magnet and magnet-to-coil forces. Such a disturbance test may be run if it is desired to reinforce earlier experiments showing the nonlinear nature of the magnetics.). Typical disturbance plots are shown in Figure 6.6-2i.

There is some significant steady state error due to the interaction of the lower drive coil field and the upper magnet (i.e., the term  $F_{u12}$  in Section 5.1). While this force is relatively small as compared to the upper coil control forces it has a significant effect under the present scheme because the upper magnet is supported only by the relatively soft "spring"  $k_{12}$ '.

- 3) The step response at  $y_2$  in Step 5 are shown in Figure 6.6-1ib where  $k_p = 1$ ,  $k_d = 0.05$  were selected. Here the overshoot in  $y_2$  are less severe than in the high gain case, but the response is slower. Both magnets have less static stiffness,

and hence greater steady state error, than those of the higher gain controller of Step 3.

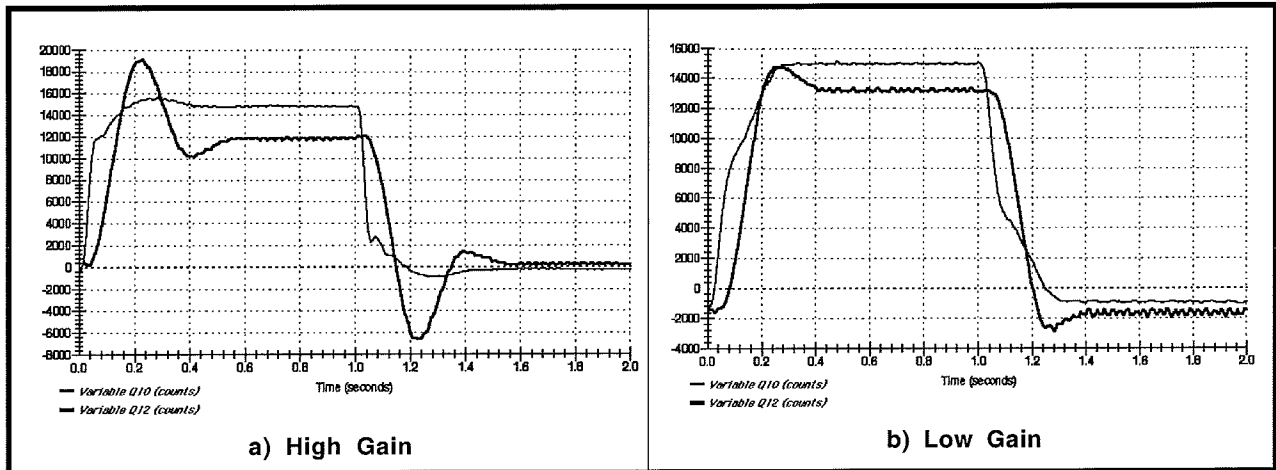


Figure 6.6-1i. Step Responses At  $y_1$  and  $y_2$  (Steps 3 & 5)

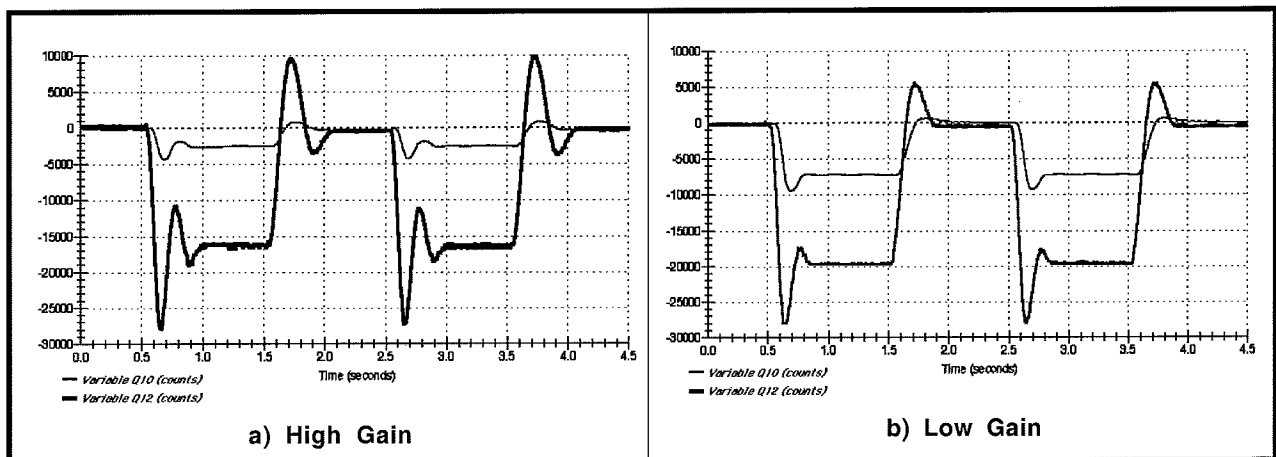


Figure 6.6-2i. Disturbance Responses At  $y_1$  and  $y_2$

**Answers to Questions**

A. The closed loop poles for the gains above are roughly  $\{-6.5 \pm 5.2i, -0.08 \pm 2.7i\}$  (Hz, from Step 3), and  $\{-3.0 \pm 4.3i, -0.3 \pm 2.5i\}$  (Hz, Step 5). (These results are more lightly damped than the actual system due to the presence of friction.) The closed loop zeros are identical to the open loop ones with the additional zero at  $-k_p/k_d$ . The high PD gains in Step 3 have brought the closed loop poles very near the lightly damped collocated zeros. This pole pair is not canceled in the  $y_2$  output. To reduce the oscillatory response, the proportional gain must be decreased resulting in the more damped poles in Step 5. The oscillations are also reduced by the slower system response due to the lower frequency real poles. A view of the root loci of this system for various ratios  $k_d/k_p$  is shown in Figure 6.4-3i. Notice that the poles remain close to the imaginary axis for high and low values of  $k_d/k_p$ . These plots are easily generated using the Matlab™ command ( $k_d/k_p = 0.05$  case):

```
rlocus(conv([.05 1], Num1), Den)
```

B. The transfer function is

$$\frac{y_2(s)}{r(s)} = \frac{(k_p + k_d s) k_{sys} N_2 / D(s)}{1 + (k_p + k_d s) k_{sys} N_1(s) / D(s)} \quad (6.6-1i)$$

The Nyquist plot is shown in Figure 6.6-4i<sup>1</sup>. As can be seen in the figure, the phase margin for both systems is roughly 60 degrees. The gain margin is infinite in both cases. Because the denominator is unchanged by the choice of output location, the stability margins are identical for  $y_1(s)/r(s)$ . (It is worth mentioning to the students that in practical systems there are issues such as sensor phase lag and sampling delays that eventually lead to instability at sufficiently high gain. There are also issues such as drive saturation and noise propagation that limit the practical bandwidth.

C. The static servo stiffness of the lower magnet for a disturbance at that location is

$$F_{d1}/y_1 = k_p k_{sys} \text{ (N/m)} \quad (6.6-2i)$$

For disturbances at the upper magnet, the static servo stiffness at  $y_1$  couples in series with the “spring”  $k_{12}'$  and reduces the effective stiffness at  $y_2$  according to:

$$F_{d2}/y_2 = (k_p k_{sys}) k_{12}' / (k_p k_{sys} + k_{12}') \quad (6.6-3i)$$

When applied at the second magnet alone, the disturbance force imparts, in the absence of friction, the same steady state force to both magnets, i.e.  $F_{d2} \approx F_{d1}$ . Because the intermagnet stiffness,  $k_{12}'$ , is less than  $k_p$ , the resulting error at  $y_2$  is significantly greater than at  $y_1$ . For this same reason, the effect of reduced gain on steady state error at  $y_2$  is not great. At  $y_1$  however the effect is proportional to gain and a 3:1 increase in steady state error for the gains given above results from the low gain system. These effects are readily seen in the disturbance response results of Figure 6.6-2i.

With integral action, the static servo stiffness is infinite, and the stiffness at  $y_2$  in this case is  $k_{12}'$ .

<sup>1</sup> The “loops” in the figure are associated with the resonant poles and zeros for the system modeled as having no friction.

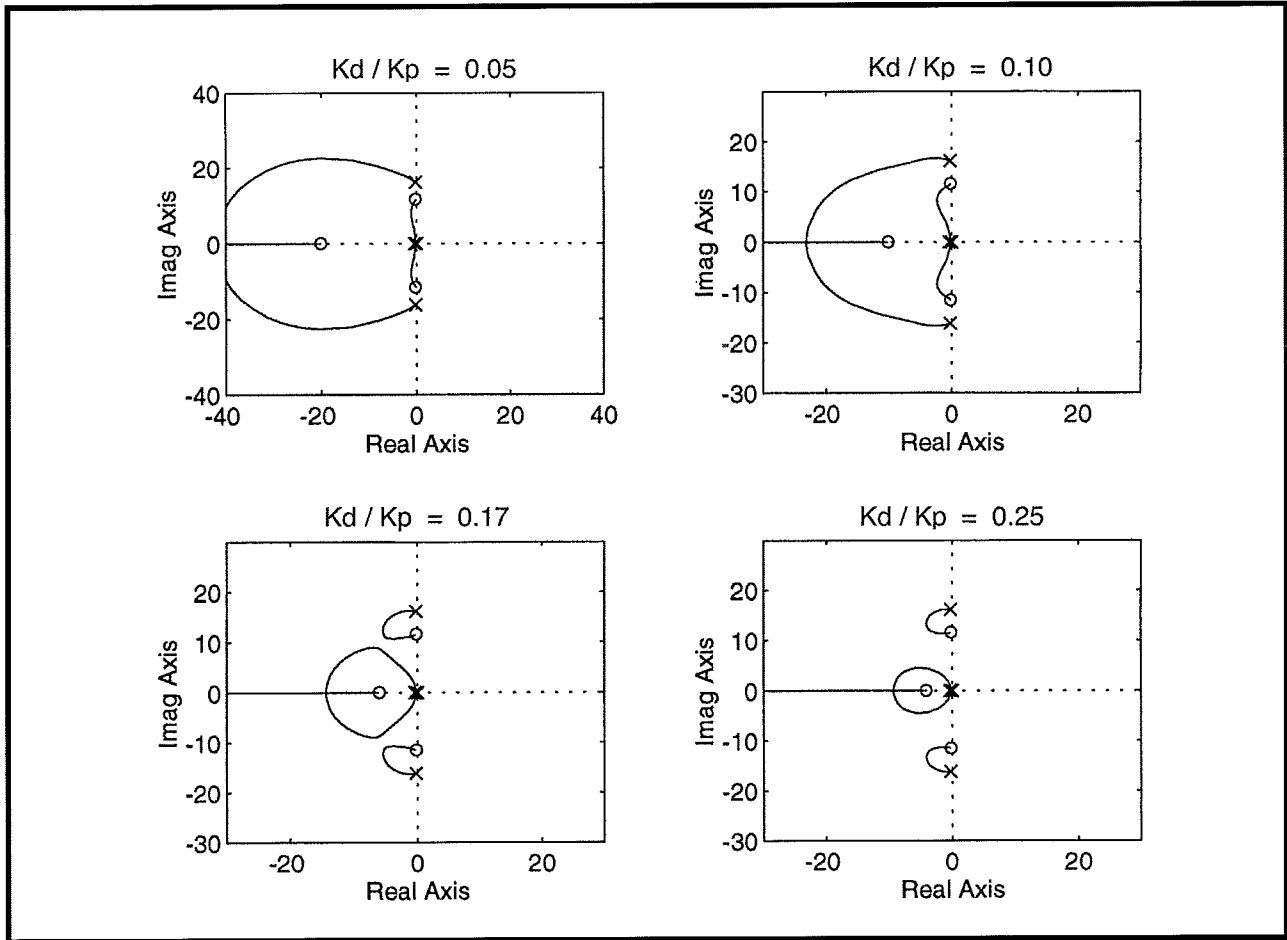


Figure 6.6-3i. Root Loci For Various  $k_d/k_p$

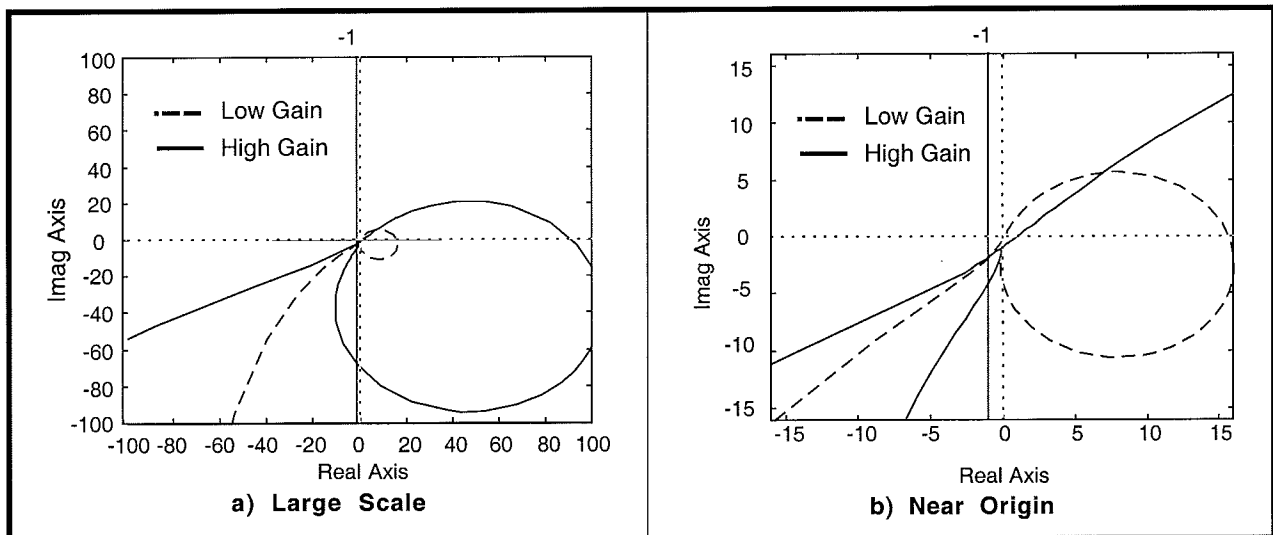


Figure 6.6-4i. Nyquist Plots Show Large Phase Margins and Infinite Gain Margins

**This Section Showed**

1. High gain control may be effective for flexible systems where the control objective is at the actuator location ( $y_1$ ); but may be largely ineffective for control of the noncollocation ( $y_2$ ) due to flexible plant oscillations.
2. Plant overshoot and oscillations may be damped via lower gain control, but at the expense of collocated performance and system stiffness.
3. The static stiffness at the collocation is the same as that of a rigid body. At the noncollocation, it is equal to the collocated static servo stiffness in series with the structural ("magnetic/gravity spring" in this case) stiffness.
4. Collocated PD control is ideally stable for all gains but has lightly damped closed loop poles at both low and high gain.

**6.7i Noncollocated SIMO Control: Successive Loop Closure**

This approach has the advantage that by closing the high gain collocated loop, system sensitivity to nonideal such effects as sensor and actuator nonlinearities and Coulomb friction at  $y_1(s)$  is dramatically reduced. The success of the approach depends greatly on the ability to attain sufficiently high bandwidth at the collocation so that the assumption of unity gain (and zero phase lag) through the ensuing system bandwidth is valid. Because it utilizes pole placement, success also strongly depends on the accuracy and validity of the pseudo-plant model  $N_2/N_1$ . In cases where this model is not well known or involves significant nonlinearity, this approach may be inappropriate.

This general approach may be successfully employed using other methods of control design for the outer loop (e.g. Bode design, linear quadratic,  $H_\infty$ ,  $\mu$ -synthesis, or QFT). The outer loop controller may be either a forward path cascade or return path/prefilter type. State space controllers are easily expressed in one of these forms.

**Notes on Safety and Performance:**

1. The laboratory staff should always be on hand when students implement their controllers. This is particularly important during the testing of the relatively higher gain designs such as the ones here.
2. For a dynamic filter design in general, and pole placement in particular, it is important to maintain relatively high numerical precision. Students should work in high precision and enter  $S(s)$  and  $R(s)$  in at least 4 significant digits. Use of only 3 digits has been shown to yield significantly altered results.
3. Due to the high associated gains, this approach is robust against model uncertainty and nonlinearities at the collocation. Because the remaining plant is reasonably well approximated by its linear model between  $y_1$  and  $y_2$  (Eq. 6.6-1i), the approach here may be employed with success. In order to get the best possible model of  $y_2(s)/y_1(s)$ , the user may wish to identify

that portion of the plant directly.  $y_2(s)/y_1(s)$  is found more precisely by letting the lower magnet rest against its hard stop and plotting and measuring the free oscillation frequency ( $\approx \omega_n$ ) and damping ratio ( $\approx \zeta$  – use logarithmic decrement technique) of the upper magnet. (Students will see the nonlinear spring effect on the oscillation shape).

$$\frac{N_2(s)}{N_1(s)} = \frac{\omega_n^2}{s^2 + 2\zeta\omega_n s + \omega_n^2} \quad (6.6-1i)$$

The data may be collected by setting the gains in any of the previous controllers equal to zero and dropping the magnet during the *Execute* period of any trajectory set to zero amplitude. Students will see the nonlinear spring effect on the oscillation shape.

4. It is possible to create a sufficiently high bandwidth controller that causes a nonlinear response with very large overshoot of the upper magnet in the upward direction. This is because of the nonlinear nature of the “spring”,  $k_{12}$ . In relatively large positive displacements  $y_2 - y_1$ , the spring become dramatically softer resulting in large overshoot.

#### Expected Results:

See answers to questions for expected control design values

- 1) In Step 3, under the high gain collocated control, the lower magnet is quite stiff ( $k_p k_{sys} \approx 300$  N/m) while the upper magnet stiffness is essentially that of  $k_{12}$  ( $\approx 40$  N/m)
- 2) A script for generating the inner and outer loop control gains entitled *SIMOpoleplace.m* is listed in Appendix A. A suitable algorithm for implementing the desired control is as follows:

```
;Set Ts=0.001768 s
;*****Declare variables*****
#define y1cal q2
#define y1rawo q3
#define kpl q4
#define kd1 q5
#define kddl q6
#define Ts q7
#define y1str q8
#define comp_effort q9
#define y1str_last q15
#define ulstr q16
#define ulo q17
#define ul q18
#define y1o q20
#define uterm1 q21
#define uterm2 q22
#define error1 q23
#define refl q24
#define kid1 q25
#define uil q26
#define refl_last q27
#define delta_y1 q28
#define y2cal q30
#define y2rawo q31
#define y2str q32
#define y2str_last q33
#define y2s q34
```

```

#define y2o q36
#define error2 q37
#define s0d q38
#define s1d q39
#define r1d q40
#define kpf q46
;*****Initialize*****
Ts=0.001768 ;for local use only must set Ts in dialog box for sampling period
;Specify Parameters
ulo=11900*2 ;gravity offset
y1o=10000
y2o=-42500
kpl=3
kdl=0.1
s0d=4.402
s1d=-4.364
r1d=-0.8713
kddl=kdl/Ts ;Discrete time terms, compute here to save real-time computation
ref1_last=0
error1=0
y2s=0
kpf=s0d+s1d+1+r1d

;*****Begin Real-time Algorithm*****
begin
y1str=sensor1_pos-y1o
y2str=sensor2_pos-y2o
;OUTER LOOP
y2s=s0d*y2str+s1d*y2str_last; RETURN PATH: S(z)*y2str-->y2s
error2=kpf*cmd1_pos-y2s; OUTER LOOP ERROR
ref1=error2-r1d*ref1_last; 1/R(z)*OUTER LOOP ERROR --> INNER LOOP REFERENCE INPUT
;INNER LOOP
error1=ref1-y1str
delta_y1=y1str-y1str_last
ulstr=kpl*error1-kddl*delta_y1 ;INNER LOOP CONTROL LAW
;OUTPUT
ul=ulstr+ulo ;Add gravity offset
uterm1=6.2+sensor1_pos/10000 ;nonlinear actuator compensation in three steps
uterm2=uterm1*uterm1
comp_effort=0.000165*uterm2*uterm2*ul
control_effort1=comp_effort
control_effort2=cmd2_pos
;INCREMENT VALUES
y2str_last=y2str
ref1_last=ref1
y1str_last=y1str
q10=y1str
q12=y2str
end

```

- 3) In Step 8,  $k_{pf} = (r_0 n_{10} + s_0 n_{20})/n_{10}$  where  $n_{i0}$  ( $i=1,2$ ) is the constant term in  $N_i$ . In this case  $n_{20}=n_{10}$  so that  $k_{pf} = (r_0 + s_0)$ . For discrete implementation this becomes  $k_{pf} = (r_{0d} + r_{1d} + s_{0d} + s_{1d})$
- 4) From Step 7, typical step response plots are shown in Figure 6.6-1i. The  $y_2$  rise time is relatively rapid with moderate overshoot. The first magnet moves quickly to accelerate the second one, then reverses motion to minimize overshoot. The disturbance responses are shown in Figure 6.7-2i.

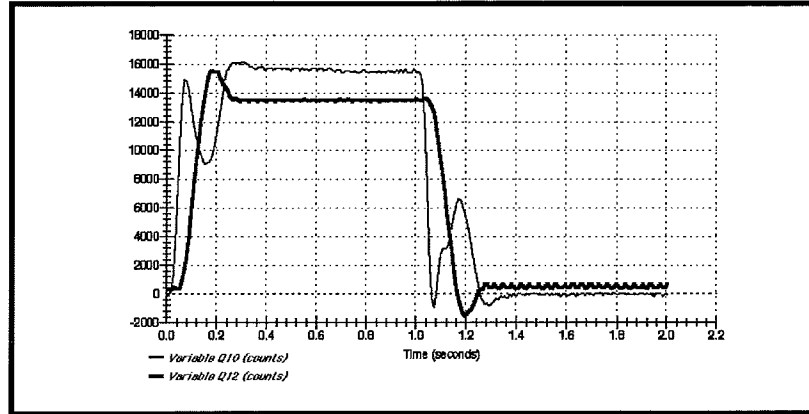


Figure 6.7-1i. Step Response At  $y_1$  and  $y_2$  Shows Relatively High System Performance. Lower Magnet Leads, Then Reverses, To Minimize Error In Upper Magnet.

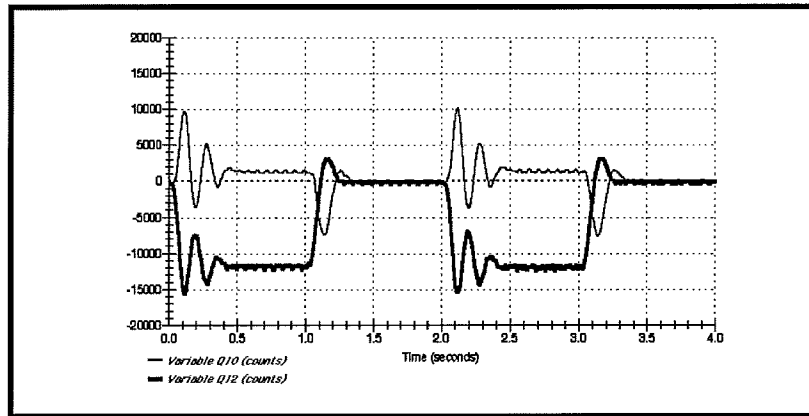


Figure 6.7-2i. Disturbance Response Shows Reduced Error At  $y_2$  Compared With Collocated Control. Polarity Of Response At  $y_1$  Reversed Due To Control Regulation

**Questions:**

A. Expected values (consistent with others in this manual) are:

$$k_p = 3.0, k_d = 0.086$$

$$s_0 = 22.692, s_1 = 4.6842, r_0 = 77.809, r_1 = 1$$

Discrete coefficients using the Tustin transformation are

$$s_{0d} = 4.402, s_{1d} = -4,364, r_{0d} = 1, r_{1d} = -0.8713$$

The prefilter gain for these discrete coefficients is

$$k_{pf} = 0.1687$$

B. The reduced and “full” order (design) closed loop transfer functions are:

$$\frac{y_2(s)}{r_r(s)} = \frac{k_{pf}k_{sys}k_pN_2}{R(s)(D(s)+k_{sys}N_1(s)(k_d s + k_p)) + S(s)k_{sys}N_2k_p} \quad (6.7-1i)$$



$$\left(\frac{y_2(s)}{r_1(s)}\right)_{design} = \frac{k_{pf}N_2}{R(s)N_1(s) + S(s)N_2} \quad (6.7-2i)$$

The simulated frequency responses for the two expressions are given in Figure 6.7-3i. Both magnitude and phase are similar through the system bandwidth and the assumption of unity gain in  $C(s)$  is generally valid.

- C. The reduced and “full” order open loop transfer functions for the outer loop are respectively

$$\left(\frac{Num_{ol}}{Den_{ol}}\right)_{reduced\ order} = \frac{N_2S(s)}{N_1R(s)} \quad (6.7-3i)$$

$$\left(\frac{Num_{ol}}{Den_{ol}}\right)_{full\ order} = \frac{k_{sys}k_pN_2S(s)}{D(s)R(s) + k_{sys}(k_d s + k_p)N_1R(s)} \quad (6.7-4i)$$

The Bode plots of these are shown in Figure 6.7-4i. The phase margin is approximately 60 degrees in the reduced order case and 25 in the full order one. The gain margin is approximately 14 Db for the full order case and infinite for the reduced order one. Thus the stability margin is reduced in the actual system as compared to the idealized low order one.

Note that both the open and closed loop Bode “full order” responses can ideally be made arbitrarily close to the reduced order one by sufficiently increasing the inner loop bandwidth. In practice however, the bandwidth is limited due to signal noise amplification and stability limits from unmodeled effects such as sampling delays and other signal lags.

- D. The static stiffnesses are readily found by referring to the static system diagram of Figure 6.7-5i. At equilibrium and in the absence of static friction, the drive force  $F_u$  is equal and opposite to the disturbance force regardless of which inertia (magnet) the disturbance acts on. We also have that

$$\text{for disturbances at the lower magnet: } y_2^* = y_1^* \quad (6.7-5i)$$

$$\text{for disturbances at the upper magnet: } y_2^* = y_1^* + F_{d2}/k_{12}' \quad (6.6-6i)$$

where  $k_{12}'$  is the “spring” constant. From these, we have the static stiffness expressions and their values (for the parameters in this manual):

$$\frac{F_{d1}}{y_1} = \frac{F_{d1}}{y_2} = k_p k_{sys} \left(1 + \frac{s_0}{r_0}\right) \quad (= 394 \text{ N/m}) \quad (6.6-7i)$$

$$\frac{F_{d2}}{y_1} = k_p k_{sys} \frac{k_{12}'(r_0 + s_0)}{r_0 k_{12}' - k_p k_{sys} s_0} \quad (= -296 \text{ N/m}) \quad (6.6-8i)$$

$$\frac{F_{d2}}{y_2} = k_p k_{sys} \frac{k_{12}'(r_0 + s_0)}{r_0(k_{12}' + k_p k_{sys})} \quad (= 44 \text{ N/m}) \quad (6.6-9i)$$

By comparing Eq's (6.7-7i) and (6.7-9i) it is seen that for this system, the upper

magnet is less stiff than the lower one for all  $k_p > 0$ . Eq. (6.7-6i) shows that the lower magnet will undergo reverse motion in response to disturbances on the upper one whenever  $k_p k_{sys} s_0 > r_0 k_{l2}'$ . This occurs whenever the outer loop control gain  $s_0/r_0$  is high relative to spring  $k_p'$  as is the case in the present system (see the reversed displacement in  $y_l$  under disturbance at the upper magnet in Figure 6.7-2)

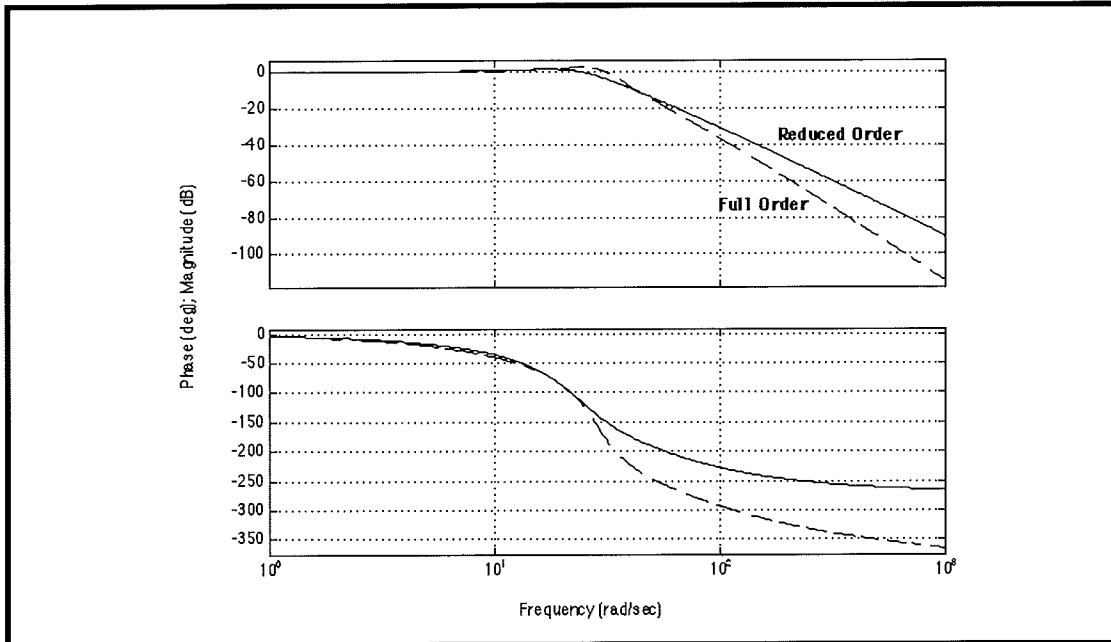


Figure 6.7-3i. Frequency Response of Reduced and Full Order Closed Loop Transfer Functions are Similar Through System Bandwidth

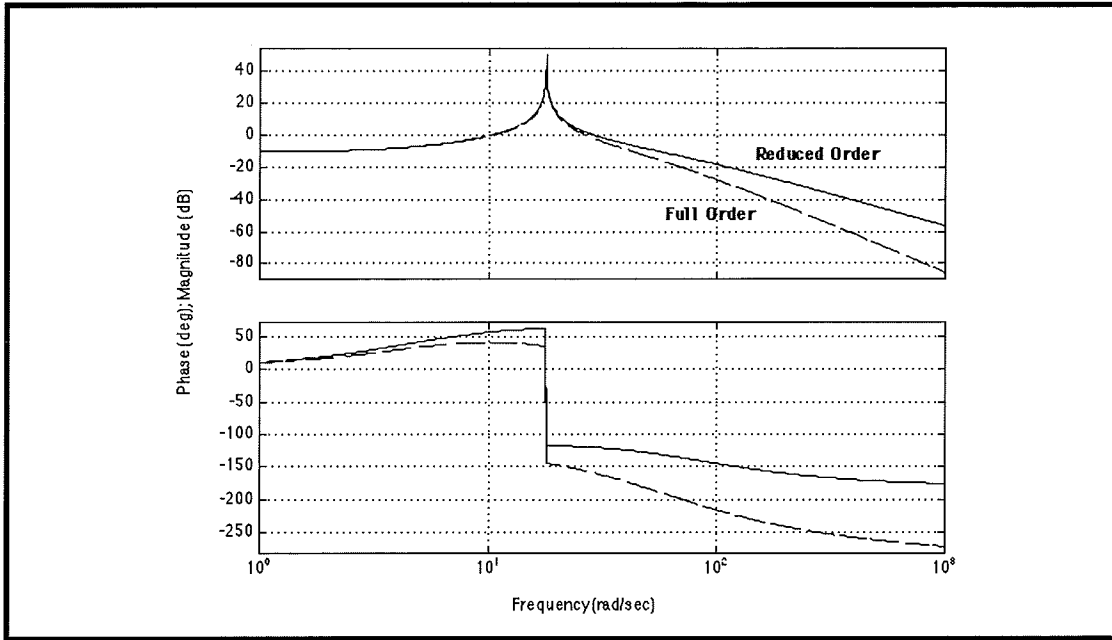


Figure 6.7-4i. Full Order Open Loop Transfer Function Reflects Reduced Phase and Gain Margins From Idealized Reduced Order System

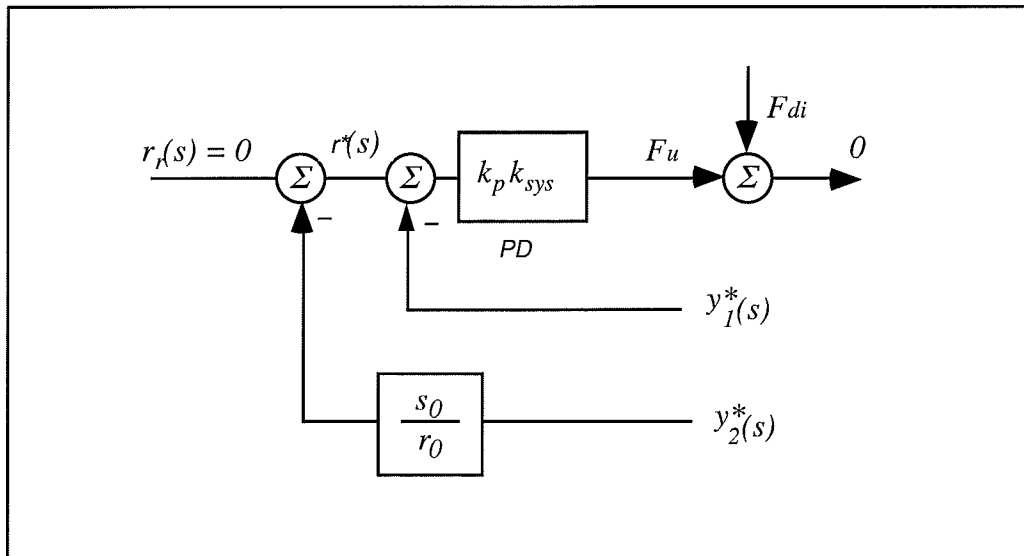


Figure 6.7-5i. Static System Block Diagram

**Optional Experiments & Results**

A. LQR Control of Outer Loop

Any number of methodologies may be used to design the outer loop controller. Shown in Figure 6.7-6i are the step and disturbance responses of such a system where the controller is generated using LQR synthesis. The script for the synthesis is listed in Appendix A as *SIMOLQR.m* where the control gains for various values of control effort weight are solved

for and the closed loop poles and step responses are plotted. The states defined for the SISO outer loop are  $y_2$  and  $\dot{y}_2$  and the associated gains used are  $k_1=0.87$  and  $k_2=0.053$ .

The step response shows a faster rise but with greater overshoot than that of the pole placement design. As in the previous design, the collocated magnet leads the noncollocated one (the object of objective control) in order to accelerate it, then reverses direction to “automatically” reduce the overshoot. The disturbance response is reduced compared to the pole placement design due to the higher steady state gain – note the significant reversed motion of the lower magnet due to control regulation. The response is nonlinear (higher overshoot in the positive direction than the negative) due to the nonlinear spring characteristic,  $k_{12}$ . The real-time routine that generated these responses is given below and includes a low pass filter at the DAC input to reduce noise resulting from differentiated sensor signals. This filter is useful for the intended purpose but begins to noticeably affect system stability at cutoff frequencies below 40 Hz.

```
;Set Ts=0.001768 s;*****Declare variables*****

#define kp1 q4

#define kd1 q5

#define kdd1 q6

#define Ts q7

#define ylstr q8

#define comp_effort q9

#define ylstr_last q14

#define ulstr q15

#define ulo q16
#define ul q17
#define ylo q18
#define uterm1 q19
#define uterm2 q20
#define error1 q21
#define refl q22
#define refl_last q23
#define delta_y1 q24
#define y2str q25
#define y2str_last q26
#define delta_y2 q27
#define y2o q28
#define error2 q29
#define k1 q30
#define k2 q31
#define kd2 q32
#define filtpole q33
#define k1filt q34
#define k2filt q35
#define filt_comp_effort q36
#define filt_comp_effort_last q37
#define kpf q38
#define dummy q40
;*****Initialize*****
Ts=0.001768 ;for local use only must specify Ts in dialog box to set sampling period
```

```

;Specify Parameters
ulo=11800*2 ;gravity offset
ylo=10000
y2o=-43000
kp1=3
kdl=0.1
;k1=0.8
;k2=0.053
k1=.6 ;Gain For Modified Design
k2=.07 ;Gain For Modified Design
filtpole=90 ;Low Pass noise filter pole in Hz
kddl=kdl/Ts ;Discrete time terms, compute here to save real-time computation
kd2=k2/Ts
ref1_last=0
error1=0
k1filt=filtpole*6.28*Ts/(1+filtpole*6.28*Ts)
k2filt=1-k1filt
kpf=1+1/k1
;*****Begin Real-time Algorithm*****
begin
y1str=sensor1_pos-ylo
y2str=sensor2_pos-y2o
;OUTER LOOP
error2=cmd1_pos*kpf-y2str; OUTER LOOP ERROR
delta_y2=y2str-y2str_last
ref1=k1*error2-kd2*delta_y2; RETURN PATH: S(z)*y2str-->y2s
;INNER LOOP
error1=ref1-y1str
delta_y1=y1str-y1str_last
ulstr=kp1*error1-kddl*delta_y1 ;INNER LOOP CONTROL LAW
;OUTPUT
u1=ulstr+ulo ;Add gravity offset
uterm1=6.2+sensor1_pos/10000 ;nonlinear actuator compensation in three steps
uterm2=uterm1*uterm1
comp_effort=0.000165*uterm2*uterm2*u1
filt_comp_effort=k1filt*comp_effort+k2filt*filt_comp_effort_last
control_effort1=filt_comp_effort
control_effort2=cmd2_pos
;SET PAST VALUES (for next time)
y2str_last=y2str
ref1_last=ref1
y1str_last=y1str
filt_comp_effort_last=filt_comp_effort
q10=y1str
q11=control_effort1
q12=y2str
end

```

### B. Empirically Modified Design

The control gains generated from the LQR synthesis are easily changed and the response checked so that generally improved system behavior is obtained through interactive design. This is rather straightforward in that for the states chosen the LQR gains are simply proportional and derivative terms in the outer loop return path. Shown in Figure 6.7-7i are the step and disturbance responses of such a design where  $k_1=0.6$  and  $k_2=0.07$  were chosen to provide a more damped response than the LQR system and with similar rise time. The asymmetry of response (overshoot) is much less pronounced. The disturbance response has similar amplitude but is also more damped.

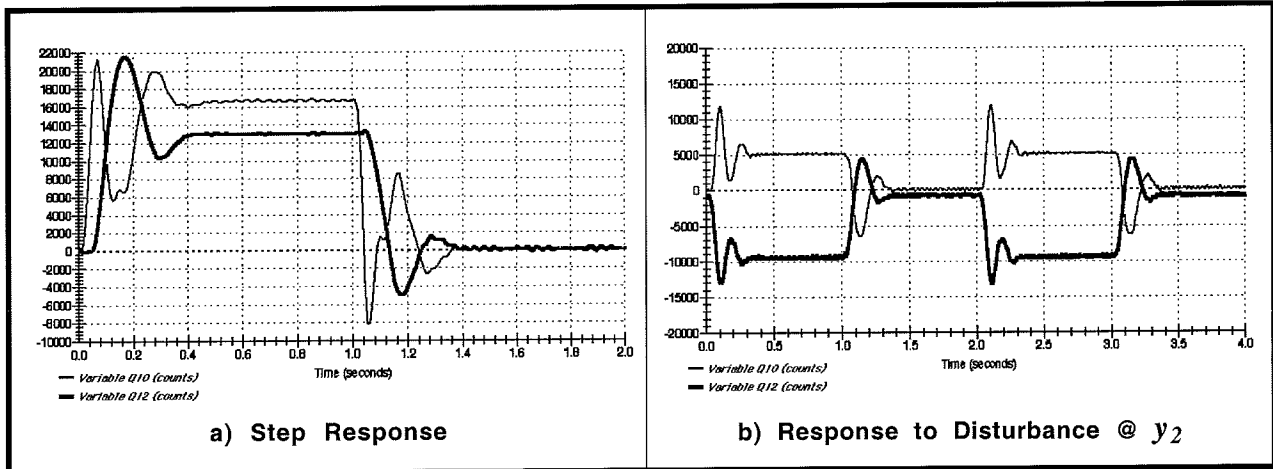


Figure 6.7-6i. Performance of LQR Outer Loop Design

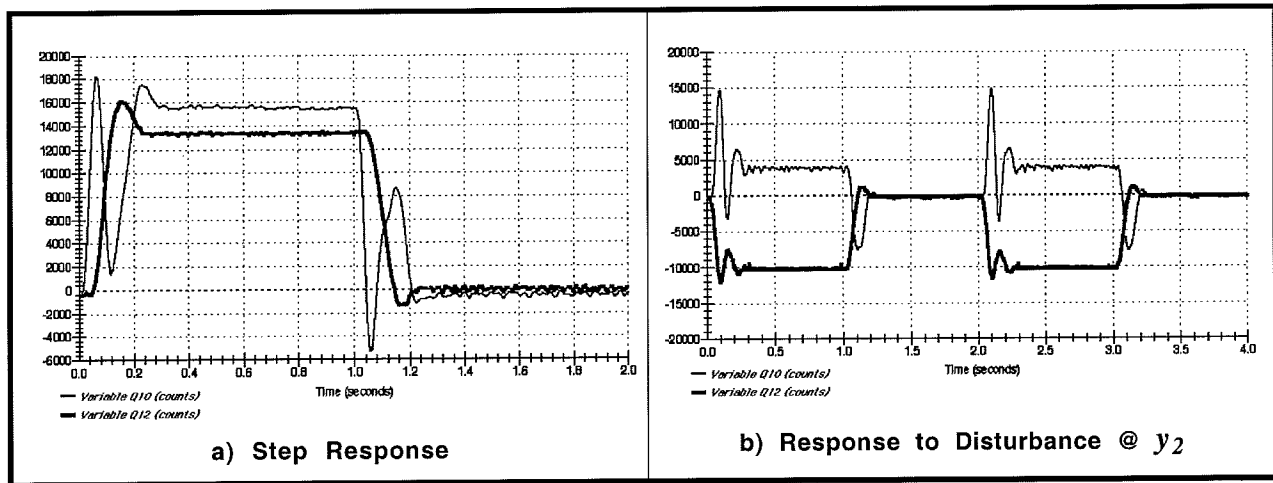


Figure 6.7-6i. Performance of Empirically Modified Outer Loop Design

**This section showed:**

1. The concept of successive loop closure for SIMO systems.
2. High gain inner loop control may be used to desensitize the system to nonlinear and uncertain parameters at the collocation. The outer loop may then be closed by any of several methodologies.
3. The technique of pole placement design.
4. Relatively high performance characteristics relative to the noncollocated output, i.e. relatively rapid step response, and strong disturbance rejection as compared to these characteristics for the same output under collocated control.

## 6.8i MIMO Control

### Expected Results:

- 1) In Steps 2 and 3, the LQR design for the indicated control effort weights and resulting closed loop poles may be obtained via the script *MIMOLQR.m* given in the Appendix.
- 2) In Step 4, a suitable routine for the LQR full state feedback control is:

```

;Set Ts=0.001768 s
;*****Declare variables*****
#define kp1 q2
#define kd1 q3
#define kdd1 q4
#define Ts q5
#define y1str q6
#define comp_effort1 q7
#define y1str_last q8
#define u1str q9
#define u1o q14
#define u1 q15
#define y1o q16
#define uterm1 q17
#define uterm2 q18
#define delta_y1 q22
#define y2str q23
#define y2str_last q24
#define delta_y2 q25
#define y2o q26
#define comp_effort2 q28
#define k11 q29
#define k12 q30
#define k13 q31
#define k14 q32
#define k21 q33
#define k22 q34
#define k23 q35
#define k24 q36
#define k12d q37
#define k14d q38
#define k22d q39
#define k24d q40
#define kpf1 q41
#define kpf2 q42
#define u2str q43
#define u2o q44
#define u2 q45
;*****Initialize*****
Ts=0.001768 ;for local use only must specify Ts in dialog box to set sampling period
;Specify Parameters
u1o=18000 ;gravity/control effort offset
u2o=5800 ;gravity/control effort offset
y1o=10000
y2o=-20000
k11=1.7
k12=0.064
k13=0.15
k14=.003
k21=.15
k22=.003
;k13=0

```

```

;k14=0
;k21=0
;k22=0
k23=1.7
k24=.064
k12d=k12/Ts ;Discrete time terms, compute here to save real-time computation
k14d=k14/Ts
k22d=k22/Ts
k24d=k24/Ts
kpf1=k11+k13
kpf2=k21+k23
;*****Begin Real-time Algorithm*****
begin
y1str=sensor1_pos-y1o
y2str=sensor2_pos-y2o
delta_y1=y1str-y1str_last
delta_y2=y2str-y2str_last
;LQR ALGORITHM
ulstr=kpf1*cmd1_pos-k11*y1str-k12d*delta_y1-k13*y2str-k14d*delta_y2
u2str=kpf2*cmd2_pos-k21*y1str-k22d*delta_y1-k23*y2str-k24d*delta_y2
;OUTPUT
u1=ulstr+ulo ;Add gravity offset
uterm1=6.2+sensor1_pos/10000 ;nonlinear actuator compensation in three steps
uterm2=uterm1*uterm1
comp_effort1=0.000165*uterm2*uterm2*u1
control_effort1=comp_effort1
;Again For Output 2
u2=u2str+u2o ;Add gravity offset
uterm1=-6.2+sensor2_pos/10000 ;nonlinear actuator compensation in three steps
uterm2=uterm1*uterm1
comp_effort2=0.000165*uterm2*uterm2*u2
control_effort2=-comp_effort2;reverse polarity for S pole of magnet upward
;SET PAST VALUES (for next time)
y1str_last=y1str
y2str_last=y2str
q10=y1str
q12=y2str
end

```

- 2) In Step 5, a suitable routine for the independent SISO controllers is the same as that used in Section 6.5 for the disturbance study where the lower is controller setup for basic PD (only) control and the gains set to approximately  $k_p=1.7$ ,  $k_d=0.6$  for both the upper and lower systems. Alternatively and perhaps more efficiently, the above LQR algorithm may be used with the gains  $k_{11}$  and  $k_{23}$  set equal to 1.7,  $k_{12}$  and  $k_{24}$  equal to 0.6 and the remaining gains to zero.
- 3) In Step 6, a plot of the multivariable step maneuver is on the dual SISO controllers is shown in Figure 6.8-1i. The cross coupling in the outputs is apparent.
- 4) In Step 7 the step series maneuver for the multivariable LQR plant is shown in Figure 6.8-2i. The cross coupling in the responses is significantly reduced from the dual SIOS controlled case. Shown in Figure 6.8-3i are the upper and lower magnet responses where Trajectory 1 is set up for a unidirectional *Impulse* of 15000 count amplitude, 250 ms pulse width, 14 repetitions, and 750 ms dwell time. Trajectory 2 is setup for a bidirectional *Ramp* of 15000 count amplitude, 15000 counts/s velocity, 1000 ms dwell time and 2 repetitions. The maneuver is executed with a 500 ms delay of Trajectory 1 after Trajectory 2. The system



motion is visually stimulating to watch and shows relatively rapid response with only moderate cross coupling.

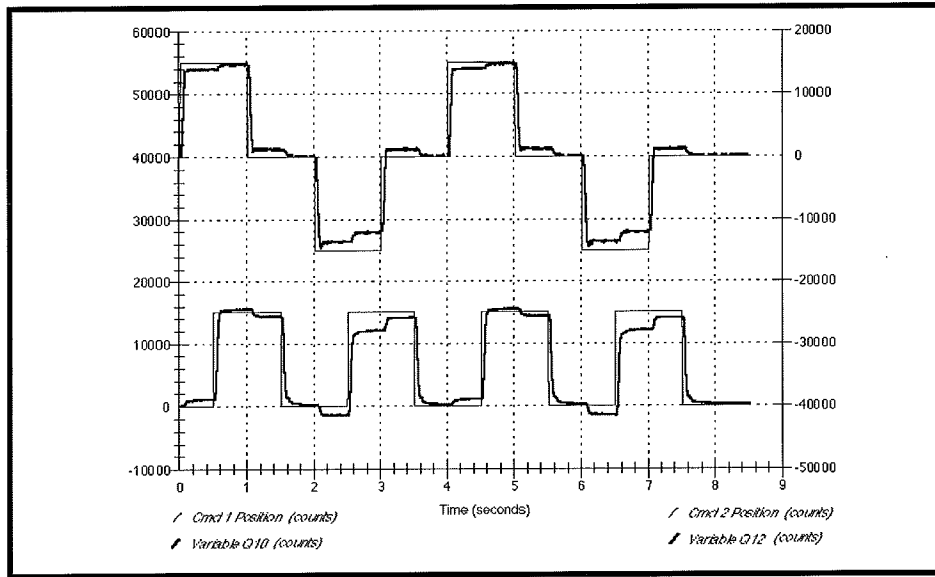


**Figure 6.8-1i. Typical Response of Dual SISO Control System To Step Type Trajectories At Each Input**

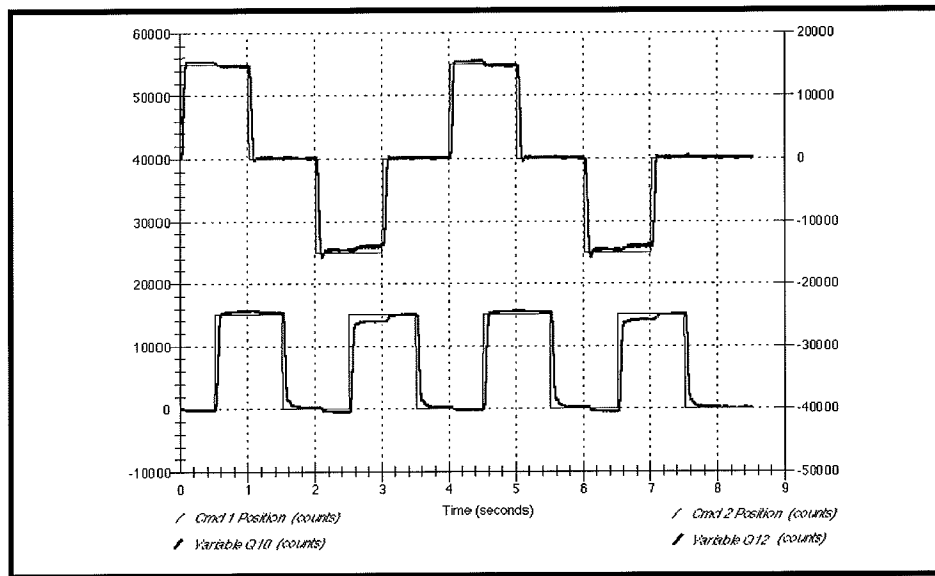


**Figure 6.8-2i. Typical Response of Multivariable LQR Controlled System**

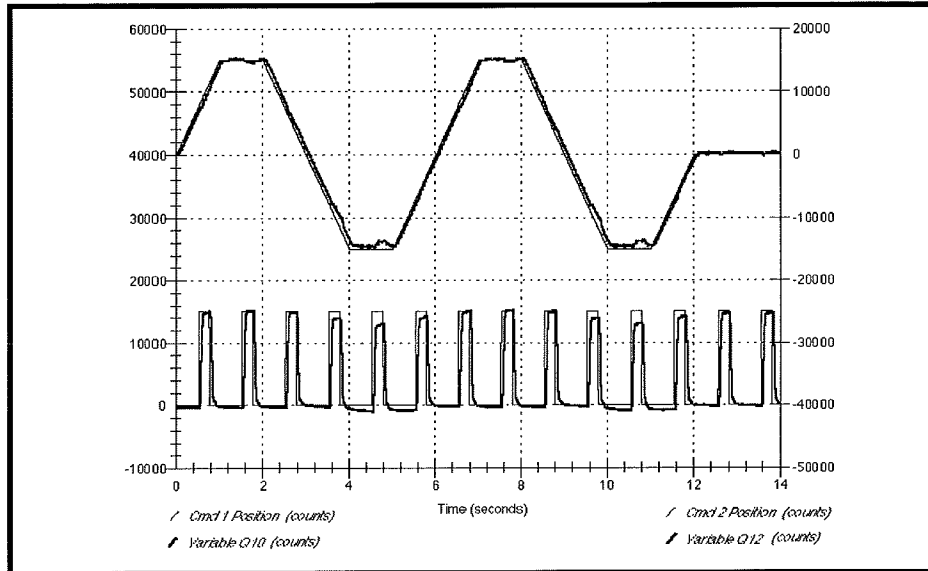


Figure 6.8-3i. LQR Controlled System Response to Ramp & Impulsive Inputs

**Answers to Questions / Exercises**

- A. Using the numerical plant of Eq. (6.1-21i) the poles of the closed loop transfer function for the specified values of  $r$  are plotted in Figure 6.8-4i. A suitable controller from these which meets the closed loop pole specification is the case of  $r = 0.3$  which has a corresponding controller:

$$K = \begin{bmatrix} 1.67 & 0.064 & 0.15 & 0.0029 \\ 0.15 & 0.0029 & 1.67 & 0.064 \end{bmatrix} \quad (6.7-1i)$$

(That the PD gains in item 2 above turned out very similar to those of the LQR controlled system is not coincidental. The closed loop roots of LQR controlled systems as the control effort becomes small approach the angles  $-135$  deg. and  $-225$  deg. from positive real axis. The SOSI design also put the poles at these angles from the origin ( $\zeta=0.707$ ) and in both cases the closed loop roots were designed to be at roughly 6 Hz.)

- B. The dual SISO control shows maximum cross coupling when the two magnets are closest together. This is because of the nonlinear nature of the “spring”  $k_{12}$ . Which has greater intermagnet force at small separation and low force at large separation. The multivariable controlled system shows much reduced cross coupling but does show some residual coupling with the nonlinear nature of  $k_{12}$  being apparent (i.e. the output error is greatest when the magnets are closest, there is a slight over-correction by the controller when the magnets are most widely separated. This characteristic may vary somewhat from system to system.)

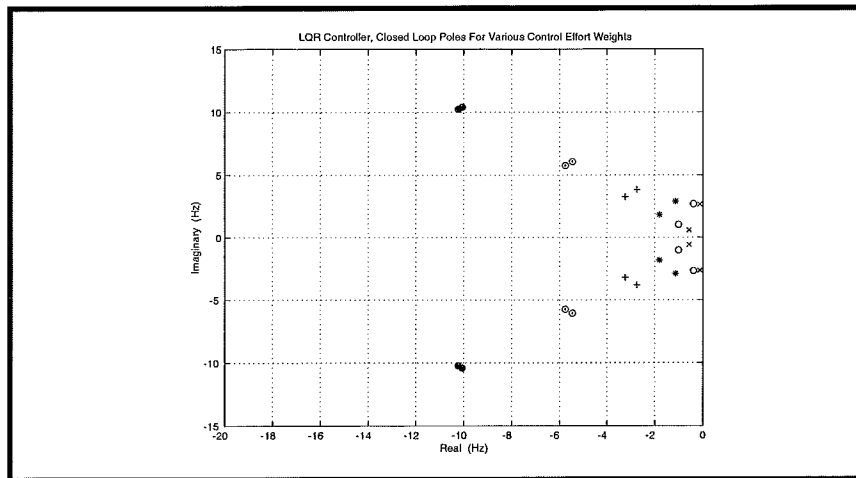


Figure 6.8-4i. Closed Loop LQR Pole Locations For Various Control Effort Weights

#### Optional Exercises & Solutions

- A. Measure the singular value response of the system and compare it with the simulated response.

Ans.: The singular value response for the  $r_1$  input as measured at  $y_1$  is found by executing a Sine Sweep via Trajectory 1. Figure 6.8-5ia shows such a response with the trajectory set to 10000 count amplitude and frequency ranging from 0.1 to 30 Hz (30 sec sweep duration). The 6 Hz rolloff and  $-40$  Db/dec asymptotic slope is clearly seen. Figure 6.8-5b shows the response where the control gain,  $k_{12}$ , is reduced to 0.034. The effect was to more lightly dampen a closed loop pole pair resulting in the resonance seen at 6-7 Hz. (The offset  $y_{10}$  was increased to 15000 counts so that the magnet would not strike the mechanical stop during resonance.) The simulated singular value response (generated in MIMOLQR.m) is shown in Figure 6.8-6i and agrees with the experimental plot.

- B. Construct a real-time control algorithm in which the nonlinear “spring”  $k_{12}'$  is compensated for as shown in Figure 6.8-7i. Compare the system response with the others of this section.

Ans.: An algorithm that implements Figure 6.8-7i is given below. The step series and impulse/ramp responses are shown in Figures 6.8-8i & -9i respectively. The responses show an improvement in the cross coupling relative to the other controllers of this section. Some cross-coupling effects remain due to inexact cancellation of  $k_{12}'$ . These are likely more the result of sensor errors (the sensor signals drive the nonlinearity inversion routine) than in the differences between the physical and modeled spring and actuator nonlinearities. Note that this implementation effectively decouples the upper and lower system so that the control design may be approached for each SISO system independently. The cross coupling errors may be further reduced by increased gain or loop shaping to address the frequency band of interest.

```

;Set Ts=0.001768 s
;*****Declare variables*****
#define kp1 q2
#define kd1 q3
#define kdd1 q4
#define Ts q5
#define ylstr q6
#define comp_effort1 q7
#define ylstr_last q8
#define ulstr q9
#define ulo q14
#define u1 q15
#define y1o q16
#define uterm1 q17
#define uterm2 q18
#define delta_y1 q22
#define y2str q23
#define y2str_last q24
#define delta_y2 q25
#define y2o q26
#define comp_effort2 q28
#define k11 q29
#define k12 q30
#define k23 q35
#define k24 q36
#define k12d q37
#define k14d q38
#define k22d q39
#define k24d q40
#define kpf1 q48
#define kpf2 q49
#define u2str q50
#define u2o q51
#define u2 q52
#define W q53
#define c q54
#define d q55
#define y12 q56
#define ul2term q57
#define ul2 q58
#define ulc q59
#define u2c q60
;*****Initialize*****
Ts=0.001768 ;for local use only must specify Ts in dialog box to set sampling
period
;Specify Parameters
ulc=0 ;Control effort offset (fine adjustment for initial offset)
u2c=0 ;Control effort offset (fine adjustment for initial offset)
y1o=10000
y2o=-20000
k11=1.7
k12=0.064
k23=1.7
k24=.064
k12d=k12/Ts ;Discrete time terms, compute here to save real-time computation
k24d=k24/Ts
W=11900; weight of magnet (N*10000)
c=26900; Nonlin magnet coefficient
d=42000; Nonlin magnet offset (cm*10000)
kpf1=k11
kpf2=k23
;*****Begin Real-time Algorithm
begin
ylstr=sensor1_pos-y1o

```

```

y2str=sensor2_pos-y2o
delta_y1=y1str-y1str_last
delta_y2=y2str-y2str_last
;CONTROLLER
ulstr=kpf1*cmd1_pos-k11*y1str-k12d*delta_y1
u2str=kpf2*cmd2_pos-k23*y2str-k24d*delta_y2
;NONLIN SPRING INVERSION PLUS MAG WEIGHT OFFSET
y12=133000-sensor1_pos+sensor2_pos; Magnet separation scaled to 1 cm=10000 counts
u12term=(y12+d)*(y12+d)/1000000 ;Intermediate term for u12 divide by 10^6 makes
u12 units N/10000 counts
u12=c/(u12term*u12term)*100000000
u1o=W+u12+u1c
u2o=W-u12+u2c
;OUTPUT
u1=u1str+u1o ;Add gravity offset
u1term1=6.2+sensor1_pos/10000 ;nonlinear actuator compensation in three steps
u1term2=u1term1*u1term1
comp_effort1=0.000165*u1term2*u1term2*u1
control_effort1=comp_effort1
;Again For Output 2
u2=u2str+u2o ;Add gravity offset
u2term1=-6.2+sensor2_pos/10000 ;nonlinear actuator compensation in three steps
u2term2=u2term1*u2term1
comp_effort2=0.000165*u2term2*u2term2*u2
control_effort2=-comp_effort2;reverse polarity for S pole of magnet upward
;SET PAST VALUES (for next time)
y1str_last=y1str
y2str_last=y2str
q10=y1str
q11=control_effort1
q12=y2str
q13=control_effort2
end
    
```

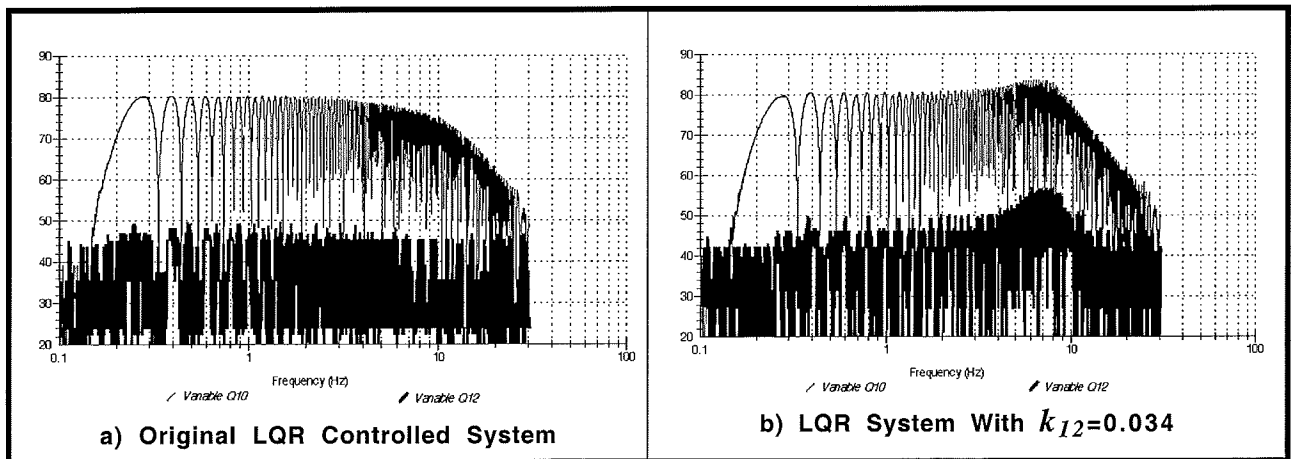


Figure 6.8-5i. Experimental Singular Value Plot

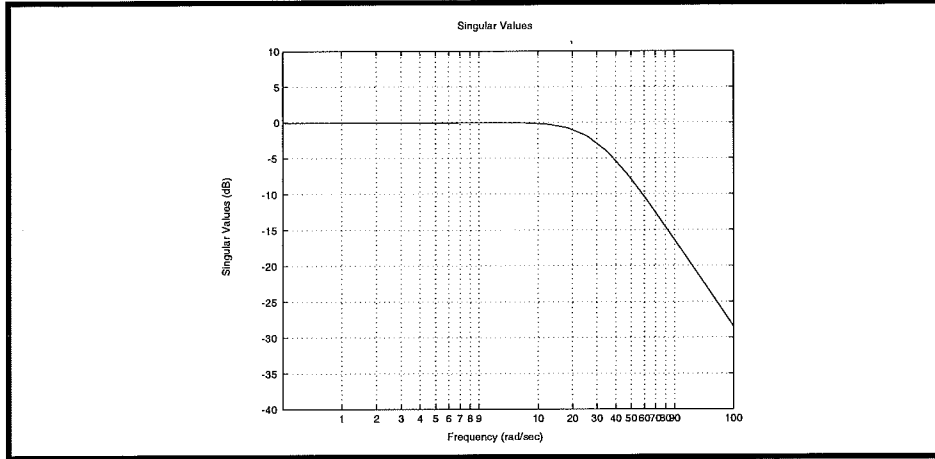


Figure 6.8-6i. Simulated Singular Value Response Of Original LQR System

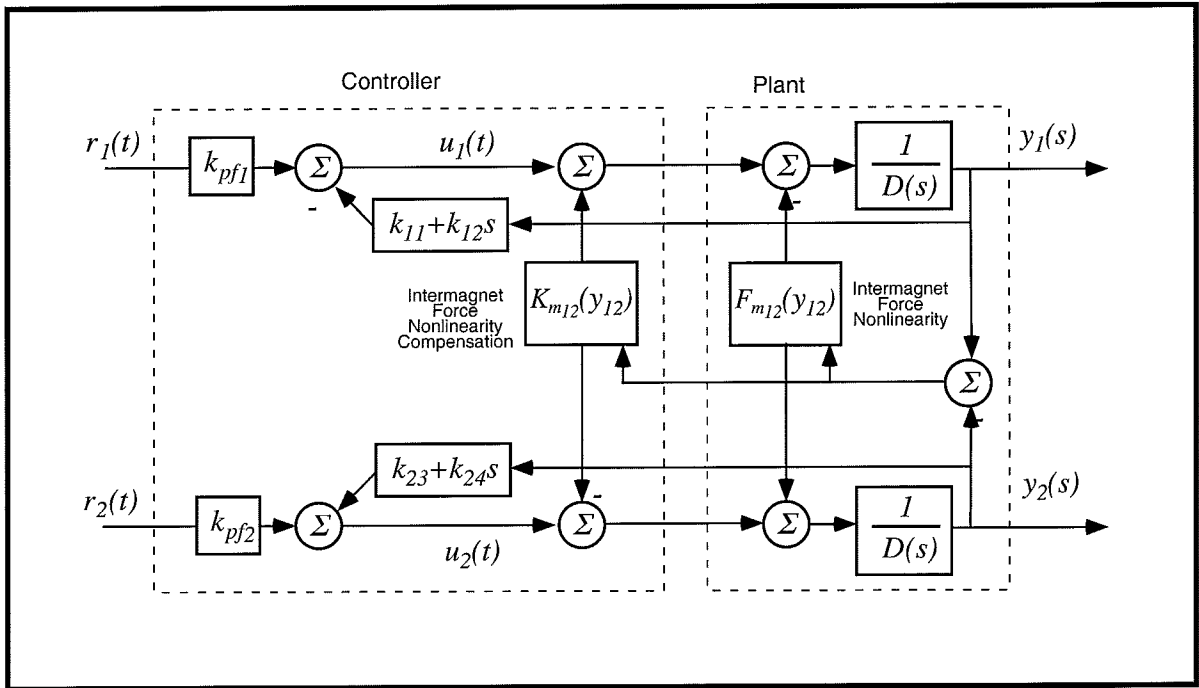


Figure 6.8-7i. Inversion Of Intermagnet Force Nonlinearity

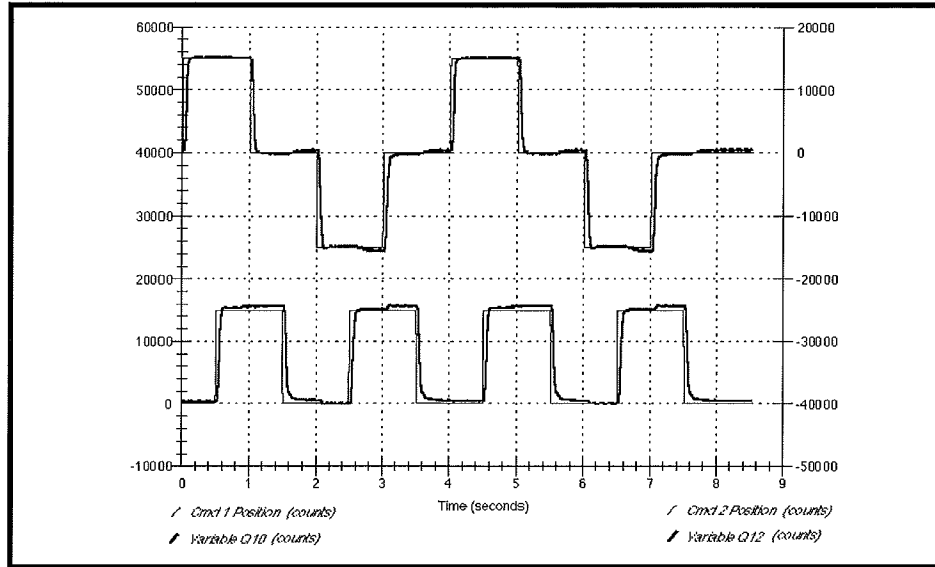


Figure 6.8-8i. Step Series Response Of Intermagnet Force Compensated System

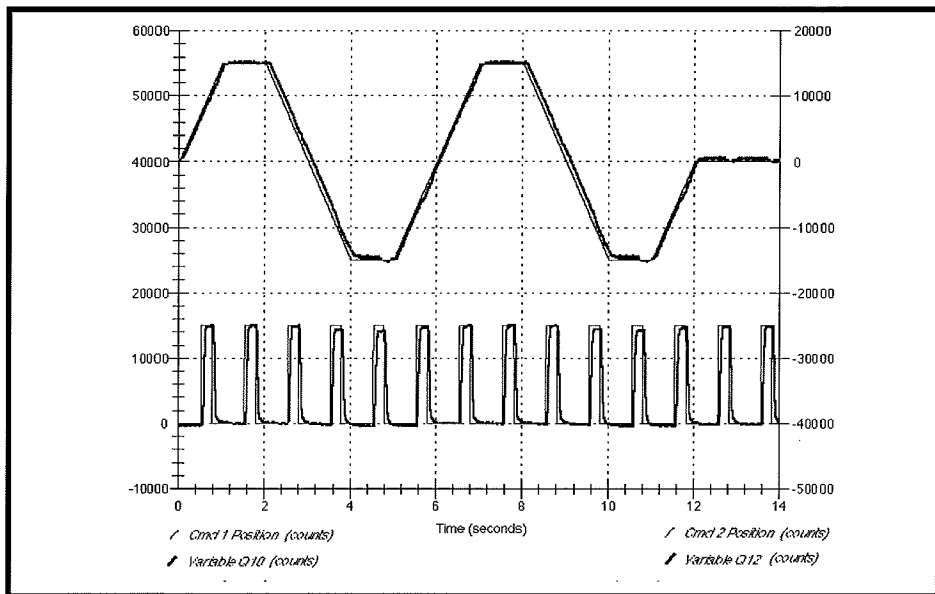


Figure 6.8-9i. Ramp/Impulse Response Of Intermagnet Force Compensated System

**This section showed:**

1. Implementation of multivariable control on 2-input, 2 output plant
2. Multivariable LQR design synthesis and control implementation.
3. Benefits of multivariable control v. SISO control of systems with significant cross coupling
4. Singular value response of multi-variable system
- 5 Decoupling of the system through real-time inversion of the nonlinear coupling term.

## 6.9i Suggestions For Further Experiments

### 6.9.1 Induced Field Levitation

The fascinating phenomenon of levitation through an induced repulsive field in a moving conductor is readily demonstrated using the optional turntable accessory. Here the magnet's levitation height is controlled through regulation of the turntable speed. The upper laser sensor of the basic apparatus is used to measure magnet height and the drive coil is used to apply disturbances to the system when configured in SISO. Additionally the system is readily configured for MIMO where the wheel speed and magnet height are outputs and coil current and wheel torque are inputs. This accessory may also be used to demonstrate control of second order rigid body systems and fundamental servo based motion control.

### 6.9.2 Practical Control Issues

Many important practical control implementation issues are readily studied using the Model 730 system including the following.

#### a. Drive Saturation.

The output will saturate for control effort values greater than 10 V. (32768 counts). The effect can lead to qualitative changes in the shape of the system response and to limit cycle instability in the extreme. This can be demonstrated on the SISO system with the initial offset increased (to say 3 cm) and rapid maneuvers such as an "impulse" of 250 ms followed by a dwell of 750 ms. For small amplitude, the system responds nominally; as amplitude increases, the response becomes highly irregular. These tests should be run for only a brief duration to avoid overheating of the amplifier and drive coils.

#### b. Effect of Discrete Time Sampling.



The time delay associated with discrete time sampling leads to instability as the sample period becomes excessively long. For the Model 730 system and the controllers studied here, these effects become apparent for sample periods greater than several milliseconds and can lead to instability for periods on the order of 10 ms or less. This is readily demonstrated by performing closed loop step responses and incrementally increasing sample period.

#### c. Effect of Finite Wordlength and Sensor Quantization.

Finite wordlength effects are a potential issue in all sampled digitally controlled systems. The effects may be demonstrated by truncating the precision of the S and R terms in the pole placement controller of Section 6.7. As the numerical precision is decreased the system response departs from the nominal and can become unstable. Truncation of the derived rate signal can also be a significant issue. As sample period becomes short, the sensor signal associated with derived rate (e.g. via backwards difference) loses resolution creating noise in the output. This source of noise increases with reduced sample rate

#### d. Effect of Sensor Noise

Sensor noise is amplified in the differentiation of the signal to estimate rate. As the rate feedback gain becomes large relative to the sample rate, noise is generated and seen in the output (and heard audibly). This may be demonstrated by increasing the derivative gain. It may be mitigated by using a low pass filter in the forward control path such as the one in the SIMO LQR controller given in Section 6.7i. This may be a higher order filter for more effective attenuation, however there is attendant phase loss and system stability is adversely affected as the filter cutoff frequency is reduced (typically 30-40 Hz is the lower practical limit). As stated above, sensor noise may also propagate due to truncation of the derived rate obtained by discrete sampling.

### 6.9.3. Discrete Control Design.

The designs in this Manual are based on continuous time modeling and implementation using backwards difference or bilinear transformations to transform the control laws to discrete time. In some cases more effective control designs (improved performance/stability characteristics) may be obtained through the use of discrete design techniques.

### 6.9.4 System Stability

Stability margin metrics such as gain and phase margins were addressed in some of the above sections, but not in a comprehensive fashion. The experimental gain margins are easily measured by simply increasing gain until incipient instability is exhibited (typically oscillations in the output increasing in magnitude with gain). Phase margin may be shown by increasing sample period. The effect may be approximated as being that of a pure time delay so that phase loss,  $\phi$ , at the crossover frequency,  $\omega_c$ , as a function of sample period  $T_s$ , is found as.  $\phi(s) = e^{-sT_s}$ , where  $s$  is evaluated at  $\omega_c$ .

### 6.9.5 Sensitivity & Robustness to Parameter Changes

The sensitivity of the system to parameter changes is a fundamental and important concept. This may be studied analytically as in the exercises in Section 6.4i. Experimentally, the inertia may be increased and the changes in the system response measured. (e.g. use a modeling clay type material that may be later removed without leaving permanent residue on the white diffuse reflective magnet surface. The user is responsible to assure that whatever material is used it does not permanently damage the surface. Ferromagnetic materials will alter the magnetic field and should not be used. Distribute the added mass such that the c.g. remains in the center of the magnet and do not block the laser light path for the active sensor.) The experimental responses can be compared with that of the nominal plant and the indications of the sensitivity analysis predictions. An experimental frequency response is particularly useful in this comparison.

### 6.9.6 Advanced Control

Virtually any control methodology may be implemented on the Model 730 system including linear (e.g. observer based, LQG/LTR,  $H^\infty$ , QFT) and nonlinear (e.g. adaptive, fuzzy logic, variable structure) forms. Feedforward elements may be added to study improved tracking performance. Customized inputs can be implemented for the study of optimal trajectory synthesis (e.g. least peak power, most rapid settling) using the *User-defined* trajectory option.

## Appendix Ai. Useful Scripts and Algorithms

### A.1i Matlab® Scripts

Listed in the table below are scripts that are used in the instructor's edition of the manual and others. These are shown in the approximate order that they appear in the manual and are included on diskette with the Model 730 system when shipped. These are not represented as being numerically or methodologically optimal, but some should be useful to most users.

Script Name	Description
<i>Sensorcal.m</i>	Solves for coefficients of sensor linearization/calibration function. User inputs raw sensor data and magnet position.
<i>Actuatorcal.m</i>	Solves for coefficients of actuator linearization/calibration function. User inputs raw control effort (counts) and levitated magnet height.
<i>Magnet2magnetcal.m</i>	Solves for coefficients of nonlinear intermagnet force function. User inputs force and magnet separation distance.
<i>SISOplant.m</i>	Solves for the linearized or "linear" (via nonlinear compensation algorithms) SISO plant models for the upper and lower magnet positions. User must first run <i>Sensorcal.m</i> , <i>Actuatorcal.m</i> , and <i>Magnet2magnetcal.m</i> , and for the linearized forms, the raw sensor outputs at the nominal operating position.
<i>MIMOplant.m</i>	Solves for the linearized or "linear" (via nonlinear compensation algorithms) MIMO plant models. User must first run <i>Sensorcal.m</i> , <i>Actuatorcal.m</i> , and <i>Magnet2magnetcal.m</i> , and for the linearized forms, the raw sensor outputs at the nominal operating position.
<i>PDdesigner.m</i>	Simple script solves for the proportional and derivative gains of a second order PD controlled system. User inputs $\omega_n$ and $\zeta$ .
<i>Secondorderresponse</i>	Simple script plots the step and Bode responses of a second order system. User inputs $\omega_n$ and $\zeta$ .
<i>DisturbBode.m</i>	Generates the open and closed loop Bode plots for the output /disturbance transfer function of a second order system with lead/lag and integral compensation. It also generates the discrete time coefficients of the lead/lag filter. User must first run <i>SISOplant.m</i> , and input the lead/lag zero and pole frequencies.
<i>SIMOpoleplace.m</i>	Solves the diophantine equation for the pole placement controller numerator and denominator used in the successive loop SIMO design of Section 6.7. It also calculates the inner loop PD gains and generates the closed loop step response of the idealized system. The user inputs the desired inner loop natural frequency and damping and the desired outer loop poles. User must first run <i>SISOplant.m</i>

<i>SIMOLQR.m</i>	Solves the linear quadratic control gain optimization for the outer loop SIMO design of Section 6.7. It also calculates the inner loop PD gains and generates the closed loop poles and step response of the idealized system. The user inputs the desired inner loop natural frequency and control effort weights. User must first run <i>SISOplant.m</i>
<i>MIMOLQR.m</i>	Solves the linear quadratic control gain optimization for control of the MIMO system of Section 6.8. It also calculates the closed loop poles and plots the step response for one input of the idealized system. The user inputs the desired inner loop natural frequency and control effort weights. User must first run <i>MIMOplant.m</i>

### A.2i Real-time Routines

Listed in the table below are real-time routines that implement the controllers and other functions described in the instructor's section of this manual. These are shown in the approximate order that they appear in the manual and are included on diskette with the Model 730 system when shipped. There may be slight differences between the version shown in the manual and those on the diskette. The furnished diskette contains the latest version of these routines and should be used for actual implementation. Also, the algorithms have parameters consistent with a particular apparatus. For more representative performance/stability results, the user should run the appropriate scripts to generate the numerical plant models and control designs for a particular apparatus and adjust the real-time control parameters accordingly.

Script Name	Description
Sensor Comp.alg	Implements the sensor nonlinear compensation / calibration routine used in Section 6.1 for demonstration purposes. (For most purposes the compensation is effected through the Setup Sensor Calibration dialog box.)
Actuator Comp.alg	Implements the actuator nonlinear compensation / calibration routine used in Section 6.1. Allows the user to input the magnet weight to render the magnet "weightless" in demonstration and for control design purposes. This compensation is used within all "compensated" routines that follow.
PDuncomp1.m	Implements PD control on the fully nonlinear lower magnet (repulsive) plant without sensor or actuator calibration.
PDuncomp2.m	Implements PD control on the fully nonlinear upper magnet (attractive) plant without sensor or actuator calibration.
SISO Comp Lower.alg	Implements PD and PID control on the lower (repulsive) SISO plant using sensor and actuator nonlinearity compensation.
SISO Comp Upper.alg	Implements PD control on the upper (attractive) SISO plant using sensor and actuator nonlinearity compensation.

SISO Disturbance.alg	Controls the position of the upper magnet to provide a commandable disturbance to the lower magnet. Implements controllers at the bottom magnet of the following forms (user-selectable) PD, PD+ Integrator, or PD+ lead/lag. The objective is to measure the disturbance rejection properties of the various lower magnet systems.
SIMO Collocated.alg	Performs collocated control of the two magnet system with control effort input and sensor feedback at the lower magnet but control objective to regulate the position of the upper magnet.
SIMO Poleplace.alg	Performs successive loop noncollocated control of the two magnet system with control effort input at the lower magnet and outer loop feedback at the upper magnet. The inner loop is high bandwidth PD and the outer one is a pole placement design.
SIMO LQR.alg	Performs successive loop noncollocated control of the two magnet system with control effort input at the lower magnet and outer loop feedback at the upper magnet. The inner loop is high bandwidth PD and the outer one is a LQR design.
MIMO LQR.alg	Performs full state feedback LQR based control of the two input, two output plant. User may characterize performance across any of the input/output vectors.
MIMO k12 Comp.alg	Compensates for the nonlinear intermagnet force coupling to implement independent upper and lower magnet controllers.